frontiers | Research Topics

Novel strategies for caries control

Edited by
Keke Zhang, Yaping Gou and
Xuelian Huang

Published in
Frontiers in Cellular and Infection Microbiology

ISSN 1664-8714
ISBN 978-2-8325-7347-1
DOI 10.3389/978-2-8325-7347-1

Generative AI statement
Any alternative text (Alt text) provided alongside figures in the articles in this ebook has been generated by Frontiers with the support of artificial intelligence and reasonable efforts have been made to ensure accuracy, including review by the authors wherever possible. If you identify any issues, please contact us.

About Frontiers

Frontiers is more than just an open access publisher of scholarly articles: it is a pioneering approach to the world of academia, radically improving the way scholarly research is managed. The grand vision of Frontiers is a world where all people have an equal opportunity to seek, share and generate knowledge. Frontiers provides immediate and permanent online open access to all its publications, but this alone is not enough to realize our grand goals.

Frontiers journal series

The Frontiers journal series is a multi-tier and interdisciplinary set of open-access, online journals, promising a paradigm shift from the current review, selection and dissemination processes in academic publishing. All Frontiers journals are driven by researchers for researchers; therefore, they constitute a service to the scholarly community. At the same time, the *Frontiers journal series* operates on a revolutionary invention, the tiered publishing system, initially addressing specific communities of scholars, and gradually climbing up to broader public understanding, thus serving the interests of the lay society, too.

Dedication to quality

Each Frontiers article is a landmark of the highest quality, thanks to genuinely collaborative interactions between authors and review editors, who include some of the world's best academicians. Research must be certified by peers before entering a stream of knowledge that may eventually reach the public - and shape society; therefore, Frontiers only applies the most rigorous and unbiased reviews. Frontiers revolutionizes research publishing by freely delivering the most outstanding research, evaluated with no bias from both the academic and social point of view. By applying the most advanced information technologies, Frontiers is catapulting scholarly publishing into a new generation.

What are Frontiers Research Topics?

Frontiers Research Topics are very popular trademarks of the *Frontiers journals series*: they are collections of at least ten articles, all centered on a particular subject. With their unique mix of varied contributions from Original Research to Review Articles, Frontiers Research Topics unify the most influential researchers, the latest key findings and historical advances in a hot research area.

Find out more on how to host your own Frontiers Research Topic or contribute to one as an author by contacting the Frontiers editorial office: frontiersin.org/about/contact

Novel strategies for caries control

Topic editors

Keke Zhang — Wenzhou Medical University, China

Yaping Gou — Lanzhou University, China

Xuelian Huang — The Ohio State University, United States

Citation

Zhang, K., Gou, Y., Huang, X., eds. (2026). *Novel strategies for caries control*. Lausanne: Frontiers Media SA. doi: 10.3389/978-2-8325-7347-1

Table of contents

frontiers | Frontiers in Cellular and Infection Microbiology

TYPE Editorial
PUBLISHED 19 December 2025
DOI 10.3389/fcimb.2025.1756613

OPEN ACCESS

EDITED AND REVIEWED BY
Christophe Beloin,
Institut Pasteur, France

*CORRESPONDENCE
Xuelian Huang
huang.6337@osu.edu

RECEIVED 28 November 2025
ACCEPTED 04 December 2025
PUBLISHED 19 December 2025

CITATION
Huang X and Zandoná AF (2025) Editorial: Novel strategies for caries control. *Front. Cell. Infect. Microbiol.* 15:1756613. doi: 10.3389/fcimb.2025.1756613

Editorial: Novel strategies for caries control

Xuelian Huang* and Andréa Ferreira Zandoná

Division of Restorative and Prosthetic Dentistry, The Ohio State University College of Dentistry, Columbus, OH, United States

KEYWORDS

artificial intelligence (AI), caries control, dental biofilm, dental caries, novel strategies, post-antibiotic era, probiotics

Editorial on the Research Topic
Novel strategies for caries control

Dental biofilm (plaque) is one of the primary contributors in the development of oral diseases, including dental caries, a "biofilm-mediated, sugar-driven, multifactorial, dynamic disease that poses significant public health concerns." Dental caries is more than a localized oral health concern—it is intricately linked to systemic health, underscoring its significance as a broader public health issue. According to the caries ecology hypothesis, a sugar-driven imbalance in oral biofilms triggers caries development, making biofilm control and dietary interventions central to caries prevention. Despite extensive research and clinical practice targeting oral biofilms, current strategies remain insufficient. In the Post-Antibiotic Era, there is an urgent need for the development of novel strategies for caries control whether through direct targeting of oral biofilms or through modulation of the oral environment."

This Research Topic assembles original research and reviews on novel caries control strategies, including: antibacterial agents and novel molecules (allulose, L-arginine, lysine acetylation), novel potential targets (fungi, particularly *Candida albicans*), advanced anti-biofilm dental materials (anti-caries hydrogels, zein-based curcumin nanocapsules, drug-delivery nanosystems), probiotics (*Lactobacillus salivarius*), and novel strategies to prevent secondary caries.

Han et al. evaluated the cariogenic potential of allulose using multi-tiered *in vitro* models, including single-species, dual-species, and saliva-derived biofilms. Compared to sucrose, glucose, and fructose, allulose significantly reduced bacterial growth, acid production, and biofilm formation, resembling non-fermentable sugar alcohols such as xylitol and erythritol. Biofilms grown with allulose lacked dense EPS-rich structures, while saliva-derived biofilms maintained higher microbial diversity with health-associated genera. These findings suggest that allulose has low cariogenic potential and may serve as a non-cariogenic, microbiome-friendly sugar alternative.

Gao et al. investigated the effects of L-arginine on key cariogenic oral microbes *Streptococcus mutans* and *C. albicans*. Using planktonic growth assays, biofilm biomass measurements, crystal violet staining, CFU counts, fluorescence *in situ* hybridization (FISH), and assessments of extracellular polysaccharide and lactic acid production in dual-species biofilms, they found that L-arginine inhibited both planktonic growth and biofilm formation in single-species and dual-species cultures, reduced biofilm adhesion, and suppressed extracellular polysaccharide and acid production. L-arginine may therefore represent a novel strategy to disrupt cross-kingdom interactions and synergistic cariogenicity.

Wang et al. reviewed secondary caries, a major cause of restoration failure, emphasizing the need for antimicrobial strategies in restorative materials. They categorized materials as releasing or non-releasing based on their antimicrobial mechanisms. Traditional release-based approaches often lack precision, durability, and adaptability for long-term caries prevention. The review focused on next-generation controlled-release antimicrobial systems, discussing the design of novel nanomaterials, their functional efficacy, and the mechanisms of representative antimicrobial agents. These advanced systems aim to provide sustained, targeted antimicrobial activity, enhancing restoration longevity and effectively inhibiting secondary caries.

Chen et al. summarized advances in anti-caries hydrogels for the prevention and treatment of dental caries. The review discussed natural and semi-synthetic polymers as hydrogel matrices and various hydrogel types, including probiotic, antibacterial, remineralization-inducing, and saliva-related caries-reducing hydrogels. Mechanisms, functional efficacy, current research status, and limitations were highlighted. These hydrogels show promise in modulating microbial dysbiosis, promoting remineralization, and providing targeted caries prevention, offering a versatile platform for future oral health therapeutics.

Erckmann et al. developed zein-based curcumin nanocapsules (Nano-curcumin) for minimally invasive caries management. Synthesized via nanoprecipitation, nanocapsules were characterized for size, morphology, encapsulation efficiency, release, and biocompatibility, and tested against *S. mutans* on dentin slices with or without photodynamic therapy (PDT). Nano-curcumin exhibited high encapsulation (~100%), spherical morphology, low polydispersity, sustained 24-hour release, and good cytocompatibility. Both Nano-curcumin and PDT-enhanced Nano-curcumin significantly reduced bacterial CFU, with PDT providing the greatest reduction, demonstrating their potential as safe and minimally invasive anti-caries agents.

Zhou et al. reviewed the role of fungi, particularly *Candida albicans*, in dental caries. Fungal biofilms release extracellular DNA (eDNA) and DNA-containing extracellular vesicles (EVs), which, together with bacterial eDNA, form the biofilm matrix and activate the host cGAS-STING signaling pathway. The review detailed molecular mechanisms of STING activation by viral, bacterial, and fungal DNA, explored direct and indirect fungal-mediated activation, and highlighted dual immune effects—enhancing antifungal defense while potentially promoting tissue damage via inflammation. Knowledge gaps were identified, with directions proposed for targeted prevention and treatment.

Yang et al. summarized the role of lysine acetylation, a post-translational modification, in regulating oral microbiota. Lysine acetylation influences bacterial metabolism, virulence, stress responses, and EPS production, affecting biofilm formation and colonization. For instance, acetylation of lactate dehydrogenase in *S. mutans* reduces acid production and tolerance, lowering cariogenic potential. Acetylation also enables bacterial adaptation to fluctuating oral environments, including hypoxia, and interacts with other PTMs to modulate protein function. Understanding these mechanisms offers insights into microbial adaptation and pathogenesis, providing potential therapeutic targets for oral disease prevention.

Ma et al. investigated the antibiofilm effects of *L. salivarius* supernatant on *S. mutans*. Biofilms were treated with cell-free supernatant, followed by RNA-seq, qRT-PCR, and non-targeted metabolomic analysis. The supernatant inhibited biofilm formation by suppressing phosphoenolpyruvate-dependent phosphotransferase systems, ATP-binding cassette transporters, two-component systems, quorum sensing, acid stress responses, and EPS production, without directly affecting glucosyltransferase genes. Metabolomic analysis identified active compounds, including phenyllactic acid, sorbitol, and honokiol, suggesting *L. salivarius* as a promising probiotic for caries prevention.

Du et al. reviewed nanosystems for drug delivery in dental caries management. Traditional drug delivery suffers from poor tissue penetration, short action duration, and low specificity. Nanosystems enhance drug stability, solubility, and bioavailability while minimizing side effects. Their roles include inhibiting bacterial survival, preventing biofilm formation, reducing demineralization, and promoting remineralization. These properties position nanosystems as next-generation strategies, with the potential to become mainstream approaches for caries prevention and treatment.

Collectively, these studies underscore cutting-edge achievements and outline future directions for caries prevention and management. Beyond biofilm control, another critical approach involves inhibiting demineralization and promoting remineralization. Therefore, developing novel strategies that integrate biofilm management with mineralization regulation represents a promising research direction. Dietary intervention constitutes a further key component in achieving effective caries management. Furthermore, advancements in artificial intelligence (AI) offer new opportunities, such as creating intelligent systems for caries risk assessment and early screening, and discovering novel antimicrobial agents like antimicrobial peptides, which could significantly contribute to caries control.

Author contributions

XH: Writing – original draft. AZ: Writing – review & editing.

Conflict of interest

The author(s) declared that this work was conducted in the absence of any commercial or financial relationships that could be construed as a potential conflict of interest.

Generative AI statement

The author(s) declared that financial support was not received for this work and/or its publication.

Any alternative text (alt text) provided alongside figures in this article has been generated by Frontiers with the support of artificial intelligence and reasonable efforts have been made to ensure accuracy, including review by the authors wherever possible. If you identify any issues, please contact us.

Publisher's note

frontiers | Frontiers in Cellular and Infection Microbiology

TYPE Review
PUBLISHED 11 February 2025
DOI 10.3389/fcimb.2025.1546816

OPEN ACCESS

EDITED BY
Keke Zhang,
Wenzhou Medical University, China

REVIEWED BY
Haohao Wang,
Sichuan University, China
Yilan Miao,
University of Michigan, United States

*CORRESPONDENCE
Deqin Yang
500246@hospital.cqmu.edu.cn

†These authors have contributed equally to this work

RECEIVED 17 December 2024
ACCEPTED 14 January 2025
PUBLISHED 11 February 2025

CITATION
Du H, Wang Z, Long S, Li Y and Yang D (2025) The advancement of nanosystems for drug delivery in the prevention and treatment of dental caries. *Front. Cell. Infect. Microbiol.* 15:1546816. doi: 10.3389/fcimb.2025.1546816

The advancement of nanosystems for drug delivery in the prevention and treatment of dental caries

Han Du[1†], Zheng Wang[1†], Shenglan Long[1], Yiding Li[1] and Deqin Yang[1,2,3*]

[1]Stomatological Hospital of Chongqing Medical University, Chongqing Key Laboratory of Oral Diseases, Chongqing, China, [2]Department of Conservative Dentistry and Endodontics, Shanghai Stomatological Hospital & School of Stomatology, Fudan University, Shanghai, China, [3]Shanghai Key Laboratory of Craniomaxillofacial Development and Diseases, Fudan University, Shanghai, China

The dental caries remains a globally prevalent disease. Although its incidence has decrease due to enhancements in sanitation policies and public health measures, the treatment and prevention of dental caries still pose significant challenges. Within the oral cavity, traditional drug delivery systems suffer from limitation such as inadequate tissue penetration, short duration of action at target site, and low specificity, which minimally affect the prevention and treatment of dental caries. Consequently, nanosystem for drug delivery, offering enhanced drug stability, solubility, and bio-availability while reducing side effects, garnering attention increasing attention in the fight against dental caries. Therefore, this review examines the role of nanosystems for drug delivery in combating dental caries by inhibiting bacteria survival, biofilm formation, demineralization, and promoting remineralization, and exploring their potential to become the mainstream means of prevention and treatment of dental caries in future.

KEYWORDS

dental caries, biofilm, nanosystems for drug delivery, remineralization, antibacterial agents

1 Introduction

Dental caries, primarily caused by bacterial infections, is a progressive and destructive disease affecting the hard tissue of teeth. When dental caries develops into periapical inflammation, it can not only lead to severe pain for the patient but also cause potentially sepsis due to the spread of localized infection (Pitts et al., 2017). Statistical data suggests that dental caries is one of the most prevalent diseases worldwide, "A Systematic Analysis for the Global Burden of Disease 2017 Study" reveals that the out of 3.5 billion cases of oral

diseases, and including 2.3 billion cases of untreated permanent tooth decay (GBD 2015 Disease and Injury Incidence and Prevalence Collaborators, 2016; Bernabe et al., 2020).

The formation of dental caries initiates when salivary proteins adhere to the tooth surface to form an acquired pellicle, which is colonized by bacteria quickly, eventually leading to form the plaque biofilm (Bowen et al., 2018). The plaque biofilm comprises various cariogenic bacteria, particularly *Streptococcus mutans, lactobacillus*, and *actinomycetes*. These bacteria metabolize carbohydrates (primarily free sugars) in the dental biofilm, producing acids through glycolysis (Zhang et al., 2022), thereby reducing the oral pH value. With the continuous acid and the lower pH value of oral environment, which leads to the loss of minerals such as calcium and phosphate from the enamel into the external environment. The gradual loss of mineral particles in hydroxyapatite results in demineralization, thus forming carious lesions (Selwitz et al., 2007). Due to the unique physiological and anatomical characteristics of the tooth (Marsh, 2010) and the growth of maturing cariogenic bacteria is protected by Extracellular polysaccharides (EPS) (Sims et al., 2018), effectively removing the plaque biofilm and the expected performance of the local antimicrobial drug pose significantly challenges.

Nowadays, most traditional anti-caries drugs exhibit low bioavailability and poor solubility, leading to they are eliminated from body quickly. Furthermore, the emergence of drug-resistant pathogens and dose-dependent adverse effects of certain chemicals severely limit the efficacy of traditional therapies (Renugalakshmi et al., 2011). Consequently, anti-caries nanosystems for drug delivery have become one of the breakthrough points in the research of caries prevention and treatment. Nanosystems for drug delivery utilize the nanoparticles with a range from 1 to 100nm (Murthy, 2007), as carriers to encapsulate, safeguard, and convey drug molecules to targeted bodily regions. Research have indicated that the nanoparticles hold remarkable potential in drug delivery (Khizar et al., 2023), attracting much attention by improving the drug stability, solubility, and bioavailability while mitigating side effects, thus enhancing the therapeutic effectiveness (Qiao et al., 2022) The most common drug delivery nanoparticles include liposomes, solid lipid nanoparticles, inorganic nanoparticles (nanosilica, gold, silver), polymer nanoparticles, and polymeric micelles (Torchilin, 2014). These nanoparticles play a key role in drug delivery. Compared with traditional drug delivery systems, nanosystems for drug delivery offer superior performance in suppressing cariogenic bacteria and advancing dental remineralization. This review elucidates the anti-caries effectiveness of nanodelivery systems, spotlighting their role in curbing the growth of cariogenic bacteria, biofilm development, and demineralization, and fostering remineralization, alongside their prospective utility in forthcoming anti-caries interventions (Figure 1).

2 Anti-biofilm

2.1 Liposomes

Liposomes are spherical nanovesicles composed of phospholipids and cholesterol, which carry a wide range of diagnostic or therapeutic hydrophobic and hydrophilic medications. They can also deliver and protect encapsulated compounds from the effects of metabolic processes (Liu et al., 2021). Studies have shown that liposomes can adsorb onto hydroxyapatite, which enables them to adhere the enamel surface for extended periods (Nguyen et al., 2010), prolonging their presence in the oral cavity. This adsorption capability, coupled with their capacity to encapsulate lipophilic or hydrophilic drugs, contributes to their effective antibacterial action against the plaque biofilm. Moreover, by physically covering the enamel surface, liposomes offer additional protection to the enamel (Nguyen et al., 2011).

Currently, the efficacy of medicine for the early prevention and treatment of dental caries is impacted by the diversity of the oral microbiome, mainly due to the drugs, poor biofilm-targeting capabilities. Lactoferrin has been proven to inhibit the proliferation of *S. mutans* and the ability of oral pathogens to form biofilms. P Habibi et al. used the thin-layer distribution method to prepare lactoferrin-containing nano-liposomes to evaluate their effect on the biofilm formed by *S. mutans*. The results showed that nano-lactoferrin was more effective in reducing the colony-forming units (CFU) of the *S. mutans* biofilm than free lactoferrin, and nano-liposomes of lactoferrin also significantly reduced the lactate production by *S. mutans* (Habibi et al., 2022). Similarly, research has shown that lipopolysaccharide -encapsulated magnolol (MAG) and fluconazole (FLC) to address their hydrophobicity and rapidly release the drugs in a pH-sensitive manner (Luo et al., 2023). This drug delivery system successfully overcame the hydrophobic characterization of the drugs, enhancing their antimicrobial efficacy against *C. albicans* and *S. mutans*. Furthermore, due to the modification of these composite particles with pyrophosphate ions (PPI), which exhibit good affinity with hydroxyapatite, the PPI - Mag/FLC-LPs can deliver drugs to teeth with high affinity, presenting a novel perspective on the use of nanosystems for drug delivery-based for cooperative drug delivery in oral anti-biofilm treatments.

The expression levels of histatin-1 in populations across different age groups who are prone to dental caries are significantly lower than in those without caries, suggesting that histatin-1 may have important implications for the prevention and treatment of dental caries (Wang et al., 2018a, 2018b). With high affinity for enamel surfaces, activities in the formation of acquired enamel pellicle and the N-terminal domain of histatin-1 could competitively reduce the adhesion of *S. mutans* onto HAP surfaces, Zhang and coworkers synthesized a novel biomimetic peptide DK5 (DpSHEK) inspired by histatin-1, it could adsorb to the surface of acid eroded HAP and guide the nucleation of calcium and phosphorus for enamel remineralization. Although it has potential for remineralization of initial enamel, it cannot be used clinically because of its remaining problems including quick elimination, easy dilution and degradation in the oral cavity.

Consequently, they prepared histatin-1 derived peptide-loaded liposomal system (DK5-Lips) indicated that DK5-Lips exhibited a sustained release profile, excellent stability in saliva, DK5-Lips group had higher surface microhardness recovery, shallower caries depth and less mineral loss in bovine enamel, moreover, it has no significant toxicity on human gingival fibroblasts (HGFs)

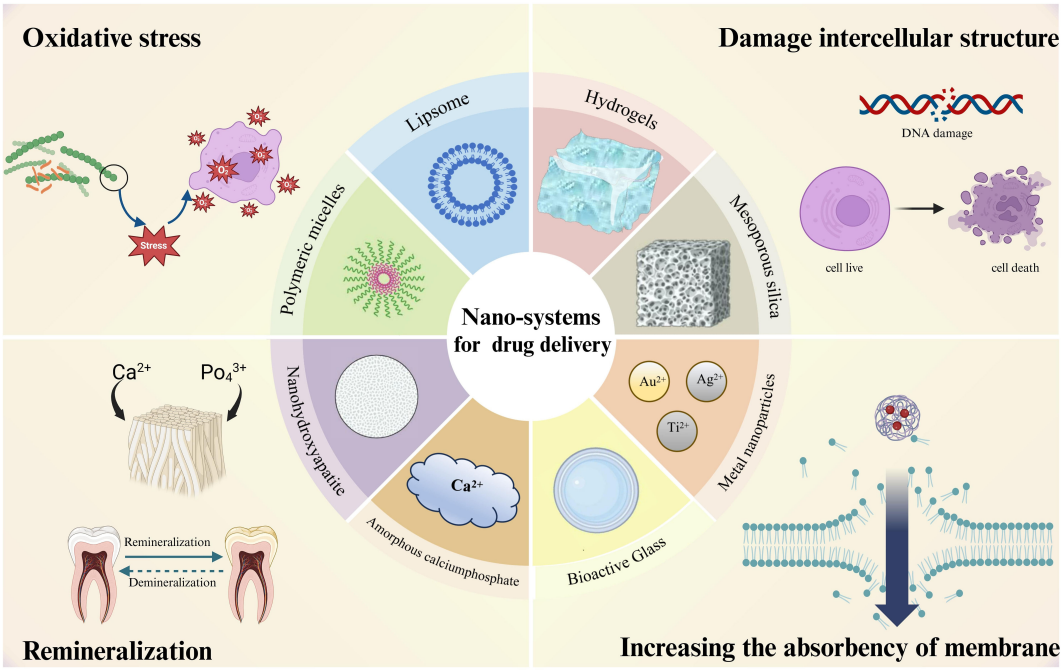

FIGURE 1
Nanodelivery systems currently used for anti - caries and their anti - caries mechanisms.

(Zhang et al., 2023). The novel liposomal delivery system for a novel peptide derived from (DK5-Lips) as a new biomimetic mineralization strategy against initial enamel caries, the system could exert significant anti-caries effect both *in vitro* and *in vivo*, evidenced by the increased level of remineralization and the reduced degree of caries decay.

Xiao et al. developed a liposome-encased formulation of indocyanine green (ICG) and rapamycin for drug delivery (ICG-rapamycin). Their investigation revealed that ICG-rapamycin, when subjected to 808 nm laser excitation, significantly enhances the levels of reactive oxygen species (ROS) and temperature, thereby activating photodynamic and photothermal mechanisms to elicit antibacterial effects. Furthermore, ICG-rapamycin promotes bacterial motility by elevating intracellular ATP concentrations within bacterial cells and simultaneously inhibiting both bacterial adhesion and biofilm formation. This innovative anti-biofilm strategy effectively addresses the challenge of disease recurrence resulting from the proliferation of residual viable bacteria, which can generate biofilms post-antibacterial treatment. Additionally, near-infrared (NIR) laser excitation facilitates M2 polarization and augments TGF-β concentrations, leading to a reduction in cellular inflammatory responses and improving the phagocytic activity of macrophages toward bacteria. The results of this investigation indicate that ICG-rapamycin has the potential to effectively treat and prevent common biofilm-associated oral diseases by modulating the microbial-cellular microenvironment, thereby offering considerable promise for future applications in dental clinics (Xiao et al., 2023).

Curcumin, functioning as a natural exogenous photosensitizer, interacts with ground-state molecular oxygen to produce reactive oxygen species (ROS) under blue light excitation (Luby et al., 2019). The recent study conducted by Hu and coworkers designed a liposome with adhesion properties to deliver curcumin (Cur@LP) into the biofilm. Curcumin can be released from the liposome near the biofilm and exert an antibacterial effect by dispersing the biofilm under blue light irradiation. The result indicates that Cur@LP group had the least residual *S. mutans* biofilm when compared with other groups. It proves that the Cur@LP has better activity of antibacterial and adhesion onto the *S. mutans* biofilm but no significant cytotoxicity compared with curcumin group. Clinically, the convenience offered by the widespread application of the blue light source and the adhesion ability to *S. mutans* biofilm will make the Cur@LP a broad application prospect (Hu et al., 2023). Liposomes show promise for targeted drug delivery in oral care, offering enhanced biofilm control, remineralization. However, more clinical experiments are still needed to prove its safety for its application.

2.2 Poly - (lactic-co-glycolic acid) (PLGA)

The combination of Lactic Acid (LA) and Glycolic Acid (GA) creates a copolymer system called PLGA, PLGA nanoparticles are used for sustainable drug delivery systems because of their excellent bioavailability, biocompatibility, biodegradability, small size, and ability to release medicine over time (Vlachopoulos et al., 2022; Narmani et al., 2023). One of the main uses of PLGA is in delivering drugs, and it can be shaped into large-scale structures (like scaffolds or gels), microparticles (MP), or even smaller nanoparticles (NP). In the realm of healthcare, these PLGA formats have shown their potential to encapsulate various kinds of medicinal agents, including antibiotic, drugs that reduce inflammation, and

antioxidants, to fulfill therapeutic objectives. Crucially, materials based on PLGA can shield the encapsulated drugs from degradation early and ensure a steady release of medication, making them exceptionally well-suited for treatments that span a longer duration.

Chlorhexidine (CHX) has been widely used in dentistry, usually in the form of an oral rinse, to prevent the formation of dental plaque and calculus, as well as to treat oral inflammation. CHX has been considered the "gold standard" (Hetrick et al., 2009) among antimicrobial agents due to its broad-spectrum antimicrobial effects. A single direct pre-treatment with CHX on the acid-etched dentin matrix significantly enhances the degradation resistance of the resin-dentin bond interface. However, without a drug-release source, the concentration of CHX cannot be guaranteed, and the non-biodegradable CHX-modified bonding resin could hinder the release of CHX due to the thickness of the adhesive layer, adversely affecting the dentin bonding system. Therefore, Priyadarshini et al. loaded CHX onto PLGA nanoparticles. These CHX@PLGA nanoparticles exhibited low cytotoxicity and strong antibacterial abilities, and CHX was continuously released over 28 days (Priyadarshini et al., 2017). In addition, when CHX@PLGA nanoparticles were in aqueous solution, they could penetrate up to 10 μm deep into dentinal tubules and tightly bond with the resin after penetration of the adhesive. It demonstrated the potential application of CHX@PLGA entering dentinal tubules for adhesive restorative treatments and its capability to deliver other drugs already used in dental treatments, thereby expanding the therapeutic methods for oral diseases continuously.

Additionally, F.O. Sousa et al. discovered that PLGA composites containing chlorhexidine diacetate and Digluconate demonstrate potent antimicrobial properties against *S. mutans* (Francisco Fábio Oliveira de et al., 2021). Specifically, the digluconate encapsulated in a solid form within PLGA exhibits a rapid release. Moreover, diacetate-loaded PLGA particles ensure a consistent and sustained release of the drug over a period of 120 days. Advances in nanotechnology and targeted delivery methods may enhance the capabilities of PLGA-based systems, allowing for improved patient outcomes and the development of personalized strategies for oral health maintenance and caries prevention.

2.3 Mesoporous silica nanoparticles (MSN)

Mesoporous materials refer to nanomaterials with pore sizes in the range of 2 to 50 nm, among which mesoporous silica has attracted considerable attention due to its excellent controllable drug delivery capabilities (María et al., 2022; Bianca et al., 2023). Mesoporous silica nanoparticles (MSNs) maintain a certain chemical stability, surface functionality (high surface area and adjustable pore size), biocompatibility, and biodegradability because of their unique mesoporous structure. With these properties, MSNs ensure the controlled release and targeted delivery of various drug molecules (Komal Sadashiv, 2015; Lanlan et al., 2023). Moreover, MSNs can respond to certain stimuli during the loading, protection, and transport of drugs to release them. Therefore, MSNs can load antimicrobial drugs and incorporate them into resin composites to produce an anticariogenic effect (Montserrat and María, 2020). In summary, due to their large surface area and pore size, which enable a higher drug load capacity and targeted drug delivery, MSNs enhance therapeutic efficacy while reducing side effects, exhibiting safer and more effective treatment outcomes.

Research has proven that L-arginine can be metabolized by the arginine deiminase system in oral bacteria, thereby raising the pH value of dental plaque and reducing the risk of caries (Marcelle et al., 2013). Researchers prepared MSNs loaded with L-arginine and integrated them into the dentin adhesive system (Arg@MSN@DAdh) (Marta et al., 2022). The experiments revealed that the adhesive system containing Arg@MSN@DAdh significantly reduced the populations of *S. mutans* and *Lactobacillus casei*, with no observed compromise in its physical, mechanical, and adhesive properties. Furthermore, this composite could continuously release L-arginine, exhibiting enduring antibacterial capabilities and preventing biofilm formation.

Studies have found that encapsulating CHX in MSNs enables it to penetrate the biofilms of *S. mutans* and interact with other microbes (Ya et al., 2011; Li et al., 2016); it even retains its biofilm-inhibitory effect after 50 hours. Based on this, Lu et al. developed biodegradable disulfide-bridged MSN, it could deliver silver nanoparticles and CHX (Ag-MSNs@CHX) concurrently (Lu et al., 2018). Experiments have shown that, due to its redox and pH-responsive release properties, this composite significantly inhibits the growth and biofilm formation of *S. mutans*, and its antibacterial effect is superior to that of an equivalent amount of free CHX. More importantly, no abnormal reactions were observed in mice after oral administration of Ag-MSNs@CHX, and Ag-MSNs@CHX significantly reduced the cytotoxicity of CHX to the oral mucosal epithelial cells.

Two-component signal transduction systems (TCSTS) are capable of modulating gene expression in response to external environmental changes. The VicRK system, one of the TCSTS, consists of a membrane-bound sensor (VicK) and a cytoplasmic response regulator (VicR). VicR is an essential regulator in exopolysaccharide (EPS) production which is one of the main cariogenic factors of S. mutans. It is reported that an Antisense vicR RNA (ASvicR) could bind to vicR mRNA, hindering the transcription and translation of the vicR gene. Moreover, ASvicR can inhibit EPS synthesis, bacterial growth, and cariogenicity of S. mutans, suggesting its potential as a strategy for caries prevention (Senadheera et al., 2005; Dongsheng et al., 2007; Lei et al., 2019; Yuting et al., 2023). Tian and coworkers had constructed a recombinant plasmid containing the ASvicR sequence (plasmid-ASvicR) and proved that it could reduce EPS synthesis, biofilm formation, and cariogenicity. However, the recombinant plasmids need protection from enzymatic degradation and require higher transformation efficiency. Consequently, they further synthesized and characterized aminated dendritic mesoporous silica nanoparticles (DMSNs-NH2) and demonstrated its capability to transport and maintain the integrity of plasmid-ASvicR (DMSNs-NH2-ASvicR). The result indicated that DMSNs-NH2 could effectively protect most of the plasmid-ASvicR from being degraded by DNase I. When loaded onto DMSNs-NH2, the

plasmid-ASvicR was able to enter *S. mutans* suppress the expression of the vicR gene, which in turn reduced the synthesis of EPS and the formation of biofilms in S. mutans. Furthermore, cytotoxicity experiments revealed that DMSNs-NH2-ASvicR exhibited no cytotoxic effects, and Keys scores outcomes demonstrated that DMSNs-NH2-ASvicR significantly lowered caries incidence in rats. This suggested that DMSNs-NH2 can protect the plasmid-ASvicR against degradation effectively and enhance its penetration into the bacteria within the rat's oral cavity. Demonstrating excellent biocompatibility, DMSNs-NH2-ASvicR sets a solid groundwork for future biomedical applications (Yuting et al., 2022).

In dental applications, MSNs demonstrate substantial antibacterial effects, effectively loading and releasing antimicrobial agents to reduce the risk of caries. Moving forward, ongoing research into the modification and functionalization of MSNs will further enhance their application potential in the prevention and treatment of oral biofilm-related diseases. Additional clinical studies will be essential to validate the long-term efficacy and safety of MSNs in biomedical applications.

2.4 Poly (amino amine) (PAMAM) dendrimers

PAMAM dendrimers, often referred to as "artificial proteins" due to their protein-like structure, are highly branched nanopolymers featuring both internal cavities and external terminal groups. These internal cavities facilitate the transport of drugs or ions (Qichao and Janet, 2015), while the external groups can be modified with various functional groups to act as carriers for drug delivery, thereby controlling the release of drugs. Notably, they exhibit both antibacterial and remineralization properties, making them effective in both treating and preventing dental caries. In aqueous solutions, PAMAM dendrimers tend to self-assemble into hierarchical structures, namely nanospheres, nanochains, microfibers, and eventually macroscopic aggregates (Jiaojiao et al., 2013). This self-assembly and the resultant hierarchical structures are capable of mimicking the function of amelogenin, which is crucial in the formation of dental enamel (Mirali and Thomas, 2021). Consequently, PAMAM dendrimers are considered a promising material for dental repair.

Previous studies showed that honokiol could inhibit the growth of many cariogenic pathogens, and could reduce acid production by cariogenic bacteria (Jun et al., 2004). However, its hydrophobicity limited its further application. Tao et al. encapsulated water-insoluble honokiol within the hydrophobic interstitial cavity of PAMAM, thereby endowing PAMAM with enduring antibacterial properties. They successfully prepared and characterized honokiol-loaded carboxyl-terminated PAMAM (PAMH), PAMH demonstrated low cytotoxicity, with its drug release dynamics elucidated via computational simulation analysis. At a low pH of 5.5, resulting in a relatively slow swelling rate and consequently a more gradual release of drug molecules in an acidic milieu compared to a neutral environment. The effective release of honokiol contributed to the sustained antibacterial properties of PAMH, They concluded that PAMH possesses antibiofilm-forming properties by inhibiting the proliferation of planktonic bacteria. Furthermore, PAMH facilitated enamel remineralization after pH cycling treatment *in vitro*, and animal studies supported its effectiveness in addressing carious lesions in rats (Tao et al., 2021).

Existing materials to induce dentin remineralization lack the ability to stabilize dentinal collagen which is the basic support for the growth of inorganic minerals and plays a role of mechanical support (Leo et al., 1999; Erika Kiyoko et al., 2020). The repeated low pH stimulation activates matrix metalloproteinases (MMPs) under pathological conditions such as dental caries, it could destroy the structure of dentinal collagen which leads to the induction of biomimetic remineralization losing its structural basis. Tao and colleagues constructed galardin-loaded poly (amido amine) (PAMAM)-NGV (PAMAM-NGV@galardin, PNG) to simultaneously induce collagen stabilization and dentin biomimetic remineralization.

In order to combat early dentin caries, NGV peptides and galardin demonstrated a dual collagen-protective effect, which lays the foundation for the dentin remineralization effect facilitated by PAMAM (Tao et al., 2022). The results suggested that in acidic environments, galardin can be more sustainably released, and a longer inhibitory effect on MMPs is achieved. The NGV peptides, modified on the surface of the dendrimer core, could form small clusters exhibiting synergistic movement over short ranges. These clusters could then create domain areas with varied properties on the PAMAM core's surface, effectively restricting collagen movement. This restriction was beneficial for collagen crosslinking. PNG induced dentin remineralization in a collagenase environment *in vitro*, and animal experiments also indicated that PNG could effectively combat dentin caries in rats. PNG showed great potential for dentin repair in future clinical applications.

Fan et al. utilized PAMAM dendrimers with different terminal groups to treat artificially demineralized bovine incisors, aiming to quantify the remineralization effects of these PAMAM dendrimers in the subsurface demineralized enamel (Menglin et al., 2020). They employed Transverse Microradiography (TMR) and cross-sectional microhardness testing for the first time to evaluate the differences in remineralization capabilities of PAMAM dendrimers with different terminal groups. After treatment with PAMAM dendrimers possessing various terminal groups, the demineralized bovine teeth examined through TMR showed a significant reduction in the translucent zone. This reduction in the area indicates the deposition of minerals in the subsurface enamel, thereby achieving remineralization. Moreover, through Scanning Electron Microscope (SEM) analysis of the bovine teeth samples, they found that compared to the control group, the PAMAM dendrimer-treated group exhibited shallower lesion depths and less mineral loss. At the same time, these samples showed a more significant recovery in microhardness on the vertical cross-sectional surfaces and absorbed more mineral deposits. These results indicate that although enamel itself can remineralize to some extent in artificial saliva, the remineralization effect of PAMAM dendrimers is more pronounced. In addition, PAMAM-NH_2 showed the strongest remineralization capability, followed by PAMAM-COOH, while PAMAM-OH had the weakest effect. The study also found that

PAMAM-NH_2 dendrimers could strongly adsorb to the enamel surface and form a stable bond with it. Therefore, PAMAM dendrimers with specific terminal groups exhibit strong enamel protection and remineralization potential, making them powerful candidates for the prevention and treatment of caries.

2.5 Chitosan

Chitosan is a natural polymer derived from the deacetylation of chitin, primarily sourced from the exoskeletons of marine crustaceans such as crabs and shrimp (Kamel et al., 2021). Its deployment as a drug delivery system, as well as its application in tissue engineering and as a therapeutic agent, has been intensively researched. Chitosan's notable antibacterial, remineralization capabilities, and adherent properties to dentin, alongside its excellent biodegradability, biocompatibility, and non-toxicity, have made it an area of significant interest in caries prevention and treatment (Shelyn Akari et al., 2022). Under acidic conditions, chitosan captures hydrogen ions through its amino groups, thereby becoming positively charged. Through electrostatic forces, the molecule adheres to negatively charged surfaces, such as tooth enamel, making it a nano drug delivery carrier that can transport ions or active substances to the tooth surface (Degli Esposti et al., 2020).

Current preventive strategies, primarily centered on fluoride, can inhibit enamel demineralization to a certain degree; however, they do not effectively prevent persistent biofilm formation and may induce adverse effects such as fluorosis or alterations in oral and gut microbiota. Consequently, there is a pressing need for a safe and effective approach to preventing dental caries (Li et al., 2019). Jiang et al. successfully synthesized a novel type of nanoparticle (CSP NPs) that exhibits both colony-suppressing and enamel demineralization-inhibiting properties (Jiang et al., 2024). These nanoparticles demonstrated efficacy in eradicating a specific strain of *S. mutans* biofilms in the absence of antibiotics. Moreover, the nanoparticles were applied to the enamel surface, enabling the binding of calcium to impede demineralization. Results from animal studies and oral microbiome analyses indicated that the CSP NPs effectively prevented dental caries without adversely affecting the microbiota or host tissues. Moreover, curcumin within chitosan nanoparticles (CSNP-Cur) were encapsulated to assess their efficacy in disrupting biofilms formed by *C. albicans* and *Staphylococcus aureus* (Ma et al., 2020). They transferred microbial cultures onto medical-grade silicone sheets to initiate biofilm formation, then treating with CSNP-Cur. The structure of biofilm on the medical silicon and the viability of bacteria within biofilm were observed by Scanning Electron Microscopy (SEM) and Confocal Laser Scanning Microscopy (CLSM). The observations from SEM and CLSM showed that CSNP -Cur could effectively reduce the thickness of the biofilms and kill the microbes embedded in the biofilms on the silicone surface. In a similar vein, Jasem et al. found that amoxicillin-loaded chitosan nanoparticles demonstrated enhanced antibacterial properties compared to chitosan alone (Abdullah and Maha Abdul Kareem, 2023). Given chitosan's versatility in forming drug delivery systems, such as gels, tablets, and micro/nanoparticles (Sevda et al., 2019), it exhibited a significant potential in preventing bacterial or plaque biofilm formation and demonstrated bactericidal properties, suggesting its utility as a prophylactic agent in early dental caries prevention.

Previous study had reported that the Cinnamaldehyde has anti-inflammatory and broad-spectrum antibacterial effects. It could be a potential anti-caries drug due to its strong effect of inhibiting *S. mutans* (Spartak, 2020; Harrison et al., 2021; Jishuai et al., 2022). Mu et al. design a novel nanosystem by loading Cinnamaldehyde (CA) into chitosan-based nanocapsules (CA@CS NC). The result indicated that CA@CS NC down-regulated QS gene, inhibited bacterial population effects such as biofilm formation and acid production, and better exerted the antibacterial effect of low-concentration CA. The keyes' score showed the development of dental caries was inhibited in CA@CS NC group. Moreover, with an oil-based core and a positively potential CS shell, which are able to adsorb *S. mutans* through electrostatic interactions and slowly release CA (Ran et al., 2023).

There are existing studies that have proven that there are inhibitory effects of Chitosan on *S. mutans* and *Porphyromonas gingivalis*, and oral care products containing Chitosan (such as water-soluble Chitosan mouthwash and chewing gum) have been shown to inhibit plaque growth and bacterial proliferation (Chih-Yu and Ying-Chien, 2012; Zahra et al., 2020). When Chitosan is functionally modified with natural compounds, metal antimicrobial particles, and antimicrobial drugs, it exhibits enhanced antibacterial effects. The antibacterial action of Chitosan primarily stems from the interaction between the cationic Chitosan molecules and the negatively charged cell membranes, leading to abnormal cell permeability and changes, thus resulting in cell death and the leakage of cellular contents. Chitosan nanoparticles (NPs) have a relatively larger surface area, leading to stronger drug loading capabilities (Somaye et al., 2021; Ashwini and Arpana, 2015). In summary, Chitosan, as a nanocarrier for dental caries prevention, not only possesses antibacterial capabilities but also, when it serves as a drug carrier, enhances the antibacterial efficacy of the drug-Chitosan composite.

2.6 Polymeric micelles

Micelles are self-assembled from amphiphilic polymers at the critical micelle concentration (CMC). These self-assembled amphiphilic polymers, containing both hydrophobic and hydrophilic ends, are known as Polymeric micelles (Suguna et al., 2022), enabling drugs with low solubility to dissolve in Polymeric micelles (Yinglan et al., 2018). Polymer micelles have numerous advantages, such as targeted delivery, stable storage of drugs, due to their nanoscale size and narrow distribution characteristics, can protect drugs from oxidation. Polymer micelles can encapsulate poorly soluble small molecule drugs, enhancing efficacy while reducing toxicity. In preclinical animal models, polymer micelles have demonstrated improved pharmacokinetic properties and better safety (Duhyeong et al., 2020). Numerous natural products and their derivatives inhibit *S. mutans*, notably components found in orange and lemon essential oils. Such components, including phellandrene, enhance the proton permeability of the bacterial cell membrane and reduce the glycolytic activity of *S. mutans* in dental plaque (Jeon et al.,

2011). Consequently, a novel polymeric micelle by conjugating Farnesal (Far) was developed to the amino groups of PEG, rendering it sensitive to low pH environments (Yi et al., 2020). This design aimed to selectively release Far in the oral environment prone to caries. They modified the polymeric micelles by coupling with pyrophosphate ions (PPi) and loading them with Far to enhance its solubility significantly, thus improving bioavailability and creating a new drug delivery system, PPi-Far-PMs. In a rat caries model, PPi-Far-PMs demonstrated a significant reduction in *S. mutans* count and continuous inhibition of its growth *in vivo* compared to the control group. Moreover, PPi-Far-PMs exhibited rapid binding to hydroxyapatite, facilitating Far release, enhancing retention in the oral cavity, prolonging the drug's action, and providing a more potent anti-caries effect. PPi-Far-PMs proved more effective than free phellandral, demonstrating their potential for targeted antimicrobial therapy for caries and the delivery of other oral disease therapeutics. Polymeric micelles, serving as carriers for drugs with low water solubility, present extensive potential in oral healthcare. Xu and coworkers developed a novel stimuli-responsive multi-drug delivery system (PMs@NaF-SAP). The system utilized the acidic pH associated with tooth decay as a trigger. It featured MAL-modified PEG-b-PLL/PBA-sheddable micelles as nanocarriers, which are loaded with the antibacterial drug tannic acid (TA) and the restorative drug NaF. Additionally, the bioinspired salivary-acquired peptide DpSpSEEK (SAP) is attached to the micellar nanoparticles, ensuring specific adhesion to the tooth. This adhesion strength, combined with the pH-sensitive boronate ester linking TA and PBA, allows PMs@NaF-SAP to firmly attach to the tooth surface. It withstands the buffering action of saliva in the oral cavity, promoting the accelerated release of TA and NaF directly to the sites of caries as the oral microenvironment becomes more acidic. Both *in vitro* and *in vivo* measurements have confirmed the intelligent drug-released system exerts effective antibacterial adhesion and cariogenic biofilm resistance, inhibits enamel demineralization and promotes remineralization to prevent tooth decay and promote enamel restoration and they evaluated the safety and biocompatibility of PMs@NaF-SAP through cell viability assays. Using CCK-8 analysis, it was observed that at dilutions ranging from 1:20 to 1:100, cell viability exceeded 80%. PMs@NaF-SAP demonstrated significantly lower cytotoxicity compared to CHX. Cytoskeleton staining confirmed that, within this dilution range, the cells maintained healthy morphology and proliferation was unaffected. Consistent results were obtained via fluorescence quantitative analysis. Therefore, it demonstrates significant promise in broadening the limited clinical options currently available for the prevention of caries and the restoration of dental defects (Xu et al., 2023). By integrating bioactive natural compounds and targeted delivery mechanisms, polymeric micelles may revolutionize oral disease management, making treatments more effective and personalized, ultimately improving patient outcomes.

2.7 Hydrogels

Hydrogels are three-dimensional (3D) networks made up of hydrophilic polymer chains. With exceptional features, such as adjustable physical, chemical, and biological p0roperties, high biocompatibility, versatility in fabrication, and their resemblance to the native extracellular matrix (ECM), hydrogels have become promising materials in the field of biomedicine (Annabi et al., 2014). These polymeric networks can consist of natural polymers (chitosan, alginate, cellulose, starch, guar gum, collagens, proteins, acacia, and acid) or synthetic polymers (polyacrylic acid, polyacrylamide, polyvinyl pyrrolidone, acrylic acid, methacrylic acid, N-isopropylacrylamide, N-vinyl-2-pyrrolidone, etc.) soluble in water (Payal et al., 2021). The hydorgels have been used to treat some diseases, including cancer, cardiovascular diseases, and eye diseases. Recently, hydorgels has been explored in the aspect of treatment of dental caries.

Lori M. and coworkers developed Nitric oxide (NO)- and fluoride ion-releasing hydrogels with highly tunable biological properties suitable for combating pathogens at the root of dental caries infections. Nitric oxide (NO), a gaseous molecule produced endogenously, possesses broad-spectrum antimicrobial and antiviral capabilities, capable of penetrating and dispersing mature biofilms. It exterminates microbes by inflicting oxidative and nitrosative stress on lipids, proteins, metabolic transporters, and DNA (Nathan et al., 2018; Mark et al., 2021). The result through a 4 h viability study against *S. mutans* showed potent antimicrobial properties in eliciting a nearly 98% reduction in viable bacteria with the combination of GSNO and NaF gels, further *in vitro* testing of the fabricated gels against human osteoblasts and gingival fibroblasts demonstrated robust cytocompatibility over 4 and 24 hours. A further extended study showed combination gels exhibited reduced porosity after acid treatment, signifying the successful prevention of demineralization of the enamel-like substrates. These results encouraged further investigation of Hydrogels contain NO and fluoride to explore more promising ways in preventing dental caries (Lori et al., 2022).

Parmanand et al. developed selective small-molecule inhibitors which targets the *S. mutans*' surface enzymes. And they have synthesized and demonstrated that the potent lead compounds HA5 was effective in the previous research. To enhance the solubility and antivirulence activities of the drug, they encapsulated HA5 within hydrogel microparticles, creating a hydrogel-encapsulated biofilm inhibitor (HEBI). The binding of HA5 to the glucosyltransferase GtfB was confirmed by resolving a high-resolution X-ray cocrystal structure of HA5 bound to the catalytic domain of GtfB and mapping its active site interactions. Additionally, HA5 effectively inhibited the glucosyltransferases of *S. mutans* and the production of glucan, with an IC50 value of 10.56μM in a Gtf inhibition assay. The HEBI demonstrated selective inhibition of the *S. mutans* biofilm similar to HA5. The result showed that treating *S. mutans* UA159-infected gnotobiotic rats with 100μM HA5 or HEBI for four weeks significantly reduced the scores for buccal, sulcal, and proximal dental caries compared to the control groups. This demonstrates their effectiveness in reducing virulence *in vivo* without significantly impacting bacterial colonization. During the test period, the rat had no loss of weight which demonstrated the compound HA5 or material HEBI have are nontoxic (Parmanand et al., 2023).

Qian et al. had produced amelogenin-derived peptide QP5, in their previous research, it can significantly promote the

remineralization of the initial caries in the bovine enamel and the rat enamel without any toxic effects (Xuebin et al., 2015; Sili et al., 2017). The QP5's application clinically is limited because its residence time with effective concentration on the tooth surface is relatively short when applied in the form of an aqueous solution. They added QP5 to chitosan hydrogel as a delivery system (CS-QP5 hydrogel) to evaluate the effects on *S. mutans* biofilm and test for its ability to promote remineralization. The result showed the *S. mutans* biofilm treated with the CS-QP5 hydrogel had a lower CFU count, lactic acid production, and metabolic activity compared with the other groups even after seven days. That's probably because a sustainable retention of the hydrogel on the tooth surface provided a consistent number of effective agents over a prolonged period of time, which may decrease the cariogenic property of the dental biofilm with fewer potential side effects. In polarized light microscopy, after inoculation for 1 day, a surface layer was clearly visible on the enamel treated with the CS-QP5 hydrogel. With an increase in the inoculation time, the lesions became significantly shallower and the negative birefringence of the enamel surface layer became more obvious in the CS-QP5 hydrogel group than in the other four groups. In addition, the CS-QP5 hydrogel group showed a significantly higher mineral content than the other groups on each day, these results provided direct evidence of the remineralization promoted by the CS-QP5 hydrogel. Therefore, as a promising deliver system of active substances, hydrogel has been proven to increase antibacterial ability which is promising application in treatment (Qian et al., 2018).

Hydrogels have emerged as promising biomaterials in biomedicine, with increasing interest in their applications for dental caries treatment. Innovations like hydrogels containing nitric oxide and fluoride ions provide novel strategies against dental caries pathogens. Additionally, QP5-enriched hydrogels demonstrate efficacy in remineralization and biofilm reduction, highlighting their potential in caries management. Future research should optimize these formulations for improved retention, effectiveness, and safety.

2.8 Metal nanoparticles

2.8.1 Silver nanoparticles

Silver ions are widely used because of their low toxicity, broad-spectrum antimicrobial characteristics, and the lack of cross-spectrum bacterial resistance (Claudia Butrón-Téllez et al., 2020). Compared to ordinary silver ions, nanosilver further increases the relative surface area, and its ability to easily penetrate biological and structural barriers results in better antimicrobial effects (Ammar, 2022). Silver nanoparticles (AgNPs) exhibit exceptionally potent toxicity toward microbes, boasting antibacterial properties 25 times stronger than those of CHX. They also possess antiviral, antifungal (Besinis et al., 2014), and anti-tumor cell activities (Noronha et al., 2017). Consequently, numerous studies have recommended their integration into various formulations, where they have demonstrated effective results in the prevention and treatment of early dental caries.

As carriers of transporting drug molecules, AgNPs can reduce side effects and enhance therapeutic effects. In addition, the use of silver nanoparticles in conjunction with other antibiotics has a stronger antibacterial effect. Studies have reported that the combined use of AgNPs with chlorhexidine and metronidazole exhibits effective bacteriostatic and bactericidal properties (Nikita et al., 2019). However, before this, there were no reports of attaching chlorhexidine or metronidazole to the surface of AgNPs. To explore the possibility of using AgNPs as carriers for drugs such as chlorhexidine and metronidazole in treating oral bacterial infections like periodontitis and other diseases. Karol P. Steckiewicz et al. developed a new type of silver nanoparticles, which are combined with Chlorhexidine (AgNPs-CHL) and Metronidazole (AgNPs-PEG-MET) (Karol et al., 2022). These innovative compounds, whether it's AgNPs-CHL or AgNPs-PEG-MET, exhibit potent antibacterial, anti-biofilm, and anti-inflammatory properties. *In vitro* models assessing the safety of its potential clinical applications have demonstrated that these silver nanoparticles (AgNPs) exhibit low cytotoxicity at high concentrations; at non-toxic concentrations, they are harmless to mammalian cells. Importantly, findings suggest that AgNPs serve as effective drug delivery carriers for Chlorhexidine and Metronidazole. However, the exploration of AgNPs as carriers for Chlorhexidine or Metronidazole in the prevention and treatment of dental caries remains uncharted territory, presenting an exciting opportunity. The anticipation is high for future researchers to delve into this area, potentially paving the way for using silver nanoparticles as drug carriers in the fight against dental caries.

Besides serving as carriers, AgNPs also demonstrate potent antibacterial effects. AgNPs adhere to the cell wall and cytoplasmic membrane through electrostatic attraction and affinity with thiol proteins, and they can change the permeability and structure of bacterial cells. When AgNPs enter the cells, they inhibit respiratory enzymes, thereby generating reactive oxygen species, causing oxidative stress response, while also interfering with DNA and inhibiting protein synthesis, leading to changes in cell structure and cell death (Lakshmi et al., 2021). Research has also found that AgNPs can inhibit *S. mutans* and its biofilm, thus having a wide range of clinical applications in the prevention of dental caries (Mario Alberto et al., 2015), for example, adding silver nanoparticles to orthodontic brackets has satisfactory effects in inhibiting *S. mutans* and preventing enamel surface caries (Gamze et al., 2016).

2.8.2 Zinc nanoparticles and zinc oxide nanoparticles

In recent years, zinc nanoparticles have shown promising anti-tumor (Sumaira et al., 2021), antibacterial, and antiviral properties (Mahda Sadat et al., 2022), with their oxides, ZnONPs, demonstrating superiorities. Owing to their expanded specific surface area, potent antibacterial activity, and excellent biocompatibility, ZnONPs demonstrate significant benefits and are therefore extensively employed in a variety of applications, including dental implants, prosthetic joints, and cardiovascular implants (An overview on zinc-oxide nanoparticles as novel drug delivery system, 2023). In the field of drug delivery, ZnONPs are considered potential candidates for targeted drug delivery carriers. Literature has reported on ZnONPs coupled with arginine-glycine-aspartic acid (RGD) peptides, as well as ZnONPs loaded in the form of a metal-doxorubicin (DOX) complex, for targeted cancer therapy (Xiaoxin et al., 2019). However, no literature was retrieved on ZnONPs as drug carriers targeting the prevention and treatment of dental caries, so only the

role of ZnONPs as nano-drugs in inhibiting oral cariogenic bacteria and biofilms is introduced below. The mechanisms by which ZnONPs inhibit bacteria include the following: (1) Through the cell's oxidative stress response, harmful oxidizing compounds, specifically H_2O_2, are generated inside the cell body to exert activity. As the concentration of zinc oxide nanoparticles increases, the production of H_2O_2 increases, and the bactericidal effect is correspondingly enhanced. (2) ZnONPs counteract bacteria by releasing Zn^{2+} ions, and Zn^{2+} ions can destroy cell membranes and internal components of the cell. (3) The presence of negative charges on the surface of microorganisms, while metal oxides carry a positive charge, leading to electromagnetic attraction between microbes and zinc nanoparticles. If attraction occurs, the microorganisms are oxidized and die rapidly (Tahreem et al., 2022). One reason for the inhibition of *S. mutans* by ZnONPs is that ZnONPs can inhibit the biofilm of dental plaque, penetrate the biofilm, disperse with the matrix, both generate reactive oxygen species (ROS) and destroy membrane transport. Therefore, Hamad et al. explored the direct effects of ZnONPs on *S. mutans*, finding that they have high antibacterial activity against both Gram-positive and Gram-negative bacteria, and the excellent antibacterial activity of ZnONPs increases with their concentration (Fairoz Ali et al., 2022). In a series of clinical experiments, for example, zinc oxide nanoparticles incorporated into dental restorations can be used to control and prevent secondary caries (Arshad Mahdi and Qanat Mahmood, 2021). Malekhoseini et al. developed a resin-modified glass ion polymer containing ZnONPs to enhance its physical properties and antibacterial potential (Zahra et al., 2021). It has been reported that the addition of ZnONPs into composite resins found that 1% ZnNPs had no significant effect on the mechanical properties of the composite resin, and as the mass fraction increased to 5%, the number of *S. mutans* significantly decreased within one day (Zahra et al., 2021). These experiments suggest that zinc and its oxide nanoparticles can be used independently or in conjunction with other antimicrobial agents in resins or adhesives, and nanoparticles may gradually emerge as significant in future bonding or filling materials.

2.8.3 Titanium nanoparticles

Due to the high ratio of surface area to volume and high reactivity, nanoparticles have become effective antimicrobial agents. Among these, titanium nanoparticles are extensively utilized in the medical field owing to their excellent reflectivity, chemical stability, biocompatibility, bioactivity, and broad antimicrobial activity (Amir Hossein et al., 2021). In the field of dentistry, titanium dioxide nanoparticles are one of the titanium nanoparticles that have been extensively studied for caries prevention. Mohammed et al. incorporated TiO_2NPs into resin composites and adhesives to assess whether the addition of TiO_2NPs would enhance the antimicrobial activity of the composite materials (Wongchai et al., 2023). One month after the experiment started, plaque was collected from the gingival margin to determine the number of *S. mutans* in the plaque. It was found that the surface of restorations with added TiO_2NPs showed a significant reduction in plaque, especially when TiO_2NPs were added to both resin composites and adhesives. More notably, the antimicrobial activity increased over time. Additionally, incorporating antimicrobial agents such as silver and TiO_2NPs into orthodontic adhesives enhanced the antimicrobial performance against *S. mutans* and *Lactobacillus acidophilus* compared to commercially available fluoride-containing composites (Mohammed et al., 2018). Therefore, adding TiO_2NPs to dental restorative materials can strengthen their anti-caries effect. The combined use with other metal nanoparticles may achieve even more ideal antimicrobial effects. These nanoparticles may be used in the development of anti-caries restorative materials in the future. However, before this, adequate *in vivo* experiments are needed to evaluate the potential side effects of these metal nanoparticles and further optimize their physicochemical properties and biosafety.

2.9 Cell membrane-coated nanoparticle (CMCNP) technology combined with nanodrug delivery systems

Recently, cell membrane-coated nanoparticles (CMCNPs) have attracted widespread attention as a novel nanodelivery system. This technique involves encapsulating nanoparticles with cell membranes, almost completely preserving the complexity of the cell membrane on the surface of the particles. Therefore, CMCNPs not only possess the advantages of nanoparticles but also retain numerous functions of the source cell membrane, such as the ability to interact with other cells. Due to the unique physiological structure of cariogenic biofilms, the effectiveness of traditional nanosystems for drug delivery is limited, this method utilizes the natural functions of the cell membrane, allowing nanoparticles to demonstrate great potential in the diagnosis and treatment of various diseases (Mahendra et al., 2022). Members of our research group, Weng et al. inspired by cell coating technology and combining the ability of *Lactobacillus strains* to adhere to *S. mutans*, coated *Lactobacillus* (LA) cell membranes onto PLGA nanoparticles carrying Triclosan (TCS) (LA/TCS @ PLGA-NPs) (Zou et al., 2020). We discovered that this composite nanoparticle demonstrated good encapsulation, controllable size, negative charge, and sustained-release kinetics inheriting the natural characteristics of the original cell surface. As a result, LA/TCS @ PLGA-NPs could adhere to *S. mutans* and extend the drug release time, thereby continuously inhibiting the formation of *S. mutans* biofilm and having a lasting inhibitory effect on the progression of dental caries. Similarly, members of our subject matter team Ye et al. constructed a biomimetic oral mucosal adhesive drug delivery system, employing *Streptococcus salivarius* K12 membrane-coated TCS @ PLGA-NPs (Lu-Ting et al., 2022; Jiajia et al., 2023). This composite could adhere to the oral mucosal epithelium and promote the antibacterial action of TCS @ PLGA-NPs at the infection site, while the outer membrane of *Streptococcus salivarius* acted as a diffusion barrier for TCS release, extending the duration of drug action. These two studies by our research group, which combined cell coating technology with nanosystems for drug delivery, improved the precision of targeted drug delivery, facilitating more effective binding to the infection site and optimizing drug delivery, thereby boosting therapeutic effects. It

offers inspiration for combining nanodelivery systems with other technologies, presenting novel strategies for the future by inhibiting the formation of plaque biofilms or suppressing bacterial growth to prevent and treat dental caries (Table 1).

3 Remineralization

3.1 Nano - hydroxyapatite (nHAp)

Hydroxyapatite constitutes the main inorganic component of dental hard tissues. With the emergence of nanotechnology, the application of nHAp has become increasingly widespread due to its excellent mechanical, physical, and chemical properties. The nHAp has higher solubility and surface energy as well as better biocompatibility, and the morphology and structure of nHAp particles are similar to the hydroxyapatite crystals in teeth (Pushpalatha et al., 2023). Furthermore, as a biocompatible synthetic material, it can serve as a source of Ca^{2+} and PO_4^{3-} in the oral cavity, particularly under acidic conditions. Increasing the levels of Ca^{2+} and PO_4^{3-} can significantly limit the enamel damage caused by acids, thereby substantially enhancing the degree of remineralization (Aiswarya et al., 2022), with the effect of mitigating demineralization and fostering remineralization, with the effect of mitigating demineralization and fostering remineralization. The nHAp chemically combines with natural hydroxyapatite crystals to form a uniform hydroxyapatite layer on the surface of demineralized enamel, thus inducing remineralization. The hardness and elastic modulus of the repaired enamel are similar to those of natural enamel. Additionally, literature indicates that nHAp, due to its high surface energy, can strongly bind to the enamel surface and fill the gaps and micropores on the enamel surface to repair it (Nebu, 2018; Aref and Alsdrani, 2023). The literature indicates that nHAp can repair early enamel damage and has the potential to serve as an auxiliary repair material as well as prevent acid erosion damage, making it a safe and effective anticaries agent in oral care (Paszynska et al., 2023). Apa Juntavee first compared the effects of two concentrations of nanohydroxyapatite gel (NHG, 20% and 30%) with nHAp -containing toothpaste (NHT) and fluoride varnish (FV) in the remineralization of artificial carious lesions (Juntavee et al., 2021). Throughout the remineralization process, the microhardness of both the tooth surface and cross-sections was evaluated, and the depth of the caries was analyzed through polarized light microscopy photos. The research results indicate that the remineralization effect of nHAp toothpaste is superior to that of two types of nanohydroxyapatite gels, and the effects of both products containing nHAp exceed those of fluoride varnish. This also demonstrates that, whether in the form of toothpaste or gel, nanohydroxyapatite's ability to remineralize is better than fluoride.

To explore the effectiveness of toothpaste containing nHAp on a model of demineralized teeth within the body, Purva Verma et al. treated teeth that had undergone orthodontic bracket detachment (due to changes in surface demineralization) separately with fluoride toothpaste and nHAp toothpaste for 15 days (Verma and Muthuswamy Pandian, 2021). Subsequently, Atomic Force Microscopy was employed to analyze the surface roughness, which served as a measure to evaluate the remineralization potential of the toothpaste. It showed the hydroxyapatite nanoparticles are incorporated into oral care products to facilitate enamel remineralization through ion supersaturation at the site of lesions, a mechanism analogous to that of other calcium-based nanoparticles. Nonetheless, these nanoparticles enhance enamel regeneration by generating a biomimetic film that resembles biological hydroxyapatite, demonstrating greater efficacy in caries repair *in vitro* when compared to fluoride and casein nanoparticles. This phenomenon occurs because the remineralization layer exhibits resistance to abrasion due to the chemical bonds formed between the synthetic and natural crystals of the enamel, even in a potentially cariogenic environment characterized by a pH of 4.

In the future, as nanotechnology advances, the application of nHAP may expand to a broader range of caries prevention, remineralization, and restorative materials, making it an essential component of oral health maintenance. The incorporation of nHAP in oral care products is expected not only to enhance product performance but also to influence consumer choices regarding oral health products, driving the development of dental materials toward safer and more effective alternatives.

3.2 Nano-sized amorphous calciumphosphate Particle (NACP)

Calcium phosphate (CaP) is a substance containing Ca^{2+} and PO_4^{3-}, Amorphous calcium phosphate (ACP) is an intermediate phase formed during the precipitation process of CaP, and the natural solid form of ACP is usually composed of a group of ACP nanoparticles, with a specific surface area of about $300m^2/g$ (Sun et al., 2019). Therefore, materials containing ACP nanoparticles are highly regarded for their effect in promoting remineralization. In a comparative study conducted by Tao et al. on the impact of NACP-containing adhesives versus commercially available fluoride-releasing adhesives on dentin remineralization in a biofilm setting, it was observed that NACP exhibited bacterial inhibition in a simulated oral environment (Tao et al., 2019). Adhesives containing NACP, by releasing Ca^{2+} and PO_4^{3-}, contribute to tooth mineralization. A measurement of the Ca^{2+} and PO_4^{3-} content in the biofilm after 10 days indicated that the adhesive with NACP, through the release of these ions, not only increases the concentration of Ca^{2+} and PO_4^{3-} in the biofilm but also restores the hardness of the dentin and achieves the sealing of the dentinal tubules, thereby confirming its effectiveness in dentin remineralization. In contrast, commercial fluoride-releasing adhesives merely inhibit further demineralization. Similarly, Fan et al. evaluated the enamel remineralization effect in the oral biofilm environment by combining antimicrobial agents and remineralizers (Fan et al., 2022). They used NACP as the remineralizer and found that the PO_4^{3-} in NACP could react with H^+ in the biofilm, thereby stopping further pH value decrease. Adhesives containing NACP were able to effectively remineralize hard dental tissues, protect the adhesive interface, and inhibit secondary caries. Moreover, the study found that the release of Ca^{2+} and PO_4^{3-} from NACP alone might offer better localized acid production limiting capabilities than using the antimicrobial agent Dimethylaminohexadecyl methacrylate

TABLE 1 The studies that used nanodrug delivery systems for caries prevention and treatment.

Ways of Anti-caries	Nanosystems for drug delivery	Types of drug carried or Combination	Response	Modify Materials	Mechanism	conclusion	Model In Vivo/ Vitro Experiment	Ref
	Liposomes	Mag and FLC PPI、histatin-1、indocyanine green	Good affinity for Hydroxyapatite、Higher surface microhardness recovery	\	(1) Deliver and protect the drug	nano-encapsulated lactoferrin reduced the CFU of biofilm up to two logarithmi cycles.	Biofilm、synthetic and biological hydroxyapatite	Luo et al., 2023; Wang et al., 2018a; Wang et al., 2018b; Xiao et al., 2023
					(2) Fuse into the cell surface and release drug			
	poly-(lactic-co-glycolic acid) (PLGA)	Chlorhexidine、Chlorhexidine diacetate (CDA) and digluconate (CDG)	\	adhesive	protect drug from degradation and provide a sustained drug release profile	TEM confirmed successful tubular penetration and retention of Nano-PLGA/CHX nanoparticles inside the structure of dentinal-tubules.	micron-sizeddentinal-tubules under pulpal-pressure simulated	Priyadarshini et al., 2017; Francisco Fábio Oliveira de et al., 2021
	Mesoporous silica nanoparticles	L-arginine、Metal particle	\	adhesive	Being able to deliver L-arginine in a sustained way with a long-term antibacterial activity enough to selectively inhibit the growth of cariogenic bacteria such as *S. mutans* and *L. casei*	relative light units(RLUs) of *S. mutans* reduce	Biofilm of *S. mutans* and *L. casei*	Marta et al., 2022; Lu et al., 2018; Yuting et al., 2022?;
	poly (aminoamine) (PAMAM)	Honokiol、NGV peptides and galardin、	\	adhesive	Drug can be encapsulated within the PAMAM dendrimer or conjugated to surface groups	triclosan encapsulated in the formulation are able to release in a controlled manner	Artificial Saliva、Dentin disks	Tao et al., 2021; Tao et al., 2022; Menglin et al., 2020
	Chitosan	FNA、Amoxicillin、Cinnamaldehyde	\	\	As the carrier of drug with biocompatibilitybiodegradability and bioadhesivity	higher fluoride uptake ability and smooth releasing profile	In vitro characterization of nanoparticles	Jiang et al., 2024; Ran et al., 2023
Anti-biofilm	Polymeric micelles	tannic acid、NaF、DpSpSEEK	PH-sensitive	\	Solubilize drug and enhance its bioavailability	exerts effective antibacterial adhesion and cariogenic biofilm resistance	Both in vitro and in vivo	Xu et al., 2023
	silver nanoparticles	\		adhesive 、resin		Having Stronger inhibit caries and better in the dental remineralization ability	decayed	Karol et al., 2022
				Prosthetics-materials、commercial fluoride varnish、a pit and fissure sealant、			teeth in vivo	
					(1)increasing the absorbency of membrane			

(Continued)

10.3389/fcimb.2025.1546816

TABLE 1 Continued

Ways of Anti-caries	Nanosystems for drug delivery	Types of drug carried or Combination	Response	Modify Materials	Mechanism	conclusion	Model In Vivo/ Vitro Experiment	Ref
	Zinc oxide nanoparticles	\		Toothpastes、resin、adhesive、sealer	(2)Destroy the DNA, proteins, and lipids are among the bacterial components	zinc oxide have an excellent anti-bacterial benefit and it can be better by increasing the solution concentration that Contains the nanoparticles.	The transferred Staphylococcus and Streptococcus in Mannitol salt agar and MSB agar base	Tahreem et al., 2022; Fairoz Ali et al., 2022
			Oxidative stress		(3)cause bacterial cell death by inducing an oxidative stress response			
	Titanium Nanoparticles	\		adhesive 、resin		TiO2NPs enhanced the antibacterial activity	Teeth in vivo	Wongchai et al., 2023; Amir Hossein et al., 2021
	Nano-Hydroxyapatite	\	\	fluoride varnish、Toothpastes	nHA remineralizes the organic scaffold in the carious attack by directly replacing lost minerals or as a carrier for lost mineral ions and increasing the supply of calcium and phosphorus ions	Remineralising effects of NanoHAP dentifrice were found to be significantly superior to routine fluoridated dentifrice.	Teeth of therapeutic extraction for the orthodontic treatment in vivo	Verma and Muthuswamy Pandian, 2021; Juntavee et al., 2021
	Nano-sizedamorphous calciumphosphate Particle	Dimethylaminohexadecyl methacrylate (DMAHDM)	\	adhesive	Nanoparticles of amorphous calcium phosphate (NACP), able to discharge much more Ca and P by virtue of the tiny particle size and large surface area	NACP+DMAHDM release a great deal of Calcium and phosphate had the highest microhardness compared NACP+DMAHDM group	Artificial initial carious lesion in Bovine incisors	Fan et al., 2022
Remineralization								
	nano-sized calcium fluoride	DMAHDM	\	experimental resins monomers	The smaller particle size and higher surface area achieved with the use of nCaF2 enabled a higher level of F ion release	nCaF2+DMAHDM composite showed a significant fluoride ion concentration	dental plaque microcosm biofilm	Daixing et al., 2022
	Bioactive Glass Nanoparticles	Ag	\	\	Antibacterial:BG release ionic dissolution products leading to the damaging of bacterial cell wall by BG sharp debris	XRD characterization: hydroxy-carbonate apatite layer formation on their surfaces following the immersion in SBF	simulated body fluid	Kazemian et al., 2021
					Remineralization:Ca2+ and P2+ can combine in solution and deposit onto silanol bonds on the glass surface, nucleating a hydroxycarbonate apatite layer.			

10.3389/fcimb.2025.1546816

(DMAHDM) alone. These findings suggest that adding NACP to dental repair materials could effectively promote enamel adhesion, protect the adhesive interface, prevent caries, and extend the lifespan of composite materials, showing broad application prospects.

3.3 Nano-sized calcium fluoride (NCaF2)

NCaF2 has been proven to effectively prevent dental caries by increasing the fluoride concentration in oral saliva, which promotes the remineralization of teeth (Sun and Chow, 2008). Additionally, it can be used to reduce the permeability of dentin. Heba Mitwalli developed a novel composite material containing dimethylaminohexadecyl methacrylate (DMAHDM) and calcium fluoride nanoparticles (NCaF2), aimed at preventing the occurrence of secondary caries at the margins of restorations (Heba et al., 2020). This material inhibits bacterial growth through the antibacterial properties of DMAHDM and significantly releases fluoride and calcium ions through the inclusion of NCaF2. Fluoride ions, acting as transmembrane proton carriers and inhibitors of glycolytic enzymes, can stimulate cytoplasmic acidification, exerting antibacterial effects at a distance and thereby preventing the formation of caries (Daixing et al., 2022). Additionally, fluoride ions can also promote the formation of fluorapatite, enhancing the remineralization effect on teeth. This novel composite exhibits strong antibacterial and ion-release capabilities, preventing the continued production of lactic acid by biofilms and significantly reducing the number of *S. mutans* on the biofilm. This bioactive nanocomposite material holds promise as a new type of anticariogenic material that protects tooth structure, inhibits demineralization, and serves as a reservoir for the release of calcium and fluoride ions.

3.4 Bioactive glass nanoparticles (BGN)

Bioactive glass (BAG) is highly valued as a regenerative material due to its controllable degradability and ability to stimulate tissue formation. It can promote bone induction and thereby bone formation by releasing ionic products. With the combination of tissue engineering and nanoscience, nanomaterials capable of imitating the characteristics of host tissues, such as bioactive glass nanoparticles (BGN), have emerged. These can adjust their size according to the host's response to facilitate cellular absorption, allowing therapeutic ions to be released inside cells (Shalumon et al., 2013; Jones, 2015; Pajares-Chamorro and Chatzistavrou, 2020).In the field of dentistry, BGN, due to its controlled ion release capability, has been applied to the remineralization of enamel and dentin (Bakry et al., 2014). It composed of sodium-calcium-amorphous phosphate, reacts with H^+ upon contact with saliva, releasing Ca^{2+} and PO_4^{3-}, leading to an immediate increase in pH value, which promotes the deposition of calcium and phosphate, followed by the formation of a hydroxyapatite layer (Taha et al., 2017). Compared to BAG, BGN has a higher ion release capacity and bioactivity, therefore, it has a wide range of application prospects in the aspect of tooth remineralization.

Zahra Kazemian et al. have prepared BGN containing silver ions using the sol-gel method, which can change the pH value of the surrounding medium through ion release (Kazemian et al., 2021). The dissolution of BG leads to the supersaturation of calcium ions in simulated body fluid, and results in the formation of reprecipitation on its surface. These precipitates, rich in calcium and phosphorus crystals, have been verified by X-ray diffraction, confirming that the hydroxyapatite layer formed on the surface of Ag-BG after soaking in simulated body fluid. Furthermore, Akbarzadeh et al. synthesized a paste containing nano-sized bioactive glass (BGN) amorphous calcium phosphate casein phosphopeptide (CPP-ACP) paste, and compared its remineralization capability with that of fluoride-containing CPP-ACP paste and commercial products (Akbarzade et al., 2022). Observations through Vickers microhardness test and scanning electron microscope (SEM) revealed that both pastes could promote the remineralization of demineralized dental enamel. However, the enamel treated with the paste containing BGN showed stronger microhardness compared to that treated with the fluoride-containing CPP-ACP paste and commercial products. Although the remineralization effect of BGN is initially recognized, the potential of different types of bioactive glass (BGs) for remineralization *in vitro* and *in vivo* still requires further research.

In addition to Bioactive Glass Nanoparticles, Mesoporous Bioactive Nanoparticles (MBN) also receive considerable attention in the field of nanomedicine due to their ability to load and deliver biomolecules, along with their nanoscale and bioactive component features. For instance, in the study conducted by Jung-Hwan Lee et al., they developed a novel drug delivery system that utilizes BGN to load strontium ions (Sr^{2+}) and phenamil (Lee et al., 2017). Sr^{2+} can promote the differentiation of precursor cells or stem cells into osteogenic cells/cementoblast thereby stimulating the growth of these cells (Kruppke et al., 2019; Miyano et al., 2023).Sr^{2+} can interact with intracellular signaling molecules in the body, and they stimulate the repair of hard tissues through the BMP2/Smad signaling pathway; similarly, phenamil has also been proven to be a potent small molecule BMP signaling activator, which enhances BMP2/Smad when acting on osteoblasts cell or cementoblast (Park et al., 2009; Xu et al., 2020). During the experimental process, they observed the formation of poorly crystallized hydroxyapatite phase in the composite (Sr^{2+}/phenamil—MBN) on the third day of soaking in simulated body fluid, and the density increased with the soaking time. *In vivo* studies, they created a drill hole defect on the extracted tooth surface, filled the defect with Sr/phenamil MBN to make it contact with dental pulp tissue as much as possible and interact with mesenchymal stem cells (MSCs), and implanted it into the subcutaneous sites of rats. Six weeks later, three-dimensional constructions and two-dimensional projection images obtained by micro-CT revealed new hard tissue formation in the tooth drill hole defect area, and histological analysis also confirmed that the new tissue was bone or dentin. They achieved for the first time the co-delivery of ions and drug molecules on nanoparticles and successfully facilitated hard tissue regeneration, indicating that MBN loaded with strontium ions and phenamil is a highly potential drug delivery platform. BGN offers broad applications in tooth remineralization due to its high ion release and bioactivity, though further research is needed on various bioactive glasses (BGs). Mesoporous Bioactive Nanoparticles (MBNs) also attract

attention for drug delivery. The co-delivery method provides a new strategy for caries remineralization, suggesting innovative approaches in dental care.

4 Conclusion

In recent years, nanotechnology has increasingly attracted attention in the field of dentistry. The development of this technology has made it possible to prevent and treat oral diseases, especially dental caries, by designing and creating nanoscale drug delivery systems. These systems can directly deliver drugs to the lesion sites of teeth, effectively preventing and treating dental caries. Moreover, studies have shown that nanoscale drug delivery systems enhance the therapeutic effect of drugs by increasing their bioavailability, thus reducing the side effects of drugs to strengthen the treatment effect. Meanwhile, researchers are also exploring the remineralization potential of nanoparticles, intending to help repair teeth damaged by dental caries by mimicking the natural mineralization process of teeth.

Future research in nanomedicine for targeted therapy aims to achieve precise drug delivery to biofilm-infected sites using diverse nanoparticles, while safeguarding the physiological function of healthy cells. This encompasses the development of adaptive drug release mechanisms responsive to physiological changes. Concurrent efforts will prioritize the optimization of nanocarriers, exploring advanced biomaterials and stimuli-responsive nanomaterials, integrating functionalities such as drug delivery, therapeutics, and diagnostics. Crucially, expediting clinical translation is essential, involving scalable manufacturing, comprehensive safety evaluations, and the establishment of clear regulatory frameworks. Novel therapeutic paradigms, including the refinement of immunotherapies, gene therapy, RNAi therapies, and the development of antimicrobial agents combating resistance, will significantly benefit from nanotechnological advancements. Furthermore, the evolution of nanomedicine in medical imaging and diagnostics, specifically via highly sensitive imaging agents and disease biomarker sensors, promises to be transformative. Lastly, employing artificial intelligence and machine learning in nanomedicine design, data analysis, and virtual screening will accelerate the entire research and development process.

Despite notable progress in dental applications of nanotechnology, several pivotal research gaps remain. Currently, the field lacks standardized evaluation protocols to systematically assess the safety and efficacy of nanosystems for oral use, resulting in limited cross-study comparability. Establishing uniform standards is essential for accurately comparing and evaluating disparate materials and approaches. Furthermore, while some nanomaterials exhibit promising laboratory and small-scale trial results, their transition to clinical practice is hampered by various challenges. Comprehensive *in vivo* studies and larger clinical trials are crucial to refining these materials' physicochemical properties and confirming their biocompatibility. With robust clinical evidence, nanosystems can become integral to standard dental treatments, providing reliable solutions. The interaction between nanosystems and the oral microbiome is another under-researched domain. The oral microbial community's complexity means that nanomaterials may engage in intricate interactions with both beneficial and harmful bacteria, influencing ecological stability and balance. In-depth investigations into these dynamics are necessary for designing nanotechnologies that effectively regulate microbial communities while minimizing adverse effects. Lastly, advancements in biomaterials and nanotechnology have ushered in emerging trends such as smart drug delivery systems and biomimetic materials, offering prospects for personalized and adaptive therapies. Although in nascent stages, these innovative technologies hold the potential to revolutionize dental care paradigms. Continued basic research alongside applied development will be pivotal in advancing these transformative applications.

Author contributions

HD: Writing – original draft, Writing – review & editing. ZW: Writing – review & editing. SL: Writing – review & editing. YL: Writing – review & editing. DY: Writing – review & editing.

Funding

The author(s) declare that financial support was received for the research, authorship, and/or publication of this article. This work was supported by the National Natural Science Foundation of China (31970783 and 82301055), Joint Funds for Innovation and Development of the Natural Science Foundation of Chongqing (CSTB2022NSCQ-LZX0039), Major Technology Innovation Project of Chongqing Medical University and Program for Youth Innovation in Future Medicine from Chongqing Medical University (No. W0060), China Postdoctoral Science Foundation (2023M730439) and the Chongqing Postdoctoral Science Foundation (No. CSTB2023NSCQ-BHX0081).

Conflict of interest

The authors declare that the research was conducted in the absence of any commercial or financial relationships that could be construed as a potential conflict of interest.

Generative AI statement

The author(s) declare that no Generative AI was used in the creation of this manuscript.

Publisher's note

References

Abdullah, J. J., and Maha Abdul Kareem, M. (2023). Preparation and characterization of amoxicillin-loaded chitosan nanoparticles to enhance antibacterial activity against dental decay pathogens. *J. Emergency Med. Trauma Acute Care*. 2023 (3). doi: 10.5339/jemtac.2023.midc.10

Aiswarya, A., Wael, I., Abdullah, A. M., Reghunathan, S. P., and Sukumaran, A. (2022). Nano-hydroxyapatite (nHAp) in the remineralization of early dental caries: A scoping review. *Int. J. Environ. Res. Public Health*. 19 (9), 5629–5629. doi: 10.3390/ijerph19095629

Akbarzade, T., Farmany, A., Farhadian, M., Khamverdi, Z., and Dastgir, R. (2022). Synthesis and characterization of nano bioactive glass for improving enamel remineralization ability of casein phosphopeptide-amorphous calcium phosphate (CPP-ACP). *BMC Oral. Health* 22, 525. doi: 10.1186/s12903-022-02549-9

Amir Hossein, M., Mohammad Sadegh Ahmad, A., Shahzad, A., Yasamin Farajzadeh, J., and Leila, J. (2021). Effect of nano–zinc oxide and nano-chitosan particles on the shear bond strength of dental composites used as orthodontic adhesive. *J. World Fed. Orthodontists*. 10 (4), 172–176. doi: 10.1016/j.ejwf.2021.08.002

Ammar, T. Q. (2022). Silver nanoparticles as drug delivery systems. doi: 10.31390/gradschool_dissertations.1069

Annabi, N., Tamayol, A., Uquillas, J. A., Akbari, M., Bertassoni, L. E., Cha, C., et al. (2014). 25th anniversary article: Rational design and applications of hydrogels in regenerative medicine. *Adv. Mater.* 26, 85–123. doi: 10.1002/adma.201303233

Aref, N. S., and Alsdrani, R. M. (2023). Surface topography and spectrophotometric assessment of white spot lesions restored with nano-hydroxyapatite-containing universal adhesive resin: an *in-vitro* study. *BMC Oral. Health* 23, 911. doi: 10.1186/s12903-023-03642-3

Arshad Mahdi, H., and Qanat Mahmood, A. (2021). *In vitro* study of the effect of zinc oxide nanoparticles on Streptococcus mutans isolated from human dental caries. *J. Physics: Conf. Series*. 1879 (2), 022041–022041. doi: 10.1088/1742-6596/1879/2/022041

Ashwini, P., and Arpana, H. J. (2015). Rutin-chitosan nanoparticles: fabrication, characterization and application in dental disorders. *Polymer-plastics Technol. Eng.* 54 (2), 202–208. doi: 10.1080/03602559.2014.935425

Bakry, A. S., Marghalani, H. Y., Amin, O. A., and Tagami, J. (2014). The effect of a bioglass paste on enamel exposed to erosive challenge. *J. Dent.* 42, 1458–1463. doi: 10.1016/j.jdent.2014.05.014

Bernabe, E., Marcenes, W., Hernandez, C. R., Bailey, J., Abreu, L. G., Alipour, V., et al. (2020). Global, regional, and national levels and trends in burden of oral conditions from 1990 to 2017: A systematic analysis for the global burden of disease 2017 study. *J. Dent. Res.* 99, 362–373. doi: 10.1177/0022034520908533

Besinis, A., De Peralta, T., and Handy, R. D. (2014). The antibacterial effects of silver, titanium dioxide and silica dioxide nanoparticles compared to the dental disinfectant chlorhexidine on Streptococcus mutans using a suite of bioassays. *Nanotoxicology* 8, 1–16. doi: 10.3109/17435390.2012.742935

Bianca, D., Verónica, C.-R., María, V. R., and Miguel, M. (2023). Natural biopolymers as smart coating materials of mesoporous silica nanoparticles for drug delivery. *Pharmaceutics*. 15 (2), 447. doi: 10.3390/pharmaceutics15020447

Bowen, W. H., Burne, R. A., Wu, H., and Koo, H. (2018). Oral biofilms: pathogens, matrix, and polymicrobial interactions in microenvironments. *Trends Microbiol.* 26, 229–242. doi: 10.1016/j.tim.2017.09.008

Chih-Yu, C., and Ying-Chien, C. (2012). Antibacterial effect of water-soluble chitosan on representative dental pathogens Streptococcus mutans and Lactobacilli brevis. *J. Appl. Oral. Sci.* 20 (6), 620–627. doi: 10.1590/s1678-77572012000600006

Claudia Butrón-Téllez, G., Juan Francisco Hernández, S., DeAlba-Montero, I., Urbano-Peña, M. A., and Facundo, R. (2020). Therapeutic use of silver nanoparticles in the prevention and arrest of dental caries. *Bioinorganic Chem. Applications*. 2020, 1–7. doi: 10.1155/2020/8882930

Daixing, Z., Shuangting, L., Hongyang, Z., Ké, L., Yiwei, Z., Yingjie, Y., et al. (2022). Improving antibacterial performance of dental resin adhesive via co-incorporating fluoride and quaternary ammonium. *J. Dentistry*. 122, 104156–104156. doi: 10.1016/j.jdent.2022.104156

Degli Esposti, L., Ionescu, A. C., Brambilla, E., Tampieri, A., and Iafisco, M. (2020). Characterization of a toothpaste containing bioactive hydroxyapatites and *in vitro* evaluation of its efficacy to remineralize enamel and to occlude dentinal tubules. *Mater. (Basel)* 13 (13), 2928–2928. doi: 10.3390/ma13132928

Dongsheng, D., Liu, M. J., Cate, J., and Wim, C. (2007). The vicRK system of streptococcus mutans responds to oxidative stress. *J. Dental Res.* 86 (7), 606–610. doi: 10.1177/154405910708600705

Duhyeong, H., Jacob, D. R., and Alexander, V. K. (2020). Polymeric micelles for the delivery of poorly soluble drugs: From nanoformulation to clinical approval. *Advanced Drug Delivery Rev.* 156, 80–118. doi: 10.1016/j.addr.2020.09.009

Erika Kiyoko, C., André Luiz Fraga, B., Rodrigo Sversut de, A., Mariana Dias, M., Paulo Henrique dos, S., and Ticiane Cestari, F. (2020). Bond strength to dentin of low-shrinkage composite resin restorations after thermocycling and mechanical loading. *Arch. Health Invest.* 9 (6), 641–647. doi: 10.21270/archi.v9i6.4906

Fairoz Ali, A.-W., Adel, A.-G., Senthil Kumar, P., Efaq Ali, N., and Shaima Abdul, F. (2022). Nanoparticles approach to eradicate bacterial biofilm-related infections: A critical review. *Chemosphere*. 288, 132603–132603. doi: 10.1016/j.chemosphere.2021.132603

Fan, M., Li, M., Yang, Y., Weir, M. D., Liu, Y., Zhou, X., et al. (2022). Dual-functional adhesive containing amorphous calcium phosphate nanoparticles and dimethylaminohexadecyl methacrylate promoted enamel remineralization in a biofilm-challenged environment. *Dent. Mater.* 38, 1518–1531. doi: 10.1016/j.dental.2022.07.003

Francisco Fábio Oliveira de, S., Nojosa, J. S., Carlos Augusto, A., Alcantara, A. P. M. P., Raquel Silva, A., Mônica, Y., et al. (2021). Design and characterization of digluconate and diacetate chlorhexidine loaded-PLGA microparticles for dental applications. *J. Drug Delivery Sci. Technol.* 62, 102361–102361. doi: 10.1016/j.jddst.2021.102361

Gamze, M.-G., Levent, T., and Gülçin, A. (2016). Nanosilver coated orthodontic brackets:*in vivo*antibacterial properties and ion release. *Eur. J. Orthodontics*. 39 (1), 9–16. doi: 10.1093/ejo/cjv097

GBD 2015 Disease and Injury Incidence and Prevalence Collaborators. (2016). Global, regional, and national incidence, prevalence, and years lived with disability for 310 diseases and injuries 1990-2015: a systematic analysis for the Global Burden of Disease Study 2015. *Lancet* 388, 1545–1602. doi: 10.1016/s0140-6736(16)31678-6

GBD. (2023). An overview on zinc-oxide nanoparticles as novel drug delivery system. *Int. J. Biol. Pharm. Allied Sci.* 388, 1545–1602. doi: 10.31032/ijbpas/2023/12.1.6794

Habibi, P., Yazdi, F. T., Mortazavi, S. A., and Farajollahi, M. M. (2022). Effects of free and nano-encapsulated bovine lactoferrin on the viability and acid production by Streptococcus mutans biofilms. *Lett. Appl. Microbiol.* 75, 689–698. doi: 10.1111/lam.13796

Harrison, J. C., Jing, L., Preety, S., Joy, R. P., Gary, J. S., and Badyal, J. P. S. (2021). Bioinspired and eco-friendly high efficacy cinnamaldehyde antibacterial surfaces. *J. Mater. Chem. B.* 9 (12), 2918–2930. doi: 10.1039/d0tb02379e

Heba, M., Abdulrahman, A. B., Rashed, A., Thomas, W. O., Mary Anne, S. M., Hockin, H. K. X., et al. (2020). Novel caF2 nanocomposites with antibacterial function and fluoride and calcium ion release to inhibit oral biofilm and protect teeth. *J. Funct. Biomater.* 11 (3), 56–56. doi: 10.3390/jfb11030056

Hetrick, E. M., Shin, J. H., Paul, H. S., and Schoenfisch, M. H. (2009). Anti-biofilm efficacy of nitric oxide-releasing silica nanoparticles. *Biomaterials* 30, 2782–2789. doi: 10.1016/j.biomaterials.2009.01.052

Hu, Z., Tang, Y., Jiang, B., Xu, Y., Liu, S., and Huang, C. (2023). Functional liposome loaded curcumin for the treatment of Streptococcus mutans biofilm. *Front. Chem.* 11. doi: 10.3389/fchem.2023.1160521

Jeon, J. G., Pandit, S., Xiao, J., Gregoire, S., Falsetta, M. L., Klein, M. I., et al. (2011). Influences of trans-trans farnesol, a membrane-targeting sesquiterpenoid, on Streptococcus mutans physiology and survival within mixed-species oral biofilms. *Int. J. Oral. Sci.* 3, 98–106. doi: 10.4248/ijos11038

Jiajia, Y., Lei, W., Lizhao, W., Guo, R. S., Wei, W., Deqin, Y., et al. (2023). Antimicrobial effect of Streptococcus salivarius outer membrane-coated nanocomplexes against Candida albicans and oral candidiasis. *Mater. Design*. 233, 112177–112177. doi: 10.1016/j.matdes.2023.112177

Jiang, W., Peng, J., Jiang, N., Zhang, W., Liu, S., Li, J., et al. (2024). Chitosan phytate nanoparticles: A synergistic strategy for effective dental caries prevention. *ACS Nano* 18, 13528–13537. doi: 10.1021/acsnano.3c11806

Jiaojiao, Y., Shuqin, C., Jiahui, L., Jianyu, X., Xingyu, C., Wei, W., et al. (2013). Staged self-assembly of PAMAM dendrimers into macroscopic aggregates with a microribbon structure similar to that of amelogenin. *Soft Matter*. 9 (31), 7553–7553. doi: 10.1039/c3sm51510a

Jishuai, S., Xiaojing, L., Jiachen, Z., and Guanghua, Z. (2022). Bio-based antibacterial food packaging films and coatings containing cinnamaldehyde: A review. *Crit. Rev. Food Sci. Nutr.* 64 (1), 140–152. doi: 10.1080/10408398.2022.2105300

Jones, J. R. (2015). Reprint of: Review of bioactive glass: From Hench to hybrids. *Acta Biomater.* 23 Suppl, S53–S82. doi: 10.1016/j.actbio.2015.07.019

Jun, L. V., Jifang, S., Miaoquan, L., Yingyan, L., and Xihong, X. (2004). Effects of Magnolol and Honokiol on the activities of streptococcal glucosyltransferases both in solution and adsorbed on an experimental pellicle. *Lett. Appl. Microbiol.* 39 (5), 459–465. doi: 10.1111/j.1472-765x.2004.01610.x

Juntavee, A., Juntavee, N., and Sinagpulo, A. N. (2021). Nano-hydroxyapatite gel and its effects on remineralization of artificial carious lesions. *Int. J. Dent.* 2021, 7256056. doi: 10.1155/2021/7256056

Kamel, R. S., Nagwa, E.-D., Moataz, M. R., Ahmed, M. K., Izabela, J., and Maged, E. K. (2021). Chitosan based-nanoparticles and nanocapsules: Overview, physicochemical features, applications of a nanofibrous scaffold, and bioprinting. *Int. J. Biol. Macromol.* 167, 1176–1197. doi: 10.1016/j.ijbiomac.2020.11.072

Karol, P. S., Piotr, C., Ewelina, B., Maciej, J., Magdalena, N., Marta, B., et al. (2022). Silver nanoparticles as chlorhexidine and metronidazole drug delivery platforms: their potential use in treating periodontitis. *Int. J. Nanomed.* 17, 495–517. doi: 10.2147/ijn.s339046

Kazemian, Z., Varzandeh, M., and Labbaf, S. (2021). A facile synthesis of mono dispersed spherical silver doped bioactive glass nanoparticle. *J. Mater. Sci. Mater. Med.* 32, 29. doi: 10.1007/s10856-021-06496-9

Khizar, S., Alrushaid, N., Alam Khan, F., Zine, N., Jaffrezic-Renault, N., Errachid, A., et al. (2023). Nanocarriers based novel and effective drug delivery system. *Int. J. Pharm.* 632, 122570. doi: 10.1016/j.ijpharm.2022.122570

Komal Sadashiv, J. (2015). Mesoporous silica nanoparticles (MSN): A nanonetwork and hierarchical structure in drug delivery. *J. Nanomed. Res*. 2 (5). doi: 10.15406/jnmr.2015.02.00043

Kruppke, B., Wagner, A. S., Rohnke, M., Heinemann, C., Kreschel, C., Gebert, A., et al. (2019). Biomaterial based treatment of osteoclastic/osteoblastic cell imbalance - Gelatin-modified calcium/strontium phosphates. *Mater. Sci. Eng. C Mater. Biol. Appl.* 104, 109933. doi: 10.1016/j.msec.2019.109933

Lakshmi, T., Abdul Habeeb, A., Sohaib, A., Devaraj, E., Sreekanth Kumar, M., Rishitha, S., et al. (2021). Antimicrobial properties of silver nitrate nanoparticle and its application in endodontics and dentistry: A review of literature. *J. Nanomater.* 2021, 1–12. doi: 10.1155/2021/9132714

Lanlan, F., Huoxiang, Z., Long, C., Yiyi, W., Fei, L., and Suping, W. (2023). The application of mesoporous silica nanoparticles as a drug delivery vehicle in oral disease treatment. *Front. Cell. Infect. Microbiol.* 13. doi: 10.3389/fcimb.2023.1124411

Lee, J. H., Mandakhbayar, N., El-Fiqi, A., and Kim, H. W. (2017). Intracellular co-delivery of Sr ion and phenamil drug through mesoporous bioglass nanocarriers synergizes BMP signaling and tissue mineralization. *Acta Biomater.* 60, 93–108. doi: 10.1016/j.actbio.2017.07.021

Lei, L., Long, L., Xin, Y., Yang, Q., Yanglin, Z., Tao, H., et al. (2019). The vicRK two-component system regulates streptococcus mutans virulence. *Curr. Issues Mol. Biol.*, 167–200. doi: 10.21775/cimb.032.167

Leo, T., Merja, S., Timo, S., Olli, T., Markku, L., and Tuula, S. (1999). The effect of MMP inhibitor metastat on fissure caries progression in rats. *Ann. New York Acad. Sci.* 878 (1), 686–688. doi: 10.1111/j.1749-6632.1999.tb07762.x

Li, Z., Hai Ming, W., Yu Yuan, Z., and Quan Li, L. (2019). Constructing an antibiofouling and mineralizing bioactive tooth surface to protect against decay and promote self-healing. *ACS Appl. Mater. Interfaces*. 12 (2), 3021–3031. doi: 10.1021/acsami.9b19745

Li, X., Wong, C. H., Ng, T. W., Zhang, C. F., Leung, K. C., and Jin, L. (2016). The spherical nanoparticle-encapsulated chlorhexidine enhances anti-biofilm efficiency through an effective releasing mode and close microbial interactions. *Int. J. Nanomed.* 11, 2471–2480. doi: 10.2147/ijn.S105681

Liu, Y., Castro Bravo, K. M., and Liu, J. (2021). Targeted liposomal drug delivery: a nanoscience and biophysical perspective. *Nanoscale Horiz* 6, 78–94. doi: 10.1039/d0nh00605j

Lori, M. E. B., Mark, G., Morgan, A., Anil, K., Huzefa, H., Elizabeth, J. B., et al. (2022). Dual action nitric oxide and fluoride ion-releasing hydrogels for combating dental caries. *ACS Appl. Mater. Interfaces*. 14 (19), 21916–21930. doi: 10.1021/acsami.2c02301

Lu, M. M., Ge, Y., Qiu, J., Shao, D., Zhang, Y., Bai, J., et al. (2018). Redox/pH dual-controlled release of chlorhexidine and silver ions from biodegradable mesoporous silica nanoparticles against oral biofilms. *Int. J. Nanomed.* 13, 7697–7709. doi: 10.2147/ijn.S181168

Luby, B. M., Walsh, C. D., and Zheng, G. (2019). Advanced photosensitizer activation strategies for smarter photodynamic therapy beacons. *Angew Chem. Int. Ed Engl.* 58, 2558–2569. doi: 10.1002/anie.201805246

Luo, Z., Lin, Y., Zhou, X., Yang, L., Zhang, Z., Liu, Z., et al. (2023). Biomineral-binding liposomes with dual antibacterial effects for preventing and treating dental caries. *Biomater. Sci.* 11, 5984–6000. doi: 10.1039/d3bm00756a

Lu-Ting, W., Lei, W., Guo, R. S., Jiajia, Y., Lei, W., Wei, W., et al. (2022). Lactobacillus cell envelope-coated nanoparticles for antibiotic delivery against cariogenic biofilm and dental caries. *J. Nanobiotechnol.* 20 (1). doi: 10.1186/s12951-022-01563-x

Ma, S., Moser, D., Han, F., Leonhard, M., Schneider-Stickler, B., and Tan, Y. (2020). Preparation and antibiofilm studies of curcumin loaded chitosan nanoparticles against polymicrobial biofilms of Candida albicans and Staphylococcus aureus. *Carbohydr. Polym.* 241, 116254. doi: 10.1016/j.carbpol.2020.116254

Mahda Sadat, N., Razieh, G., Farzin, H., Mahdi Faal, M., Mohammad, M., and Donya, P. (2022). Zinc oxide nanoparticles as a potential agent for antiviral drug delivery development: A systematic literature review. *Curr. Nanosci.* 18 (2), 147–153. doi: 10.2174/1573413717666210618103632

Mahendra, T. V. D., Muddada, V., Gorantla, S., Karri, T., Mulakala, V., Prasad, R., et al. (2022). Evaluation of antibacterial properties and shear bond strength of orthodontic composites containing silver nanoparticles, titanium dioxide nanoparticles and fluoride: An *in vitro* study. *Dental Press J. Orthod.* 27, e222067. doi: 10.1590/2177-6709.27.5.e222067.oar

Marcelle, M. N., Liu, Y., Rosy, K., Shelbi, D. P., Akanji Musbau, A., Xin, X., et al. (2013). Oral arginine metabolism may decrease the risk for dental caries in children. *J. Dental Res.* 92 (7), 604–608. doi: 10.1177/0022034513487907

María, V. R., Ferdi, S., Daniel, L., Montserrat, C., and Miguel, M. (2022). Engineering mesoporous silica nanoparticles for drug delivery: where are we after two decades? *Chem. Soc. Rev.* 51 (13), 5365–5451. doi: 10.1039/d1cs00659b

Mario Alberto, P.-D., Laura, B., Garth, A. J., Cristina, V., Roberto, S.-S., Rita Elizabeth, M.-M., et al. (2015). Silver nanoparticles with antimicrobial activities against Streptococcus mutans and their cytotoxic effect. *Mater. Sci. Eng.: C.* 55, 360–366. doi: 10.1016/j.msec.2015.05.036

Mark, G., Morgan, A., Yun, Q., Megan, D., Elizabeth, J. B., and Hitesh, H. (2021). Nitric oxide and viral infection: Recent developments in antiviral therapies and platforms. *Appl. Mater. Today*. 22, 100887–100887. doi: 10.1016/j.apmt.2020.100887

Marsh, P. D. (2010). Controlling the oral biofilm with antimicrobials. *J. Dent.* 38 Suppl 1, S11–S15. doi: 10.1016/s0300-5712(10)70005-1

Marta, L.-R., Francisco, N., Paloma, F.-G., Samuel, M.-E., Victoria, F., Isabel, G., et al. (2022). L-arginine-containing mesoporous silica nanoparticles embedded in dental adhesive (Arg@MSN@DAdh) for targeting cariogenic bacteria. *J. Nanobiotechnol.* 20 (1). doi: 10.1186/s12951-022-01714-0

Menglin, F., Min, Z., Hockin, H. K. X., Tao, S., Zhaohan, Y., Jiaojiao, Y., et al. (2020). Remineralization effectiveness of the PAMAM dendrimer with different terminal groups on artificial initial enamel caries *in vitro*. *Dental Mater.* 36 (2), 210–220. doi: 10.1016/j.dental.2019.11.015

Mingzhen, T., Zhichao, M., and Guang-Zhong, Y. (2024). Micro/nanosystems for controllable drug delivery to the brain. *The Innovation*. 5 (1), 100548–100548. doi: 10.1016/j.xinn.2023.100548

Mirali, P., and Thomas, G. H. D. (2021). Amelogenesis: Transformation of a protein-mineral matrix into tooth enamel. *J. Struct. Biol.* 213 (4), 107809–107809. doi: 10.1016/j.jsb.2021.107809

Miyano, Y., Mikami, M., Katsuragi, H., and Shinkai, K. (2023). Effects of sr(2+), BO(3)(3-), and siO(3)(2-) on differentiation of human dental pulp stem cells into odontoblast-like cells. *Biol. Trace Elem. Res.* 201, 5585–5600. doi: 10.1007/s12011-023-03625-z

Mohammed, F. H., Maha, A. N., and Doaa, E.-S. (2018). The antibacterial activity of titanium dioxide nanoparticles incorporated into resin composite restoration (*In vivo* study). *Al-Azhar Dental J. Girls* 5 (2), 173–180. doi: 10.21608/adjg.2018.9528

Montserrat, C., and María, V. R. (2020). Targeted stimuli-responsive mesoporous silica nanoparticles for bacterial infection treatment. *Int. J. Mol. Sci.* 21 (22), 8605–8605. doi: 10.3390/ijms21228605

Murthy, S. K. (2007). Nanoparticles in modern medicine: state of the art and future challenges. *Int. J. Nanomed.* 2, 129–141.

Narmani, A., Jahedi, R., Bakhshian-Dehkordi, E., Ganji, S., Nemati, M., Ghahramani-Asl, R., et al. (2023). Biomedical applications of PLGA nanoparticles in nanomedicine: advances in drug delivery systems and cancer therapy. *Expert Opin. Drug Delivery* 20, 937–954. doi: 10.1080/17425247.2023.2223941

Nathan, S., Kimberly, M., Stanley, J. H., Megan, M., and Ryan, D. (2018). Nitric oxide-releasing macromolecule exhibits broad-spectrum antifungal activity and utility as a topical treatment for superficial fungal infections. *Antimicrobial Agents Chemother.* 62 (7). doi: 10.1128/aac.01026-17

Nebu, P. (2018). State of the art enamel remineralization systems: the next frontier in caries management. *Caries Res.* 53 (3), 284–295. doi: 10.1159/000493031

Nguyen, S., Hiorth, M., Rykke, M., and Smistad, G. (2011). The potential of liposomes as dental drug delivery systems. *Eur. J. Pharm. Biopharm.* 77, 75–83. doi: 10.1016/j.ejpb.2010.09.010

Nguyen, S., Solheim, L., Bye, R., Rykke, M., Hiorth, M., and Smistad, G. (2010). The influence of liposomal formulation factors on the interactions between liposomes and hydroxyapatite. *Colloids Surf B Biointerfaces* 76, 354–361. doi: 10.1016/j.colsurfb.2009.11.020

Nikita, P. P., Prasanna, T. D., Yogesh, J. K., Mahesh, V. D., Shrikant, B. K., Ayesha, G. S., et al. (2019). *In vitro* evaluation of antimicrobial property of silver nanoparticles and chlorhexidine against five different oral pathogenic bacteria. *Saudi Dental J.* 31 (1), 76–83. doi: 10.1016/j.sdentj.2018.10.004

Noronha, V. T., Paula, A. J., Durán, G., Galembeck, A., Cogo-Müller, K., Franz-Montan, M., et al. (2017). Silver nanoparticles in dentistry. *Dent. Mater.* 33, 1110–1126. doi: 10.1016/j.dental.2017.07.002

Pajares-Chamorro, N., and Chatzistavrou, X. (2020). Bioactive glass nanoparticles for tissue regeneration. *ACS Omega* 5, 12716–12726. doi: 10.1021/acsomega.0c00180

Park, K. W., Waki, H., Kim, W. K., Davies, B. S., Young, S. G., Parhami, F., et al. (2009). The small molecule phenamil induces osteoblast differentiation and mineralization. *Mol. Cell Biol.* 29, 3905–3914. doi: 10.1128/mcb.00002-09

Parmanand, A., Veronika, K., Bhavitavya, N., Enriqueta Martínez, R., Piyasuda, P., Daniel, J. I., et al. (2023). Hydrogel-encapsulated biofilm inhibitors abrogate the cariogenic activity of streptococcus mutans. *J. Medicinal Chem.* 66 (12), 7909–7925. doi: 10.1021/acs.jmedchem.3c00272

Paszynska, E., Pawinska, M., Enax, J., Meyer, F., Schulze Zur Wiesche, E., May, T. W., et al. (2023). Caries-preventing effect of a hydroxyapatite-toothpaste in adults: a 18-month double-blinded randomized clinical trial. *Front. Public Health* 11. doi: 10.3389/fpubh.2023.1199728

Payal, K., Akansha, B., Amit, A., Vivek, S. D., and Swapnil, S. (2021). Biomedical applications of hydrogels in drug delivery system: An update. *J. Drug Delivery Sci. Technol.* 66, 102914–102914. doi: 10.1016/j.jddst.2021.102914

Pitts, N. B., Zero, D. T., Marsh, P. D., Ekstrand, K., Weintraub, J. A., Ramos-Gomez, F., et al. (2017). Dental caries. *Nat. Rev. Dis. Primers* 3, 17030. doi: 10.1038/nrdp.2017.30

Priyadarshini, B. M., Mitali, K., Lu, T. B., Handral, H. K., Dubey, N., and Fawzy, A. S. (2017). PLGA nanoparticles as chlorhexidine-delivery carrier to resin-dentin adhesive interface. *Dent. Mater.* 33, 830–846. doi: 10.1016/j.dental.2017.04.015

Pushpalatha, C., Gayathri, V. S., Sowmya, S. V., Dominic, A., Ahmed, A., Bassam, Z., et al. (2023). Nanohydroxyapatite in dentistry: A comprehensive review. *Saudi Dental J.* 35 (6), 741–752. doi: 10.1016/j.sdentj.2023.05.018

Qian, R., Zhongcheng, L., Lei, D., Xiuqing, W., Yumei, N., Xi Feng, Q., et al. (2018). Anti-biofilm and remineralization effects of chitosan hydrogel containing amelogenin-derived peptide on initial caries lesions. *Regenerative Biomater.* 5 (2), 69–76. doi: 10.1093/rb/rby005

Qiao, L., Yang, H., Gao, S., Li, L., Fu, X., and Wei, Q. (2022). Research progress on self-assembled nanodrug delivery systems. *J. Mater. Chem. B* 10, 1908–1922. doi: 10.1039/d1tb02470a

Qichao, R., and Janet, M. O. (2015). Amelogenin and enamel biomimetics. *J. Mater. Chem. B.* 3 (16), 3112–3129. doi: 10.1039/c5tb00163c

Ran, M., Hanyi, Z., Zhiyuan, Z., Xinyue, L., Jiaxuan, J., Xinyue, W., et al. (2023). Trans-cinnamaldehyde loaded chitosan based nanocapsules display antibacterial and antibiofilm effects against cavity-causing Streptococcus mutans. *J. Oral. Microbiol.* 15 (1). doi: 10.1080/20002297.2023.2243067

Renugalakshmi, A., Vinothkumar, T. S., and Kandaswamy, D. (2011). Nanodrug delivery systems in dentistry: a review on current status and future perspectives. *Curr. Drug Delivery* 8, 586–594. doi: 10.2174/156720111796642336

Selwitz, R. H., Ismail, A. I., and Pitts, N. B. (2007). Dental caries. *Lancet* 369, 51–59. doi: 10.1016/s0140-6736(07)60031-2

Senadheera, M. D., Guggenheim, B., Spatafora, G. A., Huang, Y. C., Choi, J., Hung, D. C., et al. (2005). A VicRK signal transduction system in Streptococcus mutans affects gtfBCD, gbpB, and ftf expression, biofilm formation, and genetic competence development. *J. Bacteriol.* 187, 4064–4076. doi: 10.1128/jb.187.12.4064-4076.2005

Sevda, Ş., Eda Ayşe, A., and Gülçin, A. (2019). Application of chitosan based scaffolds for drug delivery and tissue engineering in dentistry. *Springer Ser. Biomater. Sci. Eng.*, 157–178. doi: 10.1007/978-981-13-8855-2_8

Shalumon, K. T., Sowmya, S., Sathish, D., Chennazhi, K. P., Nair, S. V., and Jayakumar, R. (2013). Effect of incorporation of nanoscale bioactive glass and hydroxyapatite in PCL/chitosan nanofibers for bone and periodontal tissue engineering. *J. BioMed. Nanotechnol.* 9, 430–440. doi: 10.1166/jbn.2013.1559

Shelyn Akari, Y., Juliana Jendiroba, F., Nicolle San Nicolas Dubrull, L., Franciana Berzoti, R., Hiroe, O., and Regina Guenka, P. D. (2022). Effect of an experimental chitosan/casein gel on demineralized enamel under a cariogenic challenge. *Dental Med. Problems.* 59 (4), 531–538. doi: 10.17219/dmp/146038

Sili, H., Yingying, F., Zhen, Z., Huanxin, T., Danxue, L., Xuebin, L., et al. (2017). Promotion of enamel caries remineralization by an amelogenin-derived peptide in a rat model. *Arch. Oral. Biol.* 73, 66–71. doi: 10.1016/j.archoralbio.2016.09.009

Sims, K. R., Liu, Y., Hwang, G., Jung, H. I., Koo, H., and Benoit, D. S. W. (2018). Enhanced design and formulation of nanoparticles for anti-biofilm drug delivery. *Nanoscale* 11, 219–236. doi: 10.1039/c8nr05784b

Somaye, R., Kasra, A., Hossein, T., Maryam Alsadat, H., Mohammad Saeid, E., Hadis, F., et al. (2021). Chitosan-based nanoparticles against bacterial infections. *Carbohydr. Polymers.* 251, 117108–117108. doi: 10.1016/j.carbpol.2020.117108

Spartak, Y. (2020). Effects of cinnamon (Cinnamomum spp.) in dentistry: A review. *Molecules.* 25 (18), 4184–4184. doi: 10.3390/molecules25184184

Suguna, P., Raji, A., and Wonmok, L. (2022). A review of polymeric micelles and their applications. *Polymers.* 14 (12), 2510–2510. doi: 10.3390/polym14122510

Sumaira, A., Mariam, H., Sara Asad, M., Khan, M. Z. H., José, M. L., Bilal Haider, A., et al. (2021). Recent advances in zinc oxide nanoparticles (ZnO NPs) for cancer diagnosis, target drug delivery, and treatment. *Cancers.* 13 (18), 4570–4570. doi: 10.3390/cancers13184570

Sun, R., Åhlén, M., Tai, C. W., Bajnóczi É, G., Kleijne, F., Ferraz, N., et al. (2019). Highly porous amorphous calcium phosphate for drug delivery and bio-medical applications. *Nanomater. (Basel)* 10. doi: 10.3390/nano10010020

Sun, L., and Chow, L. C. (2008). Preparation and properties of nano-sized calcium fluoride for dental applications. *Dent. Mater.* 24, 111–116. doi: 10.1016/j.dental.2007.03.003

Taha, A. A., Patel, M. P., Hill, R. G., and Fleming, P. S. (2017). The effect of bioactive glasses on enamel remineralization: A systematic review. *J. Dent.* 67, 9–17. doi: 10.1016/j.jdent.2017.09.007

Tahreem, T., Nosheen Fatima, R., Iqra, S., Iqra, S., Sultan, M. A., Hanadi, A. A., et al. (2022). Dental composites with magnesium doped zinc oxide nanoparticles prevent secondary caries in the alloxan-induced diabetic model. *Int. J. Mol. Sci.* 23 (24), 15926–15926. doi: 10.3390/ijms232415926

Tao, S., He, L., Xu, H. H. K., Weir, M. D., Fan, M., Yu, Z., et al. (2019). Dentin remineralization via adhesive containing amorphous calcium phosphate nanoparticles in a biofilm-challenged environment. *J. Dent.* 89, 103193. doi: 10.1016/j.jdent.2019.103193

Tao, S., Jiaojiao, Y., Zhiwei, S., Fengjuan, Z., Ziyou, W., Yingming, Y., et al. (2022). A dentin biomimetic remineralization material with an ability to stabilize collagen. *Small.* 18 (38). doi: 10.1002/smll.202203644

Tao, S., Yang, X., Liao, L., Yang, J., Liang, K., Zeng, S., et al. (2021). A novel anticaries agent, honokiol-loaded poly(amido amine) dendrimer, for simultaneous long-term antibacterial treatment and remineralization of demineralized enamel. *Dent. Mater.* 37, 1337–1349. doi: 10.1016/j.dental.2021.06.003

Torchilin, V. P. (2014). Multifunctional, stimuli-sensitive nanoparticulate systems for drug delivery. *Nat. Rev. Drug Discovery* 13, 813–827. doi: 10.1038/nrd4333

Verma, P., and Muthuswamy Pandian, S. (2021). Bionic effects of nano hydroxyapatite dentifrice on demineralised surface of enamel post orthodontic debonding: *in-vivo* split mouth study. *Prog. Orthod.* 22, 39. doi: 10.1186/s40510-021-00381-5

Vlachopoulos, A., Karlioti, G., Balla, E., Daniilidis, V., Kalamas, T., Stefanidou, M., et al. (2022). Poly(Lactic acid)-based microparticles for drug delivery applications: an overview of recent advances. *Pharmaceutics* 14. doi: 10.3390/pharmaceutics14020359

Wang, K., Wang, Y., Wang, X., Ren, Q., Han, S., Ding, L., et al. (2018b). Comparative salivary proteomics analysis of children with and without dental caries using the iTRAQ/MRM approach. *J. Transl. Med.* 16, 11. doi: 10.1186/s12967-018-1388-8

Wang, K., Wang, X., Zheng, S., Niu, Y., Zheng, W., Qin, X., et al. (2018a). iTRAQ-based quantitative analysis of age-specific variations in salivary proteome of caries-susceptible individuals. *J. Transl. Med.* 16, 293. doi: 10.1186/s12967-018-1669-2

Wongchai, A., On-Uma, R., Kumchai, J., Saleh, H. S., Sulaiman Ali, A., Deepika, J., et al. (2023). Antibacterial, antifungal, antidiabetic, and antioxidant activities potential of Coleus aromaticus synthesized titanium dioxide nanoparticles. *Environ. Res.* 216, 114714–114714. doi: 10.1016/j.envres.2022.114714

Xiao, L., Feng, M., Chen, C., Xiao, Q., Cui, Y., and Zhang, Y. (2023). Microenvironment-regulating drug delivery nanoparticles for treating and preventing typical biofilm-induced oral diseases. *Adv. Mater.*, e2304982. doi: 10.1002/adma.202304982

Xiaoxin, Y., Chuang, Z., Anxia, L., Jie, W., and Xiulan, C. (2019). Red fluorescent ZnO nanoparticle grafted with polyglycerol and conjugated RGD peptide as drug delivery vehicles for efficient target cancer therapy. *Mater. Sci. Eng.: C.* 95, 104–113. doi: 10.1016/j.msec.2018.10.066

Xu, C., Yadong, Z., Jianyun, W., Chengcheng, H., Yudong, W., Hongsheng, Y., et al. (2020). Strontium modulates osteogenic activity of bone cement composed of bioactive borosilicate glass particles by activating Wnt/β-catenin signaling pathway. *Bioactive Mater.* 5 (2), 334–347. doi: 10.1016/j.bioactmat.2020.02.016

Xu, Y., You, Y., Yi, L., Wu, X., Zhao, Y., Yu, J., et al. (2023). Dental plaque-inspired versatile nanosystem for caries prevention and tooth restoration. *Bioact Mater.* 20, 418–433. doi: 10.1016/j.bioactmat.2022.06.010

Xuebin, L., Yang, Y., Sili, H., Danxue, L., Huanxin, T., Wei, L., et al. (2015). Potential of an amelogenin based peptide in promoting reminerlization of initial enamel caries. *Arch. Oral. Biol.* 60 (10), 1482–1487. doi: 10.1016/j.archoralbio.2015.07.010

Ya, S., Sonja, S., and Markus, H. (2011). Antimicrobial Efficacy of Chlorhexidine against Bacteria in Biofilms at Different Stages of Development. *J. Endodontics.* 37 (5), 657–661. doi: 10.1016/j.joen.2011.02.007

Yi, Y., Wang, L., Chen, L., Lin, Y., Luo, Z., Chen, Z., et al. (2020). Farnesal-loaded pH-sensitive polymeric micelles provided effective prevention and treatment on dental caries. *J. Nanobiotechnol.* 18, 89. doi: 10.1186/s12951-020-00633-2

Yinglan, Y., Daquan, C., Yanan, L., Wenqian, Y., Jiasheng, T., and Yan, S. (2018). Improving the topical ocular pharmacokinetics of lyophilized cyclosporine A-loaded micelles: formulation, *in vitro* and *in vivo* studies. *Drug Delivery.* 25 (1), 888–899. doi: 10.1080/10717544.2018.1458923

Yuting, S., Hong, C., Meng-Meng, X., Liwen, H., Hongchen, M., Shiyao, Y., et al. (2023). Exopolysaccharides metabolism and cariogenesis of Streptococcus mutans biofilm regulated by antisense vicK RNA. *J. Oral. Microbiol.* 15 (1). doi: 10.1080/20002297.2023.2204250

Yuting, T., Yue, Z., Mengjiao, Z., Xianchun, C., Lei, L., and Tao, H. (2022). Antisense vicR-loaded dendritic mesoporous silica nanoparticles regulate the biofilm organization and cariogenicity of streptococcus mutans. *Int. J. Nanomed.* 17, 1255–1272. doi: 10.2147/ijn.s334785

Zahra, K., Fatemeh, F., Salman, K., and Maryam, A. (2020). Efficacy of chitosan-based chewing gum on reducing salivary S. mutans counts and salivary pH: a randomised clinical trial. *Acta Odontologica Scandinavica.* 79 (4), 268–274. doi: 10.1080/00016357.2020.1836392

Zahra, M., Rezvani, M., Mohammad, N., Mohammad, A., Mahshid Mohammadi, B., Hamid Safar, A., et al. (2021). Effect of zinc oxide nanoparticles on physical and antimicrobial properties of resin-modified glass ionomer cement. *Dental Res. J.* 18 (1), 73–73. doi: 10.4103/1735-3327.326646

Zhang, Y., Chen, Y., Liu, Z., Peng, X., Lu, J., Wang, K., et al. (2023). Encapsulation of a novel peptide derived from histatin-1 in liposomes against initial enamel caries *in vitro* and in *vivo*. *Clin. Oral. Investig.* 28, 35. doi: 10.1007/s00784-023-05465-6

Zhang, J. S., Chu, C. H., and Yu, O. Y. (2022). Oral microbiome and dental caries development. *Dent. J. (Basel)* 10. doi: 10.3390/dj10100184

Zou, S., Wang, B., Wang, C., Wang, Q., and Zhang, L. (2020). Cell membrane-coated nanoparticles: research advances. *Nanomed. (Lond)* 15, 625–641. doi: 10.2217/nnm-2019-0388

frontiers | Frontiers in Cellular and Infection Microbiology

TYPE Original Research
PUBLISHED 11 March 2025
DOI 10.3389/fcimb.2025.1535539

OPEN ACCESS

EDITED BY
Keke Zhang,
Wenzhou Medical University, China

REVIEWED BY
Wei Qiu,
Southern Medical University, China
Yujie Zhou,
Sichuan University, China

*CORRESPONDENCE
Chengyue Wang
wangcy@jzmu.edu.cn
Lihong Qiu
lhqiu@cmu.edu.cn

RECEIVED 27 November 2024
ACCEPTED 14 January 2025
PUBLISHED 11 March 2025

CITATION
Ma N, Yang W, Chen B, Bao M, Li Y, Wang M, Yang X, Liu J, Wang C and Qiu L (2025) Exploration of the primary antibiofilm substance and mechanism employed by *Lactobacillus salivarius* ATCC 11741 to inhibit biofilm of *Streptococcus mutans*. *Front. Cell. Infect. Microbiol.* 15:1535539. doi: 10.3389/fcimb.2025.1535539

Exploration of the primary antibiofilm substance and mechanism employed by *Lactobacillus salivarius* ATCC 11741 to inhibit biofilm of *Streptococcus mutans*

Nan Ma[1,2], Wei Yang[2,3], Bairu Chen[2,4], Meihua Bao[2,4], Yimin Li[2,4], Meng Wang[2,4], Xiaopeng Yang[3,2], Junyi Liu[5], Chengyue Wang[2,4]* and Lihong Qiu[6]*

[1]Department of Periodontics, Affiliated Stomatology Hospital of Jinzhou Medical University, Jinzhou, China, [2]Collaborative Innovation Center for Health Promotion of Children and Adolescents of Jinzhou Medical University, Jinzhou, China, [3]Department of Pedodontics, Affiliated Stomatology Hospital of Jinzhou Medical University, Jinzhou, China, [4]Department of Prosthetics, Affiliated Stomatology Hospital of Jinzhou Medical University, Jinzhou, China, [5]Jinzhou Medical University, Jinzhou, China, [6]Department of Endodontics, School and Hospital of Stomatology, China Medical University, Liaoning Provincial Key Laboratory of Oral Diseases, Shenyang, China

Introduction: *Lactobacillus salivarius* serves as a probiotic potentially capable of preventing dental caries both *in vitro* and *in vivo*. This study focused on understanding the key antibiofilm agents and the mechanisms of action of the *Lactobacilli* supernatant against *Streptococcus mutans*.

Methods: *Streptococcus mutans* biofilm was constructed and the cell-free supernatant of *Lactobacillus salivarius* was added. After the biofilm was collected, RNA-seq and qRT-PCR were then performed to get gene information. The influence of temperature, pH and other factors on the supernatant were measured and non-targeted metabolome analysis was performed to analyze the effective components.

Results: The findings indicated that the supernatant derived from *Lactobacillus salivarius* could inhibit the biofilm formation of *Streptococcus* mutans at different times. Through transcriptome analysis, we discovered that the cell-free supernatant reduced biofilm formation, by suppressing phosphoenolpyruvate-dependent phosphotransferase systems along with two ATP-binding cassette transporters, rather than directly affecting the genes that code for glucosyltransferases; additionally, the supernatant was observed to diminish the expression of genes linked to two-component systems, polyketides/non-ribosomal peptides, acid stress response, quorum sensing, and exopolysaccharide formation. Non-targeted LC-MS/MS analysis was employed to discover a variety of potential active compounds present in the cellular filtrate of *Lactobacillus salivarius* that hinder the growth of S. mutans, including phenyllactic acid, sorbitol, and honokiol.

Discussion: In summary, our findings support the evaluation of *Lactobacillus salivarius* as a promising oral probiotic aimed at hindering the formation of biofilms by cariogenic pathogens and the development of dental caries.

KEYWORDS

Streptococcus mutans*, transcriptomics, metabolomics, biofilm, dental caries, *Lactobacillus salivarius

1 Introduction

Oral health is intricately connected to overall wellbeing. The World Health Organization explicitly identifies oral health as one of the 10 essential components of human health. Dental caries is a common oral condition that poses significant risks to public health. Its condition is a chronic and progressive disease that stems from dental plaques housing cariogenic microorganisms and characterized by demineralization of inorganic substance and decomposition of organics (Lin et al., 2022).

Streptococcus mutans is a type of Gram-positive bacterium known for its strong ability to metabolize sucrose, generate acids, and contribute to the formation of cariogenic organisms. It is the main colonizing bacteria in the beginning stage of biofilm formation, which is regarded as the main pathogen of dental caries (Li et al., 2020). Long seen as a common pathogen within the oral microbiome, *S. mutans* was confirmed to be a pivotal microorganism implicated in the progression of dental caries, which utilizes sucrose to produce acid rapidly, creating a local low pH environment to assist the colonization of other cariogenic bacteria, forming a cariogenic biofilm that ultimately generates tooth decay (Wasfi et al., 2012; Liu et al., 2021). Cariogenic biofilm is a highly dynamic and structured microbial community, covered by the extracellular polymeric substance (EPS) matrix on its surface, which comprises various polymers such as extracellular polysaccharides, proteins, and nucleic acids (Gao et al., 2023). The function of EPS in promoting biofilm formation is mainly through the following aspects: adhesion, intercellular aggregation, biofilm cohesion, barrier protection, and nutrient support (Simon-Soro and Mira, 2015). This complex three-dimensional biofilm structure creates a unique microenvironment that shields microbes from environmental stressors, such as host immune responses and pharmaceuticals, while also preventing the dissemination of acids that can result in enamel demineralization and subsequently promote the development of tooth decay (He et al., 2016). Meanwhile, the biofilm structure hinders the penetration of drugs, making it difficult for conventional antibacterial agents to exert their effects (Cugini et al., 2019).

Traditional preventive and therapeutic strategies for dental caries primarily involve mechanical interventions, antibiotics, natural plant extract therapy, and the administration of fluoride (Alshahrani and Gregory, 2020; Sun et al., 2021). However, each of these methods has its limitations (Guo et al., 2015). Mechanical therapy is limited by human will and the effect is superficial. Numerous antibiotics may disrupt the natural balance of the bacterial community, which can lead to enhanced resistance among pathogenic bacteria. Moreover, excessive fluorine usage may result in chronic fluorosis. Consequently, seeking more efficient, quick, and safe approaches to inhibit bacterial biofilm formation is essential.

Probiotics, defined as live microorganisms, are known to offer health advantages to hosts when consumed in appropriate quantities (Yeun and Lee, 2015). Currently, *Lactobacillus* is the most studied and applied probiotics. Long-term studies found that *Lactobacillus* could prevent caries by producing metabolites including lactic acid, peroxide, bacteriocin, and proteinaceous compounds, impeding adhesion and colonization, and being effective in downregulating the expressions of virulence genes linked to biofilm formation (Wasfi et al., 2018; Zhao et al., 2023; Zhang et al., 2024).

The cell-free supernatant (CFS) of microbial culture medium is the metabolites produced during microbial growth and residual nutrients in the culture medium. Studies have shown that substances that exert an antibacterial effect in the CFS include lactic acid, acetic acid, hydrogen peroxide, long-chain fatty acids and their esters, and protein compounds (van Zyl et al., 2020; Mani-Lopez et al., 2022). It was reported that the CFS of *Lactobacillus rhamnosus* contained small cyclic peptides that could inhibit the biofilm formation of *S. mutans* (Niranjan et al., 2024).

Lactobacillus salivarius is commonly found in human saliva, characterized by its ability to generate organic acids through carbohydrate fermentation, which inhibits the proliferation of surrounding microbes (Kõll-Klais et al., 2005). Because of this antagonistic property, numerous studies have revealed that they could be used to treat periodontal disease and peri-implant diseases, control body weight, and improve the host immunity (Mulla et al., 2021; Chen et al., 2022).

The limited number of studies about the specific mechanism of the probiotic *L. salivarius* against *S. mutans* in cariogenic biofilms prompted us to address this problem. Therefore, this article aimed to evaluate the influence of the *L. salivarius* ATCC11741 supernatant on cariogenic biofilms, explore the potential mechanisms through the supernatant that may intervene in cariogenic biofilms, analyze the functional

substances of the supernatant, and evaluate the effect of anti-caries in animal models.

2 Materials and methods

2.1 Bacterial strains and culture conditions

Strains of *S. mutans* (ATCC 25175) and *L. salivarius* (ATCC 11741) were sourced from the China General Microbiological Culture Collection Center (CGMCC; Beijing, China). *L. salivarius* was grown in de Man–Rogosa–Sharpe (MRS) broth and *S. mutans* was cultured with brain–heart infusion (BHI) broth at 37°C under aerobic and microaerophilic conditions, with all strains stored in the broth containing 30% glycerol at −80°C routinely and were subsequently incubated on appropriate agar plates for 24 h, followed by 2% (v/v) inoculation in the relevant broth at 37°C for an additional 18 h before experimental use.

2.2 Preparation of cell-free supernatant

The CFS of *L. salivarius* was manufactured following a modified protocol established by Liang (Liang et al., 2023). In summary, *L. salivarius* was regulated to a concentration of 1×10^7 CFU/mL during the late logarithmic growth phase and subsequently incubated for 24 h at 37°C. After the bacterial culture, the spent culture underwent centrifugation (5,000×*g*, 10 min, 4°C), and the obtained supernatant was further filtered with a 0.22-μm filter to acquire the CFS.

2.3 Biofilm formation assay

An overnight culture of *S. mutans* was diluted to a predetermined final concentration of 1.0×10^6 CFU/mL in BHI broth enriched with 1% sucrose. This diluted culture was then dispensed into a 96-well microtiter plate at a volume of 200 μL, either with or without the increase of CFS, and incubated for 24 h. The final CFS concentrations, both treated and untreated, ranged from 12.5% to 100% (v/v). For different time treatment, a certain amount of CFS was added into the 96-well microtiter plate at 0, 6, and 12 h, respectively, at 37°C for 24 h. The method of mediating the biofilm by CFS at 24 h was as follows: 200 μL of suspension of *S. mutans* was added to each well of a 96-well plate and then cultured for 24 h, the biofilm was washed with phosphate-buffered saline (PBS) two times, and then 100 μL of CFS was added and the culture was continued for another 24 h. A crystal violet staining assay was conducted to evaluate how effectively the CFS inhibited biofilm formation by *S. mutans* (Wasfi et al., 2018). Specifically, after removing the culture supernatant, the biofilm was washed with PBS and fixed in methanol for 30 min. Afterward, the wells were stained with 0.1% crystal violet solution for 30 min, and then dissolved in 33% glacial acetic acid over 30 min until fully solubilized. Finally, optical densities were recorded at 575 nm using a microplate reader (the amount of biofilm formation). As a negative control, CFS was replaced by MRS broth.

2.4 Biofilm microstructure observed using scanning electron microscopy

An overnight culture of *S. mutans* was maintained in BHI broth and subsequently diluted to 1.0×10^7 CFU/mL (with 1% sucrose). A sterile cover slide was placed into the wells of a 24-well plate. In each well, 800 μL of the *S. mutans* suspension was combined with 160 μL of CFS or MRS broth and incubated under anaerobic conditions for 24 h. The cover slides were carefully rinsed three times using PBS, fixed, and prepared for scanning electron microscopy (SEM) observation (Hitachi, SU8100) following an established protocol (Liu et al., 2021).

2.5 Fluorescence staining for observing the proportion of live and dead bacteria in biofilm

Suspensions (1.75 mL) and 350 μL of CFS were added into the confocal dishes and cultured at 37°C for 24 h. The biofilm was subjected to staining for 30 min and subsequently observed using a confocal laser scanning microscope (CLSM) according to the BBcell Probe™ live/dead bacterial staining kit. In the control conditions, MRS broth served as a substitute for the CFS.

2.6 Physical and chemical properties of active components in CFS

2.6.1 Temperature stability

The CFS was treated at 50°C, 60°C, 70°C, 80°C, 90°C, and 100°C for 30 min in a dry thermostatic metal bath, respectively. The activity of inhibiting biofilm formation mediated by these CFSs was compared.

2.6.2 pH and enzymatic stability

The pH of the supernatant was adjusted to 6.5 using 1 mol/L NaOH, maintained for 1 h, and then readjusted to the initial pH value (3.9) with 1 mol/L HCl. In addition, 5 mg/mL of catalase and 1 mg/mL of proteinase K (Solarbio, Beijing, China) were added to the CFS for enzymatic stability. Untreated CFS was used as control.

2.6.3 Non-targeted metabolome analysis

CFS and MRS culture medium were respectively divided into six biological replicates for LC-MS analysis conducted by Majorbio (Majorbio Biotech Co., Ltd., Shanghai, China) for non-targeted metabolomic evaluation, in accordance with the method depicted in the literature with minor modifications (Hou et al., 2021). A volume of 200 μL of the sample underwent ultrasonication and was obtained using 800 μL of mixture of methanol and acetonitrile (1:1, v/v) that contained an internal standard and subjected to ultrasonication at 40 kHz (5°C, 30 min). The samples were frozen at −20°C for half an hour, centrifuged for 15 min, and then evaporated with a stream of N2 gas. The resultant samples were reconstituted in 120 μL of an acetonitrile:water solution (1:1, v/v) and were

ultrasonicated again at 40 kHz (5°C, 10 min). After being centrifugated at 13,000×*g* (4°C, 10 min), we transferred the obtained supernatants into sample bottles in preparation for subsequent LC-MS/MS analysis. Furthermore, to maintain analytic stability, quality control (QC) samples were created by merging 20 µL of specimen from every sample.

The analysis was conducted via LC-MS/MS utilizing the UHPLC-Q Exactive HF-X system (Thermo Fisher, Waltham, MA, USA). Progenesis QI v3.0 was employed for processing the raw data (Waters Corporation, Milford, USA). To enhance the distinctions among the groups and identify variables of class separation, a supervised clustering method known as partial least squares discriminant analysis (PLS-DA) was implemented. We calculated variable importance in the projection (VIP) values to demonstrate the roles of different variables within the PLS-DA model. The metabolites were annotated according to KEGG for the analysis of metabolic pathways as well as for the classification of compounds. The differential metabolites were categorized using the HMDB database. A difference in metabolite production between the two groups was considered significant if $p < 0.05$ and VIP > 1.

2.7 Transcriptome analysis by RNA-seq

S. mutans were cultured statically in six-well polystyrene plates for 24 h, allowing loosely attached bacterial cells to be gently rinsed off and then the biofilms were scraped off and approximately 50 mg of biofilm mass was collected by centrifugation and frozen at −80°C until used. Library construction, sequencing, and analysis services were provided by GENEWIZ Life Sciences (Suzhou, China). Each group for transcriptomics had three replicates. The data presented in the study are deposited in the NCBI repository, accession number PRJNA1219341.

2.8 Total bacterial RNA extraction and quantitative real-time polymerase chain reaction

The biofilm formation assay adopted the same preparation as before. Following incubation, the culture suspension from the wells was discarded. The plate wells underwent two washes with sterile saline, after which biofilm was scraped and suspended in saline for transfer to a centrifuge tube. The RNAprep pure Cell/Bacteria Kit (Tiangen Biotech; Beijing; China) was used for total RNA extraction according to the instructions of this kit. RNA concentration and purity were assessed using the ND-1000 spectrophotometer. Primer [Sangon Biotech Company (Shanghai, China)] sequences are listed in Table 1. The RNA was reversely transcribed into cDNA with the NovoScript Plus All-in-one 1st Strand cDNA Synthesis SuperMix (gDNA Purge) kit (Novoprotein, E047, Suzhou, China), subsequently utilizing the NovoStart SYBR qPCR SuperMix Plus reagent (Novoprotein, E096, Suzhou, China). The internal reference was 16S rRNA. The gene transcription level was evaluated using the $2^{-\Delta\Delta CT}$ methodology.

TABLE 1 The table of primer sequences.

Primers	Sequences (5′–3′)
16S rRNA	F: CCTACGGGAGGCAGCAGTAG R: CAACAGAGCTTTACGATCCGAAA
LrgB	F: GGCAAAAGGATTGGGAACTGATG R: TGGAACGGCAAAGGCAATGG
DexA	F: AGGGCTGACTGCTTCTGGAGT R: AGTGCCAAGACTGACGCTTTG
Ldh	F: TCCTGTTGGAGGTGGCATTC R: TGCTGTACCCGCATTCCATT

2.9 Inhibitory effect of *L. salivarius* on *S. mutans* virulence *in vivo*

2.9.1 Animals and general procedures

The design of animal experiments was similar to the description by previous literature (Zhang et al., 2020). The flowchart of the animal model is shown in Figure 1A. Male SPF Sprague–Dawley rats (18 days old) were bought from the Jinzhou Medical University experiment animal center. The experiment received approval from the school's Animal Protection and Institutional Committee (approval number: 230078) in accordance with the national animal protection guidelines. All laboratory animals were operated on under anesthesia and all efforts were made to reduce pain, suffering, and mortality. A total of four groups of rats ($n = 3$) were randomly assigned, including two treatment groups (*L. salivarius* suspension and CFS), as well as the caries-free and caries model groups. The rats in the caries-free group were given normal diet and distilled water during the whole experiment. Other groups were offered a cariogenic diet 2000 (obtained from Jiangsu Xietong Pharmaceutical Bio-engineering Co., Ltd.) and water containing 5% sucrose. To suppress the oral bacteria group, 0.5 µg/mL of ampicillin and 200 µg/mL of streptomycin were administered for 3 days prior to modeling. Over a period of 5 days starting at the experiment's commencement, three groups of rats used for caries modeling were infected with *S. mutans*. This was achieved by saturating sterile cotton swabs with 1 mL of an *S. mutans* culture (10^8 CFU/mL) and applying the suspension into each quadrant of the rat's mouth for 15 s. After the application of the tooth coating, dietary and water access was restricted for 2 h to facilitate the colonization of the microorganisms. At the age of 27, 100 µL of saliva was collected and coated on a plate for culture for detecting the colonization of *S. mutans* and recording the colony-forming units (CFU) for verifying the establishment of tested strains. The treatment groups were then administered 1 mL of *L. salivarius* suspension or CFS one time per day until the experiment's conclusion (from days 28 to 63). The rats' weights were recorded weekly, and the weight gain was calculated.

2.9.2 Micro-CT analysis

After successful modeling, SD rats were euthanized. All the mandibles were harvested, fixed with 4% paraformaldehyde, and then imaged with a VENUS Micro CT instrument (Kunshan,

10.3389/fcimb.2025.1535539

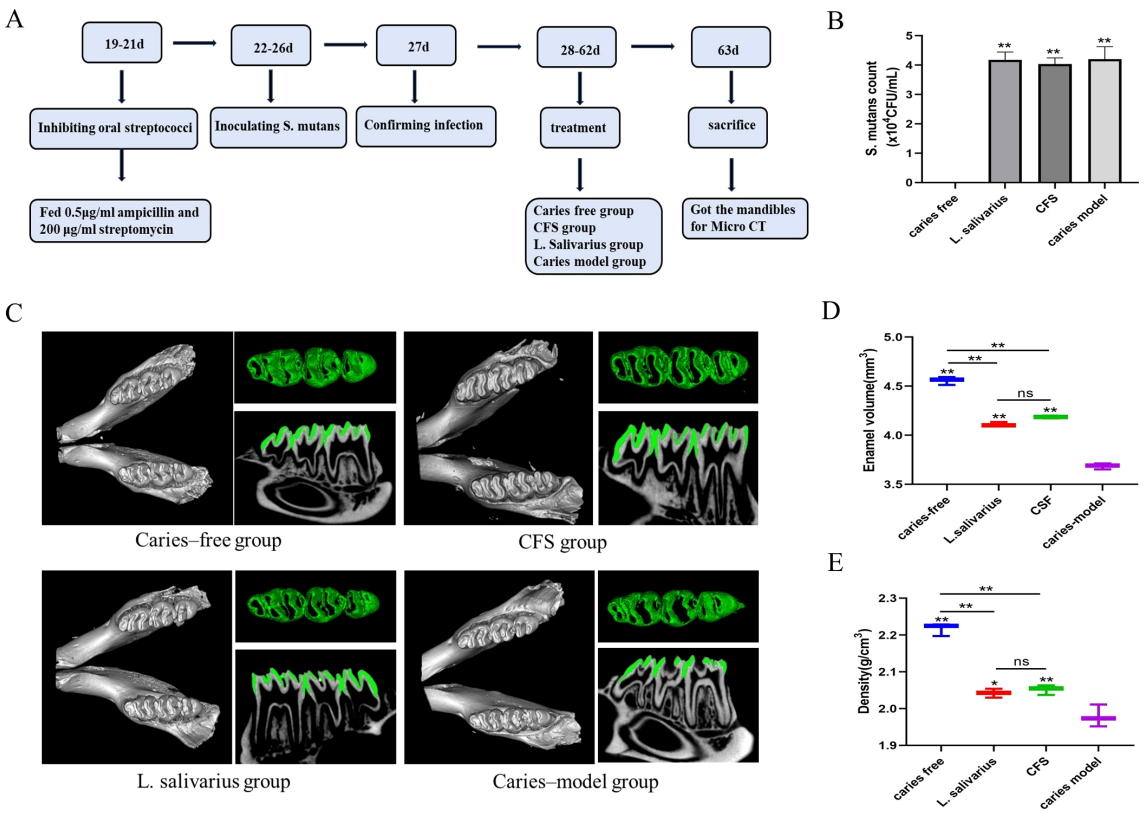

FIGURE 1
Flowchart of animal model **(A)**. *S. mutans* count from different treatment groups **(B)** ,$^{**}p < 0.01$ significantly different from the caries free group. Data were expressed as mean ± standard error of the mean ($n = 3$). 3D micro-CT image of mandibular molars, separated enamel (green), and corresponding 2D scale sagittal slice of the same molar (enamel is green) in each group **(C)**. Volume of enamel of mandibular molars **(D)** $^{**}p < 0.01$ significantly different from the caries-model group; ns, not significant. Density of enamel of mandibular molars **(E)**, $^{*}p < 0.05$, $^{**}p < 0.01$ significantly different from the caries-model group; ns, not significant.

China). 3D pictures were created utilizing AVATAR 1.5.0 software. The enamel was separated from the mandible with fixed thresholds and the mineral density and volume of the enamel were evaluated after correction for hydroxyapatite criteria.

2.10 Statistical analysis

Each experiment was performed three times, and all results were expressed as mean ± standard deviation. One-way analysis of variance (ANOVA) was used for statistical analysis along with Dunnett's test through GraphPad Prism version 8.0.1. Subsequently, all pairs of mean comparisons were assessed using the *post-hoc* Tukey method. $p < 0.05$ was considered statistically significant, while $p < 0.01$ was considered highly statistically significant.

3 Results

3.1 Antibiofilm effect of CFS of *L. salivarius* against *S. mutans*

As illustrated in Figure 2A, all CFSs at varying concentrations demonstrated efficacy in suppressing the biofilm formation of *S. mutans*. Specifically, CFS could inhibit 99% of *S. mutans* biofilm formation when used at concentrations of 50% (v/v). When the CFS was diluted to the concentration of 25%, the effect of biofilm formation decreased to 93.4% ($p < 0.05$). As the CFS was diluted to 12.5%, the inhibition decreased to 28.6% ($p < 0.01$).

The biofilm formation process included four essential time points: 0 h, where bacteria initially adhered; 6 h, marking the initial colonization of bacteria; 12 h, indicating early biofilm development; and 24 h, reflecting mature biofilm formation. As Figure 2B shows, the amount of biofilm mediated by each time point decreased significantly ($p < 0.01$); the 24-h-mediated biofilm showed a certain reduction in biofilm volume compared with the 24-h control biofilm ($p < 0.01$). The results showed that the CFS of *L. salivarius* had a strong inhibitory effect in the early stage of biofilm formation, but had a slightly destructive effect on middle and mature stage of biofilm formation.

At a dilution of 16.7% for the CFS, the SEM micrograph presented in Figure 2C demonstrated that a compact biofilm typical for *S. mutans* displayed a network-like composition identified as EPS. However, the biofilm architecture of *S. mutans* added with CFS appeared significantly more dispersed, exhibiting fewer micro-colonies on the surface compared to that of *S. mutans* alone, with a decrease in the quantity of EPS. Biofilms were created in the presence of CFS following 24 h of cultivation and analyzed by

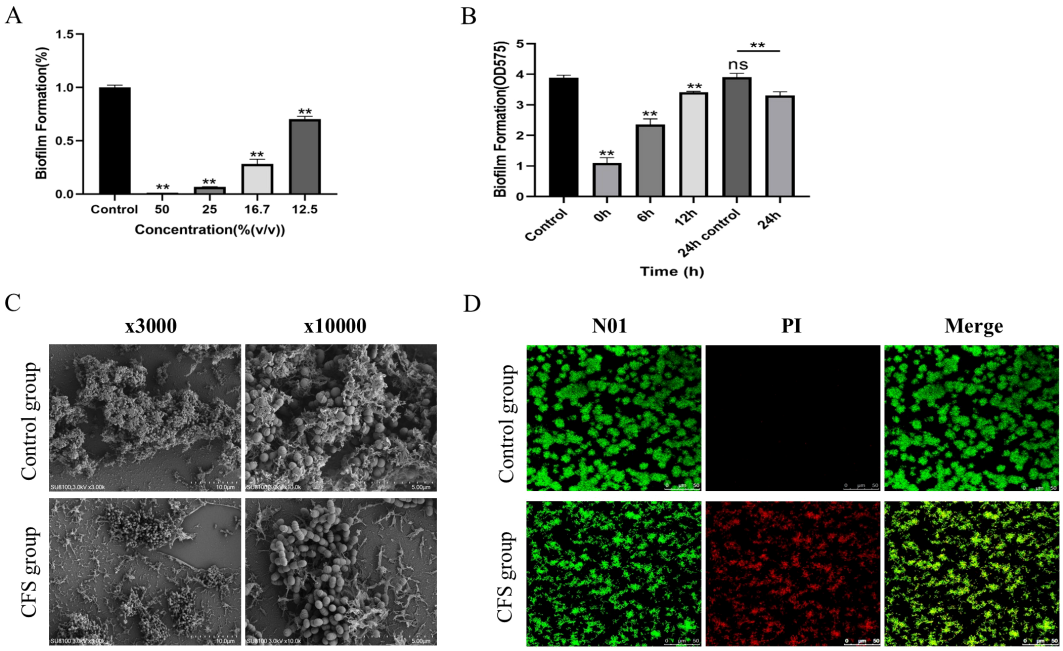

FIGURE 2
Antibiofilm effect of CFS against *S. mutans* **(A)**. Biomass of the biofilm mediated by CFS at different times **(B)**. The data are presented as the means ± SD. $^{**}p < 0.01$, compared with the control group; ns, not significant. Effect of CSF on the structure of *Streptococcus mutans* biofilm **(C)**. Effect of CSF on the activity of *Streptococcus mutans* biofilm **(D)**. Red, non-viable cells; green, viable cells; yellow, overlap of non-viable and viable cells. Bar = 50 μm.

a confocal laser scanning microscope (Figure 2D). The images demonstrate fluorescence intensities in green (live bacteria) and red (dead bacteria). The control group revealed that the biofilm was distributed uniformly, accompanied by a comparatively dense structure and total surface coverage. As shown in the CFS treatment group, the biofilms seemed significantly more dispersed and notably looser. The surface area that the biofilm occupied decreased because of CFS, leading to a marked reduction of biofilm biomass.

3.2 Analysis of antibiofilm components in CFS

Literature indicated that the antimicrobial components found in the CFS from *Lactobacillus* consist of organic acids, hydrogen peroxide, and bacteriocin (Vahedi Shahandashti et al., 2016; Liu et al., 2020). Bacteriocin is a protein synthesized by ribosomes, a metabolite secreted by bacteria during their reproductive process, possessing antibacterial properties (Kumariya et al., 2019). To preliminarily investigate the characteristics of the primary antibacterial agent, three portions of CFS were exposed to catalase and proteinase K, and pH was adjusted to neutral levels. After being treated with catalase and proteinase K, *S. mutans* showed a reduced but not lost antibiofilm effect. These findings suggested that hydrogen peroxide and a protein-like substance could serve as the principal antibiofilm agent in the CFS of *L. salivarius*. Additionally, this research revealed that the pH of the obtained CFS measured at 3.9. After adjusting the pH to 6.5, the CFS lost its antibiofilm capability; meanwhile, when the pH returned to the original value, the antibiofilm effect of CFS had not been fully restored (Figure 3A). As a result, we conducted further examinations to identify the main antibiofilm constituents of CFS. After the CFS was treated at different temperatures, there were no notable changes in its ability to inhibit biofilm formation. Even after 30-min treatment at 100°C, it still had the effect of inhibiting biofilm, and interestingly, it was slightly increased compared to that without treatment after 80°C (Figure 3B). This indicates that the active components of the CFS were thermally stable.

To analyze the effective components of CFS that enforce antibacterial properties, the extracellular metabolite profiles were compared between MRS and CFS through metabolomic analysis following a 24-h incubation period. The principal component analysis (PCA) and PLS-DA models highlighted significant metabolite differences between the two sample groups, all within the 95% confidence interval (Figures 3C, D). In the presence of the CFS, 436 metabolites were upregulated, while 694 were downregulated ($p < 0.05$, VIP > 1) compared with those in the presence of MRS broth (Figure 3E). There was a significant difference between the fermentation broths before and after cultivation, indicating that effective substances that may inhibit biofilm formation have been produced during the fermentation process. The VIP plots (Figure 3F) indicated that certain identified metabolites contributed to class differentiation. KEGG compound analysis of the upregulated metabolites was conducted, mainly including fatty acids, amino acids, nucleotides, and carboxylic acids (Figure 3G). The upregulated metabolites predominantly included various compounds including organic acids and derivatives, lipids

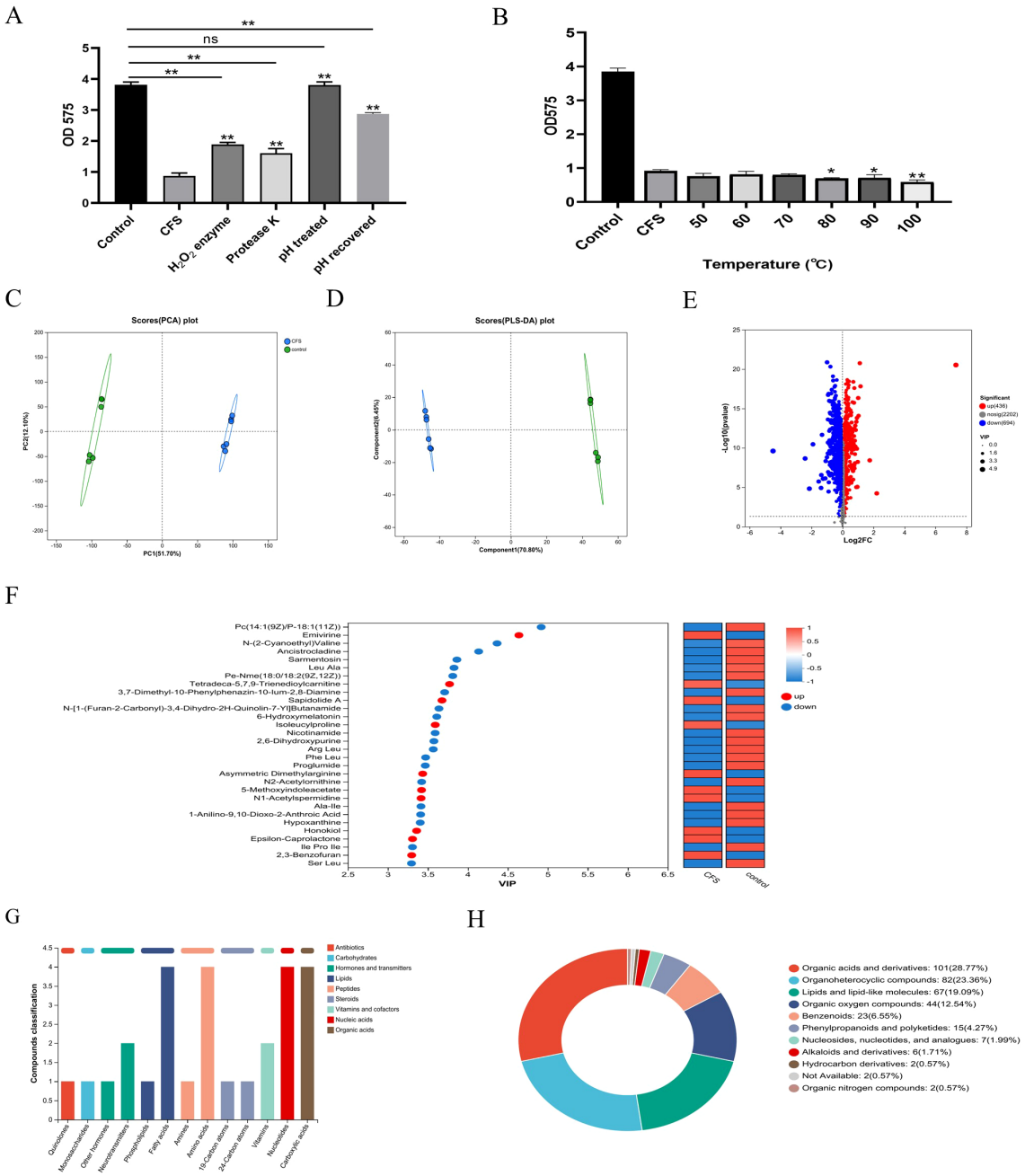

FIGURE 3
The inhibition effect on the biofilm of the CFS after different treatments. pH and enzyme **(A)** and temperature **(B)**. *$p < 0.05$, **$p < 0.01$ significantly different from the control group; ns, not significant. The metabolites in the CFS group compared to those in the control group. Principal component analysis (PCA) score plot of metabolite profiles from the treated and control groups **(C)**. Partial least squares discriminant analysis (PLS-DA) score plot of metabolite **(D)**. Volcano plot of the metabolites from CFS and control **(E)**. Variable importance for the projection (VIP) score calculated by PLS-DA **(F)**. KEGG compound analyses of upregulated metabolites **(G)**. HMDB compound classification diagram **(H)**.

and lipid-like substances, organoheterocyclic entities, organic oxygen compounds, and benzenoids were produced, as indicated by the HMDB compound classification analysis (Figure 3H). This section explored the characteristics of the effective components in CFS, which were thermally stable and possible protein and hydrogen peroxide-like substances and have a relatively narrow pH tolerance range, possibly being a type of organic acid or a substance that functions under acidic conditions. Furthermore, by combining with the non-targeted metabolomics method based on LC-MS to identify the differential metabolites between the CFS and the initial culture medium, we found that they were mainly fatty acids, amino acids, nucleotides, and carboxylic acids.

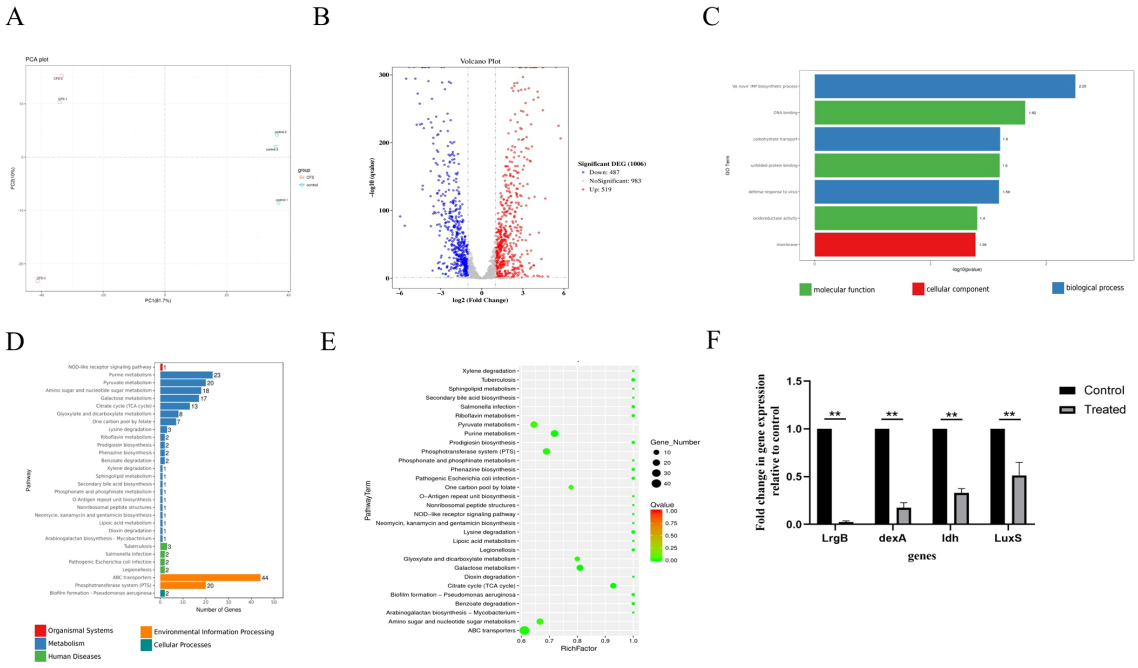

FIGURE 4
Effects of CFS through RNA-Seq analysis in *S. mutans* biofilms. Principal component analysis (PCA) score plot from the treated and control groups **(A)**. Volcano plot illustrating genes with significant expression differences of *S. mutans* biofilms in the CFS group **(B)**. GO annotation analysis of differentially expressed genes **(C)**. KEGG pathway analysis of differentially expressed genes **(D)**. KEGG rich analysis of differentially expressed genes **(E)**. Validation of differentially expressed genes using qRT-PCR **(F)** $^{**}p < 0.01$ significantly different from the control group. Fold change = $2^{-\Delta\Delta CT}$. Fold change >1 indicates upregulation, <1 indicates downregulation.

3.3 Transcriptome analysis by RNA-seq and analysis of qRT-PCR results

Given that CFS led to notable inhibition of biofilm formation by *S. mutans*, we conducted transcriptome analysis on both *S. mutans* treated with CFS and those under control conditions to monitor genome-wide gene expression alterations caused by CFS.

PCA showed that all biological replicates clustered closely, suggesting that gene expression underwent significant alteration due to CFS treatment compared to untreated controls, accounting for the 81.7% variance observed in the overall dataset (Figure 4A). The differentially expressed genes (DEGs) were identified using a modified *p*-value threshold of < 0.01 observed through the control and CFS groups. As depicted in the volcano plot and heatmap in

TABLE 2 Differentially expressed genes in *S. mutans* upon CFS treatment related to PTSs.

Gene ID	Gene name	log2FoldChange	Gene product description
gene-D820_RS08610	D820_RS08610	−4.35039416	Metal ABC transporter ATP-binding protein
gene-D820_RS08600	D820_RS08600	−5.299646868	Metal ABC transporter substrate-binding protein
gene-D820_RS08605	D820_RS08605	−4.680503916	Metal ABC transporter permease
gene-D820_RS02670	D820_RS02670	−3.320788871	Extracellular solute-binding protein
gene-D820_RS04680	D820_RS04680	−2.095828916	ABC transporter permease/substrate-binding protein
gene-D820_RS02655	ugpC	−2.274872059	sn-glycerol-3-phosphate ABC transporter ATP-binding protein
gene-D820_RS01050	D820_RS01050	−1.381214985	MetQ/NlpA family ABC transporter substrate-binding protein
gene-D820_RS02665	D820_RS02665	−2.14457111	Sugar ABC transporter permease
gene-D820_RS04675	D820_RS04675	−1.977690467	ABC transporter ATP-binding protein
gene-D820_RS05590	msmE	−2.511339465	Sugar-binding protein MsmE
gene-D820_RS04570	D820_RS04570	−1.468165245	BMP family protein

(Continued)

10.3389/fcimb.2025.1535539

TABLE 2 Continued

Gene ID	Gene name	log2FoldChange	Gene product description
gene-D820_RS08355	D820_RS08355	−1.831419345	Peptide ABC transporter substrate-binding protein
Gene-D820_RS0109815	D820_RS0109815	−1.45009996	Energy-coupling factor transporter ATPase
gene-D820_RS08420	D820_RS08420	−1.592411347	Amino acid ABC transporter ATP-binding protein
gene-D820_RS02660	D820_RS02660	−2.178411965	Sugar ABC transporter permease
gene-D820_RS05585	D820_RS05585	−1.94908875	Sugar ABC transporter permease
gene-D820_RS08415	D820_RS08415	−1.353656759	ABC transporter substrate-binding protein/permease
gene-D820_RS05580	D820_RS05580	−1.365270344	Carbohydrate ABC transporter permease
gene-D820_RS00140	D820_RS00140	−1.273980434	Energy-coupling factor transporter transmembrane protein EcfT
gene-D820_RS07555	D820_RS07555	−1.06599486	ABC transporter permease
gene-D820_RS05570	ugpC	−1.16129183	sn-glycerol-3-phosphate ABC transporter ATP-binding protein UgpC
gene-D820_RS07560	D820_RS07560	−1.092495506	ABC transporter ATP-binding protein
gene-D820_RS06575	D820_RS06575	−1.011033093	ABC transporter ATP-binding protein

Figure 4B, 487 genes were found to be upregulated, while 519 exhibited downregulation. DEGs were annotated, functionally utilizing KEGG enrichment analysis. The GO enrichment assessment concerning molecular functions, cellular components, and biological processes revealed the involvement of these DEGs in DNA binding, oxidoreductase activity, membrane, *de novo* IMP biosynthetic process, and carbohydrate transport (Figure 4C). The functional annotation of DEGs was carried out along with KEGG pathway and enrichment analysis (Figures 4D, E). Furthermore, 30 significant KEGG pathways were revealed, demonstrating potential

TABLE 3 Differentially expressed genes in *S. mutans* upon CFS treatment related to ABC transporters.

Gene ID	Gene name	log2FoldChange	Gene product description
gene-D820_RS00965	D820_RS00965	−4.232719052	PTS fructose transporter subunit IIA
gene-D820_RS01260	D820_RS01260	−3.270871468	PTS sugar transporter subunit IIB
gene-D820_RS01255	D820_RS01255	−2.777113939	PTS mannose/fructose/sorbose transporter subunit IIC
gene-D820_RS00970	D820_RS00970	−3.736814618	PTS sugar transporter subunit IIB
gene-D820_RS00975	D820_RS00975	−3.46228586	PTS sugar transporter subunit IIC
gene-D820_RS01250	D820_RS01250	−2.372420573	PTS system mannose/fructose/sorbose family transporter subunit IID
gene-D820_RS09065	D820_RS09065	−3.259542925	Fructose-specific PTS transporter subunit EIIC
gene-D820_RS08290	D820_RS08290	−2.02278172	PTS ascorbate transporter subunit IIC
gene-D820_RS09070	pfkB	−3.715535435	1-Phosphofructokinase
gene-D820_RS06470	ptsP	−1.76668403	Phosphoenolpyruvate–protein phosphotransferase
gene-D820_RS09060	D820_RS09060	−2.97617044	Fructose PTS transporter subunit IIA
gene-D820_RS03005	D820_RS03005	−3.082157304	PTS fructose transporter subunit IIB
gene-D820_RS05630	pfkB	−1.199569385	1-Phosphofructokinase
gene-D820_RS03010	D820_RS03010	−1.39127042	PTS transporter subunit IIC
gene-D820_RS03000	D820_RS03000	−2.51286028	PTS sugar transporter subunit IIA
gene-D820_RS02545	celB	−1.24228573	PTS cellobiose transporter subunit IIC
gene-D820_RS02525	D820_RS02525	−1.420784914	PTS cellobiose transporter subunit IIB
gene-D820_RS03015	lacF	−1.020431306	PTS lactose transporter subunit IIA
gene-D820_RS02535	D820_RS02535	−1.757714575	PTS cellobiose transporter subunit IIA
gene-D820_RS07210	D820_RS07210	−1.182133578	PTS sugar transporter subunit IIB

TABLE 4 Differentially expressed genes in *S. mutans* upon CFS treatment related to stress response, quorum sensing gene, and exopolysaccharide formation.

Gene ID	Gene name	log2FoldChange	Gene product description
gene-D820_RS04535	ciaH	−2.388584358	Three-component system sensor histidine kinase
gene-D820_RS04530	ciaR	−1.660277218	Three-component system response regulator
gene-D820_RS06890	lytS	−1.044404874	Two-component system sensor histidine kinase
gene-D820_RS06895	lytR	−1.490154315	Two-component system response regulator
gene-D820_RS06900	lrgA	−4.847658908	Holin-like protein
gene-D820_RS06905	lrgB	−4.310981884	Antiholin-like protein
gene-D820_RS07385	LuxS	−1.164248994	S-ribosylhomocysteine lyase
gene-D820_RS00575	dexA	−1.002077734	Dextranase
gene-D820_RS03620	mubB	−1.879608552	Mutanobactin A non-ribosomal peptide synthetase
gene-D820_RS03625	mubC	−1.996091508	Mutanobactin A non-ribosomal peptide synthetase
gene-D820_RS03630	mubD	−1.837350518	Mutanobactin A non-ribosomal peptide synthetase
gene-D820_RS03555	mubY	−5.956253759	Mutanobactin A system ABC transporter permease subunit
gene-D820_RS03610	mubH	−1.182104006	Mutanobactin A polyketide synthase
gene-D820_RS03580	mubR	−1.400053226	Mutanobactin A biosynthesis transcriptional regulator
gene-D820_RS08310	aguA	−1.50902996	Agmatine deiminase
gene-D820_RS00580	treR	−1.242887742	Trehalose operon repressor

links to the metabolic processes of *S. mutans*, including pathways related to pyruvate metabolism, purine metabolism, amino sugar and nucleotide sugar metabolism, galactose metabolism, and the TCA cycle. Certain pathways, especially pyruvate metabolism, the phosphotransferase system, and ATP-binding cassette (ABC) transporters, play vital roles in biofilm formation.

S. mutans possesses 14 phosphoenolpyruvate-dependent phosphotransferase systems (PTSs) and two ABC transporters, indicating that it can transport various sugars to meet its metabolic needs and adapt to complex and changing environments. Transcriptome analysis indicated a significant reduction in the key gene expression associated with carbohydrate metabolism because of CFS (Tables 2, 3). Selected genes related to two-component signal transduction systems (*ciaH, ciaR, lytS*, and *lytR*), polyketides/non-ribosomal peptides (*mub gene clust*), acid stress response (*aguA* and *TreR*), quorum sensing gene (*LuxS*), and exopolysaccharide-formation gene (*dexA*) were significantly downregulated and are presented in Table 4, which could inhibit oxidative stress and attenuate the virulence of *S. mutans*.

To confirm the RNA-Seq findings, randomly selected genes underwent quantification through quantitative real-time polymerase chain reaction (qRT-PCR) to assess their transcription levels. As indicated in Figure 4F, the genes *lrgB, LuxS, dexA*, and *ldh* showed significant downregulation following treatment with the supernatant, which conformed with the results derived from RNA-seq analysis.

3.4 Inhibitory effect of *L. salivarius* on *S. mutans* virulence *in vivo*

Throughout the entire experimental duration, the rats maintained stable health conditions. Weight gain among all

TABLE 5 Changes in body weight of SD rats during the experiment.

Group	Weight of SD rats at different periods (g)					
	28 d	35 d	42 d	49 d	56 d	63 d
Caries-free	79.1 ± 1.517	117.1 ± 0.945	139.2 ± 1.417	161.6 ± 0.742	182.1 ± 0.721	223.3 ± 1.627
CFS	77.2 ± 0.907	116.5 ± 0.869	139.9 ± 1.214	60.2 ± 1.229	178.7 ± 1.592	220.9 ± 1.178
L. salivarius	80.3 ± 0.624	117.1 ± 0.090	138.2 ± 0.561	160.4 ± 1.186	179.0 ± 1.733	219.7 ± 1.358
Caries-model	79.6 ± 1.444	118.5 ± 1.129	141.3 ± 1.178	158.8 ± 1.503	180.6 ± 1.389	221.1 ± 1.212

groups showed no statistically significant differences (Table 5). As shown in Figure 1B, in the caries-free group, *S. mutans* was not detected, while the levels of *S. mutans* in the caries model, *L. salivarius*, and CFS groups were approximately 4.0×10^4 CFU/mL after infection for 5 days, demonstrating successful colonization of *S. mutans* within the oral cavities.

In order to improve the visibility of caries site on rat molars, micro-CT was used for 3D reconstructions of the mandibular molars, and the enamel was isolated from the complete mandible with a predetermined threshold. Additionally, the relevant sagittal slice of the homorganic molar was extracted for comparative analysis (Figure 1C). From the complete 3D reconstruction of dental hard tissue, the sagittal slice images of the caries model group were compared with those of the caries-free group, in which it was clear that the enamel (green) areas were discontinuous in the presence of caries. Additionally, to quantitatively assess the results from micro-CT, we calculated and analyzed the enamel volume and mineral density of molar teeth across the various experimental groups. The smaller the enamel volume, the more enamel loss and the more severe the caries. As shown in Figures 1D, E, the enamel volume and mineral density of the caries model group were obviously less than those in the caries-free group, indicating that the rat caries model was successfully established. The enamel volume and mineral density of the molars treated with CFS were higher than those in the caries-model group and lower than those in the caries-free group ($p < 0.01$). In addition, no significant differences were found in enamel volume and mineral density between the CFS and *L. salivarius* groups.

4 Discussion

In the oral cavity, *S. mutans* and *Lactobacillus* are common microorganisms. Similar to the intestinal microbiota, the oral microbiota is also in a dynamic equilibrium. Once this equilibrium is disrupted, cariogenic microorganisms such as *S. mutans* will become dominant, contributing to the formation of a cariogenic biofilm (Hannig and Hannig, 2009). Hence, preventing bacterial biofilm formation is vital for maintaining dental health. In previous investigations (Wasfi et al., 2018; Liang et al., 2023), the inhibition of *S. mutans* biofilms occurred with the addition of the *L. salivarius* supernatant. The pathogenic mechanisms by which the *L. salivarius* supernatant aids in caries prevention and the potential active substances remain unclear. This study demonstrated that the inhibitory effect of the *L. salivarius* supernatant can reduce the biofilm amount and biofilm activity at different time points. It not only significantly reduced the adhesion of initial biofilms, but also has a potential inhibitory effect on 24-h mature biofilms. The biofilm structure after co-cultivation of CFS and *S. mutans* was significantly loose and sparse, which also has a significant destructive effect on the biofilm structure.

Lactobacillus, an essential category of probiotics, is widely utilized. The growth and reproduction of harmful bacteria can be inhibited by certain compounds, mainly through their metabolites such as organic acids, bacteriocins, and hydrogen peroxide (Liu et al., 2020). Neutralizing the CFS to pH 6.5 markedly diminished its antimicrobial efficacy, which found that the active components of the CFS could be organic acids or substances that exert an inhibitory effect in acidic environments. The addition of catalase and proteinase K to the CFS resulted in a reduction of its antibacterial activity against *S. mutans*. This indicated that hydrogen peroxide and protein material contribution in antimicrobial activity of the CFS were also important.

Furthermore, the non-targeted LC-MS/MS method was employed to detect the bioactive compounds present in CFS. A mountain of organic acids and derivatives were found from the HMDB analysis. Studies indicated that certain organic acids could impede biofilm formation by certain mechanisms. Among the usual organic acids found in the supernatant of *L. plantarum* CCFM8724, phenolactic acid can significantly suppress the biofilm formation of *S. mutans* and *Candida albicans*. Additionally, phenyllactic acid, a kind of postbiotics, and the secretion of *L. paracasei* ET-22 exhibited significant inhibition of a variety of pathogenic bacteria biofilm formation (Wu et al., 2023). In the characteristic monosaccharides of CFS from *L. salivarius*, sorbitol had been found to reduce acid production and the amount of bacterial biofilm as well as inhibit the acid production of *S. mutans in vitro* (Takahashi-Abbe et al., 2001). Sorbitol has been confirmed to decrease the dual-species biofilm formation of *S. mutans* and *C. albicans*, leading to change in biofilm structure and glucan production (Chan et al., 2020). Therefore, sorbitol was probably an effective substance in CFS of *L. salivarius*. Additionally, we found that the expression of honokiol was upregulated from VIP analysis, which was confirmed to suppress biofilm formation as well as the production of extracellular matrix and lactic acid in *S. mutans* (Ren et al., 2023).

Sugars are the main carbon source for bacteria, which can be used to produce adenosine triphosphate (ATP) and synthesize various cellular components (such as peptidoglycan, fatty acids, and nucleic acids) and intercellular polysaccharide. The primary means of carbohydrate transport in the dental pathogen *S. mutans* occurs through the glycolysis pathway via the PTS system and ABC transporters. *S. mutans* encodes 14 PTSs and two ABC transporters (Kawada-Matsuo et al., 2016; Zeng et al., 2017). Transcriptome analysis of *S. mutans* demonstrated that the expression of major carbohydrate metabolism genes was significantly reduced and influenced by the downregulation of CFS, PTSs for galactitol, cellobiose, fructose, lactose, and mannose. Genes involved in maltose and maltodextrin transport in the ABC transporter system such as *malK, malE*, and *malG* were also downregulated.

Two-component signal transduction system (TCSTS) is a protein phosphorylation signaling pathway widely present in bacteria, which can regulate bacterial gene expression and coordinate various bacterial activities when stimulated by environmental stimuli (Hoch, 2000). TCSTS generally involves a dimerized transmembrane receptor, specifically histidine kinase (HK), along with a cytoplasmic response regulator (RR). The HK protein, situated in the plasma membrane, is capable of sensing

specific environmental stimuli, while the RR protein, located in the cytoplasm, responds to these stimuli by modulating gene expression. In *S. mutans*, numerous TCSTS, such as *VicK/VicR*, *CiaH/CiaR*, *LytST*, and *LiaS/LiaR*, have been identified in the genome of *S. mutans* with substantial supporting lines of evidence that are associated with various functions, including acid tolerance, oxidative stress response, and biofilm formation in *S. mutans* (Lévesque et al., 2007; Liu and Burne, 2009). In our study, CFS treatment inhibited the gene expression of *ciaH, ciaR, lytS*, and *lytR* in TCSTS. In summary, our results indicate that the CFS's effect on reducing the virulence of *S. mutans* is partially influenced by the downregulation of TCSTS involved in signal transduction.

The primary components of the *S. mutans* biofilm include polysaccharides, extracellular DNA (eDNA), and adhesin proteins (Shanmugam et al., 2020). In this study, CFS was found to reduce the mRNA expression levels of *lrgA* and *lrgB*, which have a function in the production of eDNA by regulating cell autolysis and the components of membrane vesicles.

Bacterial quorum sensing (QS) is regularly present in Gram-negative and Gram-positive bacteria, which plays an important role in the information exchange among biofilm bacteria under different stress conditions (Valen and Scheie, 2018). AI-2 molecules, as a messenger molecule of QS, have been identified to play a critical role in the communication processes among *S. mutans*. The protease coded by the gene of *LuxS* is a significant catalyst for the synthesis of AI-2; therefore, the *LuxS* gene serves as a marker for producing this signaling molecule (Schauder et al., 2001). The LuxS/AI-2 QS system is known to play a role in several essential physiological functions in *S. mutans* (Hu et al., 2018). Studies indicated that mutations in *LuxS* hindered biofilm formation, decreasing acid tolerance and acid production (Yoshida et al., 2005). In this article, the gene expression of *luxS* was significantly reduced in the CFS treatment group.

The secondary metabolites of *S. mutans* mainly include bacteriocins and polyketides/non-ribosomal peptides (PKs/NRPs) (Wang et al., 2012; Xie et al., 2017). To date, in *S. mutans*, some of the PKs/NRPs that were identified include mutanobactin, mutanocyclin, and mutanofactin, and these metabolites were relatively synthesized by the *mub, muc*, and *muf* gene clusters. These compounds are involved in various functions, including competition between bacterial species, responses to oxidative stress, biofilm formation, and numerous other physiological activities (Wu et al., 2010; Li et al., 2021). Most mutanobactin operon-related genes were downregulated. Consequently, the reduced expression of these secondary metabolites could significantly impact the biofilm development of *S. mutans*.

5 Conclusion

In conclusion, the transcriptomic analysis provided new insights into the mechanism by which the supernatant of *L. salivarius* inhibits *S. mutans* biofilms, including inhibition of phosphoenolpyruvate-dependent phosphotransferase systems, two ATP-binding cassette transporters, two-component systems, PKs/NRPs, acid stress response, QS, and exopolysaccharide formation. In addition, non-targeted LC-MS/MS analysis was employed to discover a variety of potential active compounds present in the CFS of the *L. salivarius* against *S. mutans* biofilm. The above results provide a theoretical basis for further isolation and purification of the *L. salivarius* supernatant and the production and application of active components, as well as the manner and conformation of molecular docking of active components and *S. mutans* targets. Therefore, it has the potential to act as a therapeutic agent for the prevention and treatment of caries.

Data availability statement

The data presented in the study are deposited in the NCBI repository, accession number PRJNA1219341.

Ethics statement

The animal study was approved by Jinzhou Medical University Animal Protection and Institutional Committee. The study was conducted in accordance with the local legislation and institutional requirements.

Author contributions

NM: Writing – original draft, Data curation, Funding acquisition, Investigation, Methodology, Software, Writing – review & editing. WY: Data curation, Investigation, Software, Writing – review & editing. BC: Data curation, Investigation, Writing – review & editing. MB: Data curation, Investigation, Software, Writing – review & editing. YL: Investigation, Software, Writing – review & editing. MW: Software, Writing – review & editing, Data curation. XY: Methodology, Writing – review & editing. JL: Data curation, Writing – review & editing. CW: Conceptualization, Funding acquisition, Methodology, Project administration, Resources, Supervision, Writing – review & editing. LQ: Conceptualization, Methodology, Project administration, Resources, Supervision, Writing – review & editing.

Funding

The author(s) declare financial support was received for the research, authorship, and/or publication of this article. The Technology Innovation Team Program of Liaoning Province Education Department (LJ222410160037), the Young Scholars Program of Liaoning Province Education Department

(LJ212410160060), the Applied Basic Research Program of Liaoning Province (2023JH2/101700071), the Applied Basic Research Program of Liaoning Province (2022JH2/101300033), the National Natural Science Foundation of China (U21A2074), and the National Natural Science Foundation of China (62375115).

Conflict of interest

The authors declare that the research was conducted in the absence of any commercial or financial relationships that could be construed as a potential conflict of interest.

Generative AI statement

The author(s) declare that no Generative AI was used in the creation of this manuscript.

Publisher's note

References

Alshahrani, A. M., and Gregory, R. L. (2020). *In vitro* Cariostatic effects of cinnamon water extract on nicotine-induced Streptococcus mutans biofilm. *BMC Complement Med. Ther.* 20, 45. doi: 10.1186/s12906-020-2840-x

Chan, A., Ellepola, K., Truong, T., Balan, P., Koo, H., and Seneviratne, C. J. (2020). Inhibitory effects of xylitol and sorbitol on Streptococcus mutans and Candida albicans biofilms are repressed by the presence of sucrose. *Arch. Oral. Biol.* 119, 104886. doi: 10.1016/j.archoralbio.2020.104886

Chen, A. C., Fang, T. J., Ho, H. H., Chen, J. F., Kuo, Y. W., Huang, Y. Y., et al. (2022). A multi-strain probiotic blend reshaped obesity-related gut dysbiosis and improved lipid metabolism in obese children. *Front. Nutr.* 9. doi: 10.3389/fnut.2022.922993

Cugini, C., Shanmugam, M., Landge, N., and Ramasubbu, N. (2019). The role of exopolysaccharides in oral biofilms. *J. Dent. Res.* 98, 739–745. doi: 10.1177/0022034519845001

Gao, Z., Chen, X., Wang, C., Song, J., Xu, J., Liu, X., et al. (2023). New strategies and mechanisms for targeting Streptococcus mutans biofilm formation to prevent dental caries: A review. *Microbiol. Res.* 278, 127526. doi: 10.1016/j.micres.2023.127526

Guo, L., McLean, J. S., Yang, Y., Eckert, R., Kaplan, C. W., Kyme, P., et al. (2015). Precision-guided antimicrobial peptide as a targeted modulator of human microbial ecology. *Proc. Natl. Acad. Sci. U.S.A.* 112, 7569–7574. doi: 10.1073/pnas.1506207112

Hannig, C., and Hannig, M. (2009). The oral cavity–a key system to understand substratum-dependent bioadhesion on solid surfaces in man. *Clin. Oral. Investig.* 13, 123–139. doi: 10.1007/s00784-008-0243-3

He, J., Hwang, G., Liu, Y., Gao, L., Kilpatrick-Liverman, L., Santarpia, P., et al. (2016). l-Arginine Modifies the Exopolysaccharide Matrix and Thwarts Streptococcus mutans Outgrowth within Mixed-Species Oral Biofilms. *J. Bacteriol* 198, 2651–2661. doi: 10.1128/jb.00021-16

Hoch, J. A. (2000). Two-component and phosphorelay signal transduction. *Curr. Opin. Microbiol.* 3, 165–170. doi: 10.1016/s1369-5274(00)00070-9

Hou, L., Guo, S., Wang, Y., Nie, X., Yang, P., Ding, D., et al. (2021). Neuropeptide ACP facilitates lipid oxidation and utilization during long-term flight in locusts. *eLife.* 10, e65279. doi: 10.7554/eLife.65279

Hu, X., Wang, Y., Gao, L., Jiang, W., Lin, W., Niu, C., et al. (2018). The Impairment of Methyl Metabolism From luxS Mutation of Streptococcus mutans. *Front. Microbiol.* 9. doi: 10.3389/fmicb.2018.00404

Kawada-Matsuo, M., Oogai, Y., and Komatsuzawa, H. (2016). Sugar allocation to metabolic pathways is tightly regulated and affects the virulence of streptococcus mutans. *Genes (Basel)* 8, 11. doi: 10.3390/genes8010011

Köll-Klais, P., Mändar, R., Leibur, E., Marcotte, H., Hammarström, L., and Mikelsaar, M. (2005). Oral lactobacilli in chronic periodontitis and periodontal health: species composition and antimicrobial activity. *Oral. Microbiol. Immunol.* 20, 354–361. doi: 10.1111/j.1399-302X.2005.00239.x

Kumariya, R., Garsa, A. K., Rajput, Y. S., Sood, S. K., Akhtar, N., and Patel, S. (2019). Bacteriocins: Classification, synthesis, mechanism of action and resistance development in food spoilage causing bacteria. *Microb. Pathog.* 128, 171–177. doi: 10.1016/j.micpath.2019.01.002

Lévesque, C. M., Mair, R. W., Perry, J. A., Lau, P. C., Li, Y. H., and Cvitkovitch, D. G. (2007). Systemic inactivation and phenotypic characterization of two-component systems in expression of Streptococcus mutans virulence properties. *Lett. Appl. Microbiol.* 45, 398–404. doi: 10.1111/j.1472-765X.2007.02203.x

Li, Z. R., Sun, J., Du, Y., Pan, A., Zeng, L., Maboudian, R., et al. (2021). Mutanofactin promotes adhesion and biofilm formation of cariogenic Streptococcus mutans. *Nat. Chem. Biol.* 17, 576–584. doi: 10.1038/s41589-021-00745-2

Li, J., Wu, T., Peng, W., and Zhu, Y. (2020). Effects of resveratrol on cariogenic virulence properties of Streptococcus mutans. *BMC Microbiol.* 20, 99. doi: 10.1186/s12866-020-01761-3

Liang, J., Zhou, Y., Tang, G., Wu, R., and Lin, H. (2023). Exploration of the Main Antibiofilm Substance of Lactobacillus plantarum ATCC 14917 and Its Effect against Streptococcus mutans. *Int. J. Mol. Sci.* 24, 1986. doi: 10.3390/ijms24031986

Lin, Y., Zhou, X., and Li, Y. (2022). Strategies for Streptococcus mutans biofilm dispersal through extracellular polymeric substances disruption. *Mol. Oral. Microbiol.* 37, 1–8. doi: 10.1111/omi.12355

Liu, Y., and Burne, R. A. (2009). Multiple two-component systems modulate alkali generation in Streptococcus gordonii in response to environmental stresses. *J. Bacteriol* 191, 7353–7362. doi: 10.1128/jb.01053-09

Liu, Q., Guo, Q., Guo, W., Song, S., Wang, N., Chen, X., et al. (2021). Loss of CEP70 function affects acrosome biogenesis and flagella formation during spermiogenesis. *Cell Death Dis.* 12, 478. doi: 10.1038/s41419-021-03755-z

Liu, Q., Yu, Z., Tian, F., Zhao, J., Zhang, H., Zhai, Q., et al. (2020). Surface components and metabolites of probiotics for regulation of intestinal epithelial barrier. *Microb. Cell Fact* 19, 23. doi: 10.1186/s12934-020-1289-4

Mani-Lopez, E., Arrioja-Breton, D., and Lopez-Malo, A. (2022). The impacts of antimicrobial and antifungal activity of cell-free supernatants from lactic acid bacteria *in vitro* and foods. *Compr. Rev. Food Sci. Food Saf.* 21, 604–641. doi: 10.1111/1541-4337.12872

Mulla, M., Hegde, S., Koshy, A., and Mulla, M. (2021). Effect of probiotic lactobacillus salivarius on peri-implantitis pathogenic bacteria: an *in vitro* study. *Cureus* 13, e20808. doi: 10.7759/cureus.20808

Niranjan, R., Patil, S., Dubey, A., Lochab, B., and Priyadarshini, R. (2024). Small cyclic dipeptide produced by Lactobacillus rhamnosus with anti-biofilm properties against Streptococcus mutans biofilm. *Biofilm* 8, 100237. doi: 10.1016/j.bioflm.2024.100237

Ren, S., Yang, Y., Xia, M., Deng, Y., Zuo, Y., Lei, L., et al. (2023). A Chinese herb preparation, honokiol, inhibits Streptococcus mutans biofilm formation. *Arch. Oral. Biol.* 147, 105610. doi: 10.1016/j.archoralbio.2022.105610

Schauder, S., Shokat, K., Surette, M. G., and Bassler, B. L. (2001). The LuxS family of bacterial autoinducers: biosynthesis of a novel quorum-sensing signal molecule. *Mol. Microbiol.* 41, 463–476. doi: 10.1046/j.1365-2958.2001.02532.x

Shanmugam, K., Sarveswari, H. B., Udayashankar, A., Swamy, S. S., Pudipeddi, A., Shanmugam, T., et al. (2020). Guardian genes ensuring subsistence of oral Streptococcus mutans. *Crit. Rev. Microbiol.* 46, 475–491. doi: 10.1080/1040841x.2020.1796579

Simon-Soro, A., and Mira, A. (2015). Solving the etiology of dental caries. *Trends Microbiol.* 23, 76–82. doi: 10.1016/j.tim.2014.10.010

Sun, Y., Jiang, W., Zhang, M., Zhang, L., Shen, Y., Huang, S., et al. (2021). The inhibitory effects of ficin on streptococcus mutans biofilm formation. *BioMed. Res. Int.* 2021, 6692328. doi: 10.1155/2021/6692328

Takahashi-Abbe, S., Abbe, K., Takahashi, N., Tamazawa, Y., and Yamada, T. (2001). Inhibitory effect of sorbitol on sugar metabolism of Streptococcus mutans *in vitro* and on acid production in dental plaque *in vivo*. *Oral. Microbiol. Immunol.* 16, 94–99. doi: 10.1034/j.1399-302x.2001.016002094.x

Vahedi Shahandashti, R., Kasra Kermanshahi, R., and Ghadam, P. (2016). The inhibitory effect of bacteriocin produced by Lactobacillus acidophilusATCC 4356 and Lactobacillus plantarum ATCC 8014 on planktonic cells and biofilms of Serratia marcescens. *Turk J. Med. Sci.* 46, 1188–1196. doi: 10.3906/sag-1505-51

Valen, H., and Scheie, A. A. (2018). Biofilms and their properties. *Eur. J. Oral. Sci.* 126 Suppl 1, 13–18. doi: 10.1111/eos.12425

van Zyl, W. F., Deane, S. M., and Dicks, L. M. T. (2020). Molecular insights into probiotic mechanisms of action employed against intestinal pathogenic bacteria. *Gut Microbes* 12, 1831339. doi: 10.1080/19490976.2020.1831339

Wang, X., Du, L., You, J., King, J. B., and Cichewicz, R. H. (2012). Fungal biofilm inhibitors from a human oral microbiome-derived bacterium. *Org Biomol Chem.* 10, 2044–2050. doi: 10.1039/c2ob06856g

Wasfi, R., Abd-El-Rahman, O. A., Mansour, L. E., Hanora, A. S., Hashem, A. M., and Ashour, M. S. (2012). Antimicrobial activities against biofilm formed by Proteus mirabilis isolates from wound and urinary tract infections. *Indian J. Med. Microbiol.* 30, 76–80. doi: 10.4103/0255-0857.93044

Wasfi, R., Abd-El-Rahman, O. A., Zafer, M. M., and Ashour, H. M. (2018). Probiotic Lactobacillus sp. inhibit growth, biofilm formation and gene expression of caries-inducing Streptococcus mutans. *J. Cell Mol. Med.* 22, 1972–1983. doi: 10.1111/jcmm.13496

Wu, C., Cichewicz, R., Li, Y., Liu, J., Roe, B., Ferretti, J., et al. (2010). Genomic island TnSmu2 of Streptococcus mutans harbors a nonribosomal peptide synthetase-polyketide synthase gene cluster responsible for the biosynthesis of pigments involved in oxygen and H2O2 tolerance. *Appl. Environ. Microbiol.* 76, 5815–5826. doi: 10.1128/aem.03079-09

Wu, H., Guang, C., Zhang, W., and Mu, W. (2023). Recent development of phenyllactic acid: physicochemical properties, biotechnological production strategies and applications. *Crit. Rev. Biotechnol.* 43, 293–308. doi: 10.1080/07388551.2021.2010645

Xie, Z., Zhang, Z., Liu, L., Liu, X., and Chen, Y. (2017). Secondary metabolites from Streptococcus mutans and their ecological roles in dental biofilm. *Sheng Wu Gong Cheng Xue Bao* 33, 1547–1554. doi: 10.13345/j.cjb.170046

Yeun, Y., and Lee, J. (2015). Effect of a double-coated probiotic formulation on functional constipation in the elderly: a randomized, double blind, controlled study. *Arch. Pharm. Res.* 38, 1345–1350. doi: 10.1007/s12272-014-0522-2

Yoshida, A., Ansai, T., Takehara, T., and Kuramitsu, H. K. (2005). LuxS-based signaling affects Streptococcus mutans biofilm formation. *Appl. Environ. Microbiol.* 71, 2372–2380. doi: 10.1128/aem.71.5.2372-2380.2005

Zeng, L., Chakraborty, B., Farivar, T., and Burne, R. A. (2017). Coordinated Regulation of the EII(Man) and fruRKI Operons of Streptococcus mutans by Global and Fructose-Specific Pathways. *Appl. Environ. Microbiol.* 83, e01403-17. doi: 10.1128/aem.01403-17

Zhang, G., Lu, M., Liu, R., Tian, Y., Vu, V. H., Li, Y., et al. (2020). Inhibition of Streptococcus mutans Biofilm Formation and Virulence by Lactobacillus plantarum K41 Isolated From Traditional Sichuan Pickles. *Front. Microbiol.* 11. doi: 10.3389/fmicb.2020.00774

Zhang, J., Wang, Q., and Duan, Z. (2024). Preventive effects of probiotics on dental caries *in vitro* and *in vivo*. *BMC Oral. Health* 24, 915. doi: 10.1186/s12903-024-04703-x

Zhao, Z., Wu, J., Sun, Z., Fan, J., Liu, F., Zhao, W., et al. (2023). Postbiotics Derived from L. paracasei ET-22 Inhibit the Formation of S. mutans Biofilms and Bioactive Substances: An Analysis. *Molecules* 28, 1236. doi: 10.3390/molecules28031236

frontiers | Frontiers in Cellular and Infection Microbiology

TYPE Review
PUBLISHED 15 May 2025
DOI 10.3389/fcimb.2025.1594947

OPEN ACCESS

EDITED BY
Keke Zhang,
Wenzhou Medical University, China

REVIEWED BY
Yuqing Li,
Sichuan University, China
Hong Chen,
Chongqing Medical University, China
Bin Zhang,
Xi'an Jiaotong University, China

*CORRESPONDENCE
Yan Yang
yangyancsu@scu.edu.cn
Zhili Zhao
zhili-zhao@csu.edu.cn

RECEIVED 17 March 2025
ACCEPTED 28 April 2025
PUBLISHED 15 May 2025

CITATION
Yang Y, He H, Liu B, Li Z, Sun J, Zhao Z and Yang Y (2025) Protein lysine acetylation regulates oral microorganisms.
Front. Cell. Infect. Microbiol. 15:1594947.
doi: 10.3389/fcimb.2025.1594947

Protein lysine acetylation regulates oral microorganisms

Yuanchao Yang[1,2], Hailun He[3], Bingshi Liu[1,2], Zhuoyue Li[1,2], Jiaman Sun[1,2], Zhili Zhao[4]* and Yan Yang[1,2]*

[1]Xiangya Stomatological Hospital and Xiangya School of Stomatology, Central South University, Changsha, China, [2]Hunan Key Laboratory of Oral Health Research, Central South University, Changsha, China, [3]School of Life Sciences, Central South University, Changsha, China, [4]Department of Oral and Maxillofacial Surgery, The Second Xiangya Hospital, Central South University, Changsha, China

Post-translational modifications (PTMs) are integral to the regulation of protein function, stability, and cellular processes. Lysine acetylation, a widespread PTM, has been extensively characterized for its role in eukaryotic cellular functions, particularly in metabolism, gene expression, and disease progression. However, its involvement in oral microbiota remains inadequately explored. This review examines the emerging significance of lysine acetylation in modulating oral microbial communities. The oral cavity, characterized by its unique anatomical and environmental conditions, serves as a dynamic habitat where microbiota interact with host factors such as diet, immune response, pH, and the level of oxygen. Lysine acetylation enables bacterial adaptation to these fluctuating conditions, influencing microbial metabolism, virulence, and stress responses. For example, acetylation of lactate dehydrogenase in *Streptococcus mutans* reduces its acidogenicity and aciduricity, which decreases its cariogenic potential. In diverse environmental conditions, including hypoxic or anaerobic environments, acetylation regulates energy utilization pathways and enzyme activities, supporting bacterial survival and adaptation. Additionally, acetylation controls the production of extracellular polysaccharides (EPS), which are essential for biofilm formation and bacterial colonization. The acetylation of virulence factors can modulate the pathogenic potential of oral bacteria, either enhancing or inhibiting their activity depending on the specific context and regulatory mechanisms involved. This review also explores the interactions between acetylation and other PTMs, highlighting their synergistic or antagonistic effects on protein function. A deeper understanding of lysine acetylation mechanisms in oral microbiota could provide valuable insights into microbial adaptation and pathogenesis, revealing potential therapeutic targets for oral diseases.

KEYWORDS

lysine acetylation, oral microorganisms, bacterial virulence, environmental adaptation, immune escape

1 Introduction

Post-translational modification (PTM) refers to the chemical modification of proteins following translation, which influences their structure and function. These modifications can impact protein stability, affinity, activity, and subcellular localization, thereby regulating their biological roles. In the context of oral microbiota, PTMs are integral in modulating protein synthesis, metabolism, and virulence. Oral microorganisms utilize PTMs to adapt to external stimuli and control various physiological processes. To date, over 200 distinct PTMs have been cataloged (Minguez et al., 2012), including both minor chemical modifications (e.g., phosphorylation and acetylation) and the addition of complete proteins (e.g., ubiquitination). The most common PTMs observed in oral microbiota include phosphorylation, acetylation, methylation, glycosylation, sumoylation, and lactylation (Wu et al., 2019; Zeng et al., 2020; Ma et al., 2021b).

Lysine is an amphipathic residue, characterized by a hydrophobic side chain and a positively charged εN-group at physiological pH. The εN-group in the active or binding site of proteins typically engages in salt bridge formation (Moreira et al., 2007). Acylation of lysine neutralizes the amino group's positive charge, potentially altering the protein's conformation. Various acylation modifications have been identified, including acetylation (Wang et al., 2010), malonylation (Peng et al., 2011), crotonylation (Montellier et al., 2012), propionylation and butylation (Chen et al., 2007), and succinylation (Lin et al., 2012). These modifications utilize metabolic intermediates as sensors to regulate metabolism and other processes, thereby coordinating metabolic pathways and signal transduction (Wellen and Thompson, 2012).

The most extensively studied lysine modification is acetylation, which occurs through reversible catalysis by protein acetyltransferases and deacetylases. Active acetyl derivatives, such as acetyl phosphate, acetyl CoA, and acetyladenylic acid, are also known to drive protein acetylation (Ramponi et al., 1975; Wagner and Payne, 2013; Weinert et al., 2013; Kuhn et al., 2014). Initially observed in histones (Allfrey et al., 1964), lysine acetylation has since been identified in various eukaryotic non-histone proteins involved in cellular metabolism, the cell cycle, aging, growth, angiogenesis, and oncogenesis (Chuang et al., 2010; Wang et al., 2010; Zhao et al., 2010; Lu et al., 2011; Carafa et al., 2012; Lin et al., 2012). In contrast, research on prokaryotic acetylation remains limited, primarily focusing on a few microbial species. Although lysine acetylation is increasingly recognized as a significant post-translational modification in bacteria, its specific roles and regulatory mechanisms within oral microbiota remain underexplored.

The oral microenvironment is intricate, shaped by the unique anatomy of the oral cavity. Oral microorganisms are highly sensitive to host factors, including diet, immune status, pH, oral hygiene, oxygen levels, and lifestyle choices (Yan et al., 2023). In contrast to slower regulatory mechanisms such as gene expression and protein turnover, lysine acetylation enables bacteria to rapidly adjust their physiological state, offering a mechanism to respond swiftly to environmental changes. For instance, under hypoxic or anaerobic conditions, lysine acetylation modulates bacterial metabolic pathways, optimizing energy utilization and regulating enzymatic activity to mitigate external stressors (Kim et al., 2015; Martín et al., 2021; Toplak et al., 2022; Ma et al., 2024a).

In addition, protein lysine acetylation is a key regulator of microbial virulence. One noteworthy illustration is the production of extracellular polysaccharides (EPS) by oral bacteria via glucosyltransferases. EPS constitutes the primary component of dental plaque biofilms, promoting bacterial colonization and aggregation. Notably, the acetylation status of glucosyltransferase correlates with its enzymatic activity (Ma et al., 2021a). Beyond local effects, oral pathogens can release virulence factors into the bloodstream, leading to systemic infections. Acetylation plays a critical role in the onset and progression of these virulence factors (Ren et al., 2017).

Protein acetylation differs from mRNA or protein synthesis in that it is not templated, instead depending on the recognition and modification by specific enzymes. This process is typically reversible and dynamic, with chemical groups being added or removed from the polypeptide chain by specialized enzymes. Beyond enzymes, certain chemical compounds also contribute to protein acetylation. For instance, acetyl coenzyme A (Ac-CoA) directly enhances the acetylation of RprY in *Porphyromonas gingivalis* (Wagner and Payne, 2013). Proteins often undergo multiple modifications, with some residues experiencing several modifications simultaneously. For example, in *Porphyromonas gingivalis*, acetylation and succinylation frequently overlap, and RprY can concurrently undergo both acetylation and phosphorylation (Li et al., 2018). The interplay between acetylation and other PTMs can produce complementary or antagonistic effects, resulting in intricate combinations that influence the structure and function of target proteins, highlighting the complexity and adaptability of regulatory mechanisms.

Recent advances in enrichment strategies for protein lysine acetylation sites have provided substantial evidence supporting the critical role of protein acetylation in regulating both the physiological and pathological processes of oral microorganisms (Figure 1). This review explores the significance and diverse functions of protein lysine acetylation in oral microorganisms, aiming to fill current knowledge gaps and explore the potential of acetylation as a therapeutic target for oral diseases by integrating emerging evidence across major oral microorganisms, including bacteria (e.g., *Streptococcus mutans*, *Porphyromonas gingivalis*) and fungi (e.g., *Candida albicans*), and highlighting its interplay with other post-translational modifications.

2 Protein acetylation

2.1 Protein acetylation in oral microorganisms

Lysine acetylation is regulated by two distinct mechanisms: enzymatic and non-enzymatic. The enzymatic process involves the transfer of an acetyl group from acetyl-CoA to the ε-amino group of

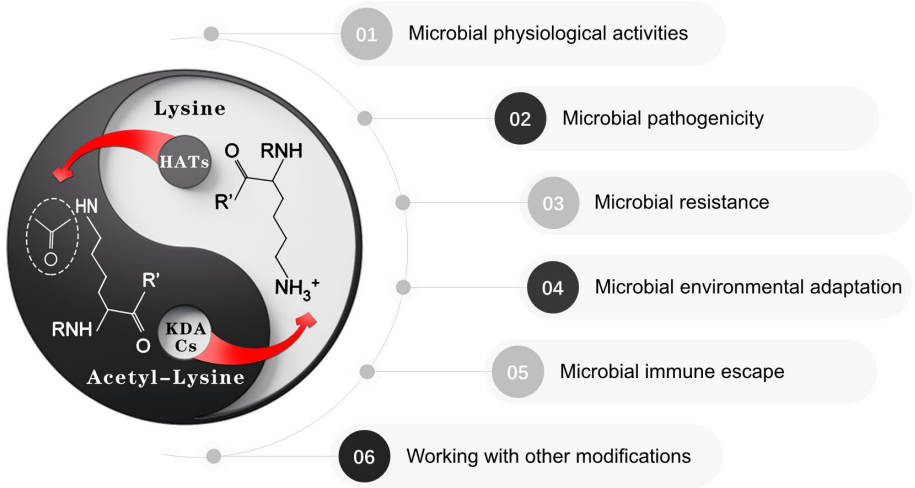

FIGURE 1
Protein lysine acetylation in oral microbiology. Oral microbiota employs dynamic acetylation/deacetylation modification mechanisms to precisely modulate critical physiological processes including physiological activities, microbial pathogenicity, drug resistance, environmental adaption, immune escape and interaction with other mechanisms. Notably, this dynamically balanced acetylation system endows pathogens with remarkable plasticity, enabling rapid epigenetic-level responses to adaptively transition between host microenvironmental conditions and external stressors. The bidirectional equilibrium inherent in this regulatory network mirrors the Taiji (Yin-Yang) philosophy in Chinese traditional thought – a cyclical interplay of complementary forces that maintains the homeostasis of living systems through dynamic equilibrium.

deprotonated lysine, a reaction catalyzed by lysine acetyltransferases (KATs). These enzymes are classified into three primary families: (i) the Gcn5-related N-acetyltransferase (GNAT) family, named after the yeast Gcn5 protein, (ii) the MYST family, which includes human MOZ, yeast Ybf2/Sas3, yeast Sas2, and human Tip60, and (iii) the p300/CBP family, named after human p300 and CBP. While the MYST and p300/CBP families are exclusive to eukaryotic cells, the GNAT family is conserved across all domains of life (Starai and Escalante-Semerena, 2004; Chen et al., 2007; Wang et al., 2010). Several KATs have been identified in various microbial species, all belonging to the GNAT family (Hentchel and Escalante-Semerena, 2015), such as ActA and ActG in *Streptococcus mutans* (Ma et al., 2021a, 2024a) and VimA and its homolog PG1842 in *Porphyromonas gingivalis* (Mishra et al., 2018), Among them, the *Salmonella enterica* protein acetyltransferase Pat (also referred to as YfiQ *Escherichia coli*) was the first to be identified and remains the most extensively studied (Starai and Escalante-Semerena, 2004).

A non-enzymatic mechanism was identified in *Escherichia coli*, where acetyl phosphate (AcP) directly transfers its acetyl group to the ε-amino group of deprotonated lysine (Weinert et al., 2013; Kuhn et al., 2014), this mechanism may similarly support rapid metabolic adaptation of oral bacteria during nutritional fluctuations or stress conditions which are common in the oral cavity (Di et al., 2023). AcP, a high-energy intermediate in the phosphotransacetylase-acetate kinase (Pta-AckA) pathway, is traditionally recognized as a donor of phosphorylation groups for specific response regulators within two-component signaling systems (Lukat et al., 1992). The *yfiQ* deletion mutant shows minimal impact on global acetylation levels, while increasing AcP concentrations correspond to elevated global acetylation, indicating that AcP-dependent acetylation is less specific than its enzymatic counterpart and may significantly influence bacterial physiological processes.

2.2 Protein deacetylation in oral microorganisms

Lysine deacetylases (KDACs) enzymatically remove acetyl groups. Currently, two primary KDAC families have been identified and categorized into four groups: the NAD+-dependent sirtuin family (class III) (Blander and Guarente, 2004) and the zinc-dependent Rpd3/Hda1 family (classes I, II, and IV) (Yang and Seto, 2008).

The NAD+-dependent CobB, the most extensively studied bacterial sirtuin, was initially characterized in *Streptococcus faecalis* (Starai et al., 2002). Its homologs have since been identified in other bacteria, including *Escherichia coli* (Zhao et al., 2004)and *Streptomyces* (Mikulik et al., 2012). CobB typically does not exhibit a preference for Pat-dependent or AcP-dependent acetylated lysine, with its substrates participating in diverse cellular processes (AbouElfetouh et al., 2015). For instance, CobB deacetylates both Pat- and AcP-dependent acetylated DnaA (Zhang et al., 2016). Initially regarded as the sole histone deacetylase (HDAC) in *Escherichia coli* due to the absence of other HDAC homologs, CobB's role was reassessed upon the identification of a novel deacetylase, YcgC, in *Escherichia coli* (Tu et al., 2015). YcgC, a member of the serine hydrolase family, lacks significant homology with known KDACs and is neither NAD+- nor Zn2+-dependent. It catalyzes substrate deacetylation through mechanisms distinct from established deacetylases, targeting a different set of acetylated proteins than those regulated by CobB in *Escherichia coli*. Thus, YcgC and its homologs may constitute a novel bacterial deacetylase family. Additionally, MSMEG_4620, a SIRT4 homolog in Mycobacterium tuberculosis, exhibits both deacetylase and auto-ADP-ribosyltransferase activities (Tan et al., 2016). Consequently, further investigation into novel microbial deacetylases and the interplay between acetylation factors and deacetylases will provide valuable insights.

3 Regulation of oral bacteria by protein acetylation

3.1 Streptococcus mutans

In *Streptococcus mutans*, lysine acetylation, a widespread and dynamic PTM, is integral to bacterial metabolic regulation and pathogenicity. It has been demonstrated that *Streptococcus mutans* utilizes sucrose to synthesize exopolysaccharide via glucosyltransferases (Gtfs), a process regulated by lysine acetylation. Analysis of protein acetylation dynamics revealed that 22.7% of proteins were acetylated, with significant enrichment in glycolysis/gluconeogenesis and RNA degradation pathways (Lei et al., 2021).

Acetyltransferase ActG has been shown to acetylate GtfB and GtfC, inhibiting their activity and thus reducing EPS synthesis and biofilm formation. However, site-directed mutagenesis of specific lysine residues was not performed to pinpoint the functional acetylation sites (Ma et al., 2021a). Furthermore, acetylation of lactate dehydrogenase (LDH) also inhibits its enzymatic activity, decreasing the cariogenic potential of *Streptococcus mutans* (Ma et al., 2022). ActA, a member of the GNAT family in *Streptococcus mutans*, regulates bacterial adaptation and competitiveness against oxidative stress through acetylation of LDH and pyruvate kinase (PykF) (Ma et al., 2024a). In contrast, the NAD^+-dependent deacetylase YkuR reverses Gtfs acetylation and restores their enzymatic activity, thereby promoting EPS production and biofilm formation. Deletion of ykuR elevates global acetylation and attenuates cariogenicity *in vivo* (Ma et al., 2024b).

Aspirin, a non-enzymatic acetylating agent, inhibits the growth and EPS production of *Streptococcus mutans* and reduces the enzymatic activity of Gtfs (Lin et al., 2024), further supporting the role of protein acetylation in antimicrobial and anti-biofilm applications.

Additionally, small RNA (sRNA) interacts with lysine acetylation in *Streptococcus mutans*. SmsR1 sRNA modulates protein acetylation levels and LDH activity by regulating the concentration of the *pdhC* gene and its metabolite acetyl-CoA (Li et al., 2024), reflecting bacterial adaptability to environmental stress.

These findings highlight the complex regulatory role of lysine acetylation in *Streptococcus mutans*, influencing bacterial virulence (e.g., biofilm formation) and pathogenicity (e.g., cariogenicity, environmental adaptation) (Table 1), and provide a theoretical foundation for developing new strategies to prevent and treat dental caries.

3.2 Porphyromonas gingivalis

Porphyromonas gingivalis, a Gram-negative anaerobic bacterium, is a key pathogen in chronic periodontitis. Through dynamic analysis of protein acetylation, 130 lysine acetylation sites from 92 *Porphyromonas gingivalis* proteins were identified, with the majority associated with 45 metabolically active proteins. These proteins are involved in multiple metabolic pathways, where enzymes catalyzing consecutive reactions within the same pathway are frequently acetylated. Notably, 12 enzymes in the anaerobic amino acid fermentation pathway, critical for energy production, also undergo lysine acetylation. This indicates that lysine acetylation plays a central role in the metabolic regulation of *Porphyromonas gingivalis*, contributing significantly to its survival and metabolic adaptation during infection (Butler et al., 2015).

VimA, a multifunctional protein in *Porphyromonas gingivalis*, regulates critical biosynthetic pathways through its acetyltransferase activity. It plays a role in the glycosylation and anchoring of bacterial surface proteins, lipid A synthesis, and the maintenance of oxidative stress tolerance. Notably, VimA and its homolog PG1842 acetylate the gingipain precursor pro-RgpB at key lysine residues (Y230, K247, and K248), facilitating its activation and maturation, which enhances both the invasive and biofilm-forming capacities of *Porphyromonas gingivalis* (Mishra et al., 2018). *VimA*-deficient mutants, such as FLL92, exhibit reduced invasion

TABLE 1 Lysine acetylation in *Streptococcus mutans*.

Lysine acetylation in *Streptococcus mutans*			
Mechanism	Effect	Biological function	References
Acetylation of GtfB and GtfC by ActG	Inhibits the enzymatic activity of GtfB and GtfC, reducing EPS synthesis and biofilm formation	Inhibits biofilm formation	Ma et al., 2021a
Acetylation of LDH	Inhibits LDH activity, reducing acidogenic potential	Decreases *Streptococcus mutans*' cariogenic potential	Ma et al., 2022
Acetylation of LDH and PykF by ActA	Inhibits bacterial adaptation to oxidative stress	Inhibits oxidative stress tolerance and competitiveness of *Streptococcus mutans*	Ma et al., 2024a
YkuR-mediated NAD^+-dependent deacetylation of Gtfs	Restores Gtf activity and increases EPS synthesis	Enhances *Streptococcus mutans* biofilm formation and virulence	Ma et al., 2024b
Non-enzymatic acetylation by ASA	Inhibits bacterial growth, reduces EPS production and Gtfs enzyme activity	Provides antimicrobial and anti-biofilm effects by targeting acetylation	Lin et al., 2024
Interaction of SmsR1 sRNA with lysine acetylation	Modulates acetylation levels and LDH activity by regulating *pdhC* and acetyl-CoA	Environmental stress response and metabolic flexibility	Li et al., 2024

efficiency into host cells; however, supplementation with VimA restores invasive potential. This highlights VimA's essential role in modulating the pathogenicity of *Porphyromonas gingivalis*. Additionally, VimA influences branched-chain amino acid metabolism by regulating acetyl-CoA levels, thereby affecting lipid A biosynthesis (Aruni et al., 2012). Lipid A, a major component of the outer membrane of *Porphyromonas gingivalis*, is crucial for immune evasion. Studies have shown that *VimA*-deficient mutants display impaired survival under oxidative stress, suggesting that VimA contributes to bacterial survival in fluctuating oral environments by enhancing membrane stability and stress tolerance.

Protein acetylation is integral to the transcriptional regulation of *Porphyromonas gingivalis*. Acetylation of the transcription factor RprY impairs its DNA-binding ability, thereby diminishing its transcriptional activation of target genes (Li et al., 2018).

A significant aspect of lysine acetylation in *Porphyromonas gingivalis* proteins is its interaction with lysine succinylation (Ksuc). In *Porphyromonas gingivalis* ATCC 33277, a substantial overlap between Ksuc and Kac occurs, particularly in ribosomal and metabolic proteins, reflecting the complexity of PTMs in bacterial physiological regulation (Zeng et al., 2020).

In conclusion, protein acetylation is central to the physiological functions, metabolic regulation, and pathogenicity of *Porphyromonas gingivalis*. By modulating various metabolic pathways, protein sorting, and surface structure synthesis, acetylation enhances the bacterium's environmental adaptability, invasiveness, and biofilm formation capabilities (Table 2). These insights present promising molecular targets for the development of novel antimicrobial therapies.

3.3 Actinomycetes

Protein lysine acetylation, a critical PTM, is integral to the regulation of various biological processes in Actinomycetes. In fact, "Amino acid sensing" was specifically observed only in Actinomycetes, based on recent studies identifying ACT domain-containing GNATs (Lu et al., 2017; Lammers, 2021). However, similar to other organisms, such as *Streptococcus mutans* and *Porphyromonas gingivalis*, akin regulatory mechanisms such as enzyme activity modulation and metabolic network regulation via acetylation are also present in Actinomycetes (Hesketh et al., 2002).

3.3.1 Amino acid sensing: GNATs and functional properties of the ACT domain

Recent studies have identified a distinct class of GNATs in Actinomycetes, which are integral to acetylation reactions via their unique domains and regulatory mechanisms. Specifically, these enzymes feature two functional domains: the ACT (amino acid binding) domain and the GNAT (N-acetyltransferase) domain. The ACT domain detects specific amino acids, thereby allosterically modulating the acetyltransferase activity of the GNAT domain (Lu et al., 2017). This "amino acid-induced allosteric regulation" implies that amino acids influence acetyltransferase catalytic activity by binding to the ACT domain. GCN5-like acetyltransferases can be classified into two groups based on the type of amino acids induction: Asn-activated PatA and Cys-activated PatA. The former is predominantly found in *Streptomyces*, while the latter is more widespread across other actinomycete species (Lu et al., 2017). This distinction highlights that acetyltransferase regulation not only fine-tunes metabolic processes through amino acid sensing but also correlates with the physiological traits and ecological adaptability of different actinomycete species.

3.3.2 Enzyme activity regulation: dynamic balance between acetyltransferases and deacetylases

In Actinomycetes, the balance between acetyltransferases (e.g., AcuA) (Gardner et al., 2006), and deacetylases (e.g., Sirtuins) (Tucker and Escalante-Semerena, 2013) plays a pivotal role in fine-tuning enzyme activity, particularly under energy stress or nutrient-limited conditions. This dynamic regulation is critical for adapting metabolic fluxes and optimizing secondary metabolite biosynthesis.Acetylation levels also influence the synthesis of secondary metabolites by modulating the activity of specific transcription factors or metabolic enzymes. By altering transcription factor binding affinity to gene promoters, acetylation can either enhance or suppress DNA binding, thereby regulating

TABLE 2 Lysine acetylation in *Porphyromonas gingivalis*.

Lysine acetylation in *Porphyromonas gingivalis*			
Mechanism	Effect	Biological function	References
VimA-mediated acetylation of pro-RgpB	VimA and its homolog PG1842 acetylate the gingipain precursor pro-RgpB at key lysine residues, facilitating its activation and maturation	Enhances bacterial invasiveness and biofilm-forming capacity	Mishra et al., 2018
VimA regulation of branched-chain amino acid metabolism	VimA indirectly affects Lipid A synthesis by modulating acetyl-CoA levels	Maintains membrane stability, enhances oxidative stress tolerance, and promotes immune evasion	Aruni et al., 2012
Acetylation of the transcription factor RprY	Acetylation of RprY reduces its DNA-binding ability	Weakens the transcriptional activation of target genes and participates in transcriptional regulation	Li et al., 2018
Crosstalk between acetylation and succinylation	There is a significant overlap between Kac (acetylation) and Ksuc (succinylation) modifications in ribosomal and metabolic proteins	Forms a complex network of post-translational regulation, modulating bacterial physiology	Zeng et al., 2020

the expression of genes involved in secondary metabolite production. This regulatory mechanism is essential for coordinating the biosynthesis of compounds such as antibiotics (e.g., streptomycin) and non-ribosomal peptides in response to environmental or metabolic signals (Martín et al., 2021).

Additionally, acetylation of key signaling enzymes or synthetases, such as acetyl-CoA synthetase (Tucker and Escalante-Semerena, 2013), can alter their catalytic efficiency and affect metabolic flux. This modification not only regulates enzyme activity but also influences the overall metabolic pathway, promoting or inhibiting the synthesis of specific metabolites. For instance, in *Streptomyces roseosporus*, acetylation of non-ribosomal peptide synthetases suggests a significant role for acetylation in secondary metabolism (Liao et al., 2014). In *Streptomyces griseus*, acetylation of the StrM enzyme, particularly at lysine site 70, reduces its activity, thereby limiting streptomycin biosynthesis (Ishigaki et al., 2017).

3.3.3 Fine regulation of metabolic networks: from amino acid metabolism to secondary metabolite biosynthesis

The coordinated regulation of amino acid sensing and enzyme activity forms a precise regulatory mechanism within the intricate metabolic network of Actinomycetes. Acetylation is not only involved in central metabolic processes but also significantly influences amino acid metabolic pathways. Studies indicate that AAPatA acetyltransferases, which utilize Asn or Cys as sensing molecules, can modulate cellular metabolic pathways by regulating enzymes involved in aspartate and cysteine metabolism (Xu et al., 2014; Lu et al., 2017).

This acetylation-driven network is particularly responsive to environmental fluctuations. Under changing nutritional conditions or stress, acetylation rapidly adjusts bacterial metabolic pathways by altering the modification states of specific transcription factors and redox enzymes, such as GrhO6 (Toplak et al., 2022). Such regulatory flexibility supports the synthesis of secondary metabolites, enabling Actinomycetes to efficiently adapt to diverse habitats and produce specialized secondary metabolites and antibiotics.

Protein acetylation regulation in Actinomycetes extends beyond traditional cellular functions, including amino acid sensing, enzyme activity modulation, and the precise regulation of metabolic networks (Table 3). Future research should focus on elucidating the specific roles of acetyltransferases in actinomycete antibiotic synthesis and their potential as targets for developing new biological agents or antibiotics. In-depth mechanistic studies could further uncover the complexities of microbial metabolic regulation, offering novel insights for bioengineering and the development of antimicrobial drugs.

4 Regulation of oral *Candida albicans* by protein acetylation

In recent years, the infection rate of *Candida albicans*, a common opportunistic fungal pathogen, has risen significantly. The growing prevalence of drug resistance and the limited availability of effective antifungal agents present substantial challenges to clinical management. During investigations into its pathogenic mechanisms and drug resistance, lysine acetylation has emerged as a key epigenetic modification. By regulating chromatin structure, gene expression, and signal transduction, lysine acetylation plays a critical role in the growth, virulence, morphological transformation, and stress response of *Candida*

TABLE 3 Lysine acetylation in Actinomycetes.

Lysine acetylation in Actinomycetes			
Mechanism	Effect	Biological function	References
Amino acid sensing via GNATs and ACT domains	Acetyltransferase activity modulated allosterically by amino acids binding to the ACT domain	Fine-tunes metabolic processes and correlates with ecological adaptability of Actinomycetes	Lu et al., 2017
Dynamic balance between acetyltransferases and deacetylases	Acetylation levels regulated by AcuA acetyltransferase and Sirtuins deacetylases	Modulates metabolic state in response to energy deprivation or stress conditions	Gardner et al., 2006; Tucker and Escalante-Semerena, 2013
Acetylation of transcription factors and metabolic enzymes	Acetylation alters transcription factor DNA binding, influencing secondary metabolite synthesis	Regulates biosynthesis of antibiotics and non-ribosomal peptides	Martín et al., 2021
Acetylation of acetyl-CoA synthetase	Modifies catalytic efficiency and metabolic flux	Influences overall metabolic pathways and secondary metabolite production	Tucker and Escalante-Semerena, 2013
Acetylation of non-ribosomal peptide synthetases	Modulates the activity of enzymes involved in secondary metabolism	Enhances or inhibits the synthesis of secondary metabolites such as antibiotics	Liao et al., 2014
Acetylation of StrM enzyme in *Streptomyces griseus*	Reduces StrM activity, limiting *streptomycin* biosynthesis	Regulates antibiotic production in response to metabolic signals	Ishigaki et al., 2017
Acetylation in amino acid metabolism	AAPatA acetyltransferases modulate aspartate and cysteine metabolism	Regulates cellular metabolic pathways and adapts to changing environmental conditions	Xu et al., 2014; Lu et al., 2017
Acetylation-driven metabolic network regulation	Alters transcription factors and redox regulatory enzymes to modulate bacterial metabolic pathways	Supports the synthesis of secondary metabolites and adaptation to diverse habitats	Toplak et al., 2022

albicans. As such, it represents a promising target for the development of novel antifungal therapies.

Histone acetylation regulates key physiological processes in *Candida albicans*, such as DNA replication, transcription, and DNA repair, influencing growth, virulence, drug resistance, and environmental adaptability. Histone acetyltransferases (HATs) and histone deacetylases (HDACs) control the acetylation and deacetylation of histones, respectively. During replication, newly synthesized histones are acetylated by HATs, deposited on DNA, and later deacetylated by HDACs; histone chaperones recognize acetylation patterns during this process (Shahbazian and Grunstein, 2007). Additionally, histone acetylation alters chromatin structure, affecting the recruitment of DNA-binding proteins and transcription factors, which in turn modulates gene transcription (Shahbazian and Grunstein, 2007). For example, in *Candida albicans*, acetylation of H3K56 promotes gene transcriptional activation by increasing chromatin accessibility, with its level closely linked to transcription factor binding on chromatin (Wurtele et al., 2010). This modification creates a favorable environment for gene transcription, reshaping the transcriptional profile of *Candida albicans*, aiding host adaptation, and enhancing pathogenicity. Rtt109, another HAT, plays a critical role in DNA damage repair and pathogenicity. Deletion of the rtt109 gene results in heightened endogenous DNA damage and increased susceptibility to host macrophages (Lopes da Rosa et al., 2010). Hat1 also contributes significantly to DNA repair; its loss leads to rapid DNA damage accumulation and shifts the growth pattern from yeast to pseudohyphal form, ultimately reducing survival of *Candida albicans* (Tscherner et al., 2012). These findings emphasize the essential role of histone acetylation in the physiological and pathogenic processes of *Candida albicans*.

Histone acetylation influences the morphological plasticity of *Candida albicans*, determining its environmental adaptability and virulence. *Candida albicans* can transition between yeast, pseudohyphal, and hyphal forms, with the filamentous forms (pseudohyphae and hyphae) playing a critical role in promoting fungal infection and the formation of drug-resistant biofilms (Odds, 1985; Sudbery, 2011). Various enzymes, including HATs and HADCs, are key regulators of this morphological transition. Altered HAT expression significantly impacts *Candida albicans*'s ability to adapt to environmental changes. For example, deletion of the SWR1 gene, which is involved in H2A.Z histone variant deposition, induces chromatin structure changes, promoting the transition between white and opaque morphologies. The SWR1 complex also regulates nucleosome positioning at the WOR1 promoter, a master regulator of the white-opaque switch essential for maintaining phenotypic plasticity (Guan and Liu, 2015). Additionally, MYST family HATs, such as Esa1 and Sas2, contribute to hyphal growth. Loss of Esa1 specifically impairs hyphal formation without affecting overall growth, highlighting the significance of HATs in regulating morphology and pathogenicity. Moreover, certain HADCs, like the NuA4 complex, regulate histone acetylation via enzymes such as Yng2, further influencing morphological transitions (Wang et al., 2013). These insights emphasize the critical role of histone acetylation in controlling *Candida albicans*'s morphological plasticity and its adaptation to various host environments and pathogenic states.

Lysine acetylation is integral to *Candida albicans*' ability to respond to host immune defenses. This pathogen evades immune detection by modulating the expression of oxidative stress response genes, a process tightly regulated by dynamic histone acetylation (Kim et al., 2018). In addition to transcriptional regulation, acetylation also influences structural adaptations that facilitate immune evasion, as the histone deacetylase Sir2 has been shown to promote systemic candidiasis by remodeling the fungal cell wall, thereby reducing the exposure of immunogenic components like mannan and β-glucan. This remodeling diminishes recognition by the host's innate immune system and enhances fungal adhesion to host cells, contributing to increased virulence (Yang et al., 2024). Notably, lysine acetylation at specific sites, such as H3K56, influences *Candida albicans*'s capacity to tolerate oxidative stress and escape immune surveillance (Conte et al., 2024). By altering chromatin structure, histone acetylation modulates gene expression in response to stressors like reactive oxygen species generated by the host immune system. The role of HATs in this process is critical; for instance, *Candida albicans* deficient in the lysine acetyltransferase Gcn5 exhibits reduced survival in THP-1 macrophages and heightened susceptibility to various stressors (Yu et al., 2022).

Furthermore, interactions between host-derived signals and epigenetic modifications, such as lysine acetylation, influence pathogen morphology, enhancing its adaptability to the host environment. Although the molecular mechanisms underlying these processes remain under investigation, it is evident that lysine acetylation plays a key mediating role in *Candida albicans*' resistance to host immune responses.

Lysine acetyltransferases are essential in mediating drug resistance and pathogenicity. The glucosamine-6-phosphate acetyltransferase encoded by the GNA1 gene influences the growth and virulence of *Candida albicans*, with its deletion resulting in a marked reduction in pathogenicity (Mio et al., 2000). Similarly, the HAT encoded by the NGG1 gene is involved in morphological transformation and virulence; its knockout substantially diminishes the strain's pathogenic potential (Li et al., 2017a). Furthermore, Hsp90 plays a critical role in drug resistance and morphogenesis. Research has shown that KDACs exhibit functional redundancy in regulating Hsp90 activity, and their inhibition can enhance the effectiveness of antifungal treatments (Li et al., 2017b).

In conclusion, lysine acetylation contributes significantly to the morphological adaptability, immune evasion, and drug resistance of *Candida albicans* by modulating chromatin structure, gene expression, and stress responses (Table 4). These epigenetic mechanisms not only enhance understanding of *Candida albicans* pathogenicity but also open avenues for the development of novel antifungal therapies. Although direct evidence of oral-specific acetylation mechanisms is currently lacking, the unique characteristics of the oral environment and the role of acetylation in gene regulation warrant further investigation into this area.

TABLE 4 Lysine acetylation in oral *Candida albicans*.

Lysine acetylation in *oral Candida albicans*			
Mechanism	Effect	Biological function	References
Acetylation of H3K56	Promotes gene transcription by increasing chromatin accessibility	Enhances transcriptional activation, aiding host adaptation and pathogenicity	Wurtele et al., 2010
Rtt109-mediated acetylation	Plays a role in DNA damage repair and pathogenicity	Protects against DNA damage and enhances survival in macrophages	Lopes da Rosa et al., 2010
Hat1-mediated acetylation	Modifies chromatin structure and promotes DNA repair	Impacts DNA damage response and growth pattern changes, reducing survival	Tscherner et al., 2012
SWR1 complex-mediated acetylation	Modulates nucleosome positioning and chromatin structure changes	Regulates white-opaque morphological transition and phenotypic plasticity	Guan and Liu, 2015
MYST family HATs, including Esa1 and Sas2, acetylation	Impairs hyphal growth upon Esa1 deletion	Contributes to hyphal growth and virulence	Wang et al., 2013
Histone acetylation by NuA4 complex	Regulates histone acetylation, influencing morphological transitions	Affects hyphal transition and virulence	Wang et al., 2013
Gcn5-mediated acetylation in response to host signals	Alters histone acetylation, influencing survival in macrophages	Regulates stress response and immune evasion	Yu et al., 2022
Glucosamine-6-phosphate acetyltransferase by GNA1	Regulates growth and virulence	Modulates pathogenicity and immune evasion	Mio et al., 2000
NGG1 gene-encoded HAT activity	Involves in morphological transformation and virulence	Influences pathogenic potential through morphological regulation	Li et al., 2017a
Hsp90 regulation by KDACs	Enhances antifungal treatment effectiveness by regulating Hsp90 activity	Plays a critical role in drug resistance and morphogenesis	Li et al., 2017b

5 Potential of protein acetylation in the prevention and treatment of oral diseases

Protein lysine acetylation plays a critical role in microbial physiology, influencing both metabolism and pathogenic potential. Recently, it has garnered significant attention in the context of oral diseases. Lysine acetylation influences the onset and progression of conditions such as dental caries, periodontal disease, and oral mucosal disorders by modulating microbial growth, metabolism, and virulence, offering novel insights and therapeutic strategies for their prevention and treatment.

Histone acetyltransferase-based treatments have been utilized in various clinical applications. Many cellular proteins undergo acetylation post-translationally, resulting in alterations to their structure and function. Consequently, HDAC inhibitors have been developed as therapeutic agents, with two currently approved by the US FDA for the treatment of cutaneous T-cell lymphoma (Richon et al., 2009). Moreover, lysine acetyltransferases are emerging as promising drug targets (Folders et al., 2000).

In dental caries research, aspirin, a non-enzymatic acetylating agent, reduces Gtfs activity in *Streptococcus mutans*. It also inhibits the growth of *Streptococcus mutans* and the production of EPS, highlighting the potential of protein acetylation in anti-caries therapies (Lin et al., 2024).

In the gingival tissue of periodontitis patients, dysregulated histone acetylation and deacetylation, along with alterations in DNA methylation, are closely linked to immune and inflammatory responses. In experimental periodontitis models, histone acetylation-targeting treatments, such as HDAC inhibitors (HDACi) or acetylated histone mimetics, effectively prevent alveolar bone loss (Cantley et al., 2011; Meng et al., 2014; Li et al., 2020), offering a novel therapeutic approach for periodontal diseases.

In *Candida albicans*, lysine 56 of histone H3 undergoes acetylation by the acetyltransferase Rtt109p, and pharmacological inhibition or genetic modulation of this enzyme has been proposed as a potential antifungal therapeutic strategy. Acetylation events, often challenging to detect, can significantly impact protein functions, including stability and crystallinity (Mahon et al., 2015). For therapeutic proteins, such modifications may influence immunogenicity and biological activity, thereby affecting safety and efficacy in clinical applications (Walsh and Jefferis, 2006).

Overall, lysine acetylation plays a key role in regulating the metabolism and pathogenicity of oral pathogens by modulating the activity of critical enzymes. Research in this area not only enhances understanding of the pathogenic mechanisms of oral pathogens but also lays a foundation for the development of novel antibacterial and antifungal therapies. Targeting specific acetylases could substantially improve the efficacy of current treatments and offer potential solutions to manage drug resistance. Future investigations should focus on the role of acetylation in the oral microbiota and its impact on host-pathogen interactions, thus paving the way for new strategies in maintaining oral health and addressing oral diseases.

6 Conclusion and prospect

Acetylation, a key PTM, is central to the functional regulation of oral microorganisms. It modulates various bacterial physiological processes, including metabolism, cell signaling, virulence factor expression, and host-pathogen interactions, by altering protein properties such as structure, activity, localization, and interactions with other biomolecules.

This modification significantly impacts the metabolic state of oral bacteria. While acetylation is typically catalyzed by acetyltransferases, it can also occur non-enzymatically via Ac-CoA (Paik et al., 1970; Yan et al., 2008) or acetyladenylate (Ramponi et al., 1975). As a metabolic intermediate, acetylation enables bacteria to adapt to environmental fluctuations and shifts in metabolic activity, thereby playing a crucial role in the regulation of bacterial physiology and pathogenicity.

Acetylation, along with other PTMs such as succinylation and phosphorylation, collectively regulates bacterial protein functions, forming a complex modification network (Latham and Dent, 2007). This cross-regulation of multiple modifications is essential for controlling bacterial virulence factors, adaptive responses, and metabolic processes. For example, in *Porphyromonas gingivalis*, substantial overlap has been observed between acetylation and succinylation sites—especially on ribosomal and metabolic proteins—suggesting potential competitive or cooperative regulation of key cellular functions (Zeng et al., 2020). Additionally, the response regulator RprY in *Porphyromonas gingivalis* is modified by both acetylation and phosphorylation, with each modification exerting distinct effects on its DNA-binding activity and transcriptional regulation (Li et al., 2018). These findings underscore the existence of an intricate PTM crosstalk network that supports bacterial adaptation to fluctuating environmental and host-derived conditions. Nevertheless, systematic studies on the functional interplay among different PTMs in oral microorganisms remain limited. Future research should aim to elucidate the molecular mechanisms and biological consequences of these interactions—particularly the synergistic or antagonistic effects between acetylation, phosphorylation, and succinylation—in governing microbial adaptation, pathogenicity, and immune evasion.

Despite extensive research on acetylation, significant gaps remain in the study of acetylation in oral bacteria. Most investigations have concentrated on a limited number of oral pathogens, such as *Porphyromonas gingivalis* and *Streptococcus mutans*. It is important to note that lysine acetylation is a widely conserved modification across diverse oral microbial taxa. Nevertheless, functional studies and comprehensive acetylomic profiling in other clinically relevant oral species—such as *Fusobacterium nucleatum*, *Prevotella intermedia*, and *Veillonella* spp.—remain limited. To address this, future research should broaden the scope of study to include a wider range of oral bacteria and conduct comprehensive acetylomics analyses to better elucidate the acetylation patterns and functions across diverse physiological and pathological states.

From a clinical standpoint, acetylation represents a key mechanism in regulating bacterial virulence and drug resistance, offering potential new targets for the treatment of oral infections. Investigating the role of acetylation in oral microbiota could provide a theoretical foundation for the development of novel antibacterial strategies. Future research should not only examine the fundamental role of acetylation in bacterial function but also explore strategies to mitigate bacterial pathogenicity through acetylation regulation, particularly by targeting the acetylation of key virulence factors to enhance therapeutic outcomes.

In conclusion, acetylation plays a crucial role in the adaptation, virulence, and immune evasion of oral microorganisms. Advances in technologies such as metabolomics, proteomics, and mass spectrometry will further elucidate the role of acetylation in bacterial physiological and pathological processes. This enhanced understanding will not only clarify the mechanisms underlying the virulence of oral bacteria but also open new avenues for the treatment of oral diseases.

Author contributions

YCY: Writing – original draft, Investigation, Funding acquisition, Writing – review & editing. HH: Conceptualization, Supervision, Writing – review & editing. BL: Writing – review & editing. ZL: Supervision, Writing – review & editing. JS: Writing – review & editing. ZZ: Writing – review & editing, Conceptualization, Supervision. YY: Conceptualization, Funding acquisition, Supervision, Writing – review & editing.

Funding

The author(s) declare that financial support was received for the research and/or publication of this article. This work was supported by the National Natural Science Foundation of China (Grant No. 82301063), Hunan Provincial Natural Science Foundation of China (Grant No. 2023JJ30815), the Science and Technology Innovation Program of Hunan Province (Grant No. 2024RC3069) and the Hunan Provincial Innovation Foundation for Postgraduate (Grant No. 2024ZZTS0278).

Conflict of interest

The authors declare that the research was conducted in the absence of any commercial or financial relationships that could be construed as a potential conflict of interest.

Generative AI statement

The author(s) declare that no Generative AI was used in the creation of this manuscript.

Publisher's note

References

AbouElfetouh, A., Kuhn, M. L., Hu, L. I., Scholle, M. D., Sorensen, D. J., Sahu, A. K., et al. (2015). The E. coli sirtuin CobB shows no preference for enzymatic and nonenzymatic lysine acetylation substrate sites. *Microbiologyopen* 4, 66–83. doi: 10.1002/mbo3.223

Allfrey, V. G., Faulkner, R., and Mirsky, A. E. (1964). Acetylation and methylation of histones and their possible role in the regulation of RNA synthesis. *Proc. Natl. Acad. Sci. U S A* 51, 786–794. doi: 10.1073/pnas.51.5.786

Aruni, A. W., Lee, J., Osbourne, D., Dou, Y., Roy, F., Muthiah, A., et al. (2012). VimA-dependent modulation of acetyl coenzyme A levels and lipid A biosynthesis can alter virulence in Porphyromonas gingivalis. *Infect. Immun.* 80, 550–564. doi: 10.1128/IAI.06062-11

Blander, G., and Guarente, L. (2004). The Sir2 family of protein deacetylases. *Annu. Rev. Biochem.* 73, 417–435. doi: 10.1146/annurev.biochem.73.011303.073651

Butler, C. A., Veith, P. D., Nieto, M. F., Dashper, S. G., and Reynolds, E. C. (2015). Lysine acetylation is a common post-translational modification of key metabolic pathway enzymes of the anaerobe Porphyromonas gingivalis. *J. Proteomics* 128, 352–364. doi: 10.1016/j.jprot.2015.08.015

Cantley, M. D., Bartold, P. M., Marino, V., Fairlie, D. P., Le, G. T., Lucke, A. J., et al. (2011). Histone deacetylase inhibitors and periodontal bone loss. *J. Periodontal Res.* 46, 697–703. doi: 10.1111/j.1600-0765.2011.01392.x

Carafa, V., Nebbioso, A., and Altucci, L. (2012). Sirtuins and disease: the road ahead. *Front. Pharmacol.* 3. doi: 10.3389/fphar.2012.00004

Chen, Y., Sprung, R., Tang, Y., Ball, H., Sangras, B., Kim, S. C., et al. (2007). Lysine propionylation and butyrylation are novel post-translational modifications in histones. *Mol. Cell Proteomics* 6, 812–819. doi: 10.1074/mcp.M700021-MCP200

Chuang, C., Lin, S. H., Huang, F., Pan, J., Josic, D., and Yu-Lee, L. Y. (2010). Acetylation of RNA processing proteins and cell cycle proteins in mitosis. *J. Proteome Res.* 9, 4554–4564. doi: 10.1021/pr100281h

Conte, M., Eletto, D., Pannetta, M., Esposito, R., Monti, M. C., Morretta, E., et al. (2024). H3K56 acetylation affects Candida albicans morphology and secreted soluble factors interacting with the host. *Biochim. Biophys. Acta Gene Regul. Mech.* 1867, 195048. doi: 10.1016/j.bbagrm.2024.195048

Di, Y., Xu, S., Chi, M., Hu, Y., Zhang, X., Wang, H., et al. (2023). Acetylation of cyclic AMP receptor protein by acetyl phosphate modulates mycobacterial virulence. *Microbiol Spectr.* 11, e0400222. doi: 10.1128/spectrum.04002-22

Folders, J., Tommassen, J., van Loon, L. C., and Bitter, W. (2000). Identification of a chitin-binding protein secreted by Pseudomonas aeruginosa. *J. Bacteriol* 182, 1257–1263. doi: 10.1128/JB.182.5.1257-1263.2000

Gardner, J. G., Grundy, F. J., Henkin, T. M., and Escalante-Semerena, J. C. (2006). Control of acetyl-coenzyme A synthetase (AcsA) activity by acetylation/deacetylation without NAD(+) involvement in Bacillus subtilis. *J. Bacteriol* 188, 5460–5468. doi: 10.1128/JB.00215-06

Guan, Z., and Liu, H. (2015). Overlapping functions between SWR1 deletion and H3K56 acetylation in candida albicans. *Eukaryot Cell* 14, 578–587. doi: 10.1128/EC.00002-15

Hentchel, K. L., and Escalante-Semerena, J. C. (2015). Acylation of biomolecules in prokaryotes: a widespread strategy for the control of biological function and metabolic stress. *Microbiol Mol. Biol. Rev.* 79, 321–346. doi: 10.1128/MMBR.00020-15

Hesketh, A. R., Chandra, G., Shaw, A. D., Rowland, J. J., Kell, D. B., Bibb, M. J., et al. (2002). Primary and secondary metabolism, and post-translational protein modifications, as portrayed by proteomic analysis of Streptomyces coelicolor. *Mol. Microbiol* 46, 917–932. doi: 10.1046/j.1365-2958.2002.03219.x

Ishigaki, Y., Akanuma, G., Yoshida, M., Horinouchi, S., Kosono, S., and Ohnishi, Y. (2017). Protein acetylation involved in streptomycin biosynthesis in Streptomyces griseus. *J. Proteomics* 155, 63–72. doi: 10.1016/j.jprot.2016.12.006

Kim, J., Lee, J. E., and Lee, J. S. (2015). Histone deacetylase-mediated morphological transition in Candida albicans. *J. Microbiol* 53, 805–811. doi: 10.1007/s12275-015-5488-3

Kim, J., Park, S., and Lee, J. S. (2018). Epigenetic control of oxidative stresses by histone acetyltransferases in candida albicans. *J. Microbiol Biotechnol.* 28, 181–189. doi: 10.4014/jmb.1707.07029

Kuhn, M. L., Zemaitaitis, B., Hu, L. I., Sahu, A., Sorensen, D., Minasov, G., et al. (2014). Structural, kinetic and proteomic characterization of acetyl phosphate-dependent bacterial protein acetylation. *PloS One* 9, e94816. doi: 10.1371/journal.pone.0094816

Lammers, M. (2021). Post-translational lysine ac(et)ylation in bacteria: A biochemical, structural, and synthetic biological perspective. *Front. Microbiol* 12. doi: 10.3389/fmicb.2021.757179

Latham, J. A., and Dent, S. Y. (2007). Cross-regulation of histone modifications. *Nat. Struct. Mol. Biol.* 14, 1017–1024. doi: 10.1038/nsmb1307

Lei, L., Zeng, J., Wang, L., Gong, T., Zheng, X., Qiu, W., et al. (2021). Quantitative acetylome analysis reveals involvement of glucosyltransferase acetylation in Streptococcus mutans biofilm formation. *Environ. Microbiol Rep.* 13, 86–97. doi: 10.1111/1758-2229.12907

Li, D. D., Fuchs, B. B., Wang, Y., Huang, X. W., Hu, D. D., Sun, Y., et al. (2017a). Histone acetyltransferase encoded by NGG1 is required for morphological conversion and virulence of Candida albicans. *Future Microbiol* 12, 1497–1510. doi: 10.2217/fmb-2017-0084

Li, Y., Krishnan, K., and Duncan, M. J. (2018). Post-translational regulation of a Porphyromonas gingivalis regulator. *J. Microbiol* 10, 1487743. doi: 10.1080/20002297.2018.1487743

Li, Q., Liu, F., Dang, R., Feng, C., Xiao, R., Hua, Y., et al. (2020). Epigenetic modifier trichostatin A enhanced osteogenic differentiation of mesenchymal stem cells by inhibiting NF-kappaB (p65) DNA binding and promoted periodontal repair in rats. *J. Cell Physiol.* 235, 9691–9701. doi: 10.1002/jcp.29780

Li, J., Ma, Q., Huang, J., Liu, Y., Zhou, J., Yu, S., et al. (2024). Small RNA SmsR1 modulates acidogenicity and cariogenic virulence by affecting protein acetylation in Streptococcus mutans. *PloS Pathog* 20, e1012147. doi: 10.1371/journal.ppat.1012147

Li, X., Robbins, N., O'Meara, T. R., and Cowen, L. E. (2017b). Extensive functional redundancy in the regulation of Candida albicans drug resistance and morphogenesis by lysine deacetylases Hos2, Hda1, Rpd3 and Rpd31. *Mol. Microbiol* 103, 635–656. doi: 10.1111/mmi.13578

Liao, G., Xie, L., Li, X., Cheng, Z., and Xie, J. (2014). Unexpected extensive lysine acetylation in the trump-card antibiotic producer Streptomyces roseosporus revealed by proteome-wide profiling. *J. Proteomics* 106, 260–269. doi: 10.1016/j.jprot.2014.04.017

Lin, Y., Ma, Q., Yan, J., Gong, T., Huang, J., Chen, J., et al. (2024). Inhibition of Streptococcus mutans growth and biofilm formation through protein acetylation. *Mol. Microbiol* 39, 334–343. doi: 10.1111/omi.12452

Lin, H., Su, X., and He, B. (2012). Protein lysine acylation and cysteine succination by intermediates of energy metabolism. *ACS Chem. Biol.* 7, 947–960. doi: 10.1021/cb3001793

Lopes da Rosa, J., Boyartchuk, V. L., Zhu, L. J., and Kaufman, P. D. (2010). Histone acetyltransferase Rtt109 is required for Candida albicans pathogenesis. *Proc. Natl. Acad. Sci. U S A* 107, 1594–1599. doi: 10.1073/pnas.0912427107

Lu, J. Y., Lin, Y. Y., Sheu, J. C., Wu, J. T., Lee, F. J., Chen, Y., et al. (2011). Acetylation of yeast AMPK controls intrinsic aging independently of caloric restriction. *Cell* 146, 969–979. doi: 10.1016/j.cell.2011.07.044

Lu, Y. X., Liu, X. X., Liu, W. B., and Ye, B. C. (2017). Identification and characterization of two types of amino acid-regulated acetyltransferases in actinobacteria. *Biosci Rep.* 37 (4), BSR20170157. doi: 10.1042/BSR20170157

Lukat, G. S., McCleary, W. R., Stock, A. M., and Stock, J. B. (1992). Phosphorylation of bacterial response regulator proteins by low molecular weight phospho-donors. *Proc. Natl. Acad. Sci. U S A* 89, 718–722. doi: 10.1073/pnas.89.2.718

Ma, Q., Li, J., Yu, S., Liu, Y., Zhou, J., Wang, X., et al. (2024a). ActA-mediated PykF acetylation negatively regulates oxidative stress adaptability of Streptococcus mutans. *mBio* 15, e0183924. doi: 10.1128/mbio.01839-24

Ma, Q., Li, J., Yu, S., Zhou, J., Liu, Y., Wang, X., et al. (2024b). YkuR functions as a protein deacetylase in Streptococcus mutans. *Proc. Natl. Acad. Sci. U S A* 121, e2407820121. doi: 10.1073/pnas.2407820121

Ma, Q., Pan, Y., Chen, Y., Yu, S., Huang, J., Liu, Y., et al. (2021a). Acetylation of glucosyltransferases regulates Streptococcus mutans biofilm formation and virulence. *PloS Pathog* 17, e1010134. doi: 10.1371/journal.ppat.1010134

Ma, Q., Pan, Y., Chen, Y., Yu, S., Huang, J., Liu, Y., et al. (2022). Acetylation of lactate dehydrogenase negatively regulates the acidogenicity of streptococcus mutans. *mBio* 13, e0201322. doi: 10.1128/mbio.02013-22

Ma, Q., Zhang, Q., Chen, Y., Yu, S., Huang, J., Liu, Y., et al. (2021b). Post-translational modifications in oral bacteria and their functional impact. *Front. Microbiol* 12. doi: 10.3389/fmicb.2021.784923

Mahon, B. P., Lomelino, C. L., Salguero, A. L., Driscoll, J. M., Pinard, M. A., and McKenna, R. (2015). Observed surface lysine acetylation of human carbonic anhydrase II expressed in Escherichia coli. *Protein Sci.* 24, 1800–1807. doi: 10.1002/pro.2771

Martín, J. F., Liras, P., and Sanchez, S. (2021). Modulation of gene expression in actinobacteria by translational modification of transcriptional factors and secondary metabolite biosynthetic enzymes. *Front. Microbiol* 12. doi: 10.3389/fmicb.2021.630694

Meng, S., Zhang, L., Tang, Y., Tu, Q., Zheng, L., Yu, L., et al. (2014). BET inhibitor JQ1 blocks inflammation and bone destruction. *J. Dent. Res.* 93, 657–662. doi: 10.1177/0022034514534261

Mikulik, K., Felsberg, J., Kudrnacova, E., Bezouskova, S., Setinova, D., Stodulkova, E., et al. (2012). CobB1 deacetylase activity in Streptomyces coelicolor. *Biochem. Cell Biol.* 90, 179–187. doi: 10.1139/o11-086

Minguez, P., Parca, L., Diella, F., Mende, D. R., Kumar, R., Helmer-Citterich, M., et al. (2012). Deciphering a global network of functionally associated post-translational modifications. *Mol. Syst. Biol.* 8, 599. doi: 10.1038/msb.2012.31

Mio, T., Kokado, M., Arisawa, M., and Yamada-Okabe, H. (2000). Reduced virulence of Candida albicans mutants lacking the GNA1 gene encoding glucosamine-6-phosphate acetyltransferase. *Microbiol. (Reading)* 146, 1753–1758. doi: 10.1099/00221287-146-7-1753

Mishra, A., Roy, F., Dou, Y., Zhang, K., Tang, H., Fletcher, H. M., et al. (2018). Role of acetyltransferase PG1842 in gingipain biogenesis in porphyromonas gingivalis. *J. Bacteriology* 200 (21), e00385-18. doi: 10.1128/jb.00385-18

Montellier, E., Rousseaux, S., Zhao, Y., and Khochbin, S. (2012). Histone crotonylation specifically marks the haploid male germ cell gene expression program: post-meiotic male-specific gene expression. *Bioessays* 34, 187–193. doi: 10.1002/bies.201100141

Moreira, I. S., Fernandes, P. A., and Ramos, M. J. (2007). Hot spots–a review of the protein-protein interface determinant amino-acid residues. *Proteins* 68, 803–812. doi: 10.1002/prot.21396

Odds, F. C. (1985). Morphogenesis in candida albicans. *Crit. Rev. Microbiol* 12, 45–93. doi: 10.3109/10408418509104425

Paik, W. K., Pearson, D., Lee, H. W., and Kim, S. (1970). Nonenzymatic acetylation of histones with acetyl-CoA. *Biochim. Biophys. Acta* 213, 513–522. doi: 10.1016/0005-2787(70)90058-4

Peng, C., Lu, Z., Xie, Z., Cheng, Z., Chen, Y., Tan, M., et al. (2011). The first identification of lysine malonylation substrates and its regulatory enzyme. *Mol. Cell Proteomics* 10, M111 012658. doi: 10.1074/mcp.M111.012658

Ramponi, G., Manao, G., and Camici, G. (1975). Nonenzymatic acetylation of histones with acetyl phosphate and acetyl adenylate. *Biochemistry* 14, 2681–2685. doi: 10.1021/bi00683a018

Ren, J., Sang, Y., Lu, J., and Yao, Y. F. (2017). Protein acetylation and its role in bacterial virulence. *Trends Microbiol* 25, 768–779. doi: 10.1016/j.tim.2017.04.001

Richon, V. M., Garcia-Vargas, J., and Hardwick, J. S. (2009). Development of vorinostat: current applications and future perspectives for cancer therapy. *Cancer Lett.* 280, 201–210. doi: 10.1016/j.canlet.2009.01.002

Shahbazian, M. D., and Grunstein, M. (2007). Functions of site-specific histone acetylation and deacetylation. *Annu. Rev. Biochem.* 76, 75–100. doi: 10.1146/annurev.biochem.76.052705.162114

Starai, V. J., Celic, I., Cole, R. N., Boeke, J. D., and Escalante-Semerena, J. C. (2002). Sir2-dependent activation of acetyl-CoA synthetase by deacetylation of active lysine. *Science* 298, 2390–2392. doi: 10.1126/science.1077650

Starai, V. J., and Escalante-Semerena, J. C. (2004). Identification of the protein acetyltransferase (Pat) enzyme that acetylates acetyl-CoA synthetase in Salmonella enterica. *J. Mol. Biol.* 340, 1005–1012. doi: 10.1016/j.jmb.2004.05.010

Sudbery, P. E. (2011). Growth of Candida albicans hyphae. *Nat. Rev. Microbiol* 9, 737–748. doi: 10.1038/nrmicro2636

Tan, Y., Xu, Z., Tao, J., Ni, J., Zhao, W., Lu, J., et al. (2016). A SIRT4-like auto ADP-ribosyltransferase is essential for the environmental growth of Mycobacterium smegmatis. *Acta Biochim. Biophys. Sin. (Shanghai)* 48, 145–152. doi: 10.1093/abbs/gmv121

Toplak, M., Nagel, A., Frensch, B., Lechtenberg, T., and Teufel, R. (2022). An acetyltransferase controls the metabolic flux in rubromycin polyketide biosynthesis by direct modulation of redox tailoring enzymes. *Chem. Sci.* 13, 7157–7164. doi: 10.1039/d2sc01952c

Tscherner, M., Stappler, E., Hnisz, D., and Kuchler, K. (2012). The histone acetyltransferase Hat1 facilitates DNA damage repair and morphogenesis in Candida albicans. *Mol. Microbiol* 86, 1197–1214. doi: 10.1111/mmi.12051

Tu, S., Guo, S. J., Chen, C. S., Liu, C. X., Jiang, H. W., Ge, F., et al. (2015). YcgC represents a new protein deacetylase family in prokaryotes. *Elife* 4, e05322. doi: 10.7554/eLife.05322

Tucker, A. C., and Escalante-Semerena, J. C. (2013). Acetoacetyl-CoA synthetase activity is controlled by a protein acetyltransferase with unique domain organization in Streptomyces lividans. *Mol. Microbiol* 87, 152–167. doi: 10.1111/mmi.12088

Wagner, G. R., and Payne, R. M. (2013). Widespread and enzyme-independent Nepsilon-acetylation and Nepsilon-succinylation of proteins in the chemical conditions of the mitochondrial matrix. *J. Biol. Chem.* 288, 29036–29045. doi: 10.1074/jbc.M113.486753

Walsh, G., and Jefferis, R. (2006). Post-translational modifications in the context of therapeutic proteins. *Nat. Biotechnol.* 24, 1241–1252. doi: 10.1038/nbt1252

Wang, X., Chang, P., Ding, J., and Chen, J. (2013). Distinct and redundant roles of the two MYST histone acetyltransferases Esa1 and Sas2 in cell growth and morphogenesis of Candida albicans. *Eukaryot Cell* 12, 438–449. doi: 10.1128/EC.00275-12

Wang, Q., Zhang, Y., Yang, C., Xiong, H., Lin, Y., Yao, J., et al. (2010). Acetylation of metabolic enzymes coordinates carbon source utilization and metabolic flux. *Science* 327, 1004–1007. doi: 10.1126/science.1179687

Weinert, B. T., Iesmantavicius, V., Wagner, S. A., Scholz, C., Gummesson, B., Beli, P., et al. (2013). Acetyl-phosphate is a critical determinant of lysine acetylation in E. coli. *Mol. Cell* 51, 265–272. doi: 10.1016/j.molcel.2013.06.003

Wellen, K. E., and Thompson, C. B. (2012). A two-way street: reciprocal regulation of metabolism and signalling. *Nat. Rev. Mol. Cell Biol.* 13, 270–276. doi: 10.1038/nrm3305

Wu, L., Gong, T., Zhou, X., Zeng, J., Huang, R., Wu, Y., et al. (2019). Global analysis of lysine succinylome in the periodontal pathogen Porphyromonas gingivalis. *Mol. Microbiol* 34, 74–83. doi: 10.1111/omi.12255

Wurtele, H., Tsao, S., Lepine, G., Mullick, A., Tremblay, J., Drogaris, P., et al. (2010). Modulation of histone H3 lysine 56 acetylation as an antifungal therapeutic strategy. *Nat. Med.* 16, 774–780. doi: 10.1038/nm.2175

Xu, J. Y., You, D., Leng, P. Q., and Ye, B. C. (2014). Allosteric regulation of a protein acetyltransferase in Micromonospora aurantiaca by the amino acids cysteine and arginine. *J. Biol. Chem.* 289, 27034–27045. doi: 10.1074/jbc.M114.579078

Yan, J., Barak, R., Liarzi, O., Shainskaya, A., and Eisenbach, M. (2008). *In vivo* acetylation of CheY, a response regulator in chemotaxis of Escherichia coli. *J. Mol. Biol.* 376, 1260–1271. doi: 10.1016/j.jmb.2007.12.070

Yan, Y., Hailun, H., Fenghui, Y., Pingting, L., Lei, L., Zhili, Z., et al. (2023). Streptococcus mutans dexA affects exopolysaccharides production and biofilm homeostasis. *Mol. Microbiol* 38, 134–144. doi: 10.1111/omi.12395

Yang, C., Li, G., Zhang, Q., Bai, W., Li, Q., Zhang, P., et al. (2024). Histone deacetylase Sir2 promotes the systemic Candida albicans infection by facilitating its immune escape via remodeling the cell wall and maintaining the metabolic activity. *mBio* 15, e0044524. doi: 10.1128/mbio.00445-24

Yang, X. J., and Seto, E. (2008). The Rpd3/Hda1 family of lysine deacetylases: from bacteria and yeast to mice and men. *Nat. Rev. Mol. Cell Biol.* 9, 206–218. doi: 10.1038/nrm2346

Yu, S., Paderu, P., Lee, A., Eirekat, S., Healey, K., Chen, L., et al. (2022). Histone acetylation regulator gcn5 mediates drug resistance and virulence of candida glabrata. *Microbiol Spectr.* 10, e0096322. doi: 10.1128/spectrum.00963-22

Zeng, J., Wu, L., Chen, Q., Wang, L., Qiu, W., Zheng, X., et al. (2020). Comprehensive profiling of protein lysine acetylation and its overlap with lysine succinylation in the Porphyromonas gingivalis fimbriated strain ATCC 33277. *Mol. Microbiol* 35, 240–250. doi: 10.1111/omi.12312

Zhang, Q., Zhou, A., Li, S., Ni, J., Tao, J., Lu, J., et al. (2016). Reversible lysine acetylation is involved in DNA replication initiation by regulating activities of initiator DnaA in Escherichia coli. *Sci. Rep.* 6, 30837. doi: 10.1038/srep30837

Zhao, K., Chai, X., and Marmorstein, R. (2004). Structure and substrate binding properties of cobB, a Sir2 homolog protein deacetylase from Escherichia coli. *J. Mol. Biol.* 337, 731–741. doi: 10.1016/j.jmb.2004.01.060

Zhao, S., Xu, W., Jiang, W., Yu, W., Lin, Y., Zhang, T., et al. (2010). Regulation of cellular metabolism by protein lysine acetylation. *Science* 327, 1000–1004. doi: 10.1126/science.1179689

frontiers | Frontiers in Cellular and Infection Microbiology

TYPE Review
PUBLISHED 01 September 2025
DOI 10.3389/fcimb.2025.1666965

OPEN ACCESS

EDITED BY
Keke Zhang,
Wenzhou Medical University, China

REVIEWED BY
Yaling Jiang,
VU Amsterdam, Netherlands
Hong Chen,
Chongqing Medical University, China
Tao Gong,
State Key Laboratory of Oral Diseases and National Clinical Research Center for Oral Diseases, China

*CORRESPONDENCE
Yang Ning
ningyang@mail.sysu.edu.cn
Ping Li
pingli@gzhmu.edu.cn

†These authors have contributed equally to this work

RECEIVED 16 July 2025
ACCEPTED 18 August 2025
PUBLISHED 01 September 2025

CITATION
Zhou Y, Ji H, Zhang Y, Liu Y, Ning Y and Li P (2025) Mechanisms of fungal pathogenic DNA-activated STING pathway in biofilms and its implication in dental caries onset. *Front. Cell. Infect. Microbiol.* 15:1666965. doi: 10.3389/fcimb.2025.1666965

Mechanisms of fungal pathogenic DNA-activated STING pathway in biofilms and its implication in dental caries onset

Yujie Zhou[1†], Huanzhong Ji[1†], Yuzhe Zhang[1], Yukun Liu[1], Yang Ning[1*] and Ping Li[2,3*]

[1]Hospital of Stomatology, Guangdong Provincial Key Laboratory of Stomatology, Guanghua School of Stomatology, Sun Yat-sen University, Guangzhou, China, [2]Department of Prosthodontics, School and Hospital of Stomatology, Guangzhou Medical University, Guangzhou, Guangdong, China, [3]School and Hospital of Stomatology, Guangdong Engineering Research Center of Oral Restoration and Reconstruction, Guangzhou Medical University, Guangzhou, Guangdong, China

Dental caries, a prevalent oral disease, has long been attributed primarily to bacteria, but emerging evidence highlights the critical role of fungi in its pathogenesis. Fungal biofilms, predominantly *Candida albicans*, release extracellular DNA (eDNA) and DNA-carrying extracellular vesicles (EVs). Together with bacterial eDNA, these form the biofilm matrix and can activate the host cGAS-STING signaling pathway. This review systematically elaborates on the molecular architecture and biological functions of the cGAS-STING pathway, comparing mechanistic differences in its activation by viral, bacterial, and fungal DNA. It further explores direct and indirect modes of STING pathway activation by fungal eDNA and EV-carried DNA, along with their immunoregulatory roles. Specifically, it discusses the interactive mechanisms between fungal biofilms and STING activation in root caries onset, emphasizing the dual effects of STING-mediated immune responses—enhancing antifungal immunity while potentially exacerbating tissue damage via excessive inflammation. Finally, this review outlines current knowledge gaps and future research directions, aiming to provide novel insights for precision prevention and treatment of dental caries.

KEYWORDS

STING pathway, fungal biofilms, extracellular DNA, dental caries, innate immunity

1 Introduction

Dental caries is a highly prevalent chronic oral infectious disease worldwide, with its high incidence and disabling impact posing a serious threat to human oral health and quality of life (Wen et al., 2022; Yirsaw et al., 2024). For a long time, it has been widely accepted that acid production metabolism and biofilm formation by cariogenic bacteria like

Streptococcus mutans are the core mechanisms of dental caries. Related antibacterial strategies have mostly focused on bacteria (Bhat et al., 2023; Jiang et al., 2023). However, with the development of microbiome technologies in recent years, growing evidence indicates that fungi represented by *Candida albicans* play an undeniable role in the occurrence and development of dental caries, especially root caries (Ji et al., 2025; Zhang et al., 2025).

These fungi, together with bacteria, form complex mixed biofilms at carious sites. The extracellular DNA (eDNA) they secrete not only cross-links with bacterial eDNA to form the biofilm matrix skeleton—enhancing community stability and stress resistance—but also acts as a key signaling molecule in host immune regulation (Gallucci, 2024; Geng et al., 2024; Han et al., 2025). Among these, the cGAS-STING signaling pathway serves as a core innate immune hub for cytosolic DNA recognition. The molecular mechanisms by which fungal eDNA and vesicle-carried DNA activate this pathway are critical. They link fungal biofilm colonization to host immune response imbalance (Brown Harding et al., 2024; Yang et al., 2024).

This review systematically clarifies the specific mechanisms by which pathogenic DNA in fungal biofilms—including eDNA and vesicle-carried DNA—activates the STING pathway. It analyzes how these mechanisms regulate immune balance in the caries microenvironment and influence dental hard tissue destruction. It also outlines future research directions. This work lays a theoretical foundation for advancing the understanding of caries etiology and facilitating the development of precise preventive and therapeutic strategies.

2 Molecular architecture and biological functions of the STING signaling pathway

The cGAS-STING signaling pathway acts as a central hub linking cytosolic DNA recognition to innate immune responses (Decout et al., 2021). It plays pivotal roles in defending against pathogenic invasion, regulating anti-tumor immunity, and maintaining autoimmune homeostasis.Cyclic GMP-AMP synthase (cGAS) is a cytosolic DNA sensor, primarily distributed in the cytoplasm and nucleus. Its N-terminal DNA-binding domain (DBD) specifically recognizes double-stranded DNA (dsDNA), including pathogenic DNA, damaged nuclear DNA, and mitochondrial DNA (Gentili et al., 2019). Upon binding to dsDNA, cGAS undergoes conformational changes to activate its C-terminal catalytic domain. This catalyzes the synthesis of the second messenger 2',3'-cyclic GMP-AMP (2',3'-cGAMP) from ATP and GTP.As a unique cyclic dinucleotide (CDN), 2',3'-cGAMP diffuses from its binding site. It then interacts with the transmembrane domain of STING (stimulator of interferon genes), which is localized on the endoplasmic reticulum (ER) (Yu and Liu, 2021; Liu et al., 2022). This interaction induces STING tetramerization and translocation from the ER to the Golgi apparatus and perinuclear vesicles. During translocation, STING recruits the serine/threonine kinase TBK1 (TANK-binding kinase 1). TBK1 phosphorylates the C-terminal tail (CTT) of STING. Activated STING further mediates TBK1-dependent phosphorylation of transcription factors IRF3 (interferon regulatory factor 3) and NF-κB (nuclear factor κB). This drives their nuclear translocation, inducing the expression of type I interferons (IFN-α/β), proinflammatory cytokines (e.g., IL-6, TNF-α), and antiviral proteins (ISGs). This completes the signal cascade amplification (Kwon and Bakhoum, 2020).

Functionally, the cGAS-STING pathway has extensive biological significance. In antiviral immunity, it recognizes viral DNA released by herpesviruses and poxviruses. This induces type I interferons to inhibit viral replication (Decout et al., 2021; Zhang et al., 2024). It also activates innate immune cells such as dendritic cells and macrophages, promoting antigen presentation and initiating adaptive immune responses (Ou et al., 2021; Zhou et al., 2023). In tumor immunoregulation, the pathway recognizes DNA released by necrotic tumor cells. When activated via STING agonists, it enhances the infiltration and activation of cytotoxic T lymphocytes (CTLs). This induces tumor cell apoptosis or autophagy (Samson and Ablasser, 2022). Currently, STING agonists are in clinical trials for melanoma and lung cancer. Their combination with PD-1 inhibitors or chemotherapeutic drugs significantly improves anti-tumor efficacy (Pan et al., 2023; Wang et al., 2024).

However, aberrant activation of the cGAS-STING pathway is linked to various diseases. In autoimmune disorders, self-DNA (e.g., nucleosomal DNA in systemic lupus erythematosus patients) is misrecognized by cGAS. This leads to sustained STING activation and excessive type I interferon production, triggering autoimmune reactions (Zierhut and Funabiki, 2020; Skopelja-Gardner et al., 2022; Liu and Pu, 2023). Patients with Aicardi-Goutières syndrome exhibit abnormal pathway activation due to mutations in cGAS or STING. This results in severe type I interferonopathy (Crow and Manel, 2015). Additionally, mitochondrial DNA leakage into the cytoplasm (e.g., during ischemia-reperfusion injury or neurodegenerative diseases) activates the pathway (Paul et al., 2021; Guo et al., 2024b). This exacerbates inflammatory responses and tissue damage. The pathway also participates in cellular responses to DNA damage. It regulates cell cycle arrest, apoptosis, pyroptosis, and senescence, thereby influencing tissue repair and organismal aging (Bai and Liu, 2019; Schmitz et al., 2023).

3 Mechanistic differences in STING pathway activation by viral and bacterial DNA

Host recognition and clearance of pathogenic microorganisms form a critical defense line of the immune system. Innate immunity acts as the first and fastest barrier against invading microbes. The DNA-activated STING pathway is a key immune mechanism for pathogen recognition. Viruses and bacteria use distinct strategies to deliver DNA into the host cytoplasm, triggering the pathway and inducing immune responses. During viral infection, enveloped

viruses (e.g., herpesviruses, poxviruses) release dsDNA into the cytoplasm via membrane fusion or endocytosis. cGAS specifically recognizes the double-stranded structure, length, and conformational features of viral DNA through its N-terminal DBD. Upon binding, it activates the C-terminal catalytic domain to generate 2',3'-cGAMP.2',3'-cGAMP then binds to ER-localized STING, inducing its activation and translocation to the Golgi apparatus and perinuclear vesicles. This is followed by TBK1 recruitment, which phosphorylates IRF3 and NF-κB. Ultimately, this induces type I interferons and proinflammatory cytokines (Wu et al., 2022; Patel et al., 2023).Notably, some viruses (e.g., adenoviruses) bypass cGAS. They activate STING via direct binding or interference with nucleic acid metabolism (Lam et al., 2014). Retroviral cDNA intermediates and RNA virus-induced mitochondrial DNA leakage also indirectly activate the pathway. To evade immunity, viruses encode proteins that degrade cGAS or inhibit STING translocation (Lange et al., 2022; Xie and Zhu, 2024).

Bacterial activation of the STING pathway differs mechanistically. Intracellular bacteria (e.g., *Listeria monocytogenes*) secrete hemolysins to disrupt phagosomal membranes. This releases bacterial DNA rich in unmethylated CpG motifs into the cytoplasm. These motifs enhance DNA-cGAS binding affinity, promoting 2',3'-cGAMP production (Glomski et al., 2002; Fehér, 2019). Extracellular bacteria (e.g., *Escherichia coli*) inject DNA into host cells via lysis or type III secretion systems (Cornelis, 2000). Beyond the canonical cGAS-dependent pathway, some bacterial DNA is recognized by endosomally localized TLR9. This synergizes with the STING pathway to activate NF-κB and IRF3, amplifying proinflammatory responses (Temizoz et al., 2022; Danielson et al., 2024). However, bacteria also regulate the STING pathway. For example, *Mycobacterium tuberculosis* DNA activates STING, but its cell wall components inhibit STING translocation. This attenuates interferon responses to facilitate survival (Marinho et al., 2017; Sun et al., 2020).

In summary, viral and bacterial activation of the STING pathway both start with cGAS recognition of cytosolic DNA. But they differ significantly in DNA sources, cytosolic delivery modes, recognition priorities, downstream effects, and evasion mechanisms. Viruses primarily rely on their genomic DNA or replication intermediates to activate the pathway, inducing type I interferons to inhibit replication (Zevini et al., 2017). Bacteria deliver DNA via phagosomal disruption or secretion systems, synergizing with other pathways to enhance phagocytic killing (Ryan et al., 2023). These mechanisms highlight the complexity of host-pathogen interactions.

A comparative summary of the key mechanisms underlying STING pathway activation by different pathogens is provided in Table 1. Among these pathogens, fungi exhibit unique activation modes of the STING pathway, which are discussed in detail below.

TABLE 1 Key mechanisms of STING pathway activation by different pathogens (viruses, bacteria, fungi).

Mechanism Category	Viruses	Bacteria	Fungi (represented by *Candida albicans*)	Reference Sequence
DNA Source	Viral genomic DNA or replication intermediates	Bacterial genomic DNA (released into the cytoplasm by intracellular bacteria, and delivered by extracellular bacteria through secretion systems)	Extracellular DNA (eDNA), genomic DNA/mtDNA fragments carried by extracellular vesicles (EVs)	Cornelis, 2000; Bolognesi and Hayashi, 2011; Lam et al., 2014; Rodrigues et al., 2025
Cytoplasmic Delivery Mode	Envelope fusion with host cell membrane, endocytosis	Intracellular bacteria: disruption of phagosomal membrane; Extracellular bacteria: injection via type III secretion system	eDNA: endocytosis, host cell membrane damage; EVs: membrane fusion or endocytosis	Cornelis, 2000; Glomski et al., 2002; Mayer et al., 2013; Lam et al., 2014; Brown Harding et al., 2024; Rodrigues et al., 2025
Host Recognition Receptor	Primarily dependent on cGAS (some viruses can directly bind to STING)	Primarily dependent on cGAS, with some synergy with endosomal TLR9	Primarily dependent on cGAS (requires recognition of double-stranded structure and unmethylated CpG motifs)	Lam et al., 2014; Fehér, 2019; Jannuzzi et al., 2020; Decout et al., 2021; Temizoz et al., 2022
Activation Auxiliary Factors	Length and conformation of viral DNA (e.g., double-stranded structure)	Unmethylated CpG motifs in bacterial DNA (enhancing binding affinity with cGAS)	Accumulation of high-concentration eDNA, phagosomal rupture (*Cryptococcus neoformans*), release of host mtDNA (*Aspergillus fumigatus*), synergy with CLRs and other PRRs	Wagener et al., 2018; Fehér, 2019; Jang et al., 2022; Kim et al., 2023
Escape Strategies	Encoding proteins to degrade cGAS, inhibiting STING translocation	*Mycobacterium tuberculosis*: inhibiting STING translocation; degrading host recognition receptors	Methylation of CpG motifs (reducing affinity with cGAS), secreting proteases to degrade STING, formation of eDNA-polysaccharide complexes to hinder recognition	Gropp et al., 2009; Lam et al., 2014; Valiante et al., 2015; Sun et al., 2020; Jang et al., 2022; Massey et al., 2023; Zhang et al., 2023
Main Immune Effects	Inducing type I interferons (IFN-α/β) to inhibit viral replication	Inducing proinflammatory cytokines (IL-6, TNF-α) to enhance phagocytic bactericidal activity	Inducing type I interferons and proinflammatory cytokines to enhance antifungal immunity; sustained activation may lead to excessive inflammation and tissue damage	Decout et al., 2021; Salgado et al., 2021; Samson and Ablasser, 2022; Temizoz et al., 2022; Brown Harding et al., 2024; Gallucci, 2024; Sun et al., 2024

4 Activation modes and immunoregulation of host STING pathway in fungal infections

During fungal infections, host cells recognize pathogens and initiate immune responses via multiple signaling pathways. Among these, the STING pathway interacts intricately with other immune signaling networks (Chen et al., 2023). As eukaryotic pathogens, fungi exhibit unique and diverse mechanisms for activating the STING pathway, emerging as a research hotspot in recent years.

In direct activation, invasive fungi (e.g., *Candida albicans*) release genomic DNA into the host cytoplasm. This occurs via secreted hydrolases (which disrupt cell membranes) or phagosomal rupture (Naglik et al., 2003; Mayer et al., 2013). Host cGAS recognizes the double-stranded structure, unmethylated CpG motifs, or specific conformational features (dsDNA length >40 bp) of fungal DNA. It then catalyzes 2',3'-cGAMP synthesis. 2',3'-cGAMP binds to ER-localized STING, inducing conformational changes and translocation to the Golgi apparatus. This is followed by TBK1 recruitment, which phosphorylates IRF3 and NF-κB. Ultimately, this induces the expression of type I interferons (e.g., IFN-β) and proinflammatory cytokines (e.g., IL-6, TNF-α), thereby enhancing antifungal immunity (Yu and Liu, 2021; Yum et al., 2021; Su et al., 2022). However, as eukaryotic DNA, fungal DNA has higher CpG methylation levels. Theoretically, it has lower cGAS binding affinity than bacterial DNA. Thus, it requires higher concentrations or specific conditions (e.g., repeated infections, phagosomal rupture) for effective activation (Jeon et al., 2015; Sarkies, 2022). For example, capsular polysaccharides of *Cryptococcus neoformans* promote phagosomal rupture. This increases fungal DNA-cGAS interactions to indirectly enhance STING activation (Liu et al., 2023c).

Non-cGAS-dependent STING activation in fungal infections primarily involves indirect activation via induced host mitochondrial DNA (mtDNA) release (Kim et al., 2023). For instance, hyphal invasion by *Aspergillus fumigatus* causes host mitochondrial damage. Released mtDNA is recognized by cGAS, activating STING. This "self-DNA + pathogen components" dual activation mode amplifies inflammatory responses in chronic infections (e.g., candidemia) (Kim et al., 2023; Peng et al., 2023). Additionally, fungal cell wall components (e.g., β-glucan, mannose) cannot directly activate STING. But they trigger signaling via other pattern recognition receptors (PRRs), synergizing with the STING pathway. Dectin-1, a C-type lectin receptor (CLR), recognizes β-glucan and activates NF-κB via the Syk-Card9 pathway. STING-induced IFN-β upregulates Dectin-1 expression, enhancing phagocytic bactericidal capacity. This "STING-IFN-other PRRs" cascade integrates antifungal immune signals (Wagener et al., 2018; Salgado et al., 2021).

The STING pathway is indispensable for antifungal immunity. On one hand, type I interferons induced by its activation enhance natural killer (NK) cell and T cell activation. They also promote macrophage phagocytosis and bactericidal function (Chen et al., 2023). On the other hand, proinflammatory cytokines recruit neutrophils, forming an inflammatory barrier to restrict fungal diffusion (Robertson et al., 2017). In animal studies, STING-deficient mice show increased susceptibility to *Candida albicans* and *Aspergillus fumigatus* infections. They exhibit elevated fungal burden and exacerbated tissue damage, confirming STING's critical role in host antifungal immunity (Chen et al., 2023). Moreover, the STING pathway interacts with autophagy. STING activation induces autophagy-related genes (e.g., ATG5, ATG7), promoting phagosome-lysosome fusion to accelerate fungal degradation (Liu et al., 2019; Schmid et al., 2024). Autophagy also clears intracellular fungal DNA, avoiding excessive STING activation-induced immunopathological damage. This balances antifungal efficacy and tolerance (Maluquer De Motes, 2022).

Fungi have evolved multiple strategies to evade the STING pathway. At the DNA level, fungi such as *Blastomyces dermatitidis* methylate CpG motifs in their DNA, reducing cGAS binding efficiency (Yu and Liu, 2021). *Cryptococcus neoformans* capsular polysaccharides encapsulate DNA, blocking cGAS recognition (Jang et al., 2022). At the signaling level, *Candida albicans* secretes aspartic proteases (e.g., Sap2) that degrade host STING, inhibiting ER-to-Golgi translocation (Gropp et al., 2009). Mannoproteins in *Aspergillus fumigatus* cell walls competitively bind 2',3'-cGAMP with STING, blocking downstream signaling (Valiante et al., 2015). Additionally, fungi such as *Talaromyces marneffei* inhibit host mtDNA release, reducing cGAS substrates to attenuate STING pathway responses (Zhang et al., 2023).

5 Fungal extracellular DNA: a potential bridge from biofilm matrix to STING pathway activation

Fungal extracellular DNA (eDNA) is a key component of fungal biofilms. It has emerged as a research focus due to its interactions with the host immune system and potential to activate the STING pathway during infections. eDNA refers to DNA actively secreted by fungi or released into the extracellular environment upon cell lysis. It is widely present in biofilm matrices of pathogenic fungi such as *Candida albicans* and *Aspergillus fumigatus* (Rajendran et al., 2013; Juszczak et al., 2024). It is generated via two main pathways: active secretion (dependent on specific fungal secretion systems) and passive release (from cell wall/membrane rupture induced by programmed cell death, mechanical damage, or host immune attacks) (Bolognesi and Hayashi, 2011). Fungal eDNA has double-stranded structures and contains unmethylated CpG motifs, providing a structural basis for recognition by host pattern recognition receptors (Panchin et al., 2016).

Fungal eDNA has multiple biological functions. In biofilm construction and protection, eDNA forms a three-dimensional network via physical cross-linking. It connects hyphae, yeast cells, and extracellular polysaccharides to enhance mechanical stability. It also defends against antifungal drug penetration and host immune clearance. For example, *Candida albicans* eDNA chelates echinocandins, reducing their inhibition of cell wall β-glucan

synthase (Rajendran et al., 2013; Sharma and Rajpurohit, 2024). In regulating fungal physiology and virulence, eDNA acts as a signaling molecule to modulate morphological transitions and virulence factor expression. Its specific sequences bind fungal transcription factors, promoting invasion-related gene expression (Campoccia et al., 2021). Additionally, eDNA mediates intercellular communication. It transfers genetic information via horizontal gene transfer, accelerating the spread of drug resistance or virulence genes among fungal populations (Gonçalves and Gonçalves, 2022).

In host interactions, fungal eDNA both activates innate immunity and participates in immune evasion and pathological damage. It is recognized by host surface or intracellular pattern recognition receptors. Endosomally localized TLR9 recognizes unmethylated CpG motifs in eDNA, activating NF-κB to induce proinflammatory cytokines. cGAS, as a cytosolic DNA sensor, also potentially recognizes eDNA (Jannuzzi et al., 2020). Conversely, high eDNA concentrations inhibit immune functions via multiple mechanisms. These include chelating antimicrobial peptides and immune cell surface receptors to impair phagocytosis, or promoting macrophage polarization toward an anti-inflammatory phenotype to reduce antifungal efficiency (Massey et al., 2023). In chronic fungal infections, sustained eDNA stimulation may induce cytokine storms and tissue damage (Conti et al., 2018).

The potential mechanisms of fungal eDNA-activated STING pathway have attracted significant attention, involving direct and indirect activation. In direct activation, eDNA may enter the cytoplasm via endocytosis or host membrane damage. cGAS recognizes its double-stranded structure and unmethylated CpG motifs, catalyzing 2',3'-cGAMP production. This potentially activates STING, recruits TBK1, phosphorylates IRF3 and NF-κB, and induces type I interferons and proinflammatory cytokines (Liu et al., 2023a; Li et al., 2025). In indirect activation, eDNA may induce host cell damage, promoting mitochondrial DNA (mtDNA) release into the cytoplasm. Or it may synergize with TLR9 and other pattern recognition receptors to enhance STING signaling (Lou and Pickering, 2018; Liu et al., 2023b). Activation efficiency may be influenced by multiple factors. eDNA length, methylation status, and CpG density may affect cGAS binding affinity (Ben Maamar et al., 2023; Dong et al., 2025). eDNA-polysaccharide/protein complexes in biofilms may hinder recognition, while local high concentrations may increase activation probability (LuTheryn et al., 2023). Differences in cGAS-STING pathway sensitivity among host cell types may also impact activation (Li and Bakhoum, 2022).

As a core biofilm component, fungal eDNA's potential to activate the STING pathway reveals novel interaction modes between fungal infections and host immunity. Targeting the eDNA-STING axis may offer new antifungal strategies, such as developing eDNA-degrading nucleases or STING agonists to enhance immunity. However, eDNA-mediated excessive STING activation may contribute to chronic inflammation and autoimmune diseases, necessitating further research into its regulatory mechanisms in pathological states.

6 Mechanisms and immunoregulatory roles of fungal extracellular vesicle–carried DNA in STING pathway activation

Fungal extracellular vesicles (EVs) are membrane-bound vesicles (30–1000 nm in diameter) actively secreted by fungal cells. Their carried DNA plays a key role in host-pathogen interactions (Rodrigues et al., 2025). EV DNA primarily includes genomic DNA fragments, mitochondrial DNA, and cDNA derived from non-coding RNA. Most are in double-stranded or circular forms; some contain unmethylated CpG motifs, endowing potential for recognition by host pattern recognition receptors (Guo et al., 2024a; Ghanam et al., 2025). In pathogenic fungi such as *Candida albicans* and *Aspergillus fumigatus*, DNA constitutes 10%-15% of total EV content. EV secretion and DNA loading efficiency increase significantly during biofilm formation or environmental stress (Ullah et al., 2023).

Functionally, fungal EV DNA has diverse biological significance. In intercellular communication and genetic information transfer, EVs act as "molecular carriers" to transport DNA to recipient fungal cells. This enables horizontal gene transfer, accelerating the spread of drug resistance or virulence genes (Marcilla and Sánchez-López, 2022; Werner Lass et al., 2024). In regulating fungal physiology and virulence, EV DNA modulates gene expression in recipient fungi. For example, Aspergillus fumigatus EV DNA regulates morphology-related genes to promote hyphal growth and enhance invasiveness (Rizzo et al., 2023). Additionally, EV DNA has dual roles in immune regulation. It acts as a pathogen-associated molecular pattern (PAMP) to activate host immunity. It also mediates immune suppression via associated immunomodulatory components to facilitate fungal evasion (Montanari Borges et al., 2024).

In host interactions, fungal EV DNA has complex immunoregulatory properties. EVs enter host cells via endocytosis or membrane fusion, releasing DNA that is recognized by intracellular pattern recognition receptors. Endosomally localized TLR9 recognizes unmethylated CpG motifs in EV DNA, activating NF-κB to induce proinflammatory cytokines (Higuchi et al., 2024). Conversely, some fungal EVs evade immunity. For example, *Cryptococcus neoformans* EV DNA binds immunosuppressive miRNAs to downregulate host cell surface MHC-II expression, impairing antigen presentation (Sk Md et al., 2020). Sustained EV DNA stimulation also induces cytokine imbalance, leading to tissue damage (Fan et al., 2025).

The direct activation pathway of STING by fungal EV-carried DNA likely involves EV entry into host cells via membrane fusion or endocytosis, followed by DNA release. Cytosolic cGAS recognizes this DNA, potentially initiating the 2',3'-cGAMP-STING signaling cascade to induce antiviral immune responses (Brown Harding et al., 2024; Kwaku et al., 2025). Indirect activation

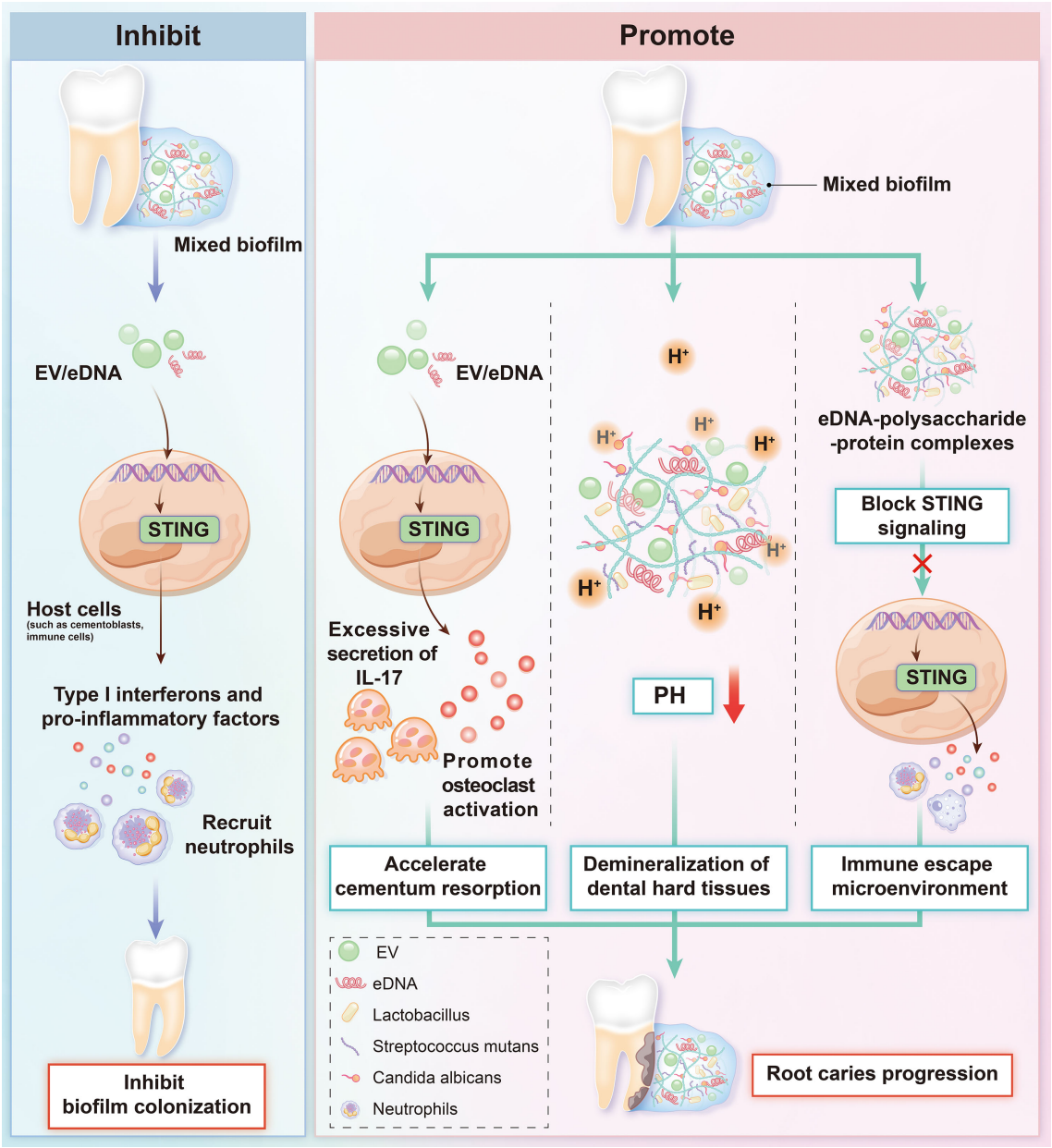

FIGURE 1
Diagram of the interaction between fungal biofilms and the STING pathway in root caries.

may involve EV DNA-induced host mitochondrial damage, releasing mtDNA to activate cGAS. Or it may synergize with EV-carried components (e.g., β-glucan) via TLR pathways to enhance STING signaling (Tao et al., 2024). This process is regulated by multiple factors. EV DNA fragment length, methylation status, and CpG motif density may affect cGAS recognition efficiency. EV source cell types, membrane components, and loaded immunomodulatory molecules may alter DNA delivery efficiency. Host cell type differences influence STING pathway responsiveness, and EV membrane proteins may regulate STING subcellular localization and activation kinetics.

7 Interactive mechanisms between fungal biofilms and STING pathway activation in root caries onset

In the pathogenesis of dental caries, particularly root caries, interactions between fungal biofilms and the STING signaling pathway may form a potential pathogenic hub. At carious sites, *Candida albicans* dominates fungal biofilms and releases extracellular DNA (eDNA) and DNA-carrying extracellular vesicles (EVs). These are recognized by host intracellular cGAS,

activating the STING pathway (Tian et al., 2022; Lattar et al., 2024; Han et al., 2025). *Candida albicans* eDNA, together with eDNA from cariogenic bacteria (e.g., *Streptococcus mutans*, *Lactobacillus*), forms a mixed biofilm matrix via physical cross-linking. This creates a dense three-dimensional network that enhances stability and acid tolerance, synergistically producing acids to exacerbate dental hard tissue demineralization (Sampaio et al., 2019; Evans et al., 2025; Han et al., 2025).

Immunologically, eDNA and EV DNA from mixed biofilms may enter the cytoplasm via endocytosis or membrane damage. This activates the STING pathway, inducing type I interferons and proinflammatory cytokines (Gallucci, 2024). This immune response has dual effects. On one hand, STING activation enhances antifungal immunity to inhibit biofilm colonization. On the other hand, sustained activation may induce excessive secretion of cytokines such as IL-17. This promotes osteoclast activation, accelerates cementum resorption, and drives root caries progression (Mao et al., 2024; Sun et al., 2024). Additionally, eDNA-polysaccharide/protein complexes in the biofilm matrix may block STING signaling, forming an immune-evasive microenvironment (Buzzo et al., 2021). Fungal and cariogenic bacterial metabolic synergies (e.g., carbon source sharing, mutual provision of growth factors) may further amplify inflammatory damage via the STING pathway (Montelongo-Jauregui et al., 2019; Kim et al., 2020). The dynamic interplay between fungal biofilms and the STING pathway offers novel insights into the mechanisms of immune dysregulation and tissue destruction in dental caries (Figure 1).

8 Conclusion and perspective

Fungal DNA released via multiple pathways—including extracellular DNA (eDNA) and extracellular vesicle (EV)-carried DNA—may activate the cGAS-STING signaling pathway to induce host immune responses. This mechanism may play a unique role in dental caries. eDNA and EV DNA from carious fungal biofilms (dominated by *Candida albicans*) may trigger STING activation. This occurs via direct cGAS stimulation or indirect induction of host mitochondrial DNA release. However, activation efficiency may be influenced by the cariogenic microenvironment (e.g., acidic pH, bacterial metabolites). Additionally, synergies between fungal biofilms and cariogenic bacteria (e.g., enhanced acid production) may amplify inflammatory damage via the STING pathway. Meanwhile, eDNA-polysaccharide complexes in the biofilm matrix may block STING signaling, forming an immune-evasive microenvironment. This complex interplay likely has unique significance in immune dysregulation and dental hard tissue destruction in caries.

Current research has not clarified the precise mechanisms of fungal DNA-activated STING pathway in the caries-specific microenvironment. For example, it remains unclear whether acidic conditions affect cGAS recognition efficiency of fungal DNA, or how the fungal-to-bacterial eDNA ratio in biofilms influences STING activation intensity. Future studies should focus on three areas: (1) developing nucleases targeting eDNA or EV inhibitors in cariogenic fungal biofilms to block excessive STING activation; (2) exploring STING pathway modulators in caries to balance antifungal immunity and inflammatory responses; (3) integrating oral microbiome research to dissect dynamic regulation of the fungal DNA-STING pathway during caries progression, providing a theoretical basis for precision caries prevention and treatment.

Author contributions

YJZ: Investigation, Funding acquisition, Writing – original draft. HJ: Writing – review & editing, Investigation, Conceptualization. YZZ: Writing – review & editing. YL: Writing – review & editing. YN: Supervision, Writing – review & editing, Funding acquisition. PL: Writing – review & editing.

Funding

The author(s) declare financial support was received for the research and/or publication of this article. This work was supported by the National Natural Science Foundation of China (Grant No. 82401116), the Guangdong Basic and Applied Basic Research Foundation (Grant No. 2022A1515110846 and No. 2022A1515111068), the Natural Science Foundation of Guangdong Province (Grant No. 2023A1515012257).

Conflict of interest

The authors declare that the research was conducted in the absence of any commercial or financial relationships that could be construed as a potential conflict of interest.

Generative AI statement

The author(s) declare that no Generative AI was used in the creation of this manuscript.

Any alternative text (alt text) provided alongside figures in this article has been generated by Frontiers with the support of artificial intelligence and reasonable efforts have been made to ensure accuracy, including review by the authors wherever possible. If you identify any issues, please contact us.

Publisher's note

References

Bai, J., and Liu, F. (2019). The cGAS-cGAMP-STING pathway: A molecular link between immunity and metabolism. *Diabetes* 68, 1099–1108. doi: 10.2337/dbi18-0052

Ben Maamar, M., Wang, Y., Nilsson, E. E., Beck, D., Yan, W., and Skinner, M. K. (2023). Transgenerational sperm DMRs escape DNA methylation erasure during embryonic development and epigenetic inheritance. *Environ. Epigenet* 9, dvad003. doi: 10.1093/eep/dvad003

Bhat, R., Godovikova, V., Flannagan, S. E., Li, Y., Seseogullari-Dirihan, R., González-Cabezas, C., et al. (2023). Targeting cariogenic streptococcus mutans in oral biofilms with charge-switching smart antimicrobial polymers. *ACS Biomater Sci. Eng.* 9, 318–328. doi: 10.1021/acsbiomaterials.2c01095

Bolognesi, C., and Hayashi, M. (2011). Micronucleus assay in aquatic animals. *Mutagenesis* 26, 205–213. doi: 10.1093/mutage/geq073

Brown Harding, H., Kwaku, G. N., Reardon, C. M., Khan, N. S., Zamith-Miranda, D., Zarnowski, R., et al. (2024). Candida albicans extracellular vesicles trigger type I IFN signalling via cGAS and STING. *Nat. Microbiol.* 9, 95–107. doi: 10.1038/s41564-023-01546-0

Buzzo, J. R., Devaraj, A., Gloag, E. S., Jurcisek, J. A., Robledo-Avila, F., Kesler, T., et al. (2021). Z-form extracellular DNA is a structural component of the bacterial biofilm matrix. *Cell* 184, 5740–5758.e5717. doi: 10.1016/j.cell.2021.10.010

Campoccia, D., Montanaro, L., and Arciola, C. R. (2021). Extracellular DNA (eDNA). A major ubiquitous element of the bacterial biofilm architecture. *Int. J. Mol. Sci.* 22, 9100. doi: 10.3390/ijms22169100

Chen, T., Feng, Y., Sun, W., Zhao, G., Wu, H., Cheng, X., et al. (2023). The nucleotide receptor STING translocates to the phagosomes to negatively regulate anti-fungal immunity. *Immunity* 56, 1727–1742.e1726. doi: 10.1016/j.immuni.2023.06.002

Conti, P., Tettamanti, L., Mastrangelo, F., Ronconi, G., Frydas, I., Kritas, S. K., et al. (2018). Impact of fungi on immune responses. *Clin. Ther.* 40, 885–888. doi: 10.1016/j.clinthera.2018.04.010

Cornelis, G. R. (2000). Type III secretion: a bacterial device for close combat with cells of their eukaryotic host. *Philos. Trans. R Soc. Lond B Biol. Sci.* 355, 681–693. doi: 10.1098/rstb.2000.0608

Crow, Y. J., and Manel, N. (2015). Aicardi-Goutières syndrome and the type I interferonopathies. *Nat. Rev. Immunol.* 15, 429–440. doi: 10.1038/nri3850

Danielson, M., Nicolai, C. J., Vo, T. T., Wolf, N. K., and Burke, T. P. (2024). Cytosolic bacterial pathogens activate TLR pathways in tumors that synergistically enhance STING agonist cancer therapies. *iScience* 27, 111385. doi: 10.1016/j.isci.2024.111385

Decout, A., Katz, J. D., Venkatraman, S., and Ablasser, A. (2021). The cGAS-STING pathway as a therapeutic target in inflammatory diseases. *Nat. Rev. Immunol.* 21, 548–569. doi: 10.1038/s41577-021-00524-z

Dong, L., Hou, Y. R., Xu, N., Gao, X. Q., Sun, Z., Yang, Q. K., et al. (2025). Cyclic GMP-AMP synthase recognizes the physical features of DNA. *Acta Pharmacol. Sin.* 46, 264–270. doi: 10.1038/s41401-024-01369-7

Evans, D. C. S., Kristensen, M. F., Minero, G. A. S., Palmén, L. G., Knap, I., Tiwari, M. K., et al. (2025). Dental biofilms contain DNase I-resistant Z-DNA and G-quadruplexes but alternative DNase overcomes this resistance. *NPJ Biofilms Microbiomes* 11, 80. doi: 10.1038/s41522-025-00694-x

Fan, X., Peng, Y., Li, B., Wang, X., Liu, Y., Shen, Y., et al. (2025). Liver-secreted extracellular vesicles promote cirrhosis-associated skeletal muscle injury through mtDNA-cGAS/STING axis. *Adv. Sci. (Weinh)* 12, e2410439. doi: 10.1002/advs.202410439

Fehér, K. (2019). Single stranded DNA immune modulators with unmethylated cpG motifs: structure and molecular recognition by toll-like receptor 9. *Curr. Protein Pept. Sci.* 20, 1060–1068. doi: 10.2174/1389203720666190830162149

Gallucci, S. (2024). DNA at the center of mammalian innate immune recognition of bacterial biofilms. *Trends Immunol.* 45, 103–112. doi: 10.1016/j.it.2023.12.004

Geng, F., Liu, J., Liu, J., Lu, Z., and Pan, Y. (2024). Recent progress in understanding the role of bacterial extracellular DNA: focus on dental biofilm. *Crit. Rev. Microbiol.* 1-19, 898–916. doi: 10.1080/1040841X.2024.2438117

Gentili, M., Lahaye, X., Nadalin, F., Nader, G. P. F., Puig Lombardi, E., Herve, S., et al. (2019). The N-terminal domain of cGAS determines preferential association with centromeric DNA and innate immune activation in the nucleus. *Cell Rep.* 26, 2377–2393.e2313. doi: 10.1016/j.celrep.2019.01.105

Ghanam, J., Lichá, K., Chetty, V. K., Pour, O. A., Reinhardt, D., Tamášová, B., et al. (2025). Unravelling the significance of extracellular vesicle-associated DNA in cancer biology and its potential clinical applications. *J. Extracell Vesicles* 14, e70047. doi: 10.1002/jev2.70047

Glomski, I. J., Gedde, M. M., Tsang, A. W., Swanson, J. A., and Portnoy, D. A. (2002). The Listeria monocytogenes hemolysin has an acidic pH optimum to compartmentalize activity and prevent damage to infected host cells. *J. Cell Biol.* 156, 1029–1038. doi: 10.1083/jcb.200201081

Gonçalves, P., and Gonçalves, C. (2022). Horizontal gene transfer in yeasts. *Curr. Opin. Genet. Dev.* 76, 101950. doi: 10.1016/j.gde.2022.101950

Gropp, K., Schild, L., Schindler, S., Hube, B., Zipfel, P. F., and Skerka, C. (2009). The yeast Candida albicans evades human complement attack by secretion of aspartic proteases. *Mol. Immunol.* 47, 465–475. doi: 10.1016/j.molimm.2009.08.019

Guo, S., Wang, X., Shan, D., Xiao, Y., Ju, L., Zhang, Y., et al. (2024a). The detection, biological function, and liquid biopsy application of extracellular vesicle-associated DNA. *biomark. Res.* 12, 123. doi: 10.1186/s40364-024-00661-2

Guo, X., Yang, L., Wang, J., Wu, Y., Li, Y., Du, L., et al. (2024b). The cytosolic DNA-sensing cGAS-STING pathway in neurodegenerative diseases. *CNS Neurosci. Ther.* 30, e14671. doi: 10.1111/cns.14671

Han, S. L., Wang, J., Wang, H. S., Yu, P., Wang, L. Y., Ou, Y. L., et al. (2025). Extracellular Z-DNA enhances cariogenicity of biofilm. *J. Dent. Res.* 104, 774–783. doi: 10.1177/00220345251316822

Higuchi, R., Tanaka, K., Saito, Y., Murakami, D., Nakagawa, T., Nutt, S. L., et al. (2024). Type I interferon promotes the fate of Toll-like receptor 9-stimulated follicular B cells to plasma cell differentiation. *PNAS Nexus* 3, pgae152. doi: 10.1093/pnasnexus/pgae152

Jang, E. H., Kim, J. S., Yu, S. R., and Bahn, Y. S. (2022). Unraveling capsule biosynthesis and signaling networks in cryptococcus neoformans. *Microbiol. Spectr.* 10, e0286622. doi: 10.1128/spectrum.02866-22

Jannuzzi, G. P., De Almeida, J. R. F., Paulo, L. N. M., De Almeida, S. R., and Ferreira, K. S. (2020). Intracellular PRRs activation in targeting the immune response against fungal infections. *Front. Cell Infect. Microbiol.* 10, 591970. doi: 10.3389/fcimb.2020.591970

Jeon, J., Choi, J., Lee, G. W., Park, S. Y., Huh, A., Dean, R. A., et al. (2015). Genome-wide profiling of DNA methylation provides insights into epigenetic regulation of fungal development in a plant pathogenic fungus, Magnaporthe oryzae. *Sci. Rep.* 5, 8567. doi: 10.1038/srep08567

Ji, M., Xiong, K., Fu, D., Chi, Y., Wang, Y., Yao, L., et al. (2025). The landscape of the microbiome at different stages of root caries. *Clin. Oral. Investig.* 29, 217. doi: 10.1007/s00784-025-06301-9

Jiang, W., Xie, Z., Huang, S., Huang, Q., Chen, L., Gao, X., et al. (2023). Targeting cariogenic pathogens and promoting competitiveness of commensal bacteria with a novel pH-responsive antimicrobial peptide. *J. Oral. Microbiol.* 15, 2159375. doi: 10.1080/20002297.2022.2159375

Juszczak, M., Zawrotniak, M., and Rapala-Kozik, M. (2024). Complexation of fungal extracellular nucleic acids by host LL-37 peptide shapes neutrophil response to Candida albicans biofilm. *Front. Immunol.* 15, 1295168. doi: 10.3389/fimmu.2024.1295168

Kim, J., Kim, H. S., and Chung, J. H. (2023). Molecular mechanisms of mitochondrial DNA release and activation of the cGAS-STING pathway. *Exp. Mol. Med.* 55, 510–519. doi: 10.1038/s12276-023-00965-7

Kim, H. E., Liu, Y., Dhall, A., Bawazir, M., Koo, H., and Hwang, G. (2020). Synergism of Streptococcus mutans and Candida albicans Reinforces Biofilm Maturation and Acidogenicity in Saliva: An *In Vitro* Study. *Front. Cell Infect. Microbiol.* 10, 623980. doi: 10.3389/fcimb.2020.623980

Kwaku, G. N., Jensen, K. N., Simaku, P., Floyd, D. J., Saelens, J. W., Reardon, C. M., et al. (2025). Extracellular vesicles from diverse fungal pathogens induce species-specific and endocytosis-dependent immunomodulation. *PloS Pathog.* 21, e1012879. doi: 10.1371/journal.ppat.1012879

Kwon, J., and Bakhoum, S. F. (2020). The cytosolic DNA-sensing cGAS-STING pathway in cancer. *Cancer Discov.* 10, 26–39. doi: 10.1158/2159-8290.CD-19-0761

Lam, E., Stein, S., and Falck-Pedersen, E. (2014). Adenovirus detection by the cGAS/STING/TBK1 DNA sensing cascade. *J. Virol.* 88, 974–981. doi: 10.1128/JVI.02702-13

Lange, P. T., White, M. C., and Damania, B. (2022). Activation and evasion of innate immunity by gammaherpesviruses. *J. Mol. Biol.* 434, 167214. doi: 10.1016/j.jmb.2021.167214

Lattar, S. M., Schneider, R. P., Eugenio, V. J., and Padilla, G. (2024). High release of Candida albicans eDNA as protection for the scaffolding of polymicrobial biofilm formed with Staphylococcus aureus and Streptococcus mutans against the enzymatic activity of DNase I. *Braz. J. Microbiol.* 55, 3921–3932. doi: 10.1007/s42770-024-01550-4

Li, J., and Bakhoum, S. F. (2022). The pleiotropic roles of cGAS-STING signaling in the tumor microenvironment. *J. Mol. Cell Biol.* 14, mjac019. doi: 10.1093/jmcb/mjac019

Li, L., He, Y., Chen, Y., and Zhou, X. (2025). cGAS-STING pathway's impact on intestinal barrier. *J. Gastroenterol. Hepatol.* 40, 1381–1392. doi: 10.1111/jgh.16974

Liu, Y., Chen, X., Zhao, Y., Wang, X. Y., Luo, Y. W., Chen, L., et al. (2023a). Small cytosolic double-stranded DNA represses cyclic GMP-AMP synthase activation and induces autophagy. *Cell Rep.* 42, 112852. doi: 10.1016/j.celrep.2023.112852

Liu, Y., and Pu, F. (2023). Updated roles of cGAS-STING signaling in autoimmune diseases. *Front. Immunol.* 14, 1254915. doi: 10.3389/fimmu.2023.1254915

Liu, H., Wang, F., Cao, Y., Dang, Y., and Ge, B. (2022). The multifaceted functions of cGAS. *J. Mol. Cell Biol.* 14, mjac031. doi: 10.1093/jmcb/mjac031

Liu, Y., Wei, F. Z., Zhan, Y. W., Wang, R., Mo, B. Y., and Lin, S. D. (2023b). TLR9 regulates the autophagy-lysosome pathway to promote dendritic cell maturation and

activation by activating the TRAF6-cGAS-STING pathway. *Kaohsiung J. Med. Sci.* 39, 1200–1212. doi: 10.1002/kjm2.12769

Liu, D., Wu, H., Wang, C., Li, Y., Tian, H., Siraj, S., et al. (2019). STING directly activates autophagy to tune the innate immune response. *Cell Death Differ* 26, 1735–1749. doi: 10.1038/s41418-018-0251-z

Liu, Y., Zhang, Y., Zhao, X., Lu, W., Zhong, Y., and Fu, Y. V. (2023c). Antifungal peptide SP1 damages polysaccharide capsule of cryptococcus neoformans and enhances phagocytosis of macrophages. *Microbiol. Spectr.* 11, e0456222. doi: 10.1128/spectrum.04562-22

Lou, H., and Pickering, M. C. (2018). Extracellular DNA and autoimmune diseases. *Cell Mol. Immunol.* 15, 746–755. doi: 10.1038/cmi.2017.136

LuTheryn, G., Ho, E. M. L., Choi, V., and Carugo, D. (2023). Cationic microbubbles for non-selective binding of cavitation nuclei to bacterial biofilms. *Pharmaceutics* 15, 1495. doi: 10.3390/pharmaceutics15051495

Maluquer De Motes, C. (2022). Autophagy takes the STING out of DNA sensing. *Cell Mol. Immunol.* 19, 125–126. doi: 10.1038/s41423-021-00797-3

Mao, H. Q., Zhou, L., Li, J. Q., Wen, Y. H., Chen, Z., and Zhang, L. (2024). STING inhibition alleviates bone resorption in apical periodontitis. *Int. Endod. J.* 57, 951–965. doi: 10.1111/iej.14057

Marcilla, A., and Sánchez-López, C. M. (2022). Extracellular vesicles as a horizontal gene transfer mechanism in Leishmania. *Trends Parasitol.* 38, 823–825. doi: 10.1016/j.pt.2022.08.004

Marinho, F. V., Benmerzoug, S., Oliveira, S. C., Ryffel, B., and Quesniaux, V. F. J. (2017). The emerging roles of STING in bacterial infections. *Trends Microbiol.* 25, 906–918. doi: 10.1016/j.tim.2017.05.008

Massey, J., Zarnowski, R., and Andes, D. (2023). Role of the extracellular matrix in Candida biofilm antifungal resistance. *FEMS Microbiol. Rev.* 47, fuad059. doi: 10.1093/femsre/fuad059

Mayer, F. L., Wilson, D., and Hube, B. (2013). Candida albicans pathogenicity mechanisms. *Virulence* 4, 119–128. doi: 10.4161/viru.22913

Montanari Borges, B., Gama De Santana, M., Willian Preite, N., De Lima Kaminski, V., Trentin, G., Almeida, F., et al. (2024). Extracellular vesicles from virulent P. brasiliensis induce TLR4 and dectin-1 expression in innate cells and promote enhanced Th1/Th17 response. *Virulence* 15, 2329573. doi: 10.3390/ijms22169100

Montelongo-Jauregui, D., Saville, S. P., and Lopez-Ribot, J. L. (2019). Contributions of Candida albicans Dimorphism, Adhesive Interactions, and Extracellular Matrix to the Formation of Dual-Species Biofilms with Streptococcus gordonii. *mBio* 10, e01179-19. doi: 10.1128/mBio.01179-19

Naglik, J. R., Challacombe, S. J., and Hube, B. (2003). Candida albicans secreted aspartyl proteinases in virulence and pathogenesis. *Microbiol. Mol. Biol. Rev.* 67, 400–428. doi: 10.1128/MMBR.67.3.400-428.2003

Ou, L., Zhang, A., Cheng, Y., and Chen, Y. (2021). The cGAS-STING pathway: A promising immunotherapy target. *Front. Immunol.* 12, 795048. doi: 10.3389/fimmu.2021.795048

Pan, X., Zhang, W., Guo, H., Wang, L., Wu, H., Ding, L., et al. (2023). Strategies involving STING pathway activation for cancer immunotherapy: Mechanism and agonists. *Biochem. Pharmacol.* 213, 115596. doi: 10.1016/j.bcp.2023.115596

Panchin, A. Y., Makeev, V. J., and Medvedeva, Y. A. (2016). Preservation of methylated CpG dinucleotides in human CpG islands. *Biol. Direct* 11, 11. doi: 10.1186/s13062-016-0113-x

Patel, D. J., Yu, Y., and Xie, W. (2023). cGAMP-activated cGAS-STING signaling: its bacterial origins and evolutionary adaptation by metazoans. *Nat. Struct. Mol. Biol.* 30, 245–260. doi: 10.1038/s41594-023-00933-9

Paul, B. D., Snyder, S. H., and Bohr, V. A. (2021). Signaling by cGAS-STING in neurodegeneration, neuroinflammation, and aging. *Trends Neurosci.* 44, 83–96. doi: 10.1016/j.tins.2020.10.008

Peng, M., Li, X., Zhang, X., and Peng, L. (2023). Inhibition of cGAS aggravated the host inflammatory response to Aspergillus fumigatus. *Exp. Lung Res.* 49, 86–100. doi: 10.1080/01902148.2023.2211663

Rajendran, R., Williams, C., Lappin, D. F., Millington, O., Martins, M., and Ramage, G. (2013). Extracellular DNA release acts as an antifungal resistance mechanism in mature Aspergillus fumigatus biofilms. *Eukaryot Cell* 12, 420–429. doi: 10.1128/EC.00287-12

Rizzo, J., Trottier, A., Moyrand, F., Coppée, J. Y., Maufrais, C., Zimbres, A. C. G., et al. (2023). Coregulation of extracellular vesicle production and fluconazole susceptibility in Cryptococcus neoformans. *mBio* 14, e0087023. doi: 10.1128/mbio.00870-23

Robertson, J. D., Ward, J. R., Avila-Olias, M., Battaglia, G., and Renshaw, S. A. (2017). Targeting neutrophilic inflammation using polymersome-mediated cellular delivery. *J. Immunol.* 198, 3596–3604. doi: 10.4049/jimmunol.1601901

Rodrigues, M. L., Janbon, G., O'connell, R. J., Chu, T. T., May, R. C., Jin, H., et al. (2025). Characterizing extracellular vesicles of human fungal pathogens. *Nat. Microbiol.* 10, 825–835. doi: 10.1038/s41564-025-01962-4

Ryan, M. E., Damke, P. P., and Shaffer, C. L. (2023). DNA transport through the dynamic type IV secretion system. *Infect. Immun.* 91, e0043622. doi: 10.1128/iai.00436-22

Salgado, R. C., Fonseca, D. L. M., Marques, A. H. C., Da Silva Napoleao, S. M., França, T. T., Akashi, K. T., et al. (2021). The network interplay of interferon and Toll-like receptor signaling pathways in the anti-Candida immune response. *Sci. Rep.* 11, 20281. doi: 10.1038/s41598-021-99838-0

Sampaio, A. A., Souza, S. E., Ricomini-Filho, A. P., Del Bel Cury, A. A., Cavalcanti, Y. W., and Cury, J. A. (2019). Candida albicans Increases Dentine Demineralization Provoked by Streptococcus mutans Biofilm. *Caries Res.* 53, 322–331. doi: 10.1159/000494033

Samson, N., and Ablasser, A. (2022). The cGAS-STING pathway and cancer. *Nat. Cancer* 3, 1452–1463. doi: 10.1038/s43018-022-00468-w

Sarkies, P. (2022). Encyclopaedia of eukaryotic DNA methylation: from patterns to mechanisms and functions. *Biochem. Soc. Trans.* 50, 1179–1190. doi: 10.1042/BST20210725

Schmid, M., Fischer, P., Engl, M., Widder, J., Kerschbaum-Gruber, S., and Slade, D. (2024). The interplay between autophagy and cGAS-STING signaling and its implications for cancer. *Front. Immunol.* 15, 1356369. doi: 10.3389/fimmu.2024.1356369

Schmitz, C. R. R., Maurmann, R. M., Guma, F., Bauer, M. E., and Barbé-Tuana, F. M. (2023). cGAS-STING pathway as a potential trigger of immunosenescence and inflammaging. *Front. Immunol.* 14, 1132653. doi: 10.3389/fimmu.2023.1132653

Sharma, D. K., and Rajpurohit, Y. S. (2024). Multitasking functions of bacterial extracellular DNA in biofilms. *J. Bacteriol* 206, e0000624. doi: 10.1128/jb.00006-24

Sk Md, O. F., Hazra, I., Datta, A., Mondal, S., Moitra, S., Chaudhuri, S., et al. (2020). Regulation of key molecules of immunological synapse by T11TS immunotherapy abrogates Cryptococcus neoformans infection in rats. *Mol. Immunol.* 122, 207–221. doi: 10.1016/j.molimm.2020.04.021

Skopelja-Gardner, S., An, J., and Elkon, K. B. (2022). Role of the cGAS-STING pathway in systemic and organ-specific diseases. *Nat. Rev. Nephrol.* 18, 558–572. doi: 10.1038/s41581-022-00589-6

Su, M., Zheng, J., Gan, L., Zhao, Y., Fu, Y., and Chen, Q. (2022). Second messenger 2'3'-cyclic GMP-AMP (2'3'-cGAMP): Synthesis, transmission, and degradation. *Biochem. Pharmacol.* 198, 114934. doi: 10.1016/j.bcp.2022.114934

Sun, X., Liu, L., Wang, J., Luo, X., Wang, M., Wang, C., et al. (2024). Targeting STING in dendritic cells alleviates psoriatic inflammation by suppressing IL-17A production. *Cell Mol. Immunol.* 21, 738–751. doi: 10.1038/s41423-024-01160-y

Sun, Y., Zhang, W., Dong, C., and Xiong, S. (2020). Mycobacterium tuberculosis mmsA (Rv0753c) interacts with STING and blunts the type I interferon response. *mBio* 11, e03254-19. doi: 10.1128/mBio.03254-19

Tao, G., Liao, W., Hou, J., Jiang, X., Deng, X., Chen, G., et al. (2024). Advances in crosstalk among innate immune pathways activated by mitochondrial DNA. *Heliyon* 10, e24029. doi: 10.1016/j.heliyon.2024.e24029

Temizoz, B., Hioki, K., Kobari, S., Jounai, N., Kusakabe, T., Lee, M. S. J., et al. (2022). Anti-tumor immunity by transcriptional synergy between TLR9 and STING activation. *Int. Immunol.* 34, 353–364. doi: 10.1093/intimm/dxac012

Tian, X., Liu, C., and Wang, Z. (2022). The induction of inflammation by the cGAS-STING pathway in human dental pulp cells: A laboratory investigation. *Int. Endod. J.* 55, 54–63. doi: 10.1111/iej.13636

Ullah, A., Huang, Y., Zhao, K., Hua, Y., Ullah, S., Rahman, M. U., et al. (2023). Characteristics and potential clinical applications of the extracellular vesicles of human pathogenic Fungi. *BMC Microbiol.* 23, 227. doi: 10.1186/s12866-023-02945-3

Valiante, V., Macheleidt, J., Föge, M., and Brakhage, A. A. (2015). The Aspergillus fumigatus cell wall integrity signaling pathway: drug target, compensatory pathways, and virulence. *Front. Microbiol.* 6, 325. doi: 10.3389/fmicb.2015.00325

Wagener, M., Hoving, J. C., Ndlovu, H., and Marakalala, M. J. (2018). Dectin-1-syk-CARD9 signaling pathway in TB immunity. *Front. Immunol.* 9, 225. doi: 10.3389/fimmu.2018.00225

Wang, B., Yu, W., Jiang, H., Meng, X., Tang, D., and Liu, D. (2024). Clinical applications of STING agonists in cancer immunotherapy: current progress and future prospects. *Front. Immunol.* 15, 1485546. doi: 10.3389/fimmu.2024.1485546

Wen, P. Y. F., Chen, M. X., Zhong, Y. J., Dong, Q. Q., and Wong, H. M. (2022). Global burden and inequality of dental caries 1990 to 2019. *J. Dent. Res.* 101, 392–399. doi: 10.1177/00220345211056247

Werner Lass, S., Smith, B. E., Camphire, S., Eutsey, R. A., Prentice, J. A., Yerneni, S. S., et al. (2024). Pneumococcal extracellular vesicles mediate horizontal gene transfer via the transformation machinery. *mSphere* 9, e0072724. doi: 10.1128/msphere.00727-24

Wu, Y., Song, K., Hao, W., Li, J., Wang, L., and Li, S. (2022). Nuclear soluble cGAS senses double-stranded DNA virus infection. *Commun. Biol.* 5, 433. doi: 10.1038/s42003-022-03400-1

Xie, F., and Zhu, Q. (2024). The regulation of cGAS-STING signaling by RNA virus-derived components. *Virol. J.* 21, 101. doi: 10.1186/s12985-024-02359-1

Yang, H., Yang, S., Guo, Q., Sheng, J., and Mao, Z. (2024). ATP-responsive manganese-based bacterial materials synergistically activate the cGAS-STING pathway for tumor immunotherapy. *Adv. Mater* 36, e2310189. doi: 10.1002/adma.202310189

Yirsaw, A. N., Bogale, E. K., Tefera, M., Belay, M. A., Alemu, A. T., Bogale, S. K., et al. (2024). Prevalence of dental caries and associated factors among primary school children in Ethiopia: systematic review and meta-analysis. *BMC Oral. Health* 24, 774. doi: 10.1186/s12903-024-04555-5

Yu, L., and Liu, P. (2021). Cytosolic DNA sensing by cGAS: regulation, function, and human diseases. *Signal Transduct Target Ther.* 6, 170. doi: 10.1038/s41392-021-00554-y

Yum, S., Li, M., Fang, Y., and Chen, Z. J. (2021). TBK1 recruitment to STING activates both IRF3 and NF-κB that mediate immune defense against tumors and viral infections. *Proc. Natl. Acad. Sci. U.S.A.* 118, e2100225118. doi: 10.1073/pnas.2100225118

Zevini, A., Olagnier, D., and Hiscott, J. (2017). Crosstalk between cytoplasmic RIG-I and STING sensing pathways. *Trends Immunol.* 38, 194–205. doi: 10.1016/j.it.2016.12.004

Zhang, K., Huang, Q., Li, X., Zhao, Z., Hong, C., Sun, Z., et al. (2024). The cGAS-STING pathway in viral infections: a promising link between inflammation, oxidative stress and autophagy. *Front. Immunol.* 15, 1352479. doi: 10.3389/fimmu.2024.1352479

Zhang, Z., Li, B., Chai, Z., Yang, Z., Zhang, F., Kang, F., et al. (2023). Evolution of the ability to evade host innate immune defense by Talaromyces marneffei. *Int. J. Biol. Macromol* 253, 127597. doi: 10.1016/j.ijbiomac.2023.127597

Zhang, R. R., Zhang, J. S., Huang, S., Lam, W. Y., Chu, C. H., and Yu, O. Y. (2025). The oral microbiome of root caries: A scoping review. *J. Dent.* 160, 105899. doi: 10.1016/j.jdent.2025.105899

Zhou, J., Zhuang, Z., Li, J., and Feng, Z. (2023). Significance of the cGAS-STING pathway in health and disease. *Int. J. Mol. Sci.* 24, 13316. doi: 10.3390/ijms241713316

Zierhut, C., and Funabiki, H. (2020). Regulation and consequences of cGAS activation by self-DNA. *Trends Cell Biol.* 30, 594–605. doi: 10.1016/j.tcb.2020.05.006

frontiers | Frontiers in Cellular and Infection Microbiology

TYPE Original Research
PUBLISHED 08 September 2025
DOI 10.3389/fcimb.2025.1614363

OPEN ACCESS

EDITED BY
Keke Zhang,
Wenzhou Medical University, China

REVIEWED BY
Xinxin Tian,
Tufts University, United States
Pan Yangyang,
Wenzhou Medical University, China

*CORRESPONDENCE
Anelise Viapiana Masiero
anemasiero@uniplaclages.edu.br

RECEIVED 18 April 2025
ACCEPTED 08 August 2025
PUBLISHED 08 September 2025

CITATION
Erckmann MC, Almeida A, Dominguini D, Becker D, Rutz JK, Hotza D, Parolia A, Dos Santos VV, Nunes MR, Da Rosa CG and Masiero AV (2025) Curcumin-photosensitized nanocapsules: biocompatibility and antimicrobial evaluation in primary tooth dentin contaminated with *Streptococcus mutans*. *Front. Cell. Infect. Microbiol.* 15:1614363. doi: 10.3389/fcimb.2025.1614363

Curcumin-photosensitized nanocapsules: biocompatibility and antimicrobial evaluation in primary tooth dentin contaminated with *Streptococcus mutans*

Michelle Cristina Erckmann[1], Aline Almeida[2], Diogo Dominguini[3], Daniela Becker[2], Josiane Khun Rutz[4], Dachamir Hotza[5,6], Abhishek Parolia[7], Vanessa Valgas Dos Santos[1], Michael Ramos Nunes[5,8], Cleonice Gonçalves Da Rosa[1] and Anelise Viapiana Masiero[1,7]*

[1]Multi-User Laboratory, Graduate Program in Environment and Health, Planalto Catarinense University, Lages, SC, Brazil, [2]Laboratory of Plasmas, Films, and Surfaces, Santa Catarina State University (UDESC), Joinville, SC, Brazil, [3]Laboratory of Experimental Pathophysiology, Graduate Program in Health Sciences, University of Extreme South of Santa Catarina (UNESC), Criciúma, Brazil, [4]Center of Biomaterials Development and Control, Faculty of Dentistry, Federal University of Pelotas, Pelotas, Rio Grande do Sul, Brazil, [5]Graduate Program in Chemical Engineering (PosENQ), Federal University of Santa Catarina (UFSC), Florianópolis, SC, Brazil, [6]Department of Chemical and Food Engineering (EQA), Federal University of Santa Catarina (UFSC), Florianópolis, SC, Brazil, [7]Department of Endodontics, College of Dentistry and Dental Clinics, University of Iowa, Iowa City, IA, United States, [8]Federal Institute of Santa Catarina, Lages, SC, Brazil

Introduction: Dental caries is a multifactorial disease with high prevalence, particularly in vulnerable populations, where *Streptococcus mutans* contributes to lesion progression via acid production and biofilm formation. Minimally invasive strategies, such as photodynamic therapy (PDT) combined with advanced delivery systems, offer promising alternatives for caries management.
Methods: Zein-based nanocapsules loaded with curcumin (Nano-curcumin) were synthesized via nanoprecipitation and characterized for encapsulation efficiency, particle size, polydispersity, zeta potential, morphology, and curcumin release. Biocompatibility was assessed using rabbit oral mucosal cells via MTT and trypan blue assays. Antimicrobial efficacy was tested in vitro on primary dentin slices contaminated with S. mutans across four groups: Nano-curcumin, Nano-curcumin + PDT, diode laser, and untreated control. Colony-forming units (CFU) were quantified after treatment. Statistical analysis was performed using ANOVA and Tukey's test ($p < 0.05$).
Results: Nano-curcumin demonstrated high encapsulation efficiency (~100%), spherical morphology, low polydispersity (0.108), and favorable colloidal stability, with sustained curcumin release over 24 hours. Cytotoxicity assays showed >50% cell viability at 100 $\mu g \cdot mL^{-1}$ and ~80% at intermediate concentrations (50–75 $\mu g \cdot mL^{-1}$). Both curcumin nanocapsules and their photosensitized versions significantly reduced *S. mutans* CFU compared to controls ($p < 0.05$), with PDT-enhanced nanocapsules showing the greatest reduction, though not statistically different from non-photosensitized nanocapsules.
Discussion: Curcumin-loaded zein nanocapsules are biocompatible and effective against *S. mutans*, with controlled release properties. Photodynamic

activation further enhances antimicrobial activity, supporting their potential as a minimally invasive approach for managing carious lesions, particularly in pediatric dentistry. This strategy integrates a natural photosensitizer with a biodegradable polymeric matrix, providing a safe and innovative alternative for caries control.

KEYWORDS

dental caries, curcumin, nanotechnology, photodynamic therapy, pediatric dentistry

1 Introduction

Dental caries continues to be a major public health issue, particularly among vulnerable populations. This is largely due to frequent carbohydrate consumption, increased acidity, and disruption of the oral microbiota (Takahashi and Nyvad, 2016). This acidic environment promotes pathogenic biofilm formation and enamel demineralization, with *Streptococcus. mutans* playing a central role. This bacterium efficiently metabolizes sugars, producing acid while thriving in low-pH conditions. It also contributes, to biofilm stability by synthesizing an extracellular polysaccharide matrix which enhances resistance to antimicrobial agents (de Oliveira et al., 2019; Pourhajibagher et al., 2019).

Although conventional treatments focus on removing caries and restoring teeth they often fall short in achieving long-term disease control. Primary teeth are especially susceptible to rapid caries progression due to their thinner dentin, larger pulp chambers, and increased permeability (Nehete et al., 2014). To address these challenges, minimally invasive techniques such as selective caries removal (SCR), stepwise caries removal (SWR), and the Hall Technique have been developed. These methods aim to preserve tooth vitality while minimizing patient discomfort (Aïem et al., 2020; Innes et al., 2011; Machiulskiene et al., 2020).

In addition to preserving tooth structure, controlling residual bacteria is essential to prevent pulp inflammation and recurrent lesion (Diniz et al., 2015). Photodynamic therapy (PDT) has emerged as a promising antimicrobial strategy, utilizing light-activated photosensitizers to selectively eliminate cariogenic bacteria (Wilson and Patterson, 2008). Among these, curcumin stands out as a photosensitizer due to its antibacterial (Carolina Alves et al., 2019), antifungal (Zorofchian Moghadamtousi et al., 2014), antineoplastic (Ghaffari et al., 2020), anti-inflammatory (Zhi et al., 2021) and antioxidant properties (Kamwilaisak et al., 2022).

When used in PDT, curcumin exhibits high cytotoxicity against pathogenic microorganisms, particularly against Gram-positive bacteria (Adamczak et al., 2020). These properties make it a promising candidate for the development of new antimicrobial therapies (Hosseinpour-Nader et al., 2022). Nanotechnology further enhances curcumin's therapeutic potential by improving its stability, bioavailability, and antimicrobial efficacy (Hosseinpour-Nader et al., 2022). Incorporating nanoparticles into dental materials has also been shown to enhance their mechanical and biological properties (Andreatta et al., 2023; Batista et al., 2024; da Rosa et al., 2022; Masiero et al., 2024; Narciso et al., 2019; Parizzi et al., 2025).

In this context, targeted strategies against *S. mutans* including the use of nanoparticles to modulate the cariogenic microbiome have shown encouraging results (Sayed et al., 2020). However, despite growing interest in PDT and the the known antimicrobial potential of curcumin, few studies have explored the combined use of curcumin-loaded nanostructures and PDT in primary dentin, which differs morphological and histological characteristics compared to permanent teeth. Moreover, limited research has assessed the biocompatibility of such systems in healthy oral tissues, particularly in pediatric settings.

To address these gaps, the present study aimed to synthesize and characterize zein-based nanocapsules loaded with curcumin, evaluate their biocompatibility with oral mucosal cells, and investigate their their *in vitro* antimicrobial efficacy on primary dentin contaminated with *S. mutans*, both with and without photodynamic activation. This innovative approach combines a natural photosensitizers with a biodegradable polymeric matrix, offering a minimally invasive and potentially safer alternative for the treatment of carious lesions in children.

2 Material and methods

This study was approved by the Research Ethics Committee (CAAE No. 6.246.02).

2.1 Materials

The materials used in this study included curcumin, zein, poloxamer 407, and Dulbecco's Modified Eagle Medium (DMEM), all from Sigma-Aldrich (Saint Louis, MO, USA). The culture media used comprised Mueller-Hinton agar and Tryptic Soy agar (Himedia, Thane, India), along with Brain and Heart Infusion Agar (BHI) (Merck, Darmstadt, Germany). The bacterial strain employed was *S. mutans* ATCC 25175. All other reagents were also obtained from Sigma-Aldrich.

2.2 Methods

2.2.1 Synthesis and physicochemical characterization of zein nanocapsules loaded with curcumin

Curcumin-loaded zein nanocapsules (Nano-curcumin) were synthesized using the nanoprecipitation method in triplicate (n=3), following the methodology described by (Gonçalves da Rosa et al., 2020; Suzuki et al., 2016). To prepare the organic phase zein (20 mg mL^{-1}) in 6.67 mL of 85% ethanol. Once fully solubilized, 134 µL of an alcoholic curcumin solution (1.5 mg mL^{-1}) was added. The organic phase was then poured into 20 mL of an aqueous phase containing the surfactant Pluronic (0.8% v/v) under constant agitation at 10,000 rpm using a homogenizer IKA T25 homogenizer (IKA, Wilmington, NC,USA) for 3 minutes.

Nanocapsule formation occurred via nanoprecipitation upon contact between the two phases. The resulting suspension was stirred under a fume hood with magnetic agitation to ensure complete evaporation of the organic solvent. A control formulation without curcumin (Nano-curcumin-free) was prepared using the same procedure.

To confirm nanoencapsulation, the encapsulation efficiency (EE) of the curcumin-loaded zein nanocapsules was evaluated in triplicate (n=3) following to the methodology described by (Gonçalves da Rosa et al., 2020). EE was determined using a centrifugal ultrafiltration method, as outlined by Parizzi et al. (2025). Samples were centrifuged using Amicon Ultra centrifugal filters with a 30 kDa Ultracel membrane at 6,000 rpm for 30 minutes, allowing non-encapsulated curcumin to pass through the membrane.

The free curcumin in the supernatant was quantified using UV-Vis spectroscopy (Spectrostar Nano, BMG Labtech, Weston Parkway Suite, NC, USA) at a wavelength of approximately 430 nm. The molar concentration of curcumin was calculated based on a calibration curve prepared with an alcoholic curcumin solution.

Encapsulation efficiency (EE) was calculated using Equation 1:

$$EE\,\% = \frac{[(initial\ \ curcumin\ -\ free\ \ curcumin)}{(initial\ \ curcumin)]\ \ x\ \ 100} \qquad (1)$$

To confirm curcumin encapsulation, UV-Vis spectrophotometry was performed using a Spectrostar Nano scanning spectrophotometer (BMG Labtech, Weston Parkway Suite, NC, USA). Measurements were taken across a wavelength range of 200 to 600 nm, with a resolution of 1 nm. The absorbance peak (λmax) of free curcumin was determined after dilution in absolute ethanol, while nanocapsule suspensions were diluted in ultrapure water prior to analysis.

Physicochemical characterization included the assessment of particle size (nm), polydispersity index (PDI), and zeta potential (mV), using dynamic light scattering (DLS) with a Zetasizer Advance (Malvern Panalytical, Worcestershire, UK). Samples of Nano-curcumin and control formulations were diluted in Milli-Q® water and analyzed at 25 °C, with a scattering angle of 173°, in triplicate (n = 3), using electrophoretic cells.

Nanocapsule morphology was examined using transmission electron microscopy (TEM) JEOL JEM 2100 (Tokyo, Japan) operating at 70 kV. Solutions containing curcumin-loaded zein nanocapsules and control samples were diluted in ultrapure Milli-Q water. Approximately 5 µL of each sample was deposited onto carbon-coated copper grids (200 mesh). After air drying at room temperature, the grids were observed under the microscope.

The curcumin release assay was conducted using a citrate–phosphate buffer at pH 7.0, as described by Parizzi et al. (2025). For each experiment, 1 mL of the nanoparticle dispersion was placed into a dialysis membrane (pore size: 25 Å; molecular weight cut-off: 12,000–16,000 Da) and immersed in 100 mL of buffer under continuous stirring. Samples of the external medium were collected at regular intervals from 1 to 8 hours, with additional aliquots taken at 12 and 24 hours. The amount of curcumin released was quantified by UV-Vis spectrophotometry using the Spectrostar Nano (BMG Labtech, Weston Parkway Suite, NC, USA) at 425 nm. Concentrations were determined using a calibration curve constructed with curcumin standards.

2.2.2 Cytotoxicity and cell viability assay

The cytotoxicity and cell viability of curcumin-loaded zein nanocapsules (Nano-curcumin) were evaluated using surface mucosal cells derived from rabbits. The cells were cultured in high-glucose Dulbecco's Modified Eagle Medium (DMEM) supplemented with 10% fetal bovine serum, 100 U/mL penicillin, and 100 mg/mL streptomycin. Cultures were maintained in a humidified atmosphere at 37 °C with 5% CO_2 and 95% air until confluence was reached.

Once confluent,the cells were seeded at a density of 10,000 cells per well in 96-well plates. A single dose of nanocapsules was added at concentrations of 25, 50, 75, and 100 µg·mL^{-1}.

Following treatment, the samples were irradiated using a low-power diode laser InGaAlP (DMC-Therapy, Sao Carlos, SP, Brazil) at a wavelength of 660 nm, continuous emission, a power output of 100 mW, and a total energy of 9 joules over 90 seconds (Knorst et al., 2019).The laser tip was positioned 10 mm above the wells, and irradiation was applied alternately to sets of four wells to ensure proper spacing between the light source and avoid overlapping light exposure.

Cell viability was assessed using the MTT assay (0.5 mg·mL^{-1}) and trypan blue exclusion (TBE). For the MTT assay, 20 µL of a stock MTT solution (5 mg·mL^{-1}) was added to each well and incubated for 4 hours. After incubation, cells were dissolved in DMSO, and optical density was measured at 490 nm in equipment Spectrostar Nano (BMG Labtech, Weston Parkway Suite NC, USA) The percentage of viable cells relative to the control was calculated based on the absorbance values, considering the ratiobetween treated cells (Abs. sample) and the absorbance of the cell-free culture medium (Abs blank), as indicated in Equation 2.

$$Cell\ \ viability\ \ (\%) = (Abs.\ \ sample)/(Abs.blank)\ \ x\ \ 100 \qquad (2)$$

2.2.3 *In vitro* antimicrobial evaluation of zein nanocapsules loaded with curcumin on primary tooth dentin contaminated with *Streptococcus mutans*

2.2.3.1 Sample preparation

Forty mandibular and maxillary primary molars free of caries, restoration and with no visible cracks or fractures were collected for this study. The teeth were donated by patients prior consent from their legal guardians. After collection, the specimens were washed to remove impurities, sterilized in an autoclave, and stored in distilled water until sectioning. For the cutting procedure, each tooth was mounted on an acrylic plate using low-melting-point plasticized wax and sectioned using a precision cutting machine (Isomet 1000, Buehler, Coventry, UK). Sections of approximately 1 mm thick were obtained using a 0.4 mm diamond disc (Buehler, Lake Bluff, IL, USA) operating at 300 rpm. Based on the inclusion criteria a final sample of 28 slices was selected. These slices were then sterilized again by autoclaving before being used in the contamination procedure.

2.2.3.2 Bacterial culture and contamination procedure

To evaluate the antimicrobial activity of the nanoparticles, lyophilized *S. mutans* (ATCC 25175) strains were rehydrated according to the manufacturer's instructions and incubated anaerobically in Tryptone Soy Broth (TSB) at 37°C for 48 hours. Following incubation, the samples were plated on solid Blood Agar using the streak plate method to obtain isolated colonies. From these colonies, a bacterial suspension equivalent to 1.5×10^8 cells·mL^{-1} was prepared using the 0.5 McFarland scale. The 1 mm dentin slices were then incubated in 990 µL of TSB medium supplemented with 10 µL of the *S. mutans* bacterial suspension and maintained under anaerobic conditions at 37°C for 48 hours.

2.2.3.3 Experimental groups and treatments

After the incubation period, the dentin slices were removed from the bacterial suspension, transferred to 1 mL of saline solution, and immediately divided into the following experimental groups (n = 7):

- Group 1: Contaminated Dentin + NanoCurcumin (Dent-NanoCurcumin)
- Group 2: Contaminated Dentin + NanoCurcumin + Photodynamic Therapy (Dent-NanoCurc-PDT)
- Group 3: Contaminated Dentin + Diode Laser
- Group 4: Contaminated Dentin (Dent) – Control

Groups 1 and 2 were incubated with 1 mL of their respective nanocapsule dispersion (containing 7.5 µg/mL of curcumin) for 4 hours at room temperature, while Groups 3 and 4 were incubated with saline solution under the same conditions. Subsequently, Groups 2 and 3 were treated with a low-power InGaAlP diode laser (DMC-Therapy, São Carlos, SP, Brazil) at a wavelength of 660 nm, in continuous emission mode, with a power output of 100 mW and a total energy of 9 joules applied over 90 seconds (Parizzi et al., 2025; Knorst et al., 2019).

2.2.3.4 Microbiological Analysis

Following the treatments, the dentin slices were transferred to 1 mL of saline solution and immediately incubated in TSB broth for 30 minutes. To assess antimicrobial activity, 10 µL of the broth was placed at the center of a sterile Petri dish, over which Mueller-Hinton agar was poured. After solidification, the plates were incubated anaerobically at 37°C for 48 hours. Colony-forming units (CFU) were then counted, and the results were expressed as CFU·mL^{-1} (Fernandes et al., 2022).

2.2.3.5 Data analysis

Results were expressed as means and standard deviations from triplicate measurements. Statistical analysis was performed using analysis of variance (ANOVA), followed by Tukey's test for multiple comparisons, with a significance level of 5%. Data were analyzed using STATISTICA 7 software.

3 Results

3.1 Physicochemical characterization of nanocapsules

The encapsulation efficiency of curcumin in zein matrices was close to 100%. Figure 1 shows the absorbance spectra of free curcumin and nanocurcumin, obtained by UV-Vis spectroscopy. Free curcumin exhibited a well-defined absorbance peak at approximately 425 nm. In contrast, the nanocurcumin spectrum displayed an altered profile, with the absence of this characteristic peak and increased absorbance in the UV region.

Table 1 presents the measurements of average particle size, polydispersity index (PDI), and zeta potential for nano-curcumin and nano-curcumin-free samples. Nano-curcumin particles exhibited a larger average size (139.4 ± 1.0 nm) compared to the nano-curcumin-free particles (128.5 ± 0.7 nm), with a statistically significant difference (Figure 2). The PDI values indicate that nano-curcumin had a lower polydispersity index (0.108 ± 0.07) whereas nano-curcumin-free showed a significantly higher PDI (0.271 ± 0.03). Regarding zeta potential, nano-curcumin exhibited a lower value (10.9 ± 0.5 mV) compared to nano-curcumin-free (40.0 ± 2.8 mV), also with a significant difference.

The transmission electron microscopy (TEM) analysis of zein nanocapsules loaded with curcumin revealed key morphological characteristics. TEM micrographs indicated that the nanocapsules exhibited a spherical shape (Figure 3).

Spectrophotometric analysis showed that nano-curcumin exhibited a sustained release in buffered aqueous medium over a 24-hour period. The release profile indicates a gradual increase in curcumin concentration in the external medium, with a more pronounced release during the first 8 hours and a tendency toward stabilization after 12 hours, as shown in Figure 4.

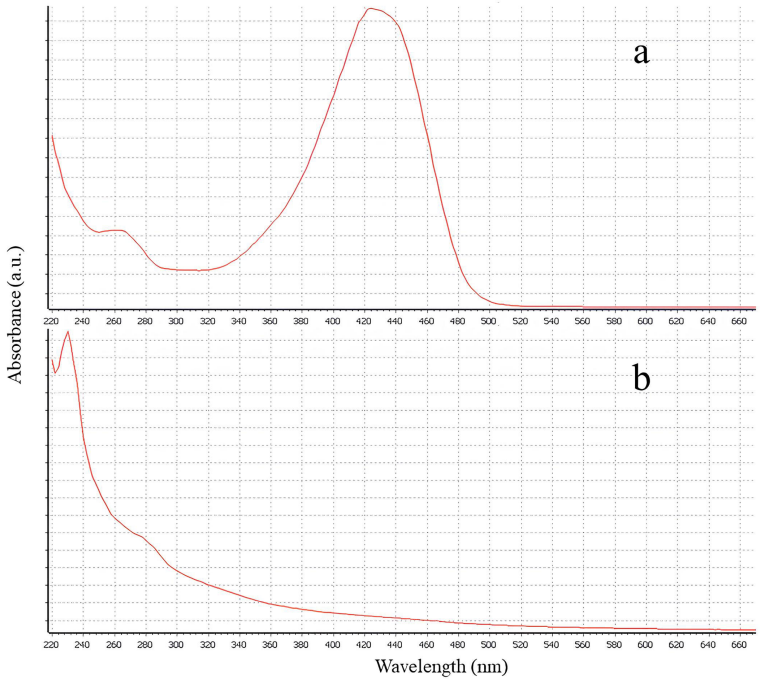

FIGURE 1
UV-Vis scan spectra: **(a)** free curcumin; **(b)** nanocurcumin.

3.2 Cytotoxicity and cell viability assay

At a 100 µg·mL-1 nanocapsule concentration, the cell survival rate exceeded 50µg·mL-1 while concentrations of 50 µg·mL-1 and 75µg·mL-1 resulted in cell survival rates approaching 80% (Figure 5).

Zein nanocapsules loaded with curcumin at a 100 µg·mL-1 concentration (7.5 µg·mL^{-1} of curcumin), indicating that half of the healthy oral mucosal cells exposed to this concentration did not survive (Figure 6).

3.3 Microbiological analysis

The results of the microbiological analysis of dentin contaminated with *S. mutans* are presented in Figure 7. Both curcumin nanocapsules and their photosensitized versions significantly reduced *S. mutans* CFU/mL compared to untreated controls ($p<0.05$). However, the group treated with photosensitized curcumin nanocapsules exhibited the lowest CFU/mL count, this reduction was not statistically different from that observed in the non-photosensitized curcumin nanocapsules group.

4 Discussion

The high encapsulation efficiency (~100%) of curcumin in zein matrices observed in this study aligns with previous reports highlighting the effectiveness of this biopolymer as a carrier for bioactive compounds (Da Rosa et al., 2020). Given curcumin's poor solubility and susceptibility to degradation (Hu et al., 2024), encapsulation within a zein matrix offers significant advantages including enhanced stability, protection against oxidation, and shielding from adverse interactions that could compromise its biological activity in the oral environment (Choi et al., 2016). This high retention capacity is particularly advantageous for controlled-release systems, where sustained bioavailability at the target site—such as infected dentin—is essential for therapeutic efficacy.

TABLE 1 Average particle size, polydispersity index (PDI), and zeta potential.

Sample	Average size (nm)	Polydispersity index (PDI)	Zeta potential (mV)
Nano-curcumin	139.4 ± 1.0a	0.108 ± 0.07b	10.9 ± 0.5b
Nano-curcumin-free	128.5 ± 0.7b	0.271 ± 0.03a	40.0 ± 2.8a

Results are expressed as mean ± standard deviation (n=3). Different letters indicate significant differences ($p<0.05$) when analyzed by Tukey's test within the column.

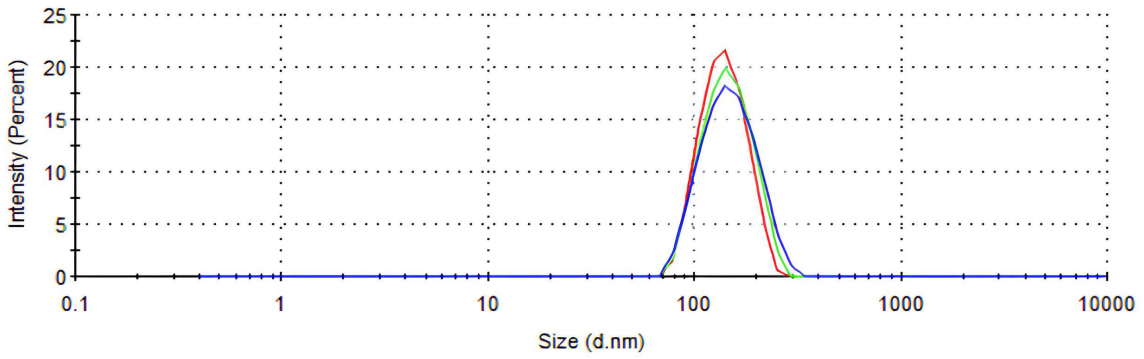

FIGURE 2
Particle size distribution of the Nano-curcumin sample.

UV-Vis spectroscopy revealed notable changes in the absorbance profile of curcumin following encapsulation. Free curcumin exhibited a distinct peak at approximately 425 nm, corresponding to $\pi \rightarrow \pi^*$ electronic transitions of the β-diketone conjugated system in its enolic form, typically observed in organic solvents (Urošević et al., 2022). In the nanoencapsulated form, this peak was significantly diminished or absent, with a relative increase in absorbance at wavelengths below 400 nm (Wu et al., 2023). These spectral changes suggest that curcumin was incorporated into the hydrophobic regions of the polymeric matrix, resulting in conformational restriction and reduced interaction with the dispersion medium.

These modifications are likely due to non-covalent interactions between curcumin and zein. Zein contains hydrophobic segments that facilitate molecular entrapment and enable additional intermolecular interactions, such as hydrogen bonding and Van der Waals forces (Chen et al., 2015). Furthermore, π–π stacking between the aromatic rings of curcumin and zein contributes to the structural stabilization of the nanoparticles (Ding et al., 2023; Liu et al., 2023).

In addition to confirming encapsulation, comparative studies have shown that encapsulated curcumin undergoes significantly less degradation under UV radiation. Literature indicates that free curcumin degrades by more than 60% after 30 minutes of exposure, whereas the encapsulated form shows less than 10% degradation under the same conditions (Wu et al., 2023). Encapsulation also promotes the dispersion of curcumin in an amorphous state, enhancing its solubility in aqueous media and absorption in the gastrointestinal tract, potentially improving oral bioavailability (Liu et al., 2023).

Thus, the attenuation of the 425 nm peak and the altered absorbance pattern observed in nano-curcumin reflect structural

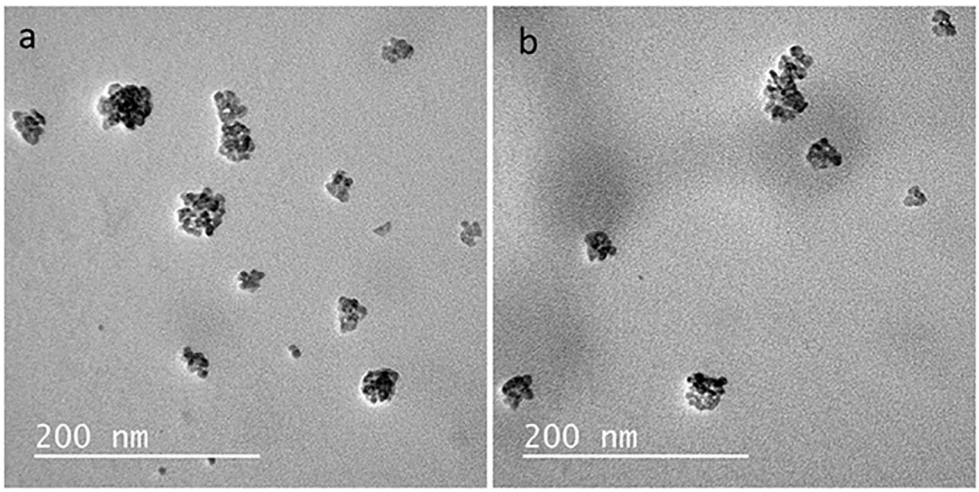

FIGURE 3
TEM micrographs of the nanocapsules: **(a)** Nano-curcumin-free **(b)** Nano-curcumin.

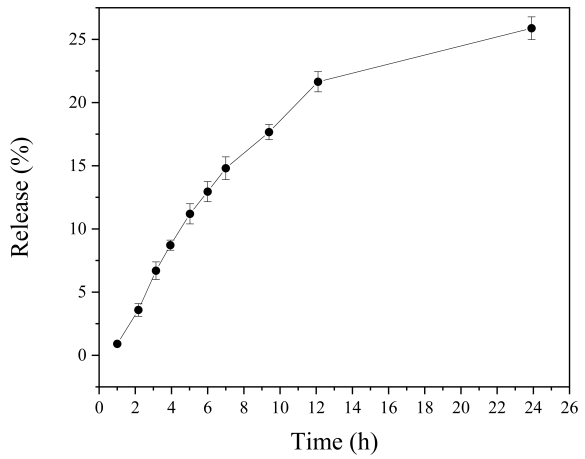

FIGURE 4
Release of nano-curcumin in citrate–phosphate buffer (pH 7.0) over 24 hours.

constraints imposed by the zein matrix, resulting in increased protection against degradation and greater potential for use in nutraceutical and pharmaceutical formulations.

The observed increase in nanoparticle size following curcumin incorporation suggests strong physicochemical interactions between zein and curcumin during nanoprecipitation process. This contributes to greater structural stability and reduced aggregation, attributed to the hydrophobic nature of curcumin (Da Rosa et al., 2015). Additionally, the lower polydispersity index (PDI) observed in curcumin-loaded formulations compared to those without the compound indicates a more uniform size distribution - an important factor for optimizing bioavailability and ensuring effective dentin penetrationthereby enhancing antimicrobial action against cariogenic microorganisms (Danaei et al., 2018).

Zeta potential results further support these findings. The lower surface charge observed in nano-curcumin formulations suggests potential alterations in colloidal stability due to interactions with zein. While higher zeta potential values typically indicate greater electrostatic stability (Nunes et al., 2022), the reduction observed here may increase the likelihood of aggregation over time, emphasizing the need for appropriate stabilization or storage strategies to preserve therapeutic efficacy (Danaei et al., 2018).

These findings underscore the potential of nano-curcumin formulations for targeted antimicrobial therapy in dentistry, particularly in minimally invasive approaches for caries management. By ensuring high encapsulation efficiency, enhanced stability, and controlled release, this formulation presents a promising alternative for dental applications. Future studies should explore its long-term stability and *in vivo* performance to validate clinical applicability and optimize formulation parameters.

The sustained release observed is consistent with the release mechanisms commonly associated with zein-based polymeric systems. Due to its hydrophobic and compact structure, zein acts as a physical barrier to drug diffusion, promoting a passive and controlled release profile (Oh and Flanagan, 2010; Gonzalez-Valdivieso et al., 2021). Hydrophobic interactions and potential hydrogen bonding between curcumin and the zein matrix further contribute to compound retention, limiting its rapid diffusion into the external medium (Lenzuni et al., 2023; Zhang et al., 2023).

Curcumin's inherently low aqueous solubility (<0.001 mg/mL) further restricts its release in buffered aqueous environments. Even after encapsulation, this intrinsic property limits immediate availability, reinforcing the gradual release profile observed (Karthikeyan et al., 2020; Omidian et al., 2023). The combination of poor solubility and the hydrophobic nature of zein results in a controlled release without burst effects.

The release of bioactive compounds from zein-based systems typically follows anomalous kinetics, often fitting the Korsmeyer–Peppas model. This suggests that both diffusion and slow matrix relaxation or degradation contribute to the release mechanism (Zhang et al., 2021; Lin et al., 2024). These processes occur simultaneously, with diffusion predominating in the initial phase and matrix reorganization influencing release behavior at later stages.

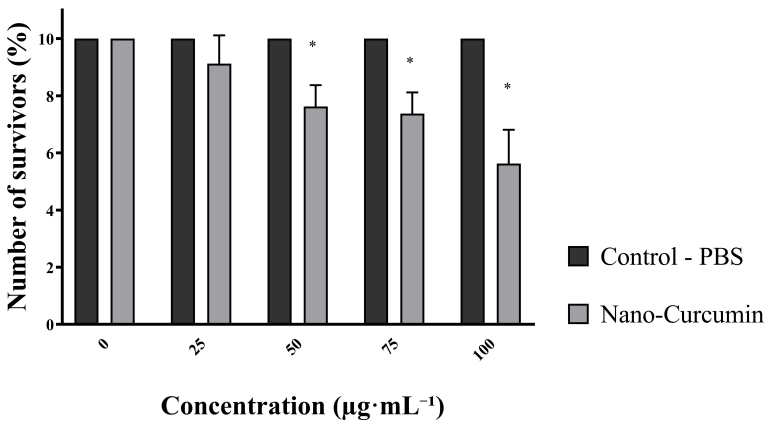

FIGURE 5
Survival of oral mucosal cells in response to different concentrations of zein nanocapsules loaded with curcumin. *The p-values: $p < 0.05$ indicate a significant difference according to Tukey's test.

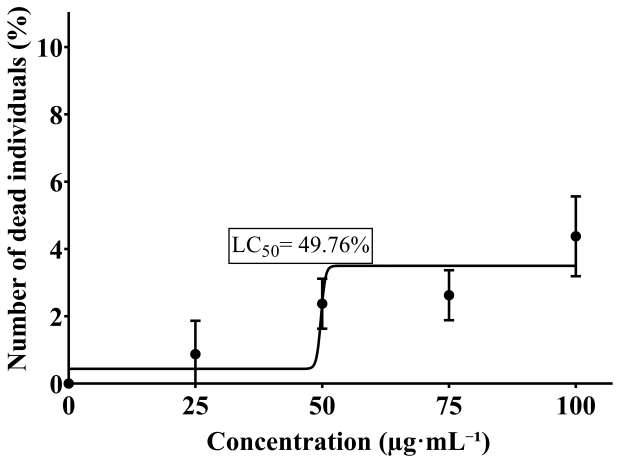

FIGURE 6
Median lethal concentration (LC50) of zein nanocapsules loaded with curcumin.

Systems with these characteristics are highly desirable for topical formulations targeting the oral cavity. Prolonged release on surfaces such as the oral mucosa, gingiva, or dentin enhances the local retention of curcumin, thereby amplifying its pharmacological activity. Curcumin is well known for its anti-inflammatory, antioxidant, and antimicrobial properties, with demonstrated benefits in the treatment of gingivitis, periodontitis, and chronic oral lesions (Inchingolo et al., 2024). Moreover, controlled release reduces the frequency of reapplication and contributes to a superior safety profile by avoiding local concentration peaks. These findings confirm that zein is an effective carrier system for the controlled release of hydrophobic compounds like curcumin, representing a promising strategy for minimally invasive therapies in oral healthcare.

The results of this study confirm the biocompatibility of zein nanocapsules loaded with curcumin for oral mucosal cells—an essential requirement for safe use in dental applications. Minimizing cytotoxicity is Inchingly critical to ensure that formulation does not harm surrounding healthy tissues while maintaining its therapeutic effects (Shahi et al., 2019). In this study, at the highest tested concentration of nanocapsules (100 µg·mL^{-1}, equivalent to 7.5 µg·mL^{-1} of curcumin), cell survival remained above 50%. At concentrations of 50 and 75 µg·mL^{-1}, viability approached 80%. Although a viability threshold above 50% is generally acceptable, these results suggest that even at full concentration, the formulation does not induce critical toxicity. This is particularly relevant for applications in the oral cavity, where direct mucosal exposure requires safe and well-tolerated materials.

The observed LC_{50} value (49.75 µg·mL^{-1}) indicates that 50% of the exposed cells did not survive at the highest tested concentration. LC_{50} is a standard toxicological parameter representing concentration at which half of the cells are affected, serving as a key indicator of formulation safety (Idrees and Kujan, 2023). The nanometric scale of the zein nanocapsules may have enhanced their penetration and interaction with oral mucosal cells, increasing curcumin's local bioavailability. While this property is advantageous for targeted antimicrobial action, it also underscores the importance of carefully optimizing dosage to mitigate toxicity risks and maintain a favorable therapeutic index.

These findings are consistent with previous studies on the Inchingly biocompatibility of curcumin when encapsulated in nanocarriers. Meng et al. (2023) demonstrated that starch-based nanocapsules loaded with curcumin exhibited low toxicity toward healthy cells while effectively inhibiting tumor cells, suggesting that encapsulation plays an important role in modulating curcumin's biological interactions. Similarly, Minhaco et al. (2023) reported over 80% cell viability at 325 µg/mL using PLGA-curcumin nanoparticles in oral cells, supporting their biomedical potential.

While reducing zein-curcumin concentrations may lower cytotoxicity, maintaining antimicrobial efficacy is key. Curcumin nanostructures remain effective at low doses; for example, 6.25 µg/mL of curcumin nanocrystals inhibited P. gingivalis growth. The 7.5 µg/mL used in this study supports the efficacy of nano-curcumin at low concentrations (Maleki Dizaj et al., 2022).

These results reinforce the promise of zein-based curcumin nanocapsules for safe, effective dental applications—especially in pediatric care, where non-invasive, biocompatible treatments are preferred.

Photodynamic therapy (PDT) with photosensitizers (PS) is well-documented for treating oral pathogens, including *S. mutans* (Cusicanqui Méndez et al., 2019; Hosseinpour-Nader et al., 2022; Manoil et al., 2014; Parizzi et al., 2025; Silvestre et al., 2023). Upon irradiation, the PS generates reactive oxygen species (ROS),

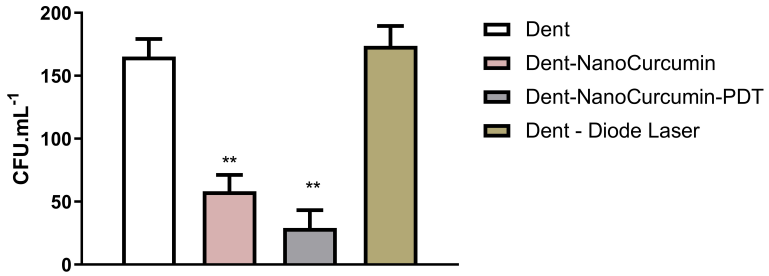

FIGURE 7
Comparison of antimicrobial effectiveness against s. mutans between the tested groups. **The p-values: $p < 0.05$ indicate a significant difference according to Tukey's test.

primarily singlet oxygen, which promotes oxidative damage to microbial DNA, organelles, and cell membranes, ultimately leading to bacterial death (Taraszkiewicz et al., 2013).

Curcumin, a natural polyphenol derived from plants, displays broad-spectrum antibacterial activity due to its unique molecular structure and antioxidant properties. It disrupts quorum sensing, impairs biofilm formation, reduces virulence factor expression, and prevents bacterial adhesion to host cell receptors. When activated, curcumin acts as a photosensitizer, generating phototoxic effects that inhibit bacterial growth and enhance the efficacy of other antimicrobials through synergistic interactions (Zheng et al., 2020).

By producing reactive oxygen species (ROS) such as hydrogen peroxide, superoxide, and singlet oxygen, curcumin damages bacterial cell structures by oxidizing membranes, proteins, and nucleic acids, leading to cell death. Gram-positive bacteria are particularly susceptible due to their permeable peptidoglycan-rich cell walls, which facilitate photosensitizer entry (Ghate et al., 2019).

Additionally, curcumin induces intracellular damage, affecting DNA and proteins, disrupting biofilm adhesion, and downregulating virulence genes involved in pathogenicity. While its effect on outer membranes is limited, photodynamic inactivation (PDI) with curcumin causes significant internal damage and cytoplasmic leakage. The superior antimicrobial effect of light-activated curcumin highlights its potential for targeting biofilm-associated infections and oral pathogens such as *Streptococcus mutans* (Ghate et al., 2015; Hu et al., 2018; Huang et al., 2020; Pereira et al., 2014; Tonon et al., 2015).

Microbiological analysis confirmed that both conventional and photosensitized curcumin nanocapsules significantly reduced *S. mutans* CFU/mL in dentin. Although the photosensitized group showed the lowest count, the difference was not statistically significant.

This may be due to the strong inherent antimicrobial activity of nano-curcumin, suboptimal PDT parameters (e.g., light dose, wavelength, pre-irradiation time), or limited light penetration into biofilms. Pre-irradiation time is crucial for PS penetration (de Oliveira et al., 2019), especially in mature biofilms, which are more resistant due to their dense extracellular matrix (Silvestre et al., 2023; Taraszkiewicz et al., 2013).

In this study, extended pre-irradiation was used to assess whether PDT efficacy could be enhanced or if nano-curcumin alone was sufficient. Less structured biofilms may respond well to nano-curcumin without PDT, as the formulation improves curcumin delivery and release.

Curcumin's poor solubility and rapid degradation limit its therapeutic use, but nanoencapsulation improves stability, lowers the MIC, and enhances antimicrobial efficacy (Pourhajibagher et al., 2018).

Studies support combining PDT with nano-curcumin. Pourhajibagher et al. (2022) found that a 5% nano-curcumin cavity liner with PDT inhibited *S. mutans* for 60 days. Araújo et al. (2017) required 5 $g{\cdot}L^{-1}$ for photoactivation effects on *S. mutans* and *L. acidophilus*. In contrast, this study used only 0.0075 $g{\cdot}L^{-1}$, yet showed efficacy—suggesting nanoencapsulation allows lower doses and reduces side effects like dental staining.

PDT also improves restoration outcomes.Clinical studies show its use in selective caries removal (SCR) reduces microbial load and enhances restoration success (Alves et al., 2019; Borges et al., 2010; Melo et al., 2015; Steiner-Oliveira et al., 2015). Long-term data confirm no compromise in restoration integrity after 6–12 months (Alves et al., 2019).

Combining nano-curcumin with PDT promotes remineralization by enhancing calcium and phosphate penetration into demineralized dentin (Koo et al., 2013; Wilson and Patterson, 2008; Zaleh et al., 2022). This approach aligns with minimally invasive dentistry, especially in pediatrics, by preserving primary teeth, reducing discomfort, and shortening treatment time. However, PDT is less effective in deeper dentin due to light scattering and absorption (Koo et al., 2013; Zanin et al., 2005), highlighting the need for personalized treatment based on lesion depth.

Despite promising results, limitations exist. *In vitro* conditions don't fully replicate the oral environment, where saliva, mechanical forces, and microbial diversity affect outcomes. While effective against *S. mutans*, further studies should assess polymicrobial biofilms. Curcumin's limited dentin penetration may reduce efficacy in deep lesions, emphasizing the need to optimize nanoencapsulation for better bioavailability.

Tooth staining is another concern. Although some *in vitro* studies report no significant discoloration (Araujo et al., 2023), these are based on simplified models. PDT with nano-curcumin may be a viable alternative to silver diamine fluoride, especially in posterior teeth where esthetics are less critical (Araujo et al., 2023).

Long-term *in vivo* studies are needed to assess safety, biocompatibility, and clinical effectiveness. Future research should refine PDT parameters—pre-irradiation time, light dose, and treatment frequency—and explore nano-curcumin's role in remineralization and its interaction with restorative materials.

5 Conclusions

This study synthesized and characterized curcumin-loaded zein nanocapsules with high encapsulation efficiency, spherical morphology, low polydispersity, and good colloidal stability. Cytotoxicity assays showed oral mucosal cell viability above 50% at high concentrations, supporting safety for topical use. Curcumin nanocapsules significantly reduced *S. mutans* on primary dentin. Although PDT further reduced bacterial load, the difference was not statistically significant, indicating the nanocarrier alone enhances antimicrobial efficacy via improved penetration and sustained release. With the limitation of this study, these results support nano-curcumin as a safe, effective, and minimally invasive strategy for caries management in primary teeth, aligning with conservative pediatric dental practices.

Data availability statement

The original contributions presented in the study are included in the article/supplementary material. Further inquiries can be directed to the corresponding author.

Ethics statement

The studies involving humans were approved by Research Ethics Committee on Human Subjects of the University of Planalto Catarinense. The studies were conducted in accordance with the local legislation and institutional requirements. Written informed consent for participation in this study was provided by the participants' legal guardians/next of kin. The animal study was approved by Ethics Committee on the Use of Animals – CEUA/UNESC. The study was conducted in accordance with the local legislation and institutional requirements.

Author contributions

ME: Formal Analysis, Methodology, Data curation, Validation, Conceptualization, Writing – original draft, Writing – review & editing, Investigation. AA: Formal Analysis, Methodology, Writing – review & editing, Data curation, Writing – original draft. DD: Writing – original draft, Writing – review & editing, Formal Analysis, Data curation, Methodology. DB: Formal Analysis, Writing – original draft, Data curation, Methodology, Writing – review & editing. JR: Data curation, Writing – original draft, Formal Analysis, Methodology, Writing – review & editing. DH: Formal Analysis, Methodology, Data curation, Writing – review & editing, Writing – original draft. AP: Conceptualization, Writing – review & editing, Formal Analysis, Writing – original draft. VS: Data curation, Formal Analysis, Methodology, Conceptualization, Writing – original draft, Writing – review & editing, Investigation. MN: Validation, Writing – review & editing, Conceptualization, Writing – original draft, Investigation, Formal Analysis, Methodology, Data curation. CR: Writing – original draft, Visualization, Formal Analysis, Project administration, Funding acquisition, Conceptualization, Methodology, Data curation, Resources, Supervision, Writing – review & editing, Validation, Investigation. AM: Conceptualization, Methodology, Visualization, Data curation, Supervision, Validation, Investigation, Funding acquisition, Writing – review & editing, Resources, Project administration, Writing – original draft, Formal Analysis.

Funding

The author(s) declare financial support was received for the research and/or publication of this article. This research was funded by Fundação de Amparo à Pesquisa e Inovação do Estado Santa Catarina (FAPESC) grant numbers FAPESC 12/2020 TO2021TR1482, FAPESC 12/2020 TO2021TR001430, FAPESC 15/2021 TO2021TR001220, FAPESC 54/2022 TO2023TR000648, FAPESC 54/2022 TO2023TR000883, FAPESC 54/2022 TO2023TR000884, FAPESC 15/2023 TO2023TR001418, FAPESC 15/2023 TO2023TR001518, FAPESC no 18/2024, FAPESC no 20/2024, and FAPESC no 61/2024. This research was also funded by the Conselho Nacional de Desenvolvimento Científico e Tecnológico (CNPq) no 69/2022-PIBPG and the Coordenação de Aperfeiçoamento de Pessoal de Nível Superior (CAPES)—Programa de Desenvolvimento da Pós-Graduação (PDPG).

Conflict of interest

The authors declare that the research was conducted in the absence of any commercial or financial relationships that could be construed as a potential conflict of interest.

Generative AI statement

The author(s) declare that Generative AI was used in the creation of this manuscript. This manuscript was entirely developed without the use of artificial intelligence tools such as ChatGPT during the research, data analysis, and initial writing phases. ChatGPT was employed only at the final stage of manuscript preparation to enhance the clarity, fluency, and readability of the English language, without altering the scientific content or the authors' original ideas.

Any alternative text (alt text) provided alongside figures in this article has been generated by Frontiers with the support of artificial intelligence and reasonable efforts have been made to ensure accuracy, including review by the authors wherever possible. If you identify any issues, please contact us.

Publisher's note

References

Adamczak, A., Ożarowski, M., and Karpiński, T. M. (2020). Curcumin, a natural antimicrobial agent with strain-specific activity. *Pharmaceuticals* 13, 153. doi: 10.3390/ph13070153

Aïem, E., Joseph, C., Garcia, A., Smaïl-Faugeron, V., and Muller-Bolla, M. (2020). Caries removal strategies for deep carious lesions in primary teeth: Systematic review. *Int. J. Paediatr. Dent.* 30, 392–404. doi: 10.1111/ipd.12616

Alves, L. V. G. L., Curylofo-Zotti, F. A., Borsatto, M. C., Salvador, S. L., de, S., Valério, R. A., et al. (2019). Influence of antimicrobial photodynamic therapy in carious lesion. Randomized split-mouth clinical trial in primary molars. *Photodiagnosis Photodyn. Ther.* 26, 124–130. doi: 10.1016/j.pdpdt.2019.02.018

Andreatta, G. B., Marcon, R. B., Da Rosa, C. G., and Masiero, A. V. (2023). Propriedades biológicas e físico-químicas de cimentos endodônticos

nanoparticulados. *Cuad. Educ. Desarro.* 15, 16209–16228. doi: 10.55905/cuadv15n12-059

Araujo, L. P., Marchesin, A. R., Gobbo, L. B., da Rosa, W. L. D. O., de Jesus Soares, A., de Almeida, J. F. A., et al. (2023). Tooth color change after photodynamic therapy in endodontics: A systematic review. *Photodiagnosis Photodyn. Ther.* 42, 103626. doi: 10.1016/j.pdpdt.2023.103626

Araújo, N. C., de Menezes, R. F., Carneiro, V. S. M., Dos Santos-Neto, A. P., Fontana, C. R., Bagnato, V. S., et al (2017). Photodynamic inactivation of cariogenic pathogens using curcumin as photosensitizer. *Photomed. Laser Surg.* 35, 259–263. doi: 10.1089/pho.2016.4156

Batista, D. G., Sganzerla, W. G., da Silva, L. R., Vieira, Y. G. S., Almeida, A. R., Dominguini, D., et al. (2024). Antimicrobial and cytotoxic potential of eucalyptus essential oil-based nanoemulsions for mouthwashes application. *Antibiotics* 13, 942. doi: 10.3390/antibiotics13100942

Borges, F. M. C., de-Melo, M. a. S., Lima, J. M. P., Zanin, I. C. J., Rodrigues, L. K. A., and Nobre-dos-Santos, M. (2010). Evaluation of the effect of photodynamic antimicrobial therapy in dentin caries: a pilot in vivo study, in: Lasers in Dentistry XVI. Presented at the Lasers in Dentistry XVI, SPIE, pp. 63–71. doi: 10.1117/12.842339

Carolina Alves, R., Fernandes, R. P., Fonseca-Santos, B., Damiani Victorelli, F., and Chorilli, M. (2019). A critical review of the properties and analytical methods for the determination of curcumin in biological and pharmaceutical matrices. *Crit. Rev. Anal. Chem.* 49, 138–149. doi: 10.1080/10408347.2018.1489216

Chen, X., Zou, L.-Q., Niu, J., Liu, W., Peng, S.-F., and Liu, C.-M. (2015). The stability, sustained release and cellular antioxidant activity of curcumin nanoliposomes. *Molecules* 20, 14293–14311. doi: 10.3390/molecules200814293

Choi, J. E., Waddell, J. N., Lyons, K. M., and Kieser, J. A. (2016). Intraoral pH and temperature during sleep with and without mouth breathing. *J. Oral Rehabil.* 43, 356–363. doi: 10.1111/joor.12372

Cusicanqui Méndez, D. A., Gutierrez, E., Campos Chaves Lamarque, G., Lopes Rizzato, V., Afonso Rabelo Buzalaf, M., Andrade Moreira MaChado, M. A., et al. (2019). The effectiveness of curcumin-mediated antimicrobial photodynamic therapy depends on pre-irradiation and biofilm growth times. *Photodiagnosis Photodyn. Ther.* 27, 474–480. doi: 10.1016/j.pdpdt.2019.07.011

Da Rosa, C. G., De Oliveira Brisola Maciel, M. V., De Carvalho, S. M., De Melo, A. P. Z., Jummes, B., Da Silva, T., et al. (2015). Characterization and evaluation of physicochemical and antimicrobial properties of zein nanoparticles loaded with phenolics monoterpenes. *Colloids Surf. A Physicochem. Eng. Asp.* 481, 337–344. doi: 10.1016/j.colsurfa.2015.05.019

Da Rosa, C. G., Sganzerla, W. G., De Oliveira Brisola Maciel, M. V., De Melo, A. P. Z., Da Rosa Almeida, A., Ramos Nunes, M., et al. (2020). Development of poly (ethylene oxide) bioactive nanocomposite films functionalized with zein nanoparticles. *Colloids Surf. A Physicochem. Eng. Asp.* 586, 124268. doi: 10.1016/j.colsurfa.2019.124268

da Rosa, C. G., Narciso, A. M., Nunes, M. R., and Masiero, A. V. (2022). "10 - Applicability of silver nanoparticles and innovation of magnetic nanoparticles in dentistry," in *Fundamentals and Industrial Applications of Magnetic Nanoparticles, Woodhead Publishing Series in Electronic and Optical Materials*. Eds. C. M. Hussain and K. K. Patankar (The Officers' Mess Business Centre, United Kingdom, Cambridge, MA, United States, Kidlington, United Kingdom: Woodhead Publishing), 317–348. doi: 10.1016/B978-0-12-822819-7.00023-5

de Oliveira, A. B., Ferrisse, T. M., Marques, R. S., De Annunzio, S. R., Brighenti, F. L., and Fontana, C. R. (2019). Effect of photodynamic therapy on microorganisms responsible for dental caries: A systematic review and meta-analysis. *Int. J. Mol. Sci.* 20, 3585. doi: 10.3390/ijms20143585

Ding, R., Zhang, M., Zhu, Q., Qu, Y., Jia, X., and Yin, L. (2023). Curcumin loaded Zein-alginate nanogels with "core-shell" structure: formation, characterization and simulated digestion. *Int. J. Biol. Macromol.* 251, 126201. doi: 10.1016/j.ijbiomac.2023.126201

Danaei, M., Dehghankhold, M., Ataei, S., Hasanzadeh Davarani, F., Javanmard, R., Dokhani, A., et al. (2018). Impact of particle size and polydispersity index on the clinical applications of lipidic nanocarrier systems. *Pharmaceutics* 10, 57. doi: 10.3390/pharmaceutics10020057

Diniz, I. M. A., Horta, I. D., Azevedo, C. S., Elmadjian, T. R., Matos, A. B., Simionato, M. R. L., et al. (2015). Antimicrobial photodynamic therapy: a promise candidate for caries lesions treatment. *Photodiagnosis Photodyn. Ther.* 12, 511–518. doi: 10.1016/j.pdpdt.2015.04.006

Fernandes, F. G. L., De Moraes, F. B., De Cezare, J. A., Degasperi, G. R., Fontana, C. E., Grandizoli, D. R. P., et al. (2022). *In vitro* evaluation of EDTA combined with photodynamic therapy to reduce Streptococcus mutans in carious dentin. *Photodiagnosis Photodyn. Ther.* 37, 102718. doi: 10.1016/j.pdpdt.2022.102718

Ghaffari, S.-B., Sarrafzadeh, M.-H., Salami, M., and Khorramizadeh, M. R. (2020). A pH-sensitive delivery system based on N-succinyl chitosan-ZnO nanoparticles for improving antibacterial and anticancer activities of curcumin. *Int. J. Biol. Macromol.* 151, 428–440. doi: 10.1016/j.ijbiomac.2020.02.141

Ghate, V., Leong, A. L., Kumar, A., Bang, W. S., Zhou, W., and Yuk, H.-G. (2015). Enhancing the antibacterial effect of 461 and 521 nm light emitting diodes on selected foodborne pathogens in trypticase soy broth by acidic and alkaline pH conditions. *Food Microbiol.* 48, 49–57. doi: 10.1016/j.fm.2014.10.014

Ghate, V. S., Zhou, W., and Yuk, H.-G. (2019). Perspectives and trends in the application of photodynamic inactivation for microbiological food safety. *Compr. Rev. Food Sci. Food Saf.* 18, 402–424. doi: 10.1111/1541-4337.12418

Gonçalves da Rosa, C., Zapelini de Melo, A. P., Sganzerla, W. G., Machado, M. H., Nunes, M. R., Vinicius de Oliveira Brisola Maciel, M., et al. (2020). Application in situ of zein nanocapsules loaded with Origanum vulgare Linneus and Thymus vulgaris as a preservative in bread. *Food Hydrocoll.* 99, 105339. doi: 10.1016/j.foodhyd.2019.105339

Gonzalez-Valdivieso, J., Girotti, A., Schneider, J., and Arias, F. J. (2021). Advanced nanomedicine and cancer: Challenges and opportunities in clinical translation. *Int. J. Pharm.* 599, 120438. doi: 10.1016/j.ijpharm.2021.120438

Hosseinpour-Nader, A., Karimi, N., Ghafari, H.-A., and Ghorbanzadeh, R. (2022). Effect of nanomicelle curcumin-based photodynamic therapy on the dynamics of white spot lesions and virulence of Streptococcus mutans in patients undergoing fixed orthodontic treatment: A randomized double-blind clinical trial. *Photodiagnosis Photodyn. Ther.* 40, 103183. doi: 10.1016/j.pdpdt.2022.103183

Hu, X., Huang, Y.-Y., Wang, Y., Wang, X., and Hamblin, M. R. (2018). Antimicrobial photodynamic therapy to control clinically relevant biofilm infections. *Front. Microbiol.* 9. doi: 10.3389/fmicb.2018.01299

Hu, Y., Rees, N. H., Qiu, C., Wang, J., Jin, Z., Wang, R., et al. (2024). Fabrication of zein/modified cyclodextrin nanofibers for the stability enhancement and delivery of curcumin. *Food Hydrocoll.* 156, 110262. doi: 10.1016/j.foodhyd.2024.110262

Huang, J., Chen, B., Li, H., Zeng, Q.-H., Wang, J. J., Liu, H., et al. (2020). Enhanced antibacterial and antibiofilm functions of the curcumin-mediated photodynamic inactivation against *Listeria monocytogenes*. *Food Control* 108, 106886. doi: 10.1016/j.foodcont.2019.106886

Idrees, M., and Kujan, O. (2023). A curcumin-based oral gel has potential protective efficacy against oral mucositis: in vitro study. *J. Pers. Med.* 14, 1. doi: 10.3390/jpm14010001

Inchingolo, F., Inchingolo, A. D., Latini, G., Trilli, I., Ferrante, L., Nardelli, P., et al. (2024). The role of curcumin in oral health and diseases: a systematic review. *Antioxidants* 13, 660. doi: 10.3390/antiox13060660

Innes, N. P. T., Evans, D. J. P., and Stirrups, D. R. (2011). Sealing caries in primary molars: randomized control trial, 5-year results. *J. Dent. Res.* 90, 1405–1410. doi: 10.1177/0022034511422064

Kamwilaisak, K., Rittiwut, K., Jutakridsada, P., Iamamorphanth, W., Pimsawat, N., Knijnenburg, J. T. N., et al. (2022). Rheology, stability, antioxidant properties, and curcumin release of oil-in-water Pickering emulsions stabilized by rice starch nanoparticles. *Int. J. Biol. Macromol.* 214, 370–380. doi: 10.1016/j.ijbiomac.2022.06.032

Karthikeyan, A., Senthil, N., and Min, T. (2020). Nanocurcumin: A promising candidate for therapeutic applications. *Front. Pharmacol.* 11. doi: 10.3389/fphar.2020.00487

Knorst, J. K., Barriquello, G. S., Villetti, M. A., Santos, R. C. V., and Kantorski, K. Z. (2019). Antimicrobial effect of methylene blue formulations with oxygen carrier at different pHs: preliminary study. *BDS* 22, 39–45. doi: 10.14295/bds.2019.v22i1.1635

Koo, H., Falsetta, M. L., and Klein, M. I. (2013). The exopolysaccharide matrix: A virulence determinant of cariogenic biofilm. *J. Dent. Res.* 92, 1065–1073. doi: 10.1177/0022034513504218

Lenzuni, M., Bonfadini, S., Criante, L., Zorzi, F., Summa, M., Bertorelli, R., et al. (2023). Dynamic investigation of zein-based degradable and hemocompatible coatings for drug-eluting stents: a microfluidic approach. *Lab. Chip* 23, 1576–1592. doi: 10.1039/D3LC00012E

Lin, Z., Zhan, L., Qin, K., Li, Y., Qin, Y., Yang, L., et al. (2024). Design and characterization of a novel core–shell nano delivery system based on zein and carboxymethylated short-chain amylose for encapsulation of curcumin. *Foods* 13, 1837. doi: 10.3390/foods13121837

Liu, G., An, D., Li, J., and Deng, S. (2023). Zein-based nanoparticles: Preparation, characterization, and pharmaceutical application. *Front. Pharmacol.* 14. doi: 10.3389/fphar.2023.1120251

Machiulskiene, V., Campus, G., Carvalho, J. C., Dige, I., Ekstrand, K. R., Jablonski-Momeni, A., et al. (2020). Terminology of dental caries and dental caries management: consensus report of a workshop organized by ORCA and cariology research group of IADR. *Caries Res.* 54, 7–14. doi: 10.1159/000503309

Manoil, D., Filieri, A., Gameiro, C., Lange, N., Schrenzel, J., Wataha, J. C., et al. (2014). Flow cytometric assessment of *Streptococcus mutans* viability after exposure to blue light-activated curcumin. *Photodiagnosis Photodyn. Ther.* 11, 372–379. doi: 10.1016/j.pdpdt.2014.06.003

Maleki Dizaj, S., Shokrgozar, H., Yazdani, J., Memar, M. Y., Sharifi, S., and Ghavimi, M. A. (2022). Antibacterial Effects of Curcumin Nanocrystals against Porphyromonas gingivalis Isolated from Patients with Implant Failure. *Clin. Pract.* 12, 809–817. doi: 10.3390/clinpract12050085

Masiero, A. V., Barletta, F. B., Nunes, M. R., Sganzerla, W. G., Erckmann, M. C., and da Rosa, C. G. (2024). "Chapter 13 - Silver nanoparticles and their role in the treatment of endodontic infections," in *Silver Nanoparticles for Drug Delivery*. Ed. P. Kesharwani (London United Kingdom, San Diego CA, United States, Cambridge, MA, United States, Oxford, United Kingdom: Academic Press), 289–311. doi: 10.1016/B978-0-443-15343-3.00011-5

Melo, M. A. S., Rolim, J. P. M. L., Passos, V. F., Lima, R. A., Zanin, I. C. J., Codes, B. M., et al. (2015). Photodynamic antimicrobial chemotherapy and ultraconservative caries removal linked for management of deep caries lesions. *Photodiagnosis Photodyn. Ther.* 12, 581–586. doi: 10.1016/j.pdpdt.2015.09.005

Meng, Q., Zhou, L., Zhong, S., Wang, J., Wang, J., Gao, Y., et al. (2023). Stimulus-responsive starch-based nanocapsules for targeted delivery and antibacterial applications. *Int. J. Biol. Macromol.* 241, 124664. doi: 10.1016/j.ijbiomac.2023.124664

Minhaco, V. M. T. R., Maquera Huacho, P. M., Mancim Imbriani, M. J., Tonon, C. C., Chorilli, M., Rastelli, A. N., et al. (2023). Improving antimicrobial activity against endodontic biofilm after exposure to blue light-activated novel curcumin nanoparticle. *Photodiagnosis Photodyn. Ther.* 42, 103322. doi: 10.1016/j.pdpdt.2023.103322

Narciso, A. M., Paim, B., Da Rosa, C. G., Paes, J. V., Nunes, M. R., et al. (2019). Síntese verde de nanopartículas de prata para uso em biomateriais odontológicos. *Revista Interdisciplinar de Estudos em Saúde*, 64–73. doi: 10.33362/ries.v8i2.2124

Nehete, A. P., Singh, J. S., Mehta, R. V., Desai, R. S., Bansal, S. P., and Kakade, A. (2014). Study of the microstructure of mineralised tissues in 50 human primary teeth. *Int. J. Oral. Maxillofac. Pathol.* 5 (4), 12–18.

Nunes, M. R., Da Rosa, C. G., De Borba, J. R., Dos Santos, G. M., Ferreira, A. L., and Barreto, P. L. M. (2022). Zein Nanoparticles: Bioactive Compounds and Controlled Delivery. In: S. Jana and S. Jana (eds.), *Nanoengineering of Biomaterials*. (Wiley), 411–436. doi: 10.1002/9783527832095.ch13

Oh, Y. K., and Flanagan, D. R. (2010). Diffusional properties of zein membranes and matrices. *Drug Dev. Ind. Pharm.* 36, 497–507. doi: 10.3109/03639040903264389

Omidian, H., Wilson, R. L., and Chowdhury, S. D. (2023). Enhancing therapeutic efficacy of curcumin: advances in delivery systems and clinical applications. *Gels* 9, 596. doi: 10.3390/gels9080596

Parizzi, M., Almeida, A. R., Salvador, G., Dominguini, D., Fernandes, M., Becker, D., et al. (2025). Photosensitized methylene blue nanoparticles: A promising approach for the control of oral infections. *Biomedicines* 13, 673. doi: 10.3390/biomedicines13030673

Pereira, M. A., Faustino, M. A. F., Tomé, J. P. C., Neves, M.G.P.M.S., Tomé, A. C., Cavaleiro, J. A. S., et al. (2014). Influence of external bacterial structures on the efficiency of photodynamic inactivation by a cationic porphyrin. *Photochem. Photobiol. Sci.* 13, 680–690. doi: 10.1039/c3pp50408e

Pourhajibagher, M., Bahrami, R., and Bahador, A. (2022). An ex vivo evaluation of physico-mechanical and anti-biofilm properties of resin-modified glass ionomer containing ultrasound waves-activated nanoparticles against *Streptococcus mutans* biofilm around orthodontic bands. *Photodiagnosis Photodyn. Ther.* 40, 103051. doi: 10.1016/j.pdpdt.2022.103051

Pourhajibagher, M., Salehi Vaziri, A., Takzaree, N., and Ghorbanzadeh, R. (2019). Physico-mechanical and antimicrobial properties of an orthodontic adhesive containing cationic curcumin doped zinc oxide nanoparticles subjected to photodynamic therapy. *Photodiagnosis Photodyn. Ther.* 25, 239–246. doi: 10.1016/j.pdpdt.2019.01.002

Pourhajibagher, M., Kazemian, H., Chiniforush, N., Hosseini, N., Pourakbari, B., Azizollahi, A., et al. (2018). Exploring different photosensitizers to optimize elimination of planktonic and biofilm forms of Enterococcus faecalis from infected root canal during antimicrobial photodynamic therapy. *Photodiagnosis Photodyn. Ther.* 24, 206–211. doi: 10.1016/j.pdpdt.2018.09.014

Sayed, M., Hiraishi, N., Matin, K., Abdou, A., Burrow, M. F., and Tagami, J. (2020). Effect of silver-containing agents on the ultra-structural morphology of dentinal collagen. *Dent. Mater.* 36, 936–944. doi: 10.1016/j.dental.2020.04.028

Shahi, S., Özcan, M., Maleki Dizaj, S., Sharifi, S., Al-Haj Husain, N., Eftekhari, A., et al (2019). A review on potential toxicity of dental material and screening their biocompatibility. *Toxicol. Mech. Methods* 29, 368–377. doi: 10.1080/15376516.2019.1566424

Silvestre, A. L. P., Dos Santos, A. M., De Oliveira, A. B., Ferrisse, T. M., Brighenti, F. L., Meneguin, A. B., et al. (2023). Evaluation of photodynamic therapy on nanoparticles and films loaded-nanoparticles based on chitosan/alginate for curcumin delivery in oral biofilms. *Int. J. Biol. Macromol.* 240, 124489. doi: 10.1016/j.ijbiomac.2023.124489

Steiner-Oliveira, C., Longo, P. L., Aranha, A. C. C., Ramalho, K. M., Mayer, M. P. A., and de Paula Eduardo, C. (2015). Randomized *in vivo* evaluation of photodynamic antimicrobial chemotherapy on deciduous carious dentin. *J. Biomed. Opt.* 20, 108003. doi: 10.1117/1.JBO.20.10.108003

Suzuki, I. L., Inada, N. M., Marangoni, V. S., Corrêa, T. Q., Zucolotto, V., Kurachi, C., et al (2016). Synthesis and characterization of PLGA nanoparticles containing mixture of curcuminoids for optimization of photodynamic inactivation. In: D. H. Kessel and T. Hasan (eds.), *SPIE Proceedings* (San Francisco, California, United States), 969413. doi: 10.1117/12.2213781

Takahashi, N., and Nyvad, B. (2016). Ecological hypothesis of dentin and root caries. *Caries Res.* 50, 422–431. doi: 10.1159/000447309

Taraszkiewicz, A., Fila, G., Grinholc, M., and Nakonieczna, J. (2013). Innovative strategies to overcome biofilm resistance. *BioMed Res. Int.* 2013, 150653. doi: 10.1155/2013/150653

Tonon, C. C., Paschoal, M. A., Correia, M., Spolidório, D. M. P., Bagnato, V. S., Giusti, J. S. M., et al. (2015). Comparative effects of photodynamic therapy mediated by curcumin on standard and clinical isolate of Streptococcus mutans. *J. Contemp Dent. Pract.* 16, 1–6. doi: 10.5005/jp-journals-10024-1626

Urošević, M., Nikolić, L., Gajić, I., Nikolić, V., Dinić, A., and Miljković, V. (2022). Curcumin: biological activities and modern pharmaceutical forms. *Antibiotics* 11, 135. doi: 10.3390/antibiotics11020135

Wilson, B. C., and Patterson, M. S. (2008). The physics, biophysics and technology of photodynamic therapy. *Phys. Med. Biol.* 53, R61–109. doi: 10.1088/0031-9155/53/9/R01

Wu, J., Chen, J., Wei, Z., Zhu, P., Li, B., Qing, Q., et al. (2023). Fabrication, evaluation, and antioxidant properties of carrier-free curcumin nanoparticles. *Molecules* 28, 1298. doi: 10.3390/molecules28031298

Zaleh, A.-A., Salehi-Vaziri, A., Pourhajibagher, M., and Bahador, A. (2022). The synergistic effect of Nano-propolis and curcumin-based photodynamic therapy on remineralization of white spot lesions: An ex vivo study. *Photodiagnosis Photodyn. Ther.* 38, 102789. doi: 10.1016/j.pdpdt.2022.102789

Zanin, I. C. J., Gonçalves, R. B., Junior, A. B., Hope, C. K., and Pratten, J. (2005). Susceptibility of Streptococcus mutans biofilms to photodynamic therapy: an *in vitro* study. *J. Antimicrob. Chemother.* 56, 324–330. doi: 10.1093/jac/dki232

Zhang, Z., Li, X., Sang, S., Julian McClements, D., Chen, L., Long, J., et al. (2023). Preparation, properties and interaction of curcumin loaded zein/HP-β-CD nanoparticles based on electrostatic interactions by antisolvent co-precipitation. *Food Chem.* 403, 134344. doi: 10.1016/j.foodchem.2022.134344

Zhang, H., Van Os, W. L., Tian, X., Zu, G., Ribovski, L., Bron, R., et al. (2021). Development of curcumin-loaded zein nanoparticles for transport across the blood–brain barrier and inhibition of glioblastoma cell growth. *Biomater. Sci.* 9, 7092–7103. doi: 10.1039/D0BM01536A

Zheng, D., Huang, C., Huang, H., Zhao, Y., Khan, M. R. U., Zhao, H., et al (2020). Antibacterial Mechanism of Curcumin: A Review. *Chem. Biodivers.* 17, e2000171. doi: 10.1002/cbdv.202000171

Zhi, K., Yang, H., Shan, Z., Huang, K., Zhang, M., and Xia, X. (2021). Dual-modified starch nanospheres encapsulated with curcumin by self-assembly: Structure, physicochemical properties and anti-inflammatory activity. *Int. J. Biol. Macromol.* 191, 305–314. doi: 10.1016/j.ijbiomac.2021.09.117

Zorofchian Moghadamtousi, S., Abdul Kadir, H., Hassandarvish, P., Tajik, H., Abubakar, S., and Zandi, K. (2014). A review on antibacterial, antiviral, and antifungal activity of curcumin. *BioMed. Res. Int.* 2014, 186864. doi: 10.1155/2014/186864

frontiers | Frontiers in Cellular and Infection Microbiology

TYPE Review
PUBLISHED 17 September 2025
DOI 10.3389/fcimb.2025.1663563

OPEN ACCESS

EDITED BY
Xuelian Huang,
University of Washington, United States

REVIEWED BY
Panpan Wang,
Sun Yat-sen University, China
Yuan Gao,
West China Hospital of Sichuan University, China

*CORRESPONDENCE
Wen Zhou
zhouwendentist@139.com

RECEIVED 10 July 2025
ACCEPTED 01 September 2025
PUBLISHED 17 September 2025

CITATION
Chen Y, Lin S, Huang X and Zhou W (2025) From biofilm control to biomimetic remineralization: Hydrogels in prevention and treatment of dental caries.
Front. Cell. Infect. Microbiol. 15:1663563.
doi: 10.3389/fcimb.2025.1663563

From biofilm control to biomimetic remineralization: Hydrogels in prevention and treatment of dental caries

Yuqing Chen, Shikang Lin, Xiaojing Huang and Wen Zhou*

Fujian Key Laboratory of Oral Diseases and Fujian Provincial Engineering Research Center of Oral Biomaterial and Stomatological Key Lab of Fujian College and University, School and Hospital of Stomatology, Fujian Medical University, Fuzhou, China

Dental caries, a prevalent chronic bacterial disease globally, poses a significant threat to public health due to its complex pathogenesis involving demineralization and microbial dysbiosis. Hydrogels, with their unique three-dimensional network structures and diverse properties, have shown great potential in prevention and treatment of dental caries. This article systematically reviews recent advances in anti-caries hydrogel development. It first introduces the basis of anti-caries hydrogels, covering the applications of natural and semi-synthetic polymers as hydrogel matrices. Then, it elaborates on the mechanisms and research status of different types of anti-caries hydrogels, including probiotic formulations, antibacterial hydrogels, remineralization-inducing hydrogels, and saliva-related caries-reducing hydrogels. Finally, it summarizes the current research achievements and limitations and looks ahead to future research directions.

KEYWORDS

dental caries, hydrogel, antibacterial, remineralization, prevention and treatment

1 Introduction

Dental caries is a chronic bacterial disease affecting the hard tissue of the teeth and is recognized as a significant, escalating global public health challenge. According to the World Health Organization (WHO) in 2023, dental caries is the most prevalent non-communicable chronic disease worldwide. Over one-third of the global population living with untreated caries (Benzian et al., 2022). The development of dental caries results from a complex interplay over time among acid-producing bacteria and fermentable carbohydrates and host factors, including the condition of teeth and saliva (Marsh, 1994; Featherstone, 2004; Mandel, 1989). The pathological changes involve the organic matter decomposition and inorganic component demineralization in dental hard tissues (Wefel et al., 1985). Targeting the key factors lead to dental caries formation is effective in preventing and treating this chronic disease.

Antibacterial materials, competitive oral probiotics, and remineralization promoters are increasingly studied for synergistic caries management (Selwitz et al., 2007). Nowadays, quite

a lot of improved anti-caries hydrogels are studied and developed, by taking use of anti-caries agents (Jenkins, 1985; Krasse, 1988; Rafiee et al., 2024; Zhen et al., 2022). Complex physicochemical oral environments and bacterial biofilms are considered critical factors compromising the clinical performance of anti-caries materials (Paula and Koo, 2017; Chen et al., 2016). Hydrogel application can enhance key properties of anti-caries agents and improve their effectiveness, such as prolonging duration of action and retention at target sites (Senel et al., 2000). This attribute to hydrogels' three-dimensional networks that possess properties including electroconductivity, swellability, environmental sensitivity, and viscosity (Jang et al., 2021; Lei et al., 2023; Zhang et al., 2020; Chen et al., 2023; Liang et al., 2021; Vinikoor et al., 2023). The strong hydrophilicity enables hydrogel remain stable for a long time after swelling in water (Thang et al., 2023). This stability enhances both the duration of action and site retention compared to traditional materials (Li et al., 2024). Moreover, hydrogels' cross-linked polymeric structure provides three-dimensional stability that enables effective loading of active ingredients while serving as a remineralization scaffold (Thang et al., 2023; Ding et al., 2022). These features make hydrogel promising material for caries management. Integrating traditional materials with hydrogels significantly enhances caries preventive and therapeutic efficacy (Rafiee et al., 2024; Zhen et al., 2022; Fathy et al., 2024; Cao et al., 2014; Estes Bright et al., 2022; Matsuda et al., 2022).

In recent years, hydrogels were increasingly studied for caries prevention and treatment (Muşat et al., 2021; Cai and Moradian-Oldak, 2023; Zhang et al., 2021c). Generally, hydrogels are composed of main body, serving as the carrier, and functional payloads. Consequently, hydrogels can be classified into natural and semi-synthetic types based on their structural composition (Loessner et al., 2016; Ho et al., 2022; Corkhill et al., 1989). The loaded ingredients endow the hydrogels with specific functions: antibacterial action, remineralization, probiotic delivery, and reducing saliva-related caries. Therefore, the present paper reviews hydrogel application in caries control, analyze their preventive/therapeutic roles, and outlines future research directions. Additionally, current challenges and potential solutions for complex hydrogels are discussed.

2 The base of anti-caries hydrogels

Commonly, gelling materials serve as the hydrogel base, functioning as the structure matrix. The matrix mainly acts as a carrier for effective ingredients (Cao et al., 2021). Hydrogel bases may comprise natural, synthetic or semi-synthetic polymers (Figure 1) (Taghipour et al., 2020). At present, only natural and semi-synthetic hydrogels are utilized in preventing or treating dental caries.

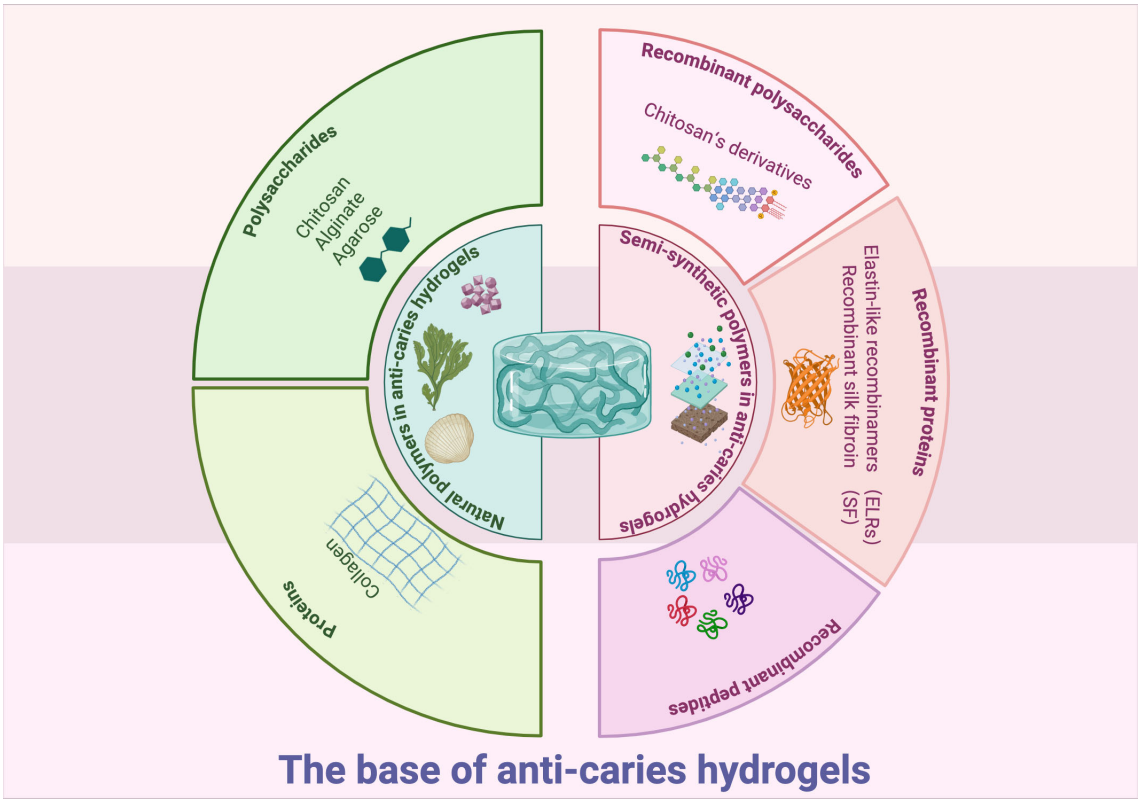

FIGURE 1
Graphical summery of the base of anti-caries hydrogels. Created in BioRender. Yuqing, C. (2025) https://BioRender.com/1phjnk0.

2.1 Natural polymers in anti-caries hydrogels

Natural polymers, such as polysaccharides (chitosan, alginate, and agarose) and proteins (collagen), have been studied as structural matrix for anti-caries hydrogels (Estes Bright et al., 2022; Rafiee et al., 2024; Mukherjee et al., 2021). As natural polymer matrix originated from living organisms, they exhibit good biocompatibility and accessibility (Coviello et al., 2007). However, many natural polymers lack inherent antibacterial efficacy (Zhong et al., 2020). The past decades have seen many researches incorporate antibiotic and antibacterial agents into natural polymer-based hydrogels to improve antibacterial properties (Zhong et al., 2020). Furthermore, cross-linking these hydrogels with other polymers has been demonstrated to improve stability, tissue adhesion, and mechanical properties (Zhen et al., 2022; Ju et al., 2023; Yuan et al., 2023; Mohanto et al., 2023; Hu et al., 2019). These advancements position natural polymer hydrogels as promising candidates for future caries management.

2.1.1 Polysaccharides

Polysaccharide hydrogels possess characteristic of thickening, stability, and gum formation (Tamo et al., 2024). To date, many natural polysaccharides, including chitosan, alginate, and agarose have great potential in making anti-caries hydrogels (Ju et al., 2023).

Chitosan is a natural polysaccharide originated from chitin within exoskeletons of crustaceans (Gholap et al., 2024). Commonly, it is easy to form hydrogels by physically cross-linking with each other, making it widely used (Pellá et al., 2018; Hamedi et al., 2022; Kalantari et al., 2019; Gholap et al., 2024). These applicable capabilities might originate from its excellent biocompatibility, biodegradability, antibacterial ability, and cell affinity (Pellá et al., 2018; Hamedi et al., 2022; Kalantari et al., 2019; Gholap et al., 2024). Due to equipped with positive charged amine groups, many chitosan-based hydrogels realize loading or releasing materials they carried, through charge interactions with other negative charged amine groups (Sereni et al., 2017; Pellá et al., 2018; Mohamed et al., 2017). Given all these features, chitosan-based hydrogels can serve as effective carriers of antibacterial or remineralization agents for prevention and treatment of dental caries. In addition, chitosan has the ability to suppress the growth of certain oral bacteria, like *Streptococcus mutans* (*S. mutans)* and *Porphyromonas gingivalis* (*P. gingivalis*), and inhibit the plaque formation (Li et al., 2020; Veltman et al., 2022). Flexibility of chitosan allows it bind to bacteria, penetrate cell membranes, alter DNA structure, prevent the formation of biological macromolecules, and reduce the production of virulence factors in pathogenic bacteria (Li et al., 2022a).

Alginate, mainly obtained from seaweeds, shows promising property in forming ionic hydrogels through coordination between polyvalent metal ions and alginate macromolecules, following the exchange of alginate ions with polyvalent cations (Zhang et al., 2021a). It also shows remarkable advantages like biocompatibility, porosity, adjustable viscosity and water retention capacity (Liu et al., 2022a). All of these features make it an ideal material for biomedical applications (Maity and Das, 2021; Song et al., 2023). At present, alginate-based hydrogels, like sodium alginate synthetic hydrogel, have been applied to remineralize hard tissues of teeth. They show excellent delivering talents, effective mineralization-inducing abilities, and even ion-triggered self-healing abilities (Zhang et al., 2021c; Estes Bright et al., 2022). However, the uncontrolled dissolution of the alginate polymer network, caused by ion exchange or loss, remains a non-negligible problem (Kharkar et al., 2013). More researches still remain to be carried out dealing with these issues.

Agarose, a water-soluble polysaccharide, is notable for its crosslinking ability and effectiveness in delivery properties (Khodadadi Yazdi et al., 2020). It has ability to expand within aqueous solution, allowing agarose-based hydrogels to load drugs when swollen, thereby maximizing drug diffusion (Kolanthai et al., 2017). Under physiological conditions, agarose-based hydrogel can mimic gel-like organic matrix environment in controlling the size and form of hydroxyapatite (HAP) crystals via interacting with calcium by hydroxyl group of agarose (Cao et al., 2014). What's more, it can also carry remineralization-inducing molecules, making it promising for anti-caries therapy (Dong et al., 2021; Khodadadi Yazdi et al., 2020). Nowadays, studies investigated the role of agarose-based gels in tooth remineralization, demonstrated that agarose hydrogel could replenish mineral precursors and control the size of calcium phosphate complex. Han et al. invented a novel agarose hydrogel system and successfully remineralized dentin *in vivo* (Han et al., 2017). Besides, Moshy et al. induced remineralizaton via agarose-based hydrogel on the caries lesion with better biosafety (El Moshy et al., 2018). With advancements in agarose-based hydrogels, researchers have successfully translated these biomaterials from *in vitro* biomimetic models to *in vivo* rabbit models, demonstrating significant efficacy in dental caries treatment.

2.1.2 Proteins

Proteins are organic macromolecules characterized by distinct three-dimensional conformations formed through the folding and coiling of polypeptide chains. These chains consistently adopt specific spatial configurations essential for biological function. The covalent and non-covalent aggregations of proteins, like collagens, facilitate the formation of gel networks. These protein-based hydrogels equip with certain stability and elasticity (Fu et al., 2023a; Zheng and Zuo, 2021; Antoine et al., 2014). While protein-based hydrogels have shown promise for dental hard tissue remineralization, their unmodified forms are rarely employed in caries management.

Collagen, which can be widely founded in the extracellular matrix, is the most common protein in the human body (Knudsen et al., 1985; Morris-Wiman and Brinkley, 1992; Singh et al., 1998). It is also crucial as the basic component of teeth tissues (Väänänen et al., 2004; Tabata et al., 1995; Lukinmaa and Waltimo, 1992). It can cross-link through chemical, physical or enzymatic way to form hydrogels (Geanaliu-Nicolae and Andronescu, 2020). Upon hydrogel formation, the material exhibits significantly enhanced stability, mechanical strength, and toughness, positioning it as an advanced biomaterial for dental applications (Yang et al., 2022).

Moreover, its distinctive triple-helix structure confers molecular recognition capabilities that facilitate efficient carrier functionality (Ruszczak and Friess, 2003; An et al., 2016). At present, collagen-based hydrogel is widely used for remineralization and anti-bacterial activities (Fu et al., 2023b; Amaya-Chantaca et al., 2023; Ikeda et al., 2022). These collagen-based carriers demonstrate significant efficacy *in vitro* when loaded with therapeutic agents. When loaded with mineralization-inducing or antibacterial agents, collagen-based hydrogels demonstrate good performance *in vitro* for both mineralization and antibacterial activities. For example, odontogenic ameloblast-associated protein (ODAM)-impregnated collagen hydrogel, has been proved to be effective in inducing mineralization (Ikeda et al., 2018).

2.2 Semi-synthetic polymers in anti-caries hydrogels

Semi-synthetic polymers are derived from chemical modifications of natural polymers. Recently, hydrogels based on these semi-synthetic polymers have shown promise for caries prevention applications.

2.2.1 Recombinant polysaccharides

Chitosan's derivatives are good examples. Active groups like amino and hydroxyl groups can be modified by etherification, esterification, crosslinking acetylation, and so on. Modified chitosan derivatives readily form hydrogels through physical cross-linking. These materials constitute ideal anti-caries hydrogels, exhibiting excellent biocompatibility, biodegradability, antibacterial efficacy, and cellular affinity (Pellá et al., 2018; Hamedi et al., 2022; Kalantari et al., 2019; Gholap et al., 2024). These modifications can effectively improve hydrogels' qualities, including antimicrobial ability, mucoadhesive property, and biocompatibility (Mohire and Yadav, 2010; Dilamian et al., 2013; Arora et al., 2023).

2.2.2 Recombinant proteins

In 2015, Li et al. creatively used a type of special biosynthetic elastin-like recombinamers (ELRs) in templating HAP nanocrystal mineralization (Li et al., 2015). These ELRs are made up of repeating pentapeptide sequences derived from tropoelastin (VPG-Xaa-G) (Arias et al., 2006). The chemical linking procedures modified the features of original polymers, enhancing mechanical stability, elasticity, bioactivity, and self-assembly properties (Li et al., 2015). Then these polymers would undergo monomer polymerization to form hybrid hydrogels. Finally, they successfully employed these ELRs to create synthesized thermo-responsive hydrogels, with promising mineralization-inducing properties (Li et al., 2015).

Recombinant silk fibroin (SF) is another type of chemically cross-linked semi-synthetic hydrogel which can deposit HAP perfectly, and with high tensile biomechanical strength, biocompatibility as well as biodegradability (Belda Marín et al., 2020). In 2022, a study showed that by combining tannic acid (TA), SF, and sodium fluoride (NaF), the composite showed remarkable biological stability and biocompatibility (Zhen et al., 2022). Currently, inspired by hagfish, Zhu et al. developed a fluid-hydrogel conversion system containing silk fibroin-TA-black phosphorene-urea (ST-BP-U) to prevent root caries (Zhu et al., 2024). This hydrogel uniformly coats the root surface and penetrates dentinal tubules. Upon aqueous exposure, it undergoes *in situ* reorganization with enhanced crosslinking density, developing stable wet-adhesion properties. Leveraging this platform, potent phototherapeutic effects and enhanced dentin remineralization are achieved.

2.2.3 Recombinant peptides

Peptides spontaneously self-assemble into ordered structures via non-covalent interactions, enabling their application in drug delivery systems (Liu et al., 2011; Caporale et al., 2021). Besides, some peptides might be effective in inhibiting the growth of cariogenic bacteria, making them the potential candidates for forming anti-caries hydrogels. Sun et al. developed a pH-responsive hydrogel coating, basing on recombinant peptide, aiming at reducing dental caries (Sun et al., 2022). This recombinant peptide-based hydrogel demonstrated significant antibacterial efficacy. However, no comparable recombinant peptide-based hydrogels have been developed for anti-caries applications to date.

In a word, the promising features of semi-synthetic hydrogels in dental fields not only maintain the ideal bioactivity of natural hydrogels but also offer multi-tunable properties derived from various chemical parameters (Park and Park, 2016). However, while many semi-synthetic polymers demonstrate excellent properties in antibacterial activity and remineralization, limited semi-synthetic polymer-based hydrogels are developed for treating dental caries (Itskovich et al., 2021; Barreto et al., 2022; Nistor et al., 2013; Barman et al., 2024). Researches focusing on the effective utilization of semi-synthetic polymer-based hybrid hydrogels for caries treatment remains largely unexplored. Further studies are needed to address this gap.

3 Hydrogels for prevention and treatment of caries

Generally, hydrogels used for preventing and treating dental caries can be classified in to five types: probiotic formulation hydrogels, antibacterial hydrogel, remineralization-inducing hydrogel, antibacterial and remineralization-inducing hydrogel, and salivary-gland-regenerating hydrogel (Figure 2).

3.1 Probiotic formulation hydrogels

Dental biofilms are highly assembled microbial communities, surrounded by an extracellular matrix that includes both commensal bacteria and opportunistic pathogens. Under healthy oral conditions, these components maintain a relative balance

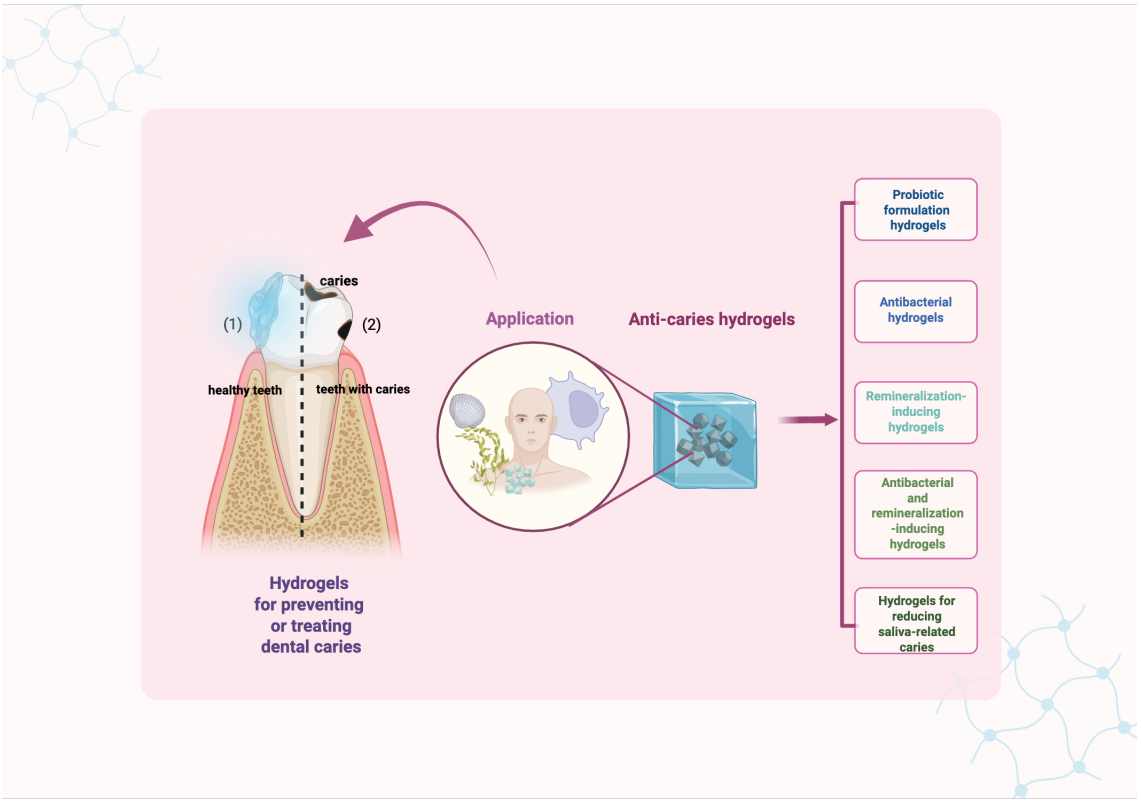

FIGURE 2
Graphical summery of anti-caries hydrogels. Created in BioRender. Yuqing, C. (2025) https://BioRender.com/uhrig6b.

(Bowen et al., 2018; Gao et al., 2018; Takahashi and Nyvad, 2011). However, once the balance was broken, like cariogenic bacteria abnormal increasing, there will be higher risk to gain dental caries (Takahashi and Nyvad, 2011). Nowadays, a novel treatment known as oral microbiome transplantation (OMT) has been developed, and might have potential to be used for clinical treatment in the future (Weyrich et al., 2024; Beikler et al., 2021; Xiao et al., 2021; Huang and Cheng, 2024). The primary aim of OMT is to address oral dysbiosis, restore ecological balance, and maintain stable homeostasis with the host's immune system. This can be achieved by using hydrogel delivery vehicle to introduce samples containing the healthiest microbiota into the oral environment. An OMT has been applied among rats and mice successfully (Nath et al., 2021). This method is emerging as a promising therapeutic strategy for dental caries prevention and management, though further validation through clinical studies is warranted.

Recent studies have indicated that *Candida albicans* (*C. albicans*) has the potential to contribute to dental caries. So, an experiment by Ribeiro et al. focused on inhibiting cariogenic *C. albicans* using gellan *gum-Lactobacillus* species (*Lactobacillus* sp.) cells (Ribeiro et al., 2020). This study marked the first investigation that utilized gellan gum hydrogel to incorporate *Lactobacillus* sp. cells to control oral candidiasis, which is relevant to inducing caries. In another study, Ribeiro et al. selected the non-toxic natural polysaccharide gellan gum as a delivery vehicle to deliver *Lacticaseibacillusparacasei* (*L. paracasei*)28.4 into the oral cavity, aiming to inhibit *C. albicans* growth and development of candidiasis. The gellan gum protected drug inside from degradation caused by physical and chemical factors in oral environments. *In vitro* experiments demonstrated that the bacteria released from the probiotic-gellan gum formulation effectively inhibited *C. albicans* growth and biofilm formation on acrylic resin surfaces. Additionally, *in vivo* experiments using a murine model confirmed that the probiotic-loaded gellan gum at concentrations of 1% (wt/vol) and 0.6% (wt/vol) facilitated oral colonization by *L. paracasei*, which was sufficient to prevent *C. albicans* growth and the associated symptomatic lesions like dental caries.

3.2 Antibacterial hydrogels

Colonization, growth and metabolism of cariogenic bacteria are important factors leading to dental caries (Selwitz et al., 2007). A lot of hydrogel materials for suppressing the caries pathogenic bacteria have been developed. These hydrogels can kill the cariogenic bacteria by incorporated molecules such as peptides, reactive oxygen species (ROS), certain enzyme and antibody (Luong et al., 2022; Li et al., 2022b; Patel, 2020).

Metal and metallic oxides have been used in controlling dental caries for quite a long time because of their outstanding features in interfering with bacterial metabolism and preventing biofilm

formation. Metal ions induce both oxidative stress and non-oxidative mechanisms to realize significant antimicrobial effect (Nizami et al., 2021). Hydrogels combined with ions or oxides of silver, zinc, titanium, and copper have shown effective in preventing dental caries. Afrasiabi et al. demonstrated the potential of zinc oxide nanoparticles (ZnO NPs) doped into a zeolite/chitosan hydrogel (ZnONC-CS) for preventing dental caries (Afrasiabi et al., 2021). ZnONC-CS gel significantly inhibited *S. mutans* growth, affected its metabolic activity, and also effectively decreased the expression of the gtfB, gtfC, and ftf genes, making it a promising candidate for caries management. In 2022, Li et al. reported an intelligent fast-cross-linking hydrogel activated by green light. Their experiments demonstrated that $Bi_{12}O_{17}Cl_2$ and Cu_2O rapidly cross-link with calcium ions (Ca^{2+}) to form an adhesive network structure on tooth surfaces. This structure releases ROS upon green light exposure, inducing localized sterilization, biofilm removal, and caries prevention in both *in vitro* and *in vivo* models (Li et al., 2022b).

Glucosyltransferases (Gtfs) are enzymes involved in the pathogenic proliferations and actions of *S. mutans* to mediate dental caries (Zhang et al., 2021b). They induce biofilm formation, leading to the colonization of cariogenic bacteria. Therefore, Gtfs are considered an important target for inhibiting cariogenic biofilms. Ahirwar et al. modified the structure of a biofilm inhibitor IIIC5 to synthesize a novel pH-responsive hydrogel: hydroxy aurones 5 (HA5) (Ahirwar et al., 2023). This compound inhibited Gtfs and suppressed glucan production. Moreover, HA5 could selectively inhibit *S. mutans* biofilms and reduce caries incidence, demonstrating its potential as an ideal candidate to address traditional challenges of anti-caries drugs. These challenges include limited solubility, poor biofilms penetration, and inability to retain efficacy in infected areas within the complex oral cavity environment.

3.3 Remineralization-inducing hydrogels

3.3.1 Demineralization and remineralization balance in caries

In oral environment, the balance between demineralization and remineralization of teeth hard tissues is significant to caries (Selwitz et al., 2007). The emergence, progression, cessation, or reemergence of caries largely depends on whether this balance is preserved (Featherstone, 2004). When the balance was broken and demineralization becomes the predominant, the process of dental caries formation is stimulated (Selwitz et al., 2007; Wang et al., 2021). Consequently, the remineralization of demineralized teeth has long been a major research focus in dental science. Some remineralization-inducing hydrogels function by directly or indirectly interacting with Ca^{2+}, PO_4^{3-}, and HAP to promote stable mineral deposition on the tooth surface (Table 1). The resulting mineralized layers cover both intact surfaces and demineralized regions, thereby protecting dental hard tissues from acid erosion (Parker et al., 2014; Sun et al., 2014).

3.3.2 Fluoride hydrogels

Historically, fluoride was the first practical approach for caries prevention due to its ability to induce remineralization (Zampetti and Scribante, 2020). However, traditional fluoride applications faced limitations imposed by the wet, dynamic oral environment, which compromised delivery efficiency and rapidly cleared drugs from tooth surfaces. These challenges were subsequently addressed through the development of fluoride hydrogel (Zhen et al., 2022). Fluoride ions released from the hydrogels interact with dental HAP to form acid-resistant fluorapatite (Bossù et al., 2019).

In 2014, Cao et al. firstly developed an effective NaF/chitosan hydrogel (Cao et al., 2014). This hydrogel restored prismatic enamel-like tissue while controlling formation, size, and mineral composition. It induced remineralization through synergistic interactions with calcium, phosphate, and fluoride ions, producing regenerated apatite crystals with strong c-axis orientation and high crystallinity. Contemporary fluoride hydrogel development has evolved from simple NaF encapsulation to advanced formulations designed for moist oral environments and physiological temperature fluctuations. These hydrogels sustain fluoride release, providing long-term anticaries and antibacterial effects with improved biocompatibility and stability. Matsuda et al. demonstrated that fluoride hydrogels significantly increase fluoride uptake on acid-etched root surfaces and inhibit hard tissue demineralization. For improved performance in moist oral conditions (Matsuda et al., 2022). For better application in moist and dynamic oral cavity environment, another study pioneered a mussel-inspired wet adhesive self-assembled fluoride hydrogel (TS@NaF) (Zhen et al., 2022). Zhen et al. used *in vitro* retention and degradation tests to simulate the drug performance under complex oral conditions. They proved this material could ideally resist the attack of enzymes and washing of liquids. This system exhibits superior stability, biocompatibility, and promotes effective calcium fluoride deposition on enamel.

However, while fluoride effectively combats caries, excessive fluoride intake poses risks like dental fluorosis, especially in children. As the primary source of fluoride exposure, community water fluoridation targets a concentration of 1 ppm. This specific level is chosen to optimize fluoride's cavity-preventing benefits while minimizing the risk of dental fluorosis (Buzalaf and Levy, 2011). Moreover, prolonged fluoride exposure may lead to the development of fluoride-resistant bacterial strains. Such strains could disrupt the microecological balance of biofilms and reduce their *in vitro* anti-caries efficacy (Shen et al., 2022). Therefore, precise control of fluoride concentration is essential in future application of fluoride hydrogels.

3.3.3 Bioactive factor-loaded hydrogels

Contemporary developments in remineralization hydrogels carrying bioactive factors represent a promising strategy for caries prevention. The mechanisms of caries formation underscore the relationship between bioactive factors and mineralization processes (Selwitz et al., 2007). Utilizing hydrogels to deliver remineralization-promoting bioactive factors offers a novel

TABLE 1 Overview of remineralization-inducing hydrogels.

Name	Type	Active ingredients	Result	Year	Ref.
NaF/chitosan hydrogel	Fluoride hydrogel	NaF	This hydrogel restored enamel-like prismatic tissue and controlled the formation, size, and mineral composition of crystals through synergistic interactions with calcium, phosphate, and fluoride ions. The regenerated apatite crystals showed strong c axis orientation and high crystallinity.	2014	(Cao et al., 2014)
Mussel-inspired wet adhesive fluoride system (denoted TS@NaF)		NaF	TS@NaF exhibited biological stability and biocompatibility. It showed consistent wet adhesion, and released fluoride ions (F-), resulting in significant calcium fluoride (CaF_2) deposition on enamel *in vitro*. Additionally, TS@NaF demonstrated an anti-caries effect and increased enamel mineral density.	2022	(Zhen et al., 2022)
NaF hydrogel coating		NaF	This fluoride gel effectively reduced early root surface caries in demineralized dentin by enhancing fluoride uptake and delivering fluorine to deeper dentin before pH cycling. Moreover, it was capable of supplying fluorine into the dentin and preventing dentin demineralization.	2022	(Matsuda et al., 2022)
NaF hydroxyapatite nanocomposite hydrogel		NaF	The 70/30 (HAp-CS) nanocomposite gel effectively increased the microhardness and mineral composition of lesions demineralized for 24 hours. But more severe lesions require stronger formulations or longer application times.	2024	(Fathy et al., 2024)
EMD-calcium chloride ($CaCl_2$) agarose hydrogel	Bioactive factor-loaded hydrogel	Enamel matrix derivative (EMD), calcium chloride ($CaCl_2$), and fluoride	The hydrogel system successfully facilitated *in vivo* regeneration of HAP crystals, with structural and mechanical properties comparable to natural dentin, on damaged dental tissues.	2017	(Han et al., 2017)
Odontogenic ameloblast-associated protein (ODAM)-impregnated collagen hydrogel		ODAM	The hydrogel resulted in formation of calcium phosphate precipitates, after treated 24 hours. Transmission electron microscopy and selected area electron diffraction analyses showed these crystals consisted of needle-like HAP.	2018	(Ikeda et al., 2018)

10.3389/fcimb.2025.1663563

TABLE 2 Antibacterial and remineralization-inducing hydrogels.

Name	Type	Active ingredients	Result	Year	Ref.
Chitosan-QP5 hydrogel	Amelogenin peptide hydrogel	QP5	Chitosan-QP5 hydrogel inhibited *S. mutans* (MIC 5 mg/mL, 95% antibiofilm), and the enhanced enamel remineralization (50% hardness recovery) and pH-responsive *in vitro* efficacy were confirmed.	2019	(Ren et al., 2019; Liu et al., 2022b)
Amelogenesis-inspired QP5 bioactive glass (BG) hydrogel		QP5, BG	The QP5 released from hydrogel triggered enamel remineralization by guiding the release of Ca^{2+} and $PO4^{3-}$ from BG. Showed excellent antibacterial effects and remineralization abilities of initial carious lesions.	2022	(Liu et al., 2022b)
rP172-releasing hydrogel		rP172, Ca^{2+}, phosphate, and fluoride	This amelogenin-hydrogel significantly increased enamel microhardness in artificial caries (static/pH/biofilm models), and reduced mineral loss with no cytotoxicity to periodontal cells.	2012	(Fan et al., 2012)
P26-chitosan (P26-CS) hydrogel and P32-chitosan (P32-CS) hydrogel		P26, P32, and chitosan	A denser coating of organized hydroxyapatite (HAP) crystals was formed covering entire demineralized enamel surfaces after treated with P26-CS and P32-CS hydrogels. And hardness and modulus of enamel were increased with no significant difference in the mechanical properties between the two peptide hydrogels.	2021	(Mukherjee et al., 2021)
P26-CS hydrogel and P32-CS hydrogel		P26, P32, and chitosan	The hydrogels ideally improved microstructure, mineral density, mineral phase, and nanomechanical properties of hard tissues.	2023	(Cai and Moradian-Oldak, 2023)
Dual-function Pluronic F127-alginate hydroge	Fluoride hydrogel	NaF and S-nitrosoglutathione (a nitric oxide donor)	The hydrogel reduced 98% micro-bacteria and effectively inhibited the demineralization of enamel-like substrates under acidic conditions.	2022	(Estes Bright et al., 2022; Ikeda et al., 2018)

therapeutic approach. And lots of studies focus on enamel matrix derivative (EMD) and ODAM-impregnated collagen systems.

The effects of EMD on biomimetic mineralization were first reported a decay ago. Cao et al. pioneered its application for enamel remineralization using an EMD-calcium chloride ($CaCl_2$) agarose hydrogel. A 2 mm-thick layer of the EMD-$CaCl_2$ hydrogel was applied onto demineralized enamel slices, overlaying by ion-free agarose and phosphate solution with fluoride. This system mediated *in vitro* mineralization of human enamel, with subsequent optimizations advanced EMD hydrogels efficacy (Han et al., 2017).

Amelotin (AMTN) is a secreted proteins in human body which can induce enamel biomineralization (Somogyi-Ganss et al., 2012; Nishio et al., 2011). Over the past few decades, researches have demonstrated the enamel mineralization inducing ability of AMTN-related complexes (Gasse et al., 2012; Núñez et al., 2016). ODAM, expressed during ameloblast maturation, strongly interacts with AMTN under physiological conditions (Nishio et al., 2013). Ikeda et al. investigated ODAM nucleation in collagen matrics after 24-hour incubation in ODAM-impregnated collagen hydrogel in simulated body fluid (SBF) buffer. They found the composite hydrogel promotes HAP nucleation both in SBF and in non-biological environments, with dose-dependent ways (Ikeda et al., 2018).

3.4 Antibacterial and remineralization-inducing hydrogels

The optimal strategy for caries prevention and treatment involves dual-action anti-caries hydrogels that simultaneously inhibit cariogenic bacteria and promote remineralization (Table 2). Currently, amelogenin peptide-based hydrogels represent the most extensively studied and clinically promising formulation.

Hydrogels carry amelogenin peptides were proved effective in antibacteria and remineralization inducing. The hydrogel containing QP5 is a good example. QP5 is effective in repairing the demineralized teeth by inducing remineralization (Ding et al., 2020). Ren et al. combined amelogenin-derived peptide QP5 with chitosan to develop a novel chitosan-QP5 hydrogel, demonstrating its long-term inhibitory effects on *S. mutans* biofilm growth, lactic acid production and metabolic activity (Ren et al., 2019; Liu et al., 2022b). Later, Liu et al. synthesized an amelogenesis-inspired hydrogel composite incorporating QP5 peptide and bioactive glass (BG) (Liu et al., 2022b). Their results revealed that QP5 promote enamel remineralization by directing the release of Ca^{2+} and $PO4^{3-}$ from BG. Therefore, chitosan-QP5 hydrogels represent promising candidates for caries control, owing to their antibacterial and remineralization abilities.

Beyond QP5, additional amelogenin peptide-chitosan hydrogels incorporating rP172, P26 and P32 have been studied. Fan et al. demonstrated rP172-releasing hydrogel loaded with Ca^{2+}, phosphate, and fluoride improved enamel microhardness while exhibiting no cytotoxicity to periodontal ligament cells (Fan et al., 2012). Mukherjee et al. induced enamel remineralization with increased hardness by using P26-chitosan (P26-CS) and P32-

chitosan (P32-CS) hydrogels (Mukherjee et al., 2021). In 2023, Cai et al. further verified the *in situ* remineralization inducing ability of P26-CS and P32-CS hydrogels (Cai and Moradian-Oldak, 2023). The results revealed that these hydrogels effectively improved the microstructure, mineral density, crystalline phase composition, and nanomechanical properties of dental hard tissues.

Fluoride-containing hydrogels demonstrate dual efficacy when combined with complementary antibacterial and remineralizing components. Bright et al. engineered a dual-functional Pluronic F127-alginate hydrogel incorporating NaF and S-nitrosoglutathione (Estes Bright et al., 2022). The hydrogel elicited nearly 98% viable bacteria while effectively inhibited the demineralization of enamel-like substrates under acidic conditions.

3.5 Hydrogels for reducing saliva-related caries

The constituents and properties of saliva play an essential role in the occurrence and progression of dental caries. As one of the most important host factors, Saliva mediates the cariogenic process (Lenander-Lumikari and Loimaranta, 2000). However, under specific pathological conditions, including post-radiotherapy/chemotherapy, autoimmune diseases which salivary gland dysfunction can occur, altering saliva composition and reducing secretion. These changes may collectively contribute to caries formation (Tappuni and Challacombe, 1994; Mansson-Rahemtulla et al., 1987; Lenander-Lumikari and Loimaranta, 2000). Hydrogel materials are now developed basing on this theory to prevent caries (Figure 3).

Some hydrogels manage caries via importing salivary substances. In 2013, Pradhan-Bhatt et al. developed a three-dimensional (3D) hyaluronic acid (HA)-based hydrogel culture system that supports salivary functional units (Pradhan-Bhatt et al., 2013). And the good structural integrity and long viability of the 3D hydrogel *in vitro* and *in vivo* was confirmed (Pradhan-Bhatt et al., 2013). The hydrogel worked like natural salivary, conducting anti-caries effectiveness.

Hydrogels can promote salivary gland regeneration showed potential of caries risk reduction. In 2017, Nam et al. pioneered this approach by developing L1 Peptide-conjugated fibrin hydrogels to promote the regeneration of salivary glands (Nam et al., 2017). Wang et al. engineered an injectable decellularized extracellular matrix hydrogel to prevent dental caries through salivary glands regeneration (Wang et al., 2023). Currently, few studies have explored this therapeutic strategy for caries prevention and treatment. The precise relationship between regeneration-induced saliva secretion and caries prevention efficacy remains to be fully elucidated.

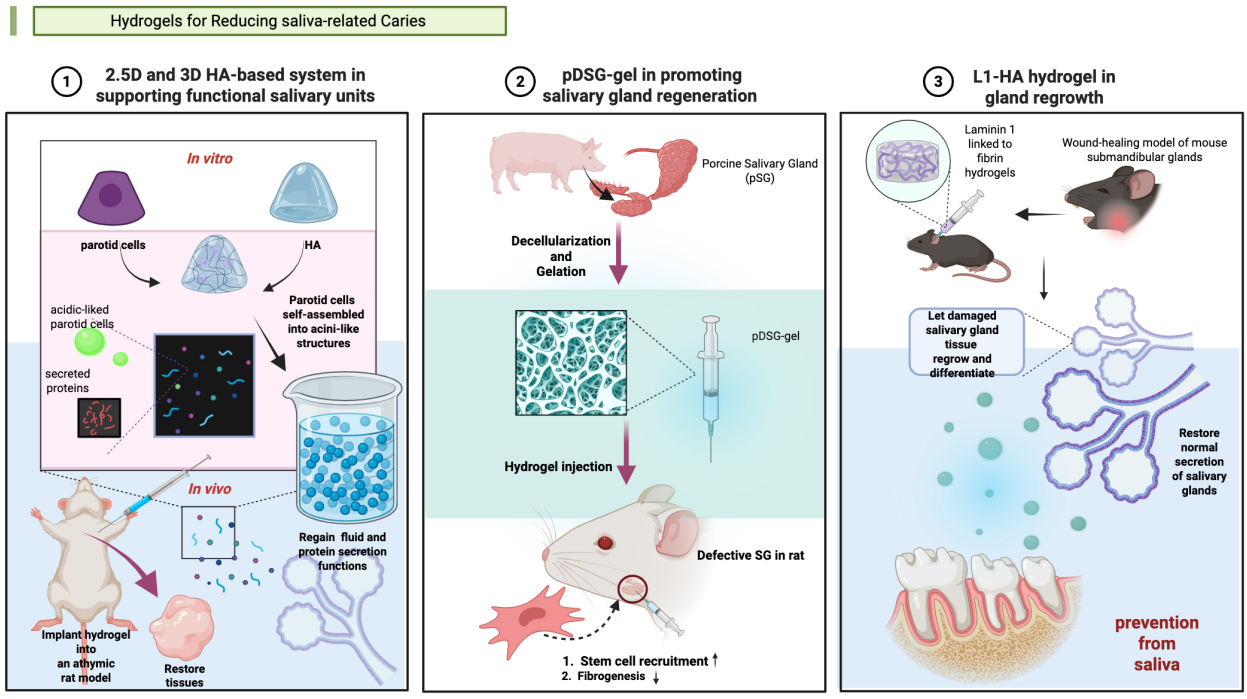

FIGURE 3
Hydrogels applied in salivary gland (SG) tissue engineering. (1) Synthesis of a 2.5-dimensional (2.5D) and a three-dimensional (3D) hyaluronic acid (HA)-based culture system in supporting functional salivary units (Pradhan-Bhatt et al., 2013). (2) Synthesis of a pDSG-gel in promoting salivary gland regeneration (Wang et al., 2023a). (3) Synthesis of a L1-HA hydrogel in gland regrowth (Nam et al., 2017). Created in BioRender. Yuqing, C. (2025) https://BioRender.com/qow0ggb.

4 Conclusion

Anti-caries hydrogels represent a critical frontier in preventive dentistry, with contemporary efforts focused on functionalized systems encompassing remineralizing, antibacterial, and dual-functional formulations. Currently, chitosan and fluoride are leading hydrogel materials for caries management, owing to their dual capacity to induce remineralization and suppress cariogenic bacteria. However, the complicated oral surroundings remain the major barrier to clinical translation of anti-caries hydrogels. Challenges in maintaining efficacy amid bacterial contamination, saliva dilution, and other interferences are still noticing. To overcome these limitations, many noticeable developments have been made. Emerging innovations, like pH-responsive and thermosensitive intelligent hydrogels enable precision strategies that dynamically respond to the oral microenvironment. Novel approaches including probiotic-loaded hydrogels and saliva-modulating systems demonstrate transformative potential, though further mechanistic validation remains essential for clinical translation.

It is worth noting that a critical limitation of multifunctional hydrogels lies in their potential biocompatibility concerns. Therefore, further research should prioritize developing non-cytotoxic hydrogels systems. Moreover, many current studies lack comprehensive biosafety evaluations and clinical validation. Future studies demand *in vitro* and *in vivo* biocompatibility assessments, and even proceed to clinical trials. In summary, development of hydrogels for caries management remains at an early stage, substantial further investigation is still required.

Author contributions

YC: Writing – original draft, Writing – review & editing. SL: Writing – original draft, Writing – review & editing. XH: Supervision, Writing – review & editing. WZ: Funding acquisition, Writing – review & editing.

Funding

The author(s) declare financial support was received for the research and/or publication of this article. This work was supported by the Natural Science Foundation of Fujian Province grant [2024J01655 (WZ)] and Introduced Talents Grant of School and Hospital of Stomatology Fujian Medical University [2023KQYJ01(WZ)].

Conflict of interest

The authors declare that the research was conducted in the absence of any commercial or financial relationships that could be construed as a potential conflict of interest.

Generative AI statement

The author(s) declare that no Generative AI was used in the creation of this manuscript.

Any alternative text (alt text) provided alongside figures in this article has been generated by Frontiers with the support of artificial intelligence and reasonable efforts have been made to ensure accuracy, including review by the authors wherever possible. If you identify any issues, please contact us.

Publisher's note

References

Afrasiabi, S., Bahador, A., and Partoazar, A. (2021). Combinatorial therapy of chitosan hydrogel-based zinc oxide nanocomposite attenuates the virulence of Streptococcus mutans. *BMC Microbiol.* 21, 62. doi: 10.1186/s12866-021-02128-y

Ahirwar, P., Kozlovskaya, V., Nijampatnam, B., Rojas, E. M., Pukkanasut, P., Inman, D., et al. (2023). Hydrogel-encapsulated biofilm inhibitors abrogate the cariogenic activity of streptococcus mutans. *J. Med. Chem.* 66, 7909–7925. doi: 10.1021/acs.jmedchem.3c00272

Amaya-Chantaca, N. J., Caldera-Villalobos, M., Claudio-Rizo, J. A., Flores-Guía, T. E., Becerra-Rodríguez, J. J., Soriano-Corral, F., et al. (2023). Semi-IPN hydrogels of collagen and gum arabic with antibacterial capacity and controlled release of drugs for potential application in wound healing. *Prog. Biomater.* 12, 25–40. doi: 10.1007/s40204-022-00210-w

An, B., Lin, Y. S., and Brodsky, B. (2016). Collagen interactions: Drug design and delivery. *Adv. Drug Delivery Rev.* 97, 69–84. doi: 10.1016/j.addr.2015.11.013

Antoine, E. E., Vlachos, P. P., and Rylander, M. N. (2014). Review of collagen I hydrogels for bioengineered tissue microenvironments: characterization of mechanics, structure, and transport. *Tissue Eng. Part B Rev.* 20, 683–696. doi: 10.1089/ten.TEB.2014.0086

Arias, F. J., Reboto, V., Martín, S., López, I., and Rodríguez-Cabello, J. C. (2006). Tailored recombinant elastin-like polymers for advanced biomedical and nano(bio) technological applications. *Biotechnol. Lett.* 28, 687–695. doi: 10.1007/s10529-006-9045-3

Arora, S., Das, G., Alqarni, M., Grover, V., Manzoor Baba, S., Saluja, P., et al. (2023). Role of chitosan hydrogels in clinical dentistry. *Gels* 9, 698. doi: 10.3390/gels9090698

Barman, S., Kurnaz, L. B., Leighton, R., Hossain, M. W., Decho, A. W., and Tang, C. (2024). Intrinsic antimicrobial resistance: Molecular biomaterials to combat microbial biofilms and bacterial persisters. *Biomaterials* 311, 122690. doi: 10.1016/j.biomaterials.2024.122690

Barreto, M. E. V., Medeiros, R. P., Shearer, A., Fook, M. V. L., Montazerian, M., and Mauro, J. C. (2022). Gelatin and bioactive glass composites for tissue engineering: A review. *J. Funct. Biomater.* 14, 23. doi: 10.3390/jfb14010023

Beikler, T., Bunte, K., Chan, Y., Weiher, B., Selbach, S., Peters, U., et al. (2021). Oral microbiota transplant in dogs with naturally occurring periodontitis. *J. Dent. Res.* 100, 764–770. doi: 10.1177/0022034521995423

Belda Marín, C., Fitzpatrick, V., Kaplan, D. L., Landoulsi, J., Guénin, E., and Egles, C. (2020). Silk polymers and nanoparticles: A powerful combination for the design of versatile biomaterials. *Front. Chem.* 8. doi: 10.3389/fchem.2020.604398

Benzian, H., Watt, R., Makino, Y., Stauf, N., and Varenne, B. (2022). WHO calls to end the global crisis of oral health. *Lancet* 400, 1909–1910. doi: 10.1016/s0140-6736(22)02322-4

Bossù, M., Saccucci, M., Salucci, A., Di Giorgio, G., Bruni, E., Uccelletti, D., et al. (2019). Enamel remineralization and repair results of Biomimetic Hydroxyapatite toothpaste on deciduous teeth: an effective option to fluoride toothpaste. *J. Nanobiotechnol.* 17, 17. doi: 10.1186/s12951-019-0454-6

Bowen, W. H., Burne, R. A., Wu, H., and Koo, H. (2018). Oral biofilms: pathogens, matrix, and polymicrobial interactions in microenvironments. *Trends Microbiol.* 26, 229–242. doi: 10.1016/j.tim.2017.09.008

Buzalaf, M., and Levy, S. M. (2011). Fluoride intake of children: considerations for dental caries and dental fluorosis. *Monogr. Oral. Sci.* 22, 1–19. doi: 10.1159/000325101

Cai, J., and Moradian-Oldak, J. (2023). Triple function of amelogenin peptide-chitosan hydrogel for dentin repair. *J. Dent. Res.* 102, 1434–1443. doi: 10.1177/00220345231198228

Cao, H., Duan, L., Zhang, Y., Cao, J., and Zhang, K. (2021). Current hydrogel advances in physicochemical and biological response-driven biomedical application diversity. *Signal Transduct Target Ther.* 6, 426. doi: 10.1038/s41392-021-00830-x

Cao, Y., Mei, M. L., Li, Q. L., Lo, E. C., and Chu, C. H. (2014). Agarose hydrogel biomimetic mineralization model for the regeneration of enamel prismlike tissue. *ACS Appl. Mater Interfaces* 6, 410–420. doi: 10.1021/am4044823

Caporale, A., Adorinni, S., Lamba, D., and Saviano, M. (2021). Peptide-protein interactions: from drug design to supramolecular biomaterials. *Molecules* 26, 1219. doi: 10.3390/molecules26051219

Chen, Y., Wang, X., Tao, S., Wang, Q., Ma, P. Q., Li, Z. B., et al. (2023). Research advances in smart responsive-hydrogel dressings with potential clinical diabetic wound healing properties. *Mil Med. Res.* 10, 37. doi: 10.1186/s40779-023-00473-9

Chen, X., Wu, G., Feng, Z., Dong, Y., Zhou, W., Li, B., et al. (2016). Advanced biomaterials and their potential applications in the treatment of periodontal disease. *Crit. Rev. Biotechnol.* 36, 760–775. doi: 10.3109/07388551.2015.1035693

Corkhill, P. H., Hamilton, C. J., and Tighe, B. J. (1989). Synthetic hydrogels. VI. Hydrogel composites as wound dressings and implant materials. *Biomaterials* 10, 3–10. doi: 10.1016/0142-9612(89)90002-1

Coviello, T., Matricardi, P., Marianecci, C., and Alhaique, F. (2007). Polysaccharide hydrogels for modified release formulations. *J. Control Release* 119, 5–24. doi: 10.1016/j.jconrel.2007.01.004

Dilamian, M., Montazer, M., and Masoumi, J. (2013). Antimicrobial electrospun membranes of chitosan/poly(ethylene oxide) incorporating poly(hexamethylene biguanide) hydrochloride. *Carbohydr. Polym.* 94, 364–371. doi: 10.1016/j.carbpol.2013.01.059

Ding, L., Han, S., Wang, K., Zheng, S., Zheng, W., Peng, X., et al. (2020). Remineralization of enamel caries by an amelogenin-derived peptide and fluoride in *vitro*. *Regener. Biomater.* 7, 283–292. doi: 10.1093/rb/rbaa003

Ding, Q., Sun, T., Su, W., Jing, X., Ye, B., Su, Y., et al. (2022). Bioinspired multifunctional black phosphorus hydrogel with antibacterial and antioxidant properties: A stepwise countermeasure for diabetic skin wound healing. *Adv. Healthc Mater* 11, e2102791. doi: 10.1002/adhm.202102791

Dong, Y., Li, S., Li, X., and Wang, X. (2021). Smart MXene/agarose hydrogel with photothermal property for controlled drug release. *Int. J. Biol. Macromol.* 190, 693–699. doi: 10.1016/j.ijbiomac.2021.09.037

El Moshy, S., Abbass, M. M. S., and El-Motayam, A. M. (2018). Biomimetic remineralization of acid etched enamel using agarose hydrogel model. *F1000Res* 7, 1476. doi: 10.12688/f1000research.16050.1

Estes Bright, L. M., Garren, M. R. S., Ashcraft, M., Kumar, A., Husain, H., Brisbois, E. J., et al. (2022). Dual action nitric oxide and fluoride ion-releasing hydrogels for combating dental caries. *ACS Appl. Mater Interfaces* 14, 21916–21930. doi: 10.1021/acsami.2c02301

Fan, Y., Wen, Z. T., Liao, S., Lallier, T., Hagan, J. L., Twomley, J. T., et al. (2012). Novel amelogenin-releasing hydrogel for remineralization of enamel artificial caries. *J. Bioact. Compat. Polym.* 27, 585–603. doi: 10.1177/0883911512458050

Fathy, S. M., Abdelhafez, A., Darwesh, F. A., and Elkhooly, T. A. (2024). Evaluation of incipient enamel-carious-like lesion treated with hydroxyapatite-chitosan nanocomposite hydrogel. *J. World Fed Orthod* 13, 211–220. doi: 10.1016/j.ejwf.2024.04.001

Featherstone, J. D. (2004). The continuum of dental caries–evidence for a dynamic disease process. *J. Dent. Res.* 83 Spec No C, C39–C42. doi: 10.1177/154405910408301s08

Fu, L., Li, L., Bian, Q., Xue, B., Jin, J., Li, J., et al. (2023a). Cartilage-like protein hydrogels engineered via entanglement. *Nature* 618, 740–747. doi: 10.1038/s41586-023-06037-0

Fu, Y. J., Shi, Y. F., Wang, L. Y., Zhao, Y. F., Wang, R. K., Li, K., et al. (2023b). All-natural immunomodulatory bioadhesive hydrogel promotes angiogenesis and diabetic wound healing by regulating macrophage heterogeneity. *Adv. Sci. (Weinh)* 10, e2206771. doi: 10.1002/advs.202206771

Gao, L., Xu, T., Huang, G., Jiang, S., Gu, Y., and Chen, F. (2018). Oral microbiomes: more and more importance in oral cavity and whole body. *Protein Cell* 9, 488–500. doi: 10.1007/s13238-018-0548-1

Gasse, B., Silvent, J., and Sire, J. Y. (2012). Evolutionary analysis suggests that AMTN is enamel-specific and a candidate for AI. *J. Dent. Res.* 91, 1085–1089. doi: 10.1177/0022034512460551

Geanaliu-Nicolae, R. E., and Andronescu, E. (2020). Blended natural support materials-collagen based hydrogels used in biomedicine. *Materials (Basel)* 13, 5641. doi: 10.3390/ma13245641

Gholap, A. D., Rojekar, S., Kapare, H. S., Vishwakarma, N., Raikwar, S., Garkal, A., et al. (2024). Chitosan scaffolds: Expanding horizons in biomedical applications. *Carbohydr. Polym.* 323, 121394. doi: 10.1016/j.carbpol.2023.121394

Hamedi, H., Moradi, S., Hudson, S. M., Tonelli, A. E., and King, M. W. (2022). Chitosan based bioadhesives for biomedical applications: A review. *Carbohydr. Polym.* 282, 119100. doi: 10.1016/j.carbpol.2022.119100

Han, M., Li, Q. L., Cao, Y., Fang, H., Xia, R., and Zhang, Z. H. (2017). *In vivo* remineralization of dentin using an agarose hydrogel biomimetic mineralization system. *Sci. Rep.* 7, 41955. doi: 10.1038/srep41955

Ho, T. C., Chang, C. C., Chan, H. P., Chung, T. W., Shu, C. W., Chuang, K. P., et al. (2022). Hydrogels: properties and applications in biomedicine. *Molecules* 27, 2902. doi: 10.3390/molecules27092902

Hu, W., Wang, Z., Xiao, Y., Zhang, S., and Wang, J. (2019). Advances in crosslinking strategies of biomedical hydrogels. *Biomater. Sci.* 7, 843–855. doi: 10.1039/c8bm01246f

Huang, Z., and Cheng, Y. (2024). Oral microbiota transplantation for intra-oral halitosis: a feasibility analysis based on an oral microbiota colonization trial in Wistar rats. *BMC Microbiol.* 24, 170. doi: 10.1186/s12866-024-03322-4

Ikeda, Y., Holcroft, J., Ikeda, E., and Ganss, B. (2022). Amelotin promotes mineralization and adhesion in collagen-based systems. *Cell Mol. Bioeng.* 15, 245–254. doi: 10.1007/s12195-022-00722-2

Ikeda, Y., Neshatian, M., Holcroft, J., and Ganss, B. (2018). The enamel protein ODAM promotes mineralization in a collagen matrix. *Connect Tissue Res.* 59, 62–66. doi: 10.1080/03008207.2017.1408603

Itskovich, Y., Meikle, M. C., Cannon, R. D., Farella, M., Coates, D. E., and Milne, T. J. (2021). Differential behaviour and gene expression in 3D cultures of femoral- and calvarial-derived human osteoblasts under a cyclic compressive mechanical load. *Eur. J. Oral. Sci.* 129, e12818. doi: 10.1111/eos.12818

Jang, K. J., Lee, W. S., Park, S., Han, J., Kim, J. E., Kim, B. M., et al. (2021). Sulfur(VI) fluoride exchange (SuFEx)-mediated synthesis of the chitosan-PEG conjugate and its supramolecular hydrogels for protein delivery. *Nanomaterials (Basel)* 11, 318. doi: 10.3390/nano11020318

Jenkins, G. N. (1985). Recent changes in dental caries. *Br. Med. J. (Clin Res. Ed)* 291, 1297–1298. doi: 10.1136/bmj.291.6505.1297

Ju, Y., Hu, Y., Yang, P., Xie, X., and Fang, B. (2023). Extracellular vesicle-loaded hydrogels for tissue repair and regeneration. *Mater Today Bio* 18, 100522. doi: 10.1016/j.mtbio.2022.100522

Kalantari, K., Afifi, A. M., Jahangirian, H., and Webster, T. J. (2019). Biomedical applications of chitosan electrospun nanofibers as a green polymer - Review. *Carbohydr. Polym.* 207, 588–600. doi: 10.1016/j.carbpol.2018.12.011

Kharkar, P. M., Kiick, K. L., and Kloxin, A. M. (2013). Designing degradable hydrogels for orthogonal control of cell microenvironments. *Chem. Soc. Rev.* 42, 7335–7372. doi: 10.1039/c3cs60040h

Khodadadi Yazdi, M., Taghizadeh, A., Taghizadeh, M., Stadler, F. J., Farokhi, M., Mottaghitalab, F., et al. (2020). Agarose-based biomaterials for advanced drug delivery. *J. Control Release* 326, 523–543. doi: 10.1016/j.jconrel.2020.07.028

Knudsen, T. B., Bulleit, R. F., and Zimmerman, E. F. (1985). Histochemical localization of glycosaminoglycans during morphogenesis of the secondary palate in mice. *Anat. Embryol. (Berl)* 173, 137–142. doi: 10.1007/bf00707312

Kolanthai, E., Abinaya Sindu, P., Thanigai Arul, K., Sarath Chandra, V., Manikandan, E., and Narayana Kalkura, S. (2017). Agarose encapsulated mesoporous carbonated hydroxyapatite nanocomposites powder for drug delivery. *J. Photochem. Photobiol. B* 166, 220–231. doi: 10.1016/j.jphotobiol.2016.12.005

Krasse, B. (1988). Biological factors as indicators of future caries. *Int. Dent. J.* 38, 219–225.

Lei, C., Song, J. H., Li, S., Zhu, Y. N., Liu, M. Y., Wan, M. C., et al. (2023). Advances in materials-based therapeutic strategies against osteoporosis. *Biomaterials* 296, 122066. doi: 10.1016/j.biomaterials.2023.122066

Lenander-Lumikari, M., and Loimaranta, V. (2000). Saliva and dental caries. *Adv. Dent. Res.* 14, 40–47. doi: 10.1177/08959374000140010601

Li, Y., Chen, X., Fok, A., Rodriguez-Cabello, J. C., and Aparicio, C. (2015). Biomimetic mineralization of recombinamer-based hydrogels toward controlled morphologies and high mineral density. *ACS Appl. Mater Interfaces* 7, 25784–25792. doi: 10.1021/acsami.5b07628

Li, Y., Chen, Y., Xue, Y., Jin, J., Xu, Y., Zeng, W., et al. (2024). Injectable hydrogel delivery system with high drug loading for prolonging local anesthesia. *Adv. Sci. (Weinh)* 11, e2309482. doi: 10.1002/advs.202309482

Li, Y., Chi, Y. Q., Yu, C. H., Xie, Y., Xia, M. Y., Zhang, C. L., et al. (2020). Drug-free and non-crosslinked chitosan scaffolds with efficient antibacterial activity against both Gram-negative and Gram-positive bacteria. *Carbohydr. Polym.* 241, 116386. doi: 10.1016/j.carbpol.2020.116386

Li, D., Liu, P., Hao, F., Lv, Y., Xiong, W., Yan, C., et al. (2022a). Preparation and application of silver/chitosan-sepiolite materials with antimicrobial activities and low cytotoxicity. *Int. J. Biol. Macromol.* 210, 337–349. doi: 10.1016/j.ijbiomac.2022.05.015

Li, Q., Liu, J., Xu, Y., Liu, H., Zhang, J., Wang, Y., et al. (2022b). Fast cross-linked hydrogel as a green light-activated photocatalyst for localized biofilm disruption and brush-free tooth whitening. *ACS Appl. Mater Interfaces* 14, 28427–28438. doi: 10.1021/acsami.2c00887

Liang, Y., He, J., and Guo, B. (2021). Functional hydrogels as wound dressing to enhance wound healing. *ACS Nano* 15, 12687–12722. doi: 10.1021/acsnano.1c04206

Liu, Z., Lu, J., Chen, X., Xiu, P., Zhang, Y., Lv, X., et al. (2022b). A novel amelogenesis-inspired hydrogel composite for the remineralization of enamel non-cavitated lesions. *J. Mater Chem. B* 10, 10150–10161. doi: 10.1039/d2tb01711c

Liu, W., Madry, H., and Cucchiarini, M. (2022a). Application of alginate hydrogels for next-generation articular cartilage regeneration. *Int. J. Mol. Sci.* 23, 1147. doi: 10.3390/ijms23031147

Liu, J., Zhang, L., Yang, Z., and Zhao, X. (2011). Controlled release of paclitaxel from a self-assembling peptide hydrogel formed in *situ* and antitumor study in *vitro*. *Int. J. Nanomed.* 6, 2143–2153. doi: 10.2147/ijn.S24038

Loessner, D., Meinert, C., Kaemmerer, E., Martine, L. C., Yue, K., Levett, P. A., et al. (2016). Functionalization, preparation and use of cell-laden gelatin methacryloyl-based hydrogels as modular tissue culture platforms. *Nat. Protoc.* 11, 727–746. doi: 10.1038/nprot.2016.037

Lukinmaa, P. L., and Waltimo, J. (1992). Immunohistochemical localization of types I, V, and VI collagen in human permanent teeth and periodontal ligament. *J. Dent. Res.* 71, 391–397. doi: 10.1177/00220345920710020801

Luong, A. D., Buzid, A., and Luong, J. H. T. (2022). Important roles and potential uses of natural and synthetic antimicrobial peptides (AMPs) in oral diseases: cavity, periodontal disease, and thrush. *J. Funct. Biomater.* 13, 175. doi: 10.3390/jfb13040175

Maity, C., and Das, N. (2021). Alginate-based smart materials and their application: recent advances and perspectives. *Top. Curr. Chem. (Cham)* 380, 3. doi: 10.1007/s41061-021-00360-8

Mandel, I. D. (1989). The role of saliva in maintaining oral homeostasis. *J. Am. Dent. Assoc.* 119, 298–304. doi: 10.14219/jada.archive.1989.0211

Mansson-Rahemtulla, B., Baldone, D. C., Pruitt, K. M., and Rahemtulla, F. (1987). Effects of variations in pH and hypothiocyanite concentrations on S. mutans glucose metabolism. *J. Dent. Res.* 66, 486–491. doi: 10.1177/00220345870660021701

Marsh, P. D. (1994). Microbial ecology of dental plaque and its significance in health and disease. *Adv. Dent. Res.* 8, 263–271. doi: 10.1177/08959374940080022001

Matsuda, Y., Altankhishig, B., Okuyama, K., Yamamoto, H., Naito, K., Hayashi, M., et al. (2022). Inhibition of demineralization of dentin by fluoride-containing hydrogel desensitizers: an *in vitro* study. *J. Funct. Biomater.* 13, 246. doi: 10.3390/jfb13040246

Mohamed, R. R., Elella, M. H., and Sabaa, M. W. (2017). Cytotoxicity and metal ions removal using antibacterial biodegradable hydrogels based on N-quaternized chitosan/poly(acrylic acid). *Int. J. Biol. Macromol.* 98, 302–313. doi: 10.1016/j.ijbiomac.2017.01.107

Mohanto, S., Narayana, S., Merai, K. P., Kumar, J. A., Bhunia, A., Hani, U., et al. (2023). Advancements in gelatin-based hydrogel systems for biomedical applications: A state-of-the-art review. *Int. J. Biol. Macromol.* 253, 127143. doi: 10.1016/j.ijbiomac.2023.127143

Mohire, N. C., and Yadav, A. V. (2010). Chitosan-based polyherbal toothpaste: as novel oral hygiene product. *Indian J. Dent. Res.* 21, 380–384. doi: 10.4103/0970-9290.70808

Morris-Wiman, J., and Brinkley, L. (1992). An extracellular matrix infrastructure provides support for murine secondary palatal shelf remodelling. *Anat. Rec* 234, 575–586. doi: 10.1002/ar.1092340413

Mukherjee, K., Chakraborty, A., Sandhu, G., Naim, S., Nowotny, E. B., and Moradian-Oldak, J. (2021). Amelogenin peptide-chitosan hydrogel for biomimetic enamel regrowth. *Front. Dent. Med.* 2. doi: 10.3389/fdmed.2021.697544

Muşat, V., Anghel, E. M., Zaharia, A., Atkinson, I., Mocioiu, O. C., Buşilă, M., et al. (2021). A chitosan-agarose polysaccharide-based hydrogel for biomimetic remineralization of dental enamel. *Biomolecules* 11, 1137. doi: 10.3390/biom11081137

Nam, K., Wang, C. S., Maruyama, C. L. M., Lei, P., Andreadis, S. T., and Baker, O. J. (2017). L1 peptide-conjugated fibrin hydrogels promote salivary gland regeneration. *J. Dent. Res.* 96, 798–806. doi: 10.1177/0022034517695496

Nath, S., Zilm, P., Jamieson, L., Kapellas, K., Goswami, N., Ketagoda, K., et al. (2021). Development and characterization of an oral microbiome transplant among Australians for the treatment of dental caries and periodontal disease: A study protocol. *PloS One* 16, e0260433. doi: 10.1371/journal.pone.0260433

Nishio, C., Wazen, R., Kuroda, S., Moffatt, P., and Nanci, A. (2011). P44-expression pattern of APIN and amelotin during formation and regeneration of the junctional epithelium. *Bull. Group Int. Rech Sci. Stomatol. Odontol.* 49, 111–112.

Nishio, C., Wazen, R., Moffatt, P., and Nanci, A. (2013). Expression of odontogenic ameloblast-associated and amelotin proteins in the junctional epithelium. *Periodontol. 2000* 63, 59–66. doi: 10.1111/prd.12031

Nistor, M. T., Chiriac, A. P., Nita, L. E., and Vasile, C. (2013). Characterization of the semi-interpenetrated network based on collagen and poly(N-isopropyl acrylamide-co-diethylene glycol diacrylate). *Int. J. Pharm.* 452, 92–101. doi: 10.1016/j.ijpharm.2013.04.043

Nizami, M. Z. I., Xu, V. W., Yin, I. X., Yu, O. Y., and Chu, C. H. (2021). Metal and metal oxide nanoparticles in caries prevention: A review. *Nanomaterials (Basel)* 11, 3446. doi: 10.3390/nano11123446

Núñez, S. M., Chun, Y. P., Ganss, B., Hu, Y., Richardson, A. S., Schmitz, J. E., et al. (2016). Maturation stage enamel malformations in Amtn and Klk4 null mice. *Matrix Biol.* 52-54, 219–233. doi: 10.1016/j.matbio.2015.11.007

Park, S., and Park, K. M. (2016). Engineered polymeric hydrogels for 3D tissue models. *Polymers (Basel)* 8, 23. doi: 10.3390/polym8010023

Parker, A. S., Patel, A. N., Al Botros, R., Snowden, M. E., Mckelvey, K., Unwin, P. R., et al. (2014). Measurement of the efficacy of calcium silicate for the protection and repair of dental enamel. *J. Dent.* 42 Suppl 1, S21–S29. doi: 10.1016/s0300-5712(14)50004-8

Patel, M. (2020). Dental caries vaccine: are we there yet? *Lett. Appl. Microbiol.* 70, 2–12. doi: 10.1111/lam.13218

Paula, A. J., and Koo, H. (2017). Nanosized building blocks for customizing novel antibiofilm approaches. *J. Dent. Res.* 96, 128–136. doi: 10.1177/0022034516679397

Pellá, M. C. G., Lima-Tenório, M. K., Tenório-Neto, E. T., Guilherme, M. R., Muniz, E. C., and Rubira, A. F. (2018). Chitosan-based hydrogels: From preparation to biomedical applications. *Carbohydr. Polym.* 196, 233–245. doi: 10.1016/j.carbpol.2018.05.033

Pradhan-Bhatt, S., Harrington, D. A., Duncan, R. L., Jia, X., Witt, R. L., and Farach-Carson, M. C. (2013). Implantable three-dimensional salivary spheroid assemblies demonstrate fluid and protein secretory responses to neurotransmitters. *Tissue Eng. Part A* 19, 1610–1620. doi: 10.1089/ten.TEA.2012.0301

Rafiee, A., Mozafari, N., Fekri, N., Memarpour, M., and Azadi, A. (2024). Preparation and characterization of a nanohydroxyapatite and sodium fluoride loaded chitosan-based in *situ* forming gel for enamel biomineralization. *Heliyon* 10, e24217. doi: 10.1016/j.heliyon.2024.e24217

Ren, Q., Ding, L., Li, Z., Wang, X., Wang, K., Han, S., et al. (2019). Chitosan hydrogel containing amelogenin-derived peptide: Inhibition of cariogenic bacteria and promotion of remineralization of initial caries lesions. *Arch. Oral. Biol.* 100, 42–48. doi: 10.1016/j.archoralbio.2019.02.004

Ribeiro, F. C., Junqueira, J. C., Dos Santos, J. D., De Barros, P. P., Rossoni, R. D., Shukla, S., et al. (2020). Development of probiotic formulations for oral candidiasis prevention: gellan gum as a carrier to deliver lactobacillus paracasei 28.4. *Antimicrob. Agents Chemother.* 64, e02323-19. doi: 10.1128/aac.02323-19

Ruszczak, Z., and Friess, W. (2003). Collagen as a carrier for on-site delivery of antibacterial drugs. *Adv. Drug Delivery Rev.* 55, 1679–1698. doi: 10.1016/j.addr.2003.08.007

Selwitz, R. H., Ismail, A. I., and Pitts, N. B. (2007). Dental caries. *Lancet* 369, 51–59. doi: 10.1016/s0140-6736(07)60031-2

Senel, S., Ikinci, G., Kaş, S., Yousefi-Rad, A., Sargon, M. F., and Hincal, A. A. (2000). Chitosan films and hydrogels of chlorhexidine gluconate for oral mucosal delivery. *Int. J. Pharm.* 193, 197–203. doi: 10.1016/s0378-5173(99)00334-8

Sereni, N., Enache, A., Sudre, G., Montembault, A., Rochas, C., Durand, P., et al. (2017). Dynamic structuration of physical chitosan hydrogels. *Langmuir* 33, 12697–12707. doi: 10.1021/acs.langmuir.7b02997

Shen, Y., Yu, F., Qiu, L., Gao, M., Xu, P., Zhang, L., et al. (2022). Ecological influence by colonization of fluoride-resistant Streptococcus mutans in oral biofilm. *Front. Cell Infect. Microbiol.* 12. doi: 10.3389/fcimb.2022.1106392

Singh, G. D., Johnston, J., Ma, W., and Lozanoff, S. (1998). Cleft palate formation in fetal Br mice with midfacial retrusion: tenascin, fibronectin, laminin, and type IV collagen immunolocalization. *Cleft Palate Craniofac J.*, 35 (1), 65–76. doi: 10.1597/1545-1569_1998_035_0065_cpfifb_2.3.co_2

Somogyi-Ganss, E., Nakayama, Y., Iwasaki, K., Nakano, Y., Stolf, D., Mckee, M. D., et al. (2012). Comparative temporospatial expression profiling of murine amelotin protein during amelogenesis. *Cells Tissues Organs* 195, 535–549. doi: 10.1159/000329255

Song, Z., Wang, S., Yang, L., Hou, R., Wang, R., Zhang, N., et al. (2023). Rotenone encapsulated in pH-responsive alginate-based microspheres reduces toxicity to zebrafish. *Environ. Res.* 216, 114565. doi: 10.1016/j.envres.2022.114565

Sun, F., Hu, W., Zhao, Y., Li, Y., Xu, X., Li, Y., et al. (2022). Invisible assassin coated on dental appliances for on-demand capturing and killing of cariogenic bacteria. *Colloids Surf B Biointerfaces* 217, 112696. doi: 10.1016/j.colsurfb.2022.112696

Sun, Y., Li, X., Deng, Y., Sun, J. N., Tao, D., Chen, H., et al. (2014). Mode of action studies on the formation of enamel minerals from a novel toothpaste containing calcium silicate and sodium phosphate salts. *J. Dent.* 42 Suppl 1, S30–S38. doi: 10.1016/s0300-5712(14)50005-x

Tabata, S., Nakayama, T., Yasui, K., and Uemura, M. (1995). Collagen fibrils in the odontoblast layer in the teeth of the rat and the house shrew, Suncus murinus, by scanning electron microscopy using a maceration method. *Connect Tissue Res.* 33, 115–121. doi: 10.3109/03008209509016990

Taghipour, Y. D., Hokmabad, V. R., Del Bakhshayesh, A. R., Asadi, N., Salehi, R., and Nasrabadi, H. T. (2020). The application of hydrogels based on natural polymers for tissue engineering. *Curr. Med. Chem.* 27, 2658–2680. doi: 10.2174/0929867326666190711103956

Takahashi, N., and Nyvad, B. (2011). The role of bacteria in the caries process: ecological perspectives. *J. Dent. Res.* 90, 294–303. doi: 10.1177/0022034510379602

Tamo, A. K., Djouonkep, L. D. W., and Selabi, N. B. S. (2024). 3D printing of polysaccharide-based hydrogel scaffolds for tissue engineering applications: A review. *Int. J. Biol. Macromol.* 270, 132123. doi: 10.1016/j.ijbiomac.2024.132123

Tappuni, A. R., and Challacombe, S. J. (1994). A comparison of salivary immunoglobulin A (IgA) and IgA subclass concentrations in predentate and dentate children and adults. *Oral. Microbiol. Immunol.* 9, 142–145. doi: 10.1111/j.1399-302x.1994.tb00050.x

Thang, N. H., Chien, T. B., and Cuong, D. X. (2023). Polymer-based hydrogels applied in drug delivery: an overview. *Gels* 9, 523. doi: 10.3390/gels9070523

Väänänen, A., Tjäderhane, L., Eklund, L., Heljasvaara, R., Pihlajaniemi, T., Herva, R., et al. (2004). Expression of collagen XVIII and MMP-20 in developing teeth and odontogenic tumors. *Matrix Biol.* 23, 153–161. doi: 10.1016/j.matbio.2004.04.003

Veltman, B., Harpaz, D., Cohen, Y., Poverenov, E., and Eltzov, E. (2022). Characterization of the selective binding of modified chitosan nanoparticles to Gram-negative bacteria strains. *Int. J. Biol. Macromol.* 194, 666–675. doi: 10.1016/j.ijbiomac.2021.11.111

Vinikoor, T., Dzidotor, G. K., Le, T. T., Liu, Y., Kan, H. M., Barui, S., et al. (2023). Injectable and biodegradable piezoelectric hydrogel for osteoarthritis treatment. *Nat. Commun.* 14, 6257. doi: 10.1038/s41467-023-41594-y

Wang, T., Huang, Q., Rao, Z., Liu, F., Su, X., Zhai, X., et al. (2023). Injectable decellularized extracellular matrix hydrogel promotes salivary gland regeneration via endogenous stem cell recruitment and suppression of fibrogenesis. *Acta Biomater.* 169, 256–272. doi: 10.1016/j.actbio.2023.08.003

Wang, Z., Zhou, Z., Fan, J., Zhang, L., Zhang, Z., Wu, Z., et al. (2021). Hydroxypropylmethylcellulose as a film and hydrogel carrier for ACP nanoprecursors to deliver biomimetic mineralization. *J. Nanobiotechnol.* 19, 385. doi: 10.1186/s12951-021-01133-7

Wefel, J. S., Clarkson, B. H., and Heilman, J. R. (1985). Natural root caries: a histologic and microradiographic evaluation. *J. Oral. Pathol.* 14, 615–623. doi: 10.1111/j.1600-0714.1985.tb00538.x

Weyrich, L. S., Nath, S., and Jamieson, L. M. (2024). Commercializing equitable, accessible oral microbiome transplantation therapy. *Community Dent. Health* 41, 83–88. doi: 10.1922/CDH_IADR24Weyrich06

Xiao, H., Fan, Y., Li, Y., Dong, J., Zhang, S., Wang, B., et al. (2021). Oral microbiota transplantation fights against head and neck radiotherapy-induced oral mucositis in mice. *Comput. Struct. Biotechnol. J.* 19, 5898–5910. doi: 10.1016/j.csbj.2021.10.028

Yang, C., Zhang, Y., Tang, P., Zheng, T., Zhang, X., Zhang, Y., et al. (2022). Collagen-based hydrogels cross-linked via laccase - mediated system incorporated with Fe(3+) for wound dressing. *Colloids Surf B Biointerfaces* 219, 112825. doi: 10.1016/j.colsurfb.2022.112825

Yuan, X., Zhu, Z., Xia, P., Wang, Z., Zhao, X., Jiang, X., et al. (2023). Tough gelatin hydrogel for tissue engineering. *Adv. Sci. (Weinh)* 10, e2301665. doi: 10.1002/advs.202301665

Zampetti, P., and Scribante, A. (2020). Historical and bibliometric notes on the use of fluoride in caries prevention. *Eur. J. Paediatr. Dent.* 21, 148–152. doi: 10.23804/ejpd.2020.21.02.10

Zhang, H., Cheng, J., and Ao, Q. (2021a). Preparation of alginate-based biomaterials and their applications in biomedicine. *Mar. Drugs* 19, 264. doi: 10.3390/md19050264

Zhang, Q., Ma, Q., Wang, Y., Wu, H., and Zou, J. (2021b). Molecular mechanisms of inhibiting glucosyltransferases for biofilm formation in Streptococcus mutans. *Int. J. Oral. Sci.* 13, 30. doi: 10.1038/s41368-021-00137-1

Zhang, R., Xie, L., Wu, H., Yang, T., Zhang, Q., Tian, Y., et al. (2020). Alginate/laponite hydrogel microspheres co-encapsulating dental pulp stem cells and VEGF for endodontic regeneration. *Acta Biomater.* 113, 305–316. doi: 10.1016/j.actbio.2020.07.012

Zhang, S., Zhao, Y., Ding, S., Zhou, C., Li, H., and Li, L. (2021c). Facile synthesis of in situ formable alginate composite hydrogels with ca(2+)-induced healing ability. *Tissue Eng. Part A* 27, 1225–1238. doi: 10.1089/ten.TEA.2020.0282

Zhen, L., Liang, K., Luo, J., Ke, X., Tao, S., Zhang, M., et al. (2022). Mussel-inspired hydrogels for fluoride delivery and caries prevention. *J. Dent. Res.* 101, 1597–1605. doi: 10.1177/00220345221114783

Zheng, H., and Zuo, B. (2021). Functional silk fibroin hydrogels: preparation, properties and applications. *J. Mater Chem. B* 9, 1238–1258. doi: 10.1039/d0tb02099k

Zhong, Y., Xiao, H., Seidi, F., and Jin, Y. (2020). Natural polymer-based antimicrobial hydrogels without synthetic antibiotics as wound dressings. *Biomacromolecules* 21, 2983–3006. doi: 10.1021/acs.biomac.0c00760

Zhu, J., Zhang, M., Qiu, R., Li, M., Zhen, L., Li, J., et al. (2024). Hagfish-inspired hydrogel for root caries: A multifunctional approach including immediate protection, antimicrobial phototherapy, and remineralization. *Acta Biomater.* 188, 117–137. doi: 10.1016/j.actbio.2024.09.014

frontiers | Frontiers in Cellular and Infection Microbiology

TYPE Review
PUBLISHED 01 October 2025
DOI 10.3389/fcimb.2025.1669643

OPEN ACCESS

EDITED BY
Xuelian Huang,
University of Washington, United States

REVIEWED BY
Chengcheng Liu,
Sichuan University, China
Santhiyagu Prakash,
Tamil Nadu Fisheries University, India
Yuncong Li,
Xi'an Jiaotong University School of Stomotology, China

*CORRESPONDENCE
Fei Liu
liufeidentist@163.com
Yingchun Cai
815560289@qq.com
Suping Wang
wangsupingdent@163.com

†These authors share first authorship

RECEIVED 20 July 2025
ACCEPTED 08 September 2025
PUBLISHED 01 October 2025

CITATION
Wang Y, Du X, Jia Y, Qin L, Liu F, Cai Y and Wang S (2025) Recent progress in antimicrobial strategies of controlled-release nanomaterials for secondary caries. *Front. Cell. Infect. Microbiol.* 15:1669643. doi: 10.3389/fcimb.2025.1669643

Recent progress in antimicrobial strategies of controlled-release nanomaterials for secondary caries

Yiyi Wang[1,2†], Xushuo Du[1,2†], Yanmin Jia[1,2], Lu Qin[1,2], Fei Liu[3*], Yingchun Cai[4*] and Suping Wang[3*]

[1]Stomatology Center, The First Affiliated Hospital of Zhengzhou University, Zhengzhou, China, [2]School of Stomatology, Zhengzhou University, Zhengzhou, China, [3]Department of Stomatology, The First Affiliated Hospital of Zhengzhou University, Zhengzhou, China, [4]Department of Orthopedics, The First Affiliated Hospital of Zhengzhou University, Zhengzhou, China

Secondary caries is a leading cause of restoration failure. Inhibiting caries through antimicrobial efficacy is essential for extending the restoration's service life. Antimicrobial agents have been incorporated into restorative materials for decades. Based on their mechanism of antimicrobial action, these materials are classified as either releasing or non-releasing types. However, the simple release strategy is often insufficient for long-term caries prevention, as it lacks the precision, durability, and adaptability now required. This necessitates the development of next-generation systems that can provide a controlled, sustained, and targeted antimicrobial activity. To this end, this review focuses on advanced, controlled-release antimicrobial strategies, exploring the design of novel nanomaterials, their functional efficacy, and the mechanisms of their representative antimicrobial agents.

KEYWORDS

antimicrobial, nanomaterials, controlled-release, stimulus-responsive, rechargeable, cascade catalytic nanoreactor, secondary caries

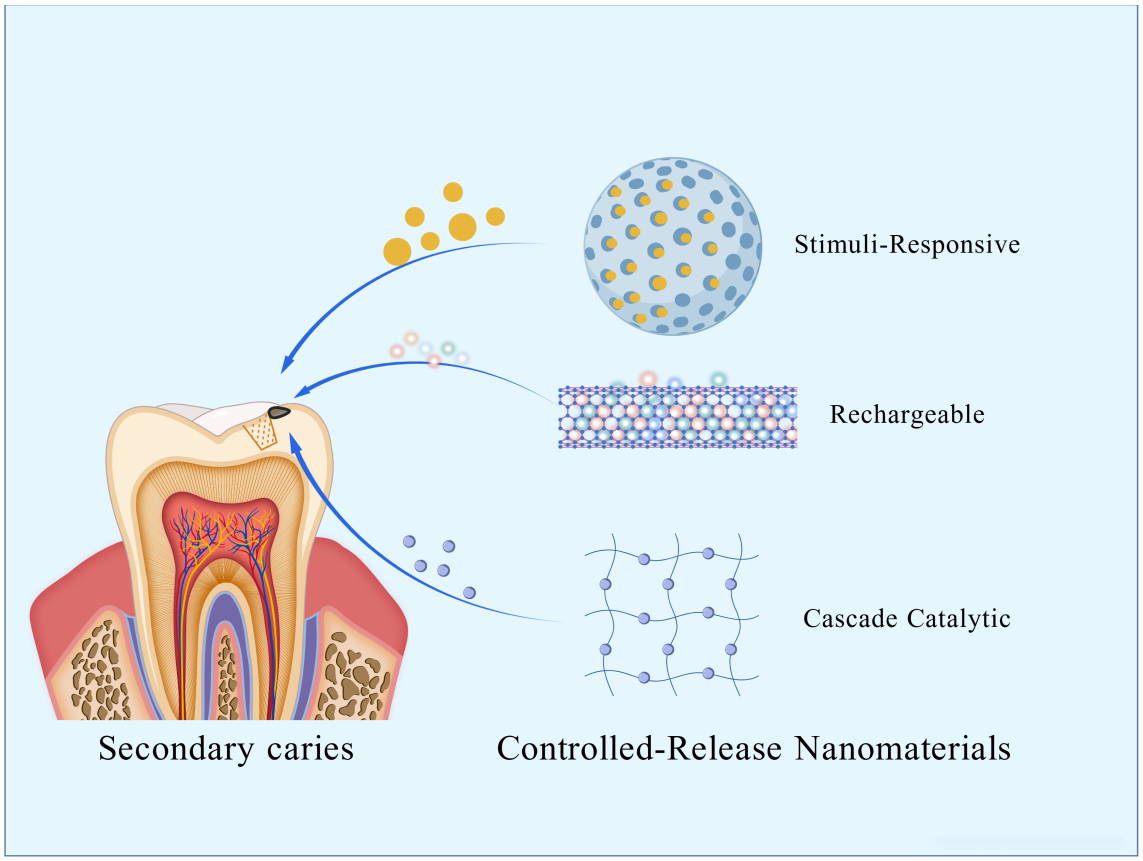

GRAPHICAL ABSTRACT
These figures were created with BioGDP.com.

1 Introduction

Secondary caries is a common reason associated with failed restorations. Factors such as polymerization shrinkage of composite resin materials, mechanical stress, and adhesive degradation can lead to microgaps forming between the restoration and the tooth structure (Alizadeh Oskoee et al., 2017). The polymerization shrinkage of composite resins, combined with mechanical stress and adhesive degradation, can create micro-gaps at the restoration-tooth interface (Bowen et al., 2018). These marginal defects allow acid-producing bacteria to penetrate, metabolizing carbohydrates into a localized acidic microenvironment. Once established, this process of secondary caries accelerates the loss of tooth structure and elevates the risk that pulp treatment will be required (Schwendicke et al., 2021). While modern restorative materials can meet functional restoration needs, they cannot actively address bacterial infections at vulnerable margins or demineralization issues.

Early efforts to extend the service life of dental composites centered on enhancing their mechanical properties and minimizing polymerization shrinkage (Zhang et al., 2015; Balhaddad et al., 2021). Advances in nanotechnology have spurred interest in multifunctional composites, marking a pivotal shift from passive to active strategies in preventing secondary caries. Antimicrobial composites reduce bacterial adhesion via antimicrobial release or contact-killing, preventing biofilm formation (Jiao et al., 2019; Xue et al., 2020). Composites designed for remineralization can provide ion sources: calcium and phosphate to compensate for structural damage caused by demineralization in early-stage caries (Besinis et al., 2014). Traditional antimicrobial agents or remineralization ions are often released linearly or uncontrolled, resulting in short release durations and uncontrollable release quantities (Sivakumar et al., 2014). However, with the continuous development of nanotechnology, this issue has been effectively addressed, enabling precise control over the release of antimicrobial agents and remineralization ions (Rostami et al., 2025). By carefully designing the structure of nanomaterials to respond to specific stimuli, targeted release can be achieved (Wang et al., 2024). Rechargeable nanomaterials allow for the repeated release of bioactive agents, while sophisticated cascade nanoreactors enable a synergistic, multi-step process of antibacterial action and remineralization within the caries microenvironment. Crucially, nanoparticles preserve the mechanical strength of restorative materials while introducing new functionalities (Amin et al., 2025).

Therefore, this paper reviews the latest progress of controlled-release antimicrobial nanomaterials (as summarized in Table 1) in

TABLE 1 Controlled-release nanomaterials.

Type	Nanomaterial	Material type	Mechanism	Release kinetics	Advantages/ disadvantages	Author (year)
pH Responsive	BioUnion	Bioactive glass powder	Release of Zn^{2+}, F^{-}, Ca^{2+}	Significantly enhanced release of Zn^{2+} and Ca^{2+} at pH 4.5–5.5	**Advantages:** Multi-ion synergistic antibacterial effect; responsive release; promotes remineralization. **Disadvantages:** F^{-} release inhibited in acidic environments, reducing anti-caries efficacy	(Liu et al., 2020)
	Eu@B-UiO-66/Zn	MOF composite	Releases eugenol, generates reactive oxygen species, disrupts biofilm	Maintains physical stability for at least 60 days with sustained release potential	**Advantages:** Synergistic pH-responsive release and ROS-based antibacterial action. **Disadvantages:** Potential toxicity from material degradation	(Wang et al., 2024)
	PMs@NaF-SAP	Polymeric micelles	Releases tannic acid and sodium fluoride	Releases 70% TA and 80% NaF within 24 hours at pH 5.0	**Advantages:** Multi-stimuli responsive release; validated both *in vitro* and *in vivo*. **Disadvantages:** Limited drug loading capacity; complex preparation.	(Xu et al., 2023)
Magnetic-Responsive	SPIONs (Fe_3O_4)	Magnetic nanocomposite	Release under magnetic field stimulation	Release exceeds 1 mg/mL within 24 hours, sufficient to inhibit MMP-9 activity	**Advantages**: Enhanced bonding strength; combines antibacterial and magnetic-guided penetration. **Disadvantages:** Slightly complex for clinical application.	(Mokeem et al., 2024)
Light/Heat-Responsive	CG-AgPB hydrogel	Hydrogel	NIR-triggered photothermal response, release of Fe^{2+} and Ag^{+}, antibacterial and anti-biofilm	808 nm laser irradiation triggers temperature rise >50 °C within 3 minutes	**Advantages:** Synergistic photothermal and ion release for highly effective antibacterial action. **Disadvantages:** Dependent on laser activation.	(Li et al., 2024)
	Sr-ZnO@PDA	Composite material	Yellow light and ultrasound synergistically catalyze ROS generation; Sr^{2+} promotes remineralization	Light/sonication-triggered release of Sr^{2+}	**Advantages:** Responsive to multiple physical stimuli; combines antibacterial and remineralization functions. **Disadvantages:** Relatively complex activation method.	(Mu et al., 2025)

(Continued)

10.3389/fcimb.2025.1669643

TABLE 1 Continued

Type	Nanomaterial	Material type	Mechanism	Release kinetics	Advantages/ disadvantages	Author (year)
	$ZnPcS_4$@GC5AF_5	Supramolecular nanomaterial	660 nm laser triggers PDT/PTT switching mechanism	Light-triggered, ATP environment-adaptive	**Advantages:** Smart switching of treatment mode; high targeting ability; low cytotoxicity. **Disadvantages:** ATP concentration-dependent; complex design.	(Zhang et al., 2024)
Fluoride-rechargeable	CaF_2 nanoparticles	Resin composite additive	Sustained release of F^- and Ca^{2+}; PMGDM in resin chelates F^- for ion recharge	Enhanced F^- release at pH 4.0, rechargeable multiple times	**Advantages:** Long-term fluoride release; rechargeability. **Disadvantages:** HEMA may cause hydrolysis; stringent recharge conditions.	(Yi et al., 2019)
NACP-based	NACP + DMAHDM	Resin composite	NACP releases calcium and phosphate ions under acidic conditions	Low pH triggers NACP release; mechanically triggered microcapsule release	**Advantages**: Self-healing, antibacterial, and remineralizing. **Disadvantages**: High microcapsule content may compromise mechanical properties.	(Wu et al., 2015)
GOx-based	HA@MRuO_2-Cip/GOx	Nanoreactor	GOx catalyzes glucose to produce acid and H_2O_2; pH-triggered antibiotic release and ROS generation	Sustained release of antibiotics and ROS under acidic conditions	**Advantages:** Cascade reaction amplifies antibacterial effect; bacteria-responsive controlled release. **Disadvantages:** High ROS concentrations may damage adjacent normal cells.	(Zhu et al., 2023)
	$Na_2S_2O_8$@ZIF-67/GOx	ROS nanogenerator	GOx-catalyzed acid production accelerates ZIF-67 decomposition, releasing SO_4^{2-} and ·OH	At pH 6.5, ZIF-67 decomposes rapidly and the release of ROS can last for 90 minutes	**Advantages:** Highly effective antibacterial; self-acidifying system; multi-mechanism synergy. **Disadvantages:** Complex preparation; potential toxicity risks.	(Ge et al., 2023)
	CoPt@G@GOx	Nanocomposite	Magnetic targeting + two-step cascade reaction to produce ·OH	Continuous production of oxTMB within 6 minutes	**Advantages:** Highly efficient cascade catalysis; magnetic targeting; pH-responsive. **Disadvantages:** Complex preparation.	(Dong et al., 2022)

(Continued)

10.3389/fcimb.2025.1669643

TABLE 1 Continued

Type	Nanomaterial	Material type	Mechanism	Release kinetics	Advantages/ disadvantages	Author (year)
	MX/AgP-GOx	Heterojunction nanomaterial	NIR photothermal release of Ag^+ + GOx consumes sugar, synergistic antibacterial effect	Instant response to NIR; release stops upon irradiation cessation; sustained release	**Advantages:** Multi-modal synergy: phototherapy + chemotherapy + metabolic intervention. **Disadvantages**: Risk of accumulation from long-term degradation products of MXene.	(Zhu et al., 2025)
Iron Oxide-based	CAT-NPs	Catalytic nanoparticles	Catalyzes H_2O_2 to produce ·OH under acidic conditions, disrupting biofilm	CAT-NP exhibits strongest catalytic activity in acidic environments; capable of killing bacteria and degrading EPS within 5 minutes	**Advantages:** Highly effective antibacterial and anti-biofilm activity; matrix degradation capability; pH-responsive. **Disadvantages:** Potential iron ion accumulation; dependent on H_2O_2.	(Gao et al., 2016)
	Ferumoxytol	Nanoparticles	Catalyzes H_2O_2 to generate free radicals under acidic conditions, disrupting biofilm	Catalytic reaction initiates within minutes when combined with H_2O_2	**Advantages:** High catalytic efficiency; simultaneously kills bacteria and degrades EPS; targets acidic environments. **Disadvantages:** Dependent on exogenous H_2O_2.	(Liu et al., 2018a)
	Dex-NZMs	Composite nanoparticles	Dex-NZM catalyzes H_2O_2 decomposition into free radicals under acidic conditions	pH-responsive catalysis when applied locally to biofilm surface	**Advantages:** High stability; high catalytic efficiency. **Disadvantages:** Dependent on exogenous H_2O_2; limited by pH dependency.	(Naha et al., 2019)

10.3389/fcimb.2025.1669643

preventing and treating secondary caries from the perspective of the strategy mechanism.

2 Stimuli-responsive strategy

Incorporating antimicrobial nano-ions into resin can address bacterial infections that cause secondary caries while maintaining the mechanical strength of the restorative material. Traditional antimicrobial agents often compromise the mechanical properties of resins (Ibrahim et al., 2020). In contrast, nano-antimicrobial agents can effectively kill bacteria at lower concentrations with their high specific surface area and extremely small volume (Sowmya et al., 2024). The nano-structure enriches the antimicrobial mechanisms, including contact killing, inducing cellular oxidative stress, and interfering with metabolism (Jowkar et al., 2025), making it less prone to bacterial resistance—a global concern. Initially, nano-antimicrobial agents faced the challenge of the burst effect: the early release of large amounts of antimicrobial agents caused local drug concentrations to rise, leading to significant cellular toxicity and a sharp decline in antimicrobial efficacy later on (de Jesus et al., 2024).

Additionally, concerns arose regarding the accumulation of metal nanoparticles in the body, their potential to induce inflammation, and the risk of breaching the blood-brain barrier (Wang et al., 2023; Yang et al., 2024). Controlled-release nano-antimicrobial materials, which can precisely respond to changes in the oral microenvironment to release antimicrobial agents, have emerged as a highly promising strategy to address this challenge. Common stimulants include exogenous magnetic fields, ultrasound, light, temperature, endogenous glutathione, enzymes, acids, glucose, ions, etc. (Figure 1). Light, temperature, and acid stimulants are commonly used to develop oral nanomedicines. Research on pH responsiveness to the special environment created by microbial acid production is the most prevalent.

2.1 pH-responsive

Dental caries-causing bacteria, such as *Streptococcus mutans* (*S. mutans*), produce organic acids (lactic acid and acetic acid) through glycolysis. This metabolic process lowers the pH at the interface between the filling material and the tooth structure, ultimately accelerating the dissolution of hydroxyapatite (Sangha et al., 2024).

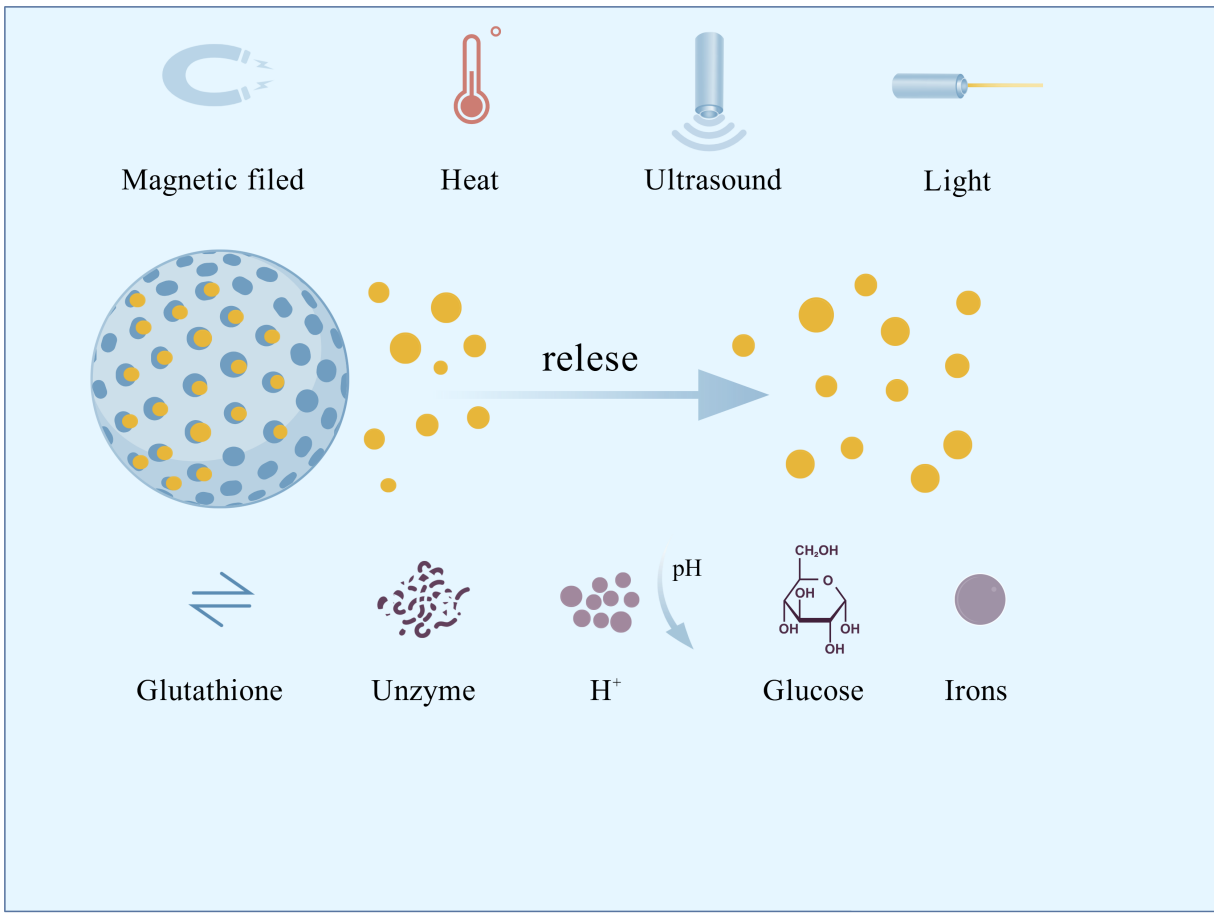

FIGURE 1
Common stimulus types for nano-responsive materials.

The mechanism of acid-responsive nanomedicines involves three points: (1) protonation or ionization of functional groups. For example, amino groups (-NH_2) protonate at low pH values to form -NH_3^+, releasing encapsulated antimicrobial agents; (2) cleavage of acid-labile bonds. Aldehyde bonds in specific mesoporous silica nanoparticles readily hydrolyze in acidic environments, enabling rapid drug release; (3) conformational changes in polymers. When pH drops below 5.5, carboxyl groups (–COOH) protonate, causing polymer contraction, which compresses internal pores and expels molecules (Meng et al., 2024; Boyuklieva et al., 2025; Tapponi et al., 2025). Their nanoscale dimensions further enhance biofilm penetration, ensuring efficient drug delivery. When functionalized with fluoride ions (F^-), these systems exhibit synergistic antimicrobial-remineralizing dual functionality, presenting a promising strategy for secondary caries prevention and therapy (Qi et al., 2025). Currently, acid-stimuli-responsive nanomaterials are the most extensively studied. Below, three typical acid-responsive materials are introduced: BioUnion, Eugenol, and Tannic acid.

2.1.1 BioUnion

BioUnion filler is a novel bioactive glass powder (Xia et al., 2025), that addresses the issue of declining fluoride release over time observed in traditional glass ionomer cements (GICs) (Dcruz et al., 2024; Da et al., 2025). It composed of silicon dioxide (SiO_2), zinc oxide (ZnO), calcium oxide (CaO), and a fluoride compound. Its particles can be incorporated into dental materials, releasing Zn^{2+} (combats oral bacteria and reduces dentin demineralization), F^- (inhibits demineralization), and Ca^{2+} (enhances remineralization) ions to prevent secondary caries (Fallahzadeh et al., 2022; Piszko et al., 2025). It also exhibits pH-dependent selective release of Zn^{2+}/Ca^{2+} (Liu et al., 2020).In bovine dentin subjected to 4-week pH-cycling, the GICs-Bio group (Control group: GICs) demonstrated superior inhibition of demineralization and promotion of remineralization. *In vitro* salivary titration assembly revealed that BioUnion™-incorporated GIC provides higher initial fluoride release and a more sustained release profile under simulated oral conditions (Htet et al., 2025).

2.1.2 Eugenol

Whereas BioUnio's strategy relies on antibacterial action and remineralization, eugenol acts primarily through pathogen inhibition and pulp inflammation modulation to prevent secondary caries (Nazemisalman et al., 2024; Patil et al., 2025). Innovative nano-delivery systems now enhance its efficacy by improving solubility and enabling controlled release.

These systems retain Eugenol's functionality while achieving slow, sustained drug release, and can be triggered to release in response to specific environmental stimuli, thereby avoiding the cytotoxicity associated with long-term high-concentration release, improving biosafety (Khan et al., 2019; Montoya et al., 2023). Specific applications include the Eu@B-UiO-66/Zn system, based on eugenol-loaded B-UiO-66 MOF complexed with Zn^{2+}, which achieves pH-responsive release via a phenolic hydroxyl-Zn^{2+} cage-like network where the released Eugenol generates reactive oxygen species (ROS) to disrupt biofilms (Wang et al., 2024); nanoencapsulation significantly enhances eugenol stability, for example up to 60 days (Vilela et al., 2023);acid-triggered nanoparticles modified with casein and based on hydroxyapatite/calcium carbonate that adhere to dentin and release Eugenol under low pH conditions (Sereda et al., 2023); synthetic eugenol derivatives containing polymerizable methacrylate groups, such as EgMA, enabling participation in resin free-radical polymerization, which maintain antibacterial activity against Gram-positive(G^+) and Gram-negative(G^-) bacteria while avoiding detrimental effects on resin polymerization and strength (Almaroof et al., 2016).

2.1.3 Tannic acid

Nanotechnology not only overcomes the limitations of natural active substances but also endows them with new functionalities. Tannic acid (TA) is a water-soluble natural polyphenol extracted from plants with antibacterial properties (Yamauchi et al., 1989; Sileika et al., 2013). When combined with phenylboronic acid (PBA), it forms a borate ester bond that can break down and release functional molecules under pH changes caused by bacteria (Springsteen and Wang, 2002). Using nano-polymer micelles (PM) with a shell-core structure as a scaffold, Sodium fluoride (NaF), tannic acid, and salivary acquired peptides (SAP)were loaded to produce multifunctional smart-release nano-antimicrobial materials PMs@NaF-SAP. At pH 5.0, nearly 70% of TA was released from PMs@NaF -SAP, while only approximately 40% was released at pH 7.4. Additionally, the more acidic the pH, the faster the NaF release rate; at pH 5.0, approximately 80% of NaF is released within 24 hours, and its antibacterial efficacy at this pH value is significantly stronger than that of the chlorhexidine (CHX) control group. As determined, PMs@NaF-SAP exhibits excellent demineralization inhibition and remineralization promotion capabilities, with relatively smooth tooth surfaces. Results from a caries-prone rodent model indicate that PMs@NaF-SAP treatment reduces the incidence and severity of lesions on smooth and fissure surfaces, effectively preventing the development of caries *in vivo* (Xu et al., 2023).

2.2 Magnetic field-responsive

Magnetically responsive materials, activated by an external magnetic field, enable the stimulation or targeting of specific objects using materials containing magnetic substances (Menezes-Silva et al., 2021). The magnetic field can adjust ion distribution within the material, enhancing the marginal sealing of restorative materials and reducing microleakage. Under its guidance, nanoparticles can penetrate dentinal tubules effectively, improving bonding strength.

Superparamagnetic iron oxide nanoparticles (SPIONs) exhibit non-magnetic behavior without an external magnetic field. However, when subjected to an external field, they respond rapidly to Lorentz forces, enabling their movement or directional alignment under magnetic guidance (Hu et al., 2017). In dental adhesives, SPIONs (Fe_3O_4) guided by a magnetic field can infiltrate

the micropores of dentin more effectively, leading to enhanced bond strength. This process generates mild thermal effects that can inhibit bacterial growth (Garcia et al., 2021). Ferroferric Oxide (Fe_3O_4) is a type of SPION. Constructing a core-shell structure with Fe_3O_4 cores and mesoporous silica shells allows for encapsulating antimicrobial agents like CHX and quaternary ammonium silane. This system achieved an inhibition rate of over 78% against *S. mutans* biofilms and maintained antibacterial activity even after 6 months of artificial aging, with no significant cytotoxicity observed (Mokeem et al., 2024). Targeted, sustained antimicrobial delivery to the critical interface prolongs restoration longevity.

Magnetic field-responsive materials provide superior spatiotemporal control and deep-tissue activation capabilities but at the cost of requiring external hardware. Acid-responsive materials are simpler, more autonomous, and highly biocompatible, but their action is less precise and confined to acidic micro-environments.

2.3 Light/heat responsive

For clinical ease-of-use, photothermal-responsive systems are ideal, as they allow therapeutic agents to be activated on-demand with a straightforward light source. Traditional nanomaterials exert antibacterial effects by releasing metal ions such as Ag^+, Cu^{2+}, and Zn^{2+}, which disrupt bacterial cell membranes and interfere with enzymatic activities (Xiu et al., 2011; Fan et al., 2021). However, their "burst release" mechanism leads to short therapeutic duration and lacks precise control (Jiang et al., 2023). Photo-responsive nanomaterials based on photodynamic therapy (PDT) offer a novel approach for preventing and managing secondary caries. PDT involves three key components: oxygen, an excitation light source, and a photosensitizer (PS). When exposed to light of specific wavelengths, the PS generates toxic ROS. These ROS possess strong oxidizing power and high reactivity, thereby inducing rapid lipid peroxidation in bacteria (Pereira et al., 2013; Fiegler-Rudol et al., 2025).

Photothermal therapy (PTT) and PDT are two complementary and promising phototherapeutic approaches. Silver-ion-doped Prussian Blue (AgPB) nanoparticles were encapsulated in cationic guar gum (CG) to form an antibacterial PTT hydrogel, CG-AgPB, exhibiting a photothermal conversion efficiency of 34.4%. Upon exposure to an 808 nm laser at a power density of 0.4 W cm^2, the hydrogel surpassed 50 °C within 3 minutes, synchronized with the release of Ag^+ ions from interstitial sites of the AgPB lattice, thereby inhibiting both individual oral cariogenic bacteria and their biofilms. *In vivo*, CG-AgPB-mediated PTT significantly reduced cariogenic bacteria to less than 1% of the original load in a rat caries model (Li et al., 2024). The laser power and irradiation duration can be precisely modulated to confine the therapeutic thermal zone, thereby minimizing collateral damage to adjacent healthy tissues (Alumutairi et al., 2020).

A polydopamine (PDA)-coated strontium-doped zinc oxide composite (Sr-ZnO@PDA) responds to yellow light and ultrasound. Synergistic piezophotocatalysis generates ROS, destroying bacterial cell membrane structures and decomposing dental surface pigments. Additionally, strontium ions (Sr^{2+}) released from SZ@PDA promote remineralization of enamel and dentin, repairing damaged tooth tissues (Mu et al., 2025). Another supramolecular nanoformulation achieves highly efficient inhibition of *S. mutans* biofilms through an adaptive PDT/PTT switching mechanism. Guanidinium groups on the material surface specifically bind to negatively charged moieties such as lipoteichoic acid and ATP on the *S. mutans* cell membrane, enabling targeted accumulation. Upon 660 nm laser irradiation, synergistic PTT and PDT effects are observed. In low-ATP environments (planktonic bacteria), the photosensitizer $ZnPcS_4$ exists as monomers that predominantly generate ROS via PDT, disrupting bacterial membrane integrity. In high-ATP environments (biofilms), $ZnPcS_4$ forms H-aggregates that chiefly produce heat through PTT for bactericidal action, circumventing the limited ROS penetration issue. Experiments also confirmed the material's low cytotoxicity; compared to the markedly demineralized control group, enamel remained notably intact in a rat dental caries model (Zhang Y. et al., 2024).

This section highlights the promise of stimuli-responsive nanomedicines for combating secondary caries. pH-responsive systems offer high clinical relevance by leveraging the cariogenic microenvironment to trigger targeted drug release and demonstrate synergistic antibacterial-remineralization effects. In comparison, external field-responsive strategies provide superior spatiotemporal control over treatment, enabling on-demand activation. Yet they face significant practical limitations. For light-responsive systems in particular, limited tissue penetration depth remains a major constraint. In morphologically complex teeth such as molars, light may be unable to effectively reach lesions in proximal or deep dentinal areas, resulting in incomplete treatment. Similarly, magnetic-responsive approaches require externally applied devices, which may complicate clinical integration and routine use.

3 Rechargeable strategy

Interventions for secondary caries primarily encompass antibacterial approaches and remineralization. For years, researchers have incorporated remineralizing ions into restorative materials. Fluoride ions(F^-) facilitate the deposition of calcium ions (Ca^{2+}) and phosphorus ions (PO_4^{3-}) within the tooth structure, forming more acid-resistant fluorapatite ($Ca_5(PO_4)_3F$), while also buffering the acidic environment created by bacteria. Sodium fluoride nanoparticles have reduced secondary caries at restoration margins by releasing F^- and Ca^{2+} (Albelasy et al., 2023). However, the short duration of effective ion release from these materials, relative to the expected lifespan of restorations, remains a critical challenge. To address this, a rechargeable strategy has been proposed to prolong ion release (Kelić et al., 2023). This approach centers on replenishing the diminishing active ions within the restorative material through exogenous ion exchange, restoring its remineralizing potential. There are three phases: 1) Release phase: Soluble active ions (F^-/Ca^{2+}) are released from the material, promoting remineralization; 2) Depletion phase:

Continued ion release depletes surface reservoirs, leading to declining ion concentration and diminished remineralization capacity; 3) Recharging phase: The material is exposed to an exogenous high-concentration ion solution. Driven by concentration gradients or ion exchange, new ions diffuse into the inorganic matrix/microporous structure, achieving reloading (Puttipanampai et al., 2025) (Figure 2).

3.1 Fluoride

As widely documented, fluoride combats dental caries through three mechanisms: inhibiting demineralization, promoting remineralization, and suppressing bacterial metabolism (Monjarás-Ávila et al., 2025). To address the transient fluoride release from existing restorative materials, rechargeable fluoride nanomaterials offer a new way for managing secondary caries.

Calcium fluoride (CaF_2) nanoparticles (average 58 nm), synthesized via spray-drying and incorporated into resin matrices, exhibit excellent biocompatibility and significantly enhanced F^- release capacity that remains stable over repeated recharging cycles (Yi et al., 2019). These materials demonstrate high pH sensitivity, where acidic conditions trigger a surge in fluoride release, particularly pronounced in systems containing CaF_2 or fluorohydroxyapatite under cariogenic pH (4.5-5.5) generated by bacterial metabolism (Morawska-Wilk et al., 2025). Studies confirm that ion release (Ca^{2+}, F^-, PO_4^{3-}) at acidic pH (4.5-5.5) is markedly higher than at neutral pH (6.5), a trend sustained even after recharging (Venkataiah et al., 2025). This pH-responsive sustained release is critical in resin-based restorations: it enhances remineralization within cariogenic microenvironments and extends restoration longevity. Both silane- and methacrylate-based composites effectively serve as rechargeable fluoride carriers (Madhyastha et al., 2025). The synergy between acid-triggered release and on-demand recharging holds significant promise for combating secondary caries.

3.2 Nanoamorphous calcium phosphate

Amorphous calcium phosphate (ACP) possesses a non-crystalline structure and exhibits high ionic release activity (Degli Esposti and Iafisco, 2022). Nanotechnology has effectively addressed the challenge of uncontrolled ion release from traditional ACP. Under acidic conditions, NACP rapidly releases significant amounts of calcium (Ca^{2+}) and phosphate (PO_4^{3-}) ions,

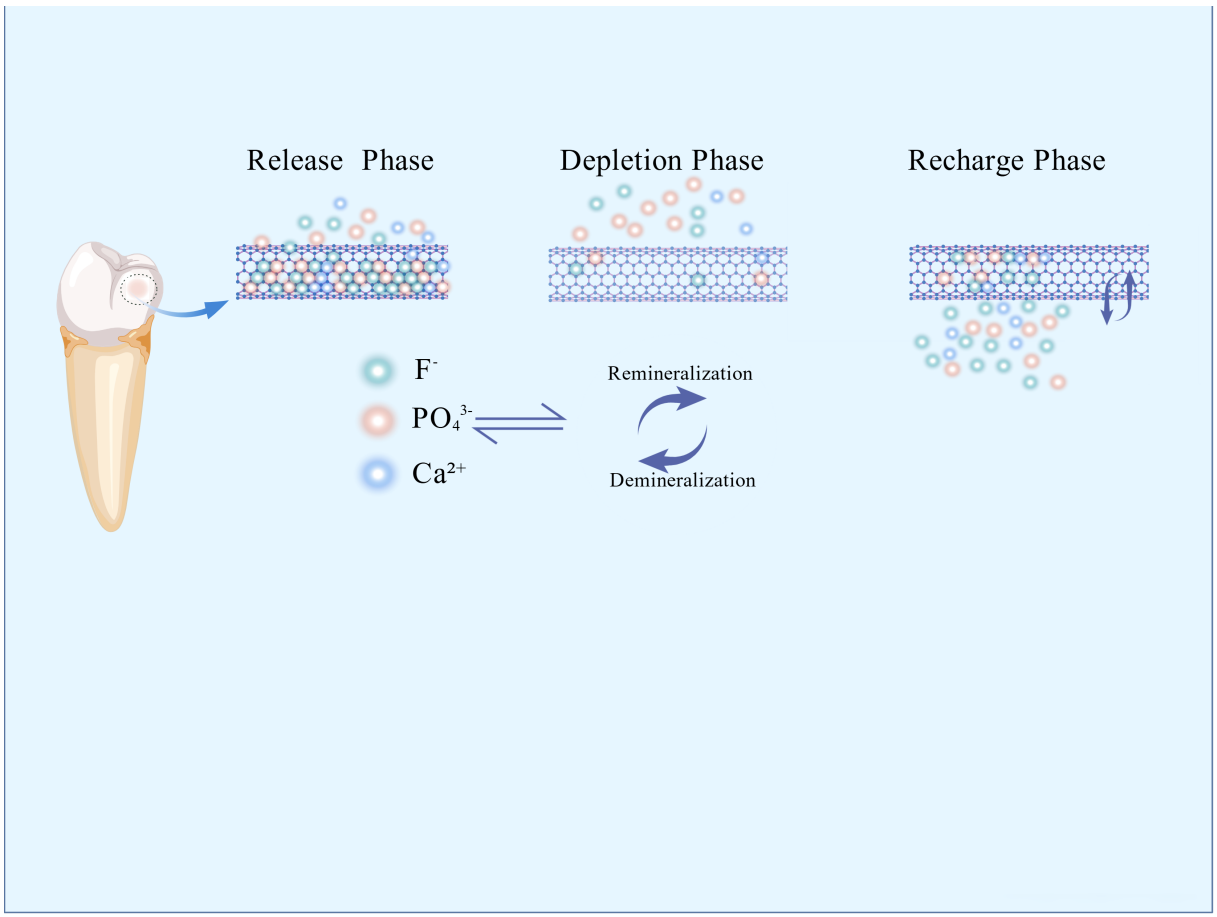

FIGURE 2
Mechanism of rechargeable nanomaterials.

while maintaining structural stability with minimal ion release in neutral or alkaline environments (Liang et al., 2019).

Incorporating nano-sized NACP alongside dimethylaminohexadecyl methacrylate (DMAHDM) nanoparticles into resin-based materials creates a dual-functional composite. The Ca^{2+} and PO_4^{3-} ions released from NACP neutralize acids produced by cariogenic bacteria, disrupting the acidic environment conducive to demineralization and promoting remineralization. Simultaneously, the DMAHDM component exerts a potent direct antibacterial effect (Wu et al., 2015; Sales-Junior et al., 2025). Furthermore, animal models have demonstrated that these composites induce minimal pulp irritation and stimulate tertiary dentin formation (Li et al., 2014). In an *in vitro* saliva-derived biofilm secondary caries model, it inhibits the growth of cariogenic bacteria at the resin margin and has no negative impact on tooth enamel hardness (Zhou et al., 2020).

NACP has also been successfully integrated into dental adhesives, often with monobasic calcium phosphate dihydrate (MCPM), to enhance their remineralization and antibacterial capabilities (Liu et al., 2018a). Despite finite ion release duration (typically months), rechargeable NACP nanocomposites overcome this limitation via periodic calcium/pHospHate solution immersion. Both rechargeable NACP and NACP-DMAHDM variants retain flexural strength and elastic modulus comparable to commercial counterparts. They significantly inhibit biofilm metabolic activity and lactic acid production, while drastically reducing biofilm colony-forming units (CFUs). A single recharge sustains effective ion release for up to 42 days (Al-Dulaijan et al., 2018). Crucially, the release profile remains stable over multiple recharge cycles, demonstrating long-term ion release and remineralization potential. This recharge strategy also shows significant anti-caries efficacy in adhesives and sealants (Ibrahim et al., 2020). For instance, a novel self-healing dental adhesive incorporating poly(urea-formaldehyde) (PUF) microcapsules, DMAHDM, and NACP achieved a 67% crack-healing efficiency without compromising dentin bond strength. Concurrently, it reduced biofilm CFUs by four orders of magnitude, confirming its potent antibacterial properties (Wu et al., 2019).

This rechargeable strategy substantially bridges the translational gap: Recharging requires mere minutes per session, with a single treatment sustaining caries-preventive efficacy for up to six months. Crucially, at-home recharge via mouth rinse empowers patient autonomy. It establishes a clinically viable protocol for long-term dynamic management of secondary caries.

Rechargeable resin-based restoratives can markedly extend the functional lifespan of dental restorations through their replenishable ion-release mechanism, simultaneously enhancing remineralization and antimicrobial efficacy. In acidic environments, these materials exhibit intelligent, pH-responsive ionic discharge while maintaining favorable biocompatibility and mechanical stability, offering a novel long-term dynamic management strategy for recurrent caries.

Nevertheless, recent investigations have highlighted several shortcomings. First, although CaF_2 and NACP nanoparticles are intrinsically cytocompatible, high fluoride loads or DMAHDM quaternary ammonium antimicrobials still display concentration-dependent cytotoxicity in 3-D spheroid cultures or human dental-pulp stem-cell assays, compromising the biosafety of the pulp and surrounding soft tissues (Fei et al., 2024). Second, even advanced CAD/CAM resin composites undergo inevitable deterioration in flexural strength and surface hardness after prolonged exposure to the moist oral milieu, primarily attributable to water sorption and hydrolytic degradation (Wendler et al., 2021). Third, fluoride-releasing materials experience significant deterioration of nanohardness, elastic modulus, and surface roughness when challenged by acidic beverages (Güner and Köse, 2024). Fourth, no consensus exists on the concentration, pH, or contact time of "recharge mouthwashes"; regulatory agencies have yet to establish *in vitro–in vivo* correlation guidelines, and published clinical trials are underpowered with follow-up periods < 2 years, precluding reliable assessment of long-term marginal integrity and secondary-caries incidence (Zhang J. et al., 2024).

4 Cascade catalytic nanoreactor

Integrating nanotechnology, catalytic chemistry, and biomedicine has led to the development of cascade catalytic nanoreactors, representing an advanced strategy for preventing and treating oral infectious diseases. Inspired by intracellular multi-enzyme cascade reactions, researchers initially attempted to construct artificial cascade systems by encapsulating natural enzymes within porous synthetic materials, including metal-organic frameworks (MOFs), covalent organic frameworks (COFs), and hydrogen-bonded organic frameworks (HOFs) (Lykourinou et al., 2011; Huang et al., 2022). However, these early systems suffered from poor enzyme stability, low reaction efficiency, and inadequate controllability (Meghwanshi et al., 2020). Subsequent advancements replaced natural enzymes with inorganic nanocatalysts (Fe_3O_4 or Au nanoparticles), effectively resolving stability issues (Li et al., 2015; Kwon et al., 2021; Ma et al., 2024). Further innovation incorporated stimuli-responsive materials (ultrasound or pH-activated components) to achieve precisely controlled activation (Chen and Li, 2020; Li et al., 2022). Self-supplying substrate systems were engineered to overcome dependence on external reactants (Figure 3). Consequently, application scenarios have expanded beyond tumor therapy to encompass anti-biofilm interventions.

4.1 Glucose oxidase

GOx exhibits catalytic properties and bioactivities uniquely suited to the cariogenic microenvironment: it oxidizes glucose and oxygen into gluconic acid and hydrogen peroxide (Dubey et al., 2017). This reaction directly depletes free glucose, competing with *S. mutans* for metabolic substrates and suppressing bacterial growth and acid production (Senol et al., 2007; Yuan et al., 2015). The in situ-generated hydrogen peroxide reduces glucosyltransferase activity, diminishing viscous glucan synthesis and disrupting biofilm formation mechanisms (Zhang et al., 2021). Concurrently, gluconic acid production triggers pH-

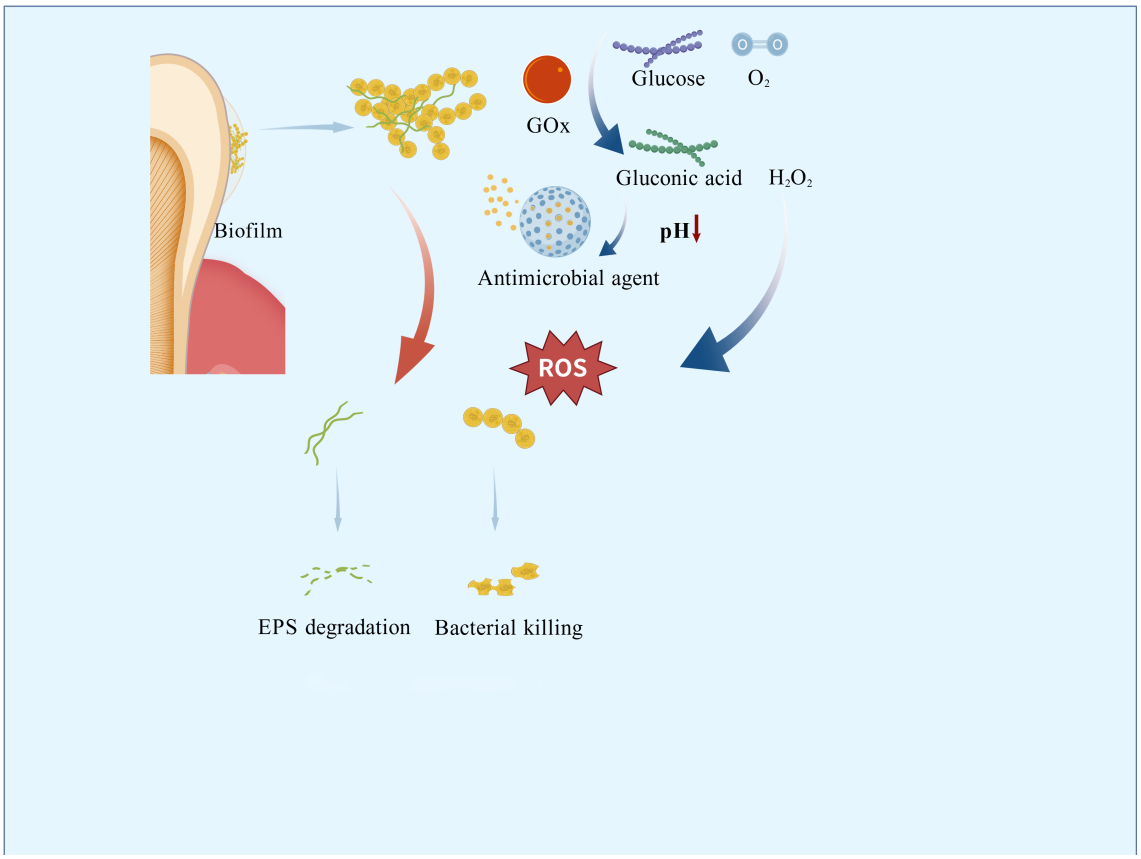

FIGURE 3
Mechanism of antimicrobial cascade nanoreactors.

responsive drug release (Wang et al., 2022). GOx is not used in isolation. It is integrated into nanocomposites that incorporate additional targeting strategies (such as magnetic guidance, pH-responsive release, or photothermal activation) which enhance spatial precision and biological specificity. GOx does not target specific bacterial species through molecular recognition, but rather functionally discriminates against cariogenic pathogens. These targeted mechanisms establish a novel paradigm for constructing multimodal antimicrobial systems.

The greatest advantage of cascade nanoreactors lies in their ability to integrate and leverage distinct molecular functions. The HA@MRuO$_2$–Cip/GOx composite (composed of hydroxyapatite, HA; mesoporous ruthenium dioxide, MRuO$_2$; ciprofloxacin, Cip; and GOx) incorporates a mesoporous RuO$_2$ core co-loaded with Cip and GOx. *In vitro*, the composite disrupts biofilms by cleaving extracellular DNA, thereby enhancing the bactericidal efficacy of Cip against planktonic bacteria. Under acidic conditions, it not only sustains ROS generation but also allows controlled release of antibiotics (Zhu et al., 2023).

Similarly leveraging acidic conditions for antibacterial activity, $Na_2S_2O_8$@ZIF-67/GOx(composed of sodium persulfate, $Na_2S_2O_8$; zeolitic imidazolate framework-67, ZIF-67; and GOx) functions as a novel ROS nanogenerator. GOx-mediated catalysis in acidic microenvironments produces H_2O_2 and gluconic acid, which further reduces pH to accelerate ZIF-67 decomposition and $Na_2S_2O_8$ release. This process yields highly toxic sulfate (SO_4^{2-}) and hydroxyl (-OH) radicals, effectively suppressing bacterial proliferation and biofilm formation (Ge et al., 2023).

Also operating under external energy stimulation, the nanozyme CoPt@G@GOx (composed of cobalt-platinum alloy, CoPt; graphene, G; and GOx) employs a two-step cascade reaction to generate potent -OH radicals in acidic environments, achieving 4-fold enhanced catalytic efficiency in disrupting *S. mutans* biofilms compared to simple mixtures. Its magnetic CoPt@grapHene core enables precise targeting of carious lesions via external magnetic fields, minimizing off-target effects (Dong et al., 2022). TiO$_2$-GOx(composed of titanium dioxide, TiO$_2$; and GOx)exhibits high catalytic activity in glucose-rich environments under UV irradiation, significantly amplifying ROS production (Kim et al., 2019).

Incorporating both photothermal and biochemical antibacterial mechanisms, MX/AgP-Gox (composed of MXene, MX; silver nanoparticles, AgNPs; and GOx) is a cascade bio-heterojunction (HJ) engineered to target both dental-plaque biofilms' chemical and biological constituents. Under near-infrared (NIR) irradiation, the HJ rapidly heats up to generate photothermal effects while exploiting H_2O_2 to burst-produce massive ROS, achieving highly efficient phototherapy. Even in darkness, the bactericidal action of

Ag^+ ions and glucose depletion mediated by GOx act synergistically to suppress bacteria, ensuring long-lasting anti-caries efficacy after light withdrawal. Rat caries models further confirmed that the material inhibits enamel demineralization and exhibits excellent biocompatibility (Zhu et al., 2025).

4.2 Iron oxide

Catalytic iron oxide nanoparticles (CAT-NPs) mimic natural peroxidases through their intrinsic catalytic activity. Under acidic conditions, they catalyze H_2O_2 decomposition into hydroxyl radicals (-OH), disrupting bacterial membranes, degrading intracellular macromolecules, and breaking down extracellular polymeric substances (EPS) within biofilms. *In vitro* studies demonstrate that CAT-NPs reduce apatite demineralization at acidic pH. Topical application combined with H_2O_2 effectively suppresses caries initiation and progression without adverse effects on oral mucosal tissues *in vivo* (Gao et al., 2016).

Ferumoxytol is a Food and Drug Administration (FDA)-approved nanoparticle formulation used for magnetic resonance imaging and the treatment of iron deficiency (Dósa et al., 2011). Ferumoxytol can penetrate the interior of biofilms and, under acidic conditions, catalyze the production of reactive radicals from H_2O_2. These radicals disrupt bacterial cell membranes and degrade extracellular polysaccharide matrices, killing the bacteria. In ex vivo biofilm models, its combination with low concentrations of H_2O_2 effectively inhibits biofilm accumulation on natural teeth and prevents enamel demineralization (Liu et al., 2018b). Notably, it enables pathogenic biofilm detection via colorimetric responses, establishing a theranostic platform for caries management (Liu et al., 2021). Dextran-coated iron oxide nanoparticles (Dex-NZMs) maintain catalytic efficiency while enhancing stability. These particles exhibit potent catalytic activity at acidic pH, enabling biofilm-specific targeting. Dex-NZMs prevent severe carious lesions in murine caries models while demonstrating excellent biosafety (Naha et al., 2019).

Cascade-catalytic nanoreactors that emulate natural enzymatic cascades have recently emerged as promising therapeutics for oral infectious diseases. They efficiently generate ROS, respond precisely to the pathological microenvironment, supply their own substrates, and exert multimodal synergistic antimicrobial effects. Collectively, these attributes substantially enhance biofilm eradication while minimizing collateral damage to healthy tissues.

Nevertheless, clinical translation remains hindered by several unresolved limitations. Catalytic activity is prone to attenuation in the complex oral milieu owing to protein adsorption, pH fluctuations, and variable ionic strength, leading to suboptimal durability and limited functional persistence (Ming et al., 2020). Moreover, the fidelity of cascade activation is still imperfect; off-target triggering or adventitious side-reactions may compromise therapeutic predictability and patient safety (Zhang et al., 2018).

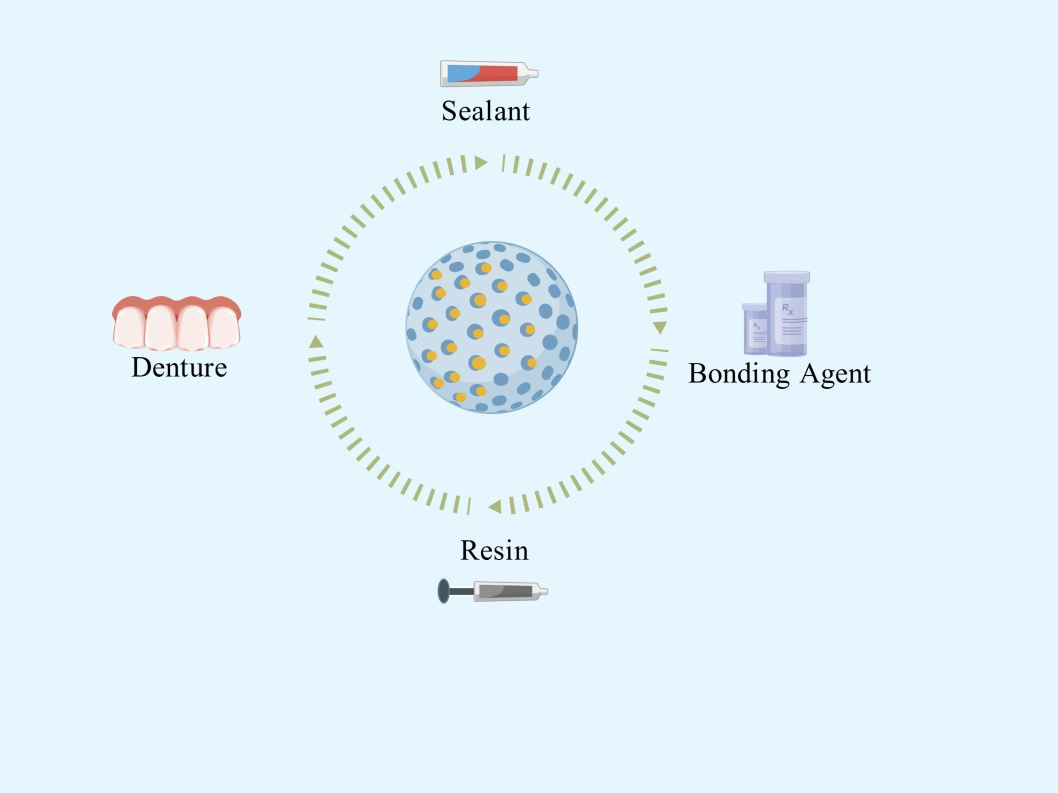

FIGURE 4
Applications of controlled-release nano-antimicrobial materials.

It constitute an innovative therapeutic platform, yet scalable manufacturing, reproducible quality control, and comprehensive regulatory frameworks are still in their infancy.

5 Opportunities and challenges in clinical translation

The heterogeneity of biofilms and the presence of salivary proteins pose challenges for oral antibacterial materials. The former has long posed a significant challenge to antimicrobial materials: the oral biofilm forms a complex three-dimensional structure. The EPS matrix acts like a "fortress wall" that blocks the penetration of antimicrobial molecules (Zhao et al., 2023). Gradients of oxygen and nutrients from the surface to the deeper layers lead to altered bacterial metabolic activity, with dormant bacteria in the deep layers exhibiting stronger drug tolerance (Liu et al., 2024).

Controlled-release nano-antimicrobial materials show promising performance in addressing biofilm heterogeneity. Physically, their nanoscale structure provides high surface energy, enhancing adhesion to negatively charged bacterial biofilms and enabling penetration through the EPS matrix to deliver antimicrobial agents directly to dormant bacteria in the deeper layers (Han et al., 2022). Moreover, the released antimicrobial molecules can disrupt bacterial membrane potential, inhibit enzymatic activity, and promote ROS generation (Sahli et al., 2022). Finally, through controlled-release mechanisms, these materials maintain effective bactericidal concentrations at the infection site, preventing exposure to sublethal doses and thereby suppressing the enrichment of drug-resistant mutants. These advantages make them highly effective against biofilms.

However, salivary proteins present a double-edged sword. Within hours after cleaning, teeth become coated with a layer of salivary proteins, which can isolate antibacterial materials from bacteria, thereby reducing antimicrobial efficiency and long-term efficacy (Heo et al., 2013). At the same time, this protein layer facilitates bacterial adhesion. However, current nano-antibacterial materials often fail to account for this effect. How to resist salivary protein adhesion through surface modification of nanomaterials is thus an important issue. Research should also be conducted under conditions that simulate the oral environment to more accurately evaluate the practical antibacterial performance of these materials. Rather than focusing solely on avoiding salivary proteins, it would be more beneficial to explore how to leverage them to enhance material functionality.

In addition to the two aforementioned oral-specific environmental resistance factors, the clinical translation of nanomaterials currently faces several challenges:(1) the long-term biosafety, biocompatibility, and functional durability of these nanomaterials within the oral cavity require rigorous assessment in live animal models and, ultimately, clinical trials (Sajithkumar et al., 2025). Many studies discussed in this article are primarily *in vitro*. Not only in the dental field, one of the biggest current challenges for nanomaterials is the lack of long-term *in vivo* experiments. While a few studies have employed rodent caries models to show efficacy in reducing lesion severity, these are often short-term and lack evaluation of critical endpoints; (2) the regulatory landscape for nano-enabled medical products remains fragmented. Harmonized characterization standards and quality-control guidelines are urgently required. Critical parameters—including particle-size distribution, surface charge, and degradation products—must be quantified through validated, standardized assays to guarantee batch-to-batch consistency and clinical reproducibility (Rodríguez-Gómez et al., 2025). (3) Since some dental materials need to meet aesthetic requirements, the coloration issue of certain metal nanoparticles also cannot be ignored. Despite these challenges, the unique properties of controlled-release nano-antimicrobial materials have led to their exploration in a wide range of dental applications. These applications aim to leverage their sustained and targeted antibacterial action to improve the longevity and success of various dental treatments and restorative procedures (Figure 4).

6 Conclusion

This paper systematically reviews the latest mechanistic advances in controlled-release nanomaterials for preventing secondary caries. Stimulus-responsive systems have evolved from single pH triggers to multi-stimulus synergistic activation, rechargeable nanocarriers have graduated from one-off ion reservoirs to "stimulus–response–re-supply" cycles, and cascade nanoplates now seamlessly integrate antibacterial, acid-neutralizing, and remineralizing functions for precise modulation of the cariogenic microenvironment.

However, the oral pH landscape is constantly perturbed by diet, saliva and microbial metabolism, making it difficult for materials to respond specifically to acid niches generated solely by cariogenic bacteria; The layer-by-layer fabrication of cascade structures still relies on complex processes, which limits large-scale production and cost control; and unified characterization protocols together with long-term biosafety regulation for nanomaterials are still absent. These challenges are compounded by patient compliance issues, as complex or expensive preventive measures may lead to poor adherence, reducing real-world effectiveness. Therefore, overcoming these technical and economic barriers while ensuring user-friendly and affordable solutions, which is essential to advancing effective caries management.

Author contributions

YW: Visualization, Writing – original draft, Writing – review & editing. XD: Investigation, Writing – original draft, Writing – review & editing. YJ: Investigation, Writing – review & editing. LQ: Investigation, Writing – review & editing. FL: Funding acquisition, Investigation, Writing – review & editing. YC: Funding acquisition, Validation, Writing – review & editing. SW: Funding acquisition, Project administration, Supervision, Writing – review & editing.

Funding

The author(s) declare financial support was received for the research and/or publication of this article. This work was supported by Henan Provincial Medical Science and Technology Research Plan Provincial Key Project (No. SBGJ202102162); Henan Provincial Department of Education Key Scientific Research Project of Higher Education Institutions (No. 22A320006); Joint Construction Project of Henan Medical Science and Technology Research and Development Program (No. LHGJ20220353).

Conflict of interest

The authors declare that the research was conducted in the absence of any commercial or financial relationships that could be construed as a potential conflict of interest.

Generative AI statement

The author(s) declare that no Generative AI was used in the creation of this manuscript.

Any alternative text (alt text) provided alongside figures in this article has been generated by Frontiers with the support of artificial intelligence and reasonable efforts have been made to ensure accuracy, including review by the authors wherever possible. If you identify any issues, please contact us.

Publisher's note

References

Albelasy, E. H., Chen, R., Fok, A., Montasser, M., Hamama, H. H., Mahmoud, S. H., et al. (2023). Inhibition of caries around restoration by ion-releasing restorative materials: an *in vitro* optical coherence tomography and micro-computed tomography evaluation. *Materials (Basel)* 16 (16), 5558. doi: 10.3390/ma16165558

Al-Dulaijan, Y. A., Cheng, L., Weir, M. D., Melo, M. A. S., Liu, H., Oates, T. W., et al. (2018). Novel rechargeable calcium phosphate nanocomposite with antibacterial activity to suppress biofilm acids and dental caries. *J. Dent.* 72, 44–52. doi: 10.1016/j.jdent.2018.03.003

Alizadeh Oskoee, P., Pournaghi Azar, F., Jafari Navimipour, E., Ebrahimi Chaharom, M. E., Naser Alavi, F., and Salari, A. (2017). The effect of repeated preheating of dimethacrylate and silorane-based composite resins on marginal gap of class V restorations. *J. Dent. Res. Dent. Clin. Dent. Prospects* 11, 36–42. doi: 10.15171/joddd.2017.007

Almaroof, A., Niazi, S. A., Rojo, L., Mannocci, F., and Deb, S. (2016). Influence of a polymerizable eugenol derivative on the antibacterial activity and wettability of a resin composite for intracanal post cementation and core build-up restoration. *Dent. Mater* 32, 929–939. doi: 10.1016/j.dental.2016.04.001

Alumutairi, L., Yu, B., Filka, M., Nayfach, J., and Kim, M. H. (2020). Mild magnetic nanoparticle hyperthermia enhances the susceptibility of Staphylococcus aureus biofilm to antibiotics. *Int. J. Hyperthermia* 37, 66–75. doi: 10.1080/02656736.2019.1707886

Amin, F., Moin, S. F., Kumar, N., Asghar, M. A., Mahmood, S. J., and Palma, P. J. (2025). The impact of zirconium oxide nanoparticles on the mechanical and physical properties of glass ionomer dental materials. *Int. J. Mol. Sci.* 26 (11), 5382. doi: 10.3390/ijms26115382

Balhaddad, A. A., Garcia, I. M., Mokeem, L., Alsahafi, R., Collares, F. M., and Sampaio de Melo, M. A. (2021). Metal oxide nanoparticles and nanotubes: ultrasmall nanostructures to engineer antibacterial and improved dental adhesives and composites. *Bioengineering (Basel)* 8 (10), 146. doi: 10.3390/bioengineering8100146

Besinis, A., van Noort, R., and Martin, N. (2014). Remineralization potential of fully demineralized dentin infiltrated with silica and hydroxyapatite nanoparticles. *Dent. Mater* 30, 249–262. doi: 10.1016/j.dental.2013.11.014

Bowen, W. H., Burne, R. A., Wu, H., and Koo, H. (2018). Oral biofilms: pathogens, matrix, and polymicrobial interactions in microenvironments. *Trends Microbiol.* 26, 229–242. doi: 10.1016/j.tim.2017.09.008

Boyuklieva, R., Zahariev, N., Simeonov, P., Penkov, D., and Katsarov, P. (2025). Next-generation drug delivery for neurotherapeutics: the promise of stimuli-triggered nanocarriers. *Biomedicines* 13 (6), 1464. doi: 10.3390/biomedicines13061464

Chen, D., and Li, J. (2020). Ultrasmall Au nanoclusters for bioanalytical and biomedical applications: the undisclosed and neglected roles of ligands in determining the nanoclusters' catalytic activities. *Nanoscale Horiz* 5, 1355–1367. doi: 10.1039/D0NH00207K

Da, Y., He, T., Ma, X., Yang, R., Lin, Y., Yang, Q., et al. (2025). Probing into the triggering effects of zinc presence on the mineral formation, hydration evolution, and mechanical properties of fluorine-bearing clinker. *Langmuir* 41, 11417–11427. doi: 10.1021/acs.langmuir.5c00302

Dcruz, M. M., Tapashetti, S., Naik, B., Shah, M. A., Mogi, P., and Horatti, P. (2024). Comparative evaluation of fluoride release profiles in new glass ionomer cements and conventional type II GIC: Implications for cariostatic efficacy. *Bioinformation* 20, 2009–2014. doi: 10.6026/9732063002002009

Degli Esposti, L., and Iafisco, M. (2022). Amorphous calcium phosphate, the lack of order is an abundance of possibilities. *Biomater Biosyst.* 5, 100037. doi: 10.1016/j.bbiosy.2021.100037

de Jesus, R. A., de Assis, G. C., de Oliveira, R. J., Costa, J. A. S., da Silva, C. M. P., Iqbal, H. M. N., et al. (2024). Metal/metal oxide nanoparticles: A revolution in the biosynthesis and medical applications. *Nano-Structures Nano-Objects* 37, 101071. doi: 10.1016/j.nanoso.2023.101071

Dong, Q., Li, Z., Xu, J., Yuan, Q., Chen, L., and Chen, Z. (2022). Versatile graphitic nanozymes for magneto actuated cascade reaction-enhanced treatment of S. *mutans biofilms. Nano Res.* 15, 9800–9808. doi: 10.1007/s12274-022-4258-x

Dósa, E., Tuladhar, S., Muldoon, L. L., Hamilton, B. E., Rooney, W. D., and Neuwelt, E. A. (2011). MRI using ferumoxytol improves the visualization of central nervous system vascular malformations. *Stroke* 42, 1581–1588. doi: 10.1161/STROKEAHA.110.607994

Dubey, M. K., Zehra, A., Aamir, M., Meena, M., Ahirwal, L., Singh, S., et al. (2017). Improvement strategies, cost effective production, and potential applications of fungal glucose oxidase (GOD): current updates. *Front. Microbiol.* 8, 1032. doi: 10.3389/fmicb.2017.01032

Fallahzadeh, F., Heidari, S., Najafi, F., Hajihasani, M., Noshiri, N., and Nazari, N. F. (2022). Efficacy of a novel bioactive glass-polymer composite for enamel remineralization following erosive challenge. *Int. J. Dent.* 2022, 6539671. doi: 10.1155/2022/6539671

Fan, X., Yahia, L., and Sacher, E. (2021). Antimicrobial properties of the ag, cu nanoparticle system. *Biol. (Basel)* 10 (2), 137. doi: 10.3390/biology10020137

Fei, X., Li, Y., Zhang, Q., Tian, C., Li, Y., Dong, Q., et al. (2024). Novel pit and fissure sealant with nano-CaF(2) and antibacterial monomer: Fluoride recharge, microleakage, sealing ability and cytotoxicity. *Dent. Mater J.* 43, 346–358. doi: 10.4012/dmj.2023-166

Fiegler-Rudol, J., Kapłon, K., Kotucha, K., Moś, M., Skaba, D., Kawczyk-Krupka, A., et al. (2025). Hypocrellin-mediated PDT: A systematic review of its efficacy, applications, and outcomes. *Int. J. Mol. Sci.* 26 (9), 4038. doi: 10.3390/ijms26094038

Gao, L., Liu, Y., Kim, D., Li, Y., Hwang, G., Naha, P. C., et al. (2016). Nanocatalysts promote Streptococcus mutans biofilm matrix degradation and enhance bacterial killing to suppress dental caries in *vivo*. *Biomaterials* 101, 272–284. doi: 10.1016/j.biomaterials.2016.05.051

Garcia, I. M., Balhaddad, A. A., Lan, Y., Simionato, A., Ibrahim, M. S., Weir, M. D., et al. (2021). Magnetic motion of superparamagnetic iron oxide nanoparticles- loaded dental adhesives: physicochemical/biological properties, and dentin bonding performance studied through the tooth pulpal pressure model. *Acta Biomater* 134, 337–347. doi: 10.1016/j.actbio.2021.07.031

Ge, G., Wu, L., Zhang, F., Wang, T., Han, L., Kong, X., et al. (2023). Na(2)S(2)O(4)@Co-metal organic framework (ZIF-67) @glucose oxidase for biofilm-infecting wound

healing with immune activation. *Int. J. Biol. Macromol* 226, 1533–1546. doi: 10.1016/j.ijbiomac.2022.11.265

Güner, Z., and Köse, H. D. (2024). Evaluation of nanohardness, elastic modulus, and surface roughness of fluoride-releasing tooth colored restorative materials. *J. Clin. Pediatr. Dent.* 48, 131–137. doi: 10.22514/jocpd.2024.112

Han, X., Lou, Q., Feng, F., Xu, G., Hong, S., Yao, L., et al. (2022). Spatiotemporal release of reactive oxygen species and NO for overcoming biofilm heterogeneity. *Angew Chem. Int. Ed Engl.* 61, e202202559. doi: 10.1002/anie.202202559

Heo, S. M., Ruhl, S., and Scannapieco, F. A. (2013). Implications of salivary protein binding to commensal and pathogenic bacteria. *J. Oral. Biosci.* 55, 169–174. doi: 10.1016/j.job.2013.06.004

Htet, K., Hiraishi, N., Sanon, K., Ubolsaard, P., Sone, K. P., and Shimada, Y. (2025). Effect of zinc-releasing glass ionomer cement on preventing dentin demineralization. *J. Dent.* 156, 105718. doi: 10.1016/j.jdent.2025.105718

Hu, P., Kang, L., Chang, T., Yang, F., Wang, H., Zhang, Y., et al. (2017). High saturation magnetization Fe3O4 nanoparticles prepared by one-step reduction method in autoclave. *J. Alloys Compounds* 728, 88–92. doi: 10.1016/j.jallcom.2017.08.290

Huang, S., Chen, G., and Ouyang, G. (2022). Confining enzymes in porous organic frameworks: from synthetic strategy and characterization to healthcare applications. *Chem. Soc. Rev.* 51, 6824–6863. doi: 10.1039/D1CS01011E

Ibrahim, M. S., Balhaddad, A. A., Garcia, I. M., Collares, F. M., Weir, M. D., Xu, H. H. K., et al. (2020). pH-responsive calcium and phosphate-ion releasing antibacterial sealants on carious enamel lesions in *vitro*. *J. Dent.* 97, 103323. doi: 10.1016/j.jdent.2020.103323

Jiang, T., Su, W., Li, Y., Jiang, M., Zhang, Y., Xian, C. J., et al. (2023). Research progress on nanomaterials for tissue engineering in oral diseases. *J. Funct. Biomater* 14 (8), 404. doi: 10.3390/jfb14080404

Jiao, Y., Tay, F. R., Niu, L. N., and Chen, J. H. (2019). Advancing antimicrobial strategies for managing oral biofilm infections. *Int. J. Oral. Sci.* 11, 28. doi: 10.1038/s41368-019-0062-1

Jowkar, Z., Askarzadeh, S., Hamidi, S. A., Fattah, Z., and Moaddeli, A. (2025). Assessment of the antimicrobial properties of mesoporous zinc oxide nanoparticles against streptococcus mutans: an *in vitro* investigation. *Int. J. Dentistry* 2025, 4438269. doi: 10.1155/ijod/4438269

Kelić, M., Kilić, D., Kelić, K., Šutej, I., Par, M., Peroš, K., et al. (2023). The fluoride ion release from ion-releasing dental materials after surface loading by topical treatment with sodium fluoride gel. *J. Funct. Biomater* 14(2), 102. doi: 10.3390/jfb14020102

Khan, I., Saeed, K., and Khan, I. (2019). Nanoparticles: Properties, applications and toxicities. *Arabian J. Chem.* 12, 908–931. doi: 10.1016/j.arabjc.2017.05.011

Kim, B. C., Jeong, E., Kim, E., and Hong, S. W. (2019). Bio-organic–inorganic hybrid photocatalyst, TiO2 and glucose oxidase composite for enhancing antibacterial performance in aqueous environments. *Appl. Catalysis B: Environ.* 242, 194–201. doi: 10.1016/j.apcatb.2018.09.102

Kwon, T., Kumari, N., Kumar, A., Lim, J., Son, C. Y., and Lee, I. S. (2021). Au/pt-egg-in-nest nanomotor for glucose-powered catalytic motion and enhanced molecular transport to living cells. *Angew Chem. Int. Ed Engl.* 60, 17579–17586. doi: 10.1002/anie.202103827

Li, K., Chen, C., Chen, C., Wang, Y., Wei, Z., Pan, W., et al. (2015). Magnetosomes extracted from Magnetospirillum magneticum strain AMB-1 showed enhanced peroxidase-like activity under visible-light irradiation. *Enzyme Microb. Technol.* 72, 72–78. doi: 10.1016/j.enzmictec.2015.02.009

Li, R., Landfester, K., and Ferguson, C. T. J. (2022). Temperature- and pH-responsive polymeric photocatalysts for enhanced control and recovery. *Angew Chem. Int. Ed Engl.* 61, e202211132. doi: 10.1002/anie.202211132

Li, S., Li, Q., Zhang, H., Li, F., Hu, J., Qian, J., et al. (2024). Dental caries management with antibacterial silver-doped pRussian blue hydrogel by the combined effects of photothermal response and ion discharge. *ACS Appl. Mater Interfaces* 16, 28172–28183. doi: 10.1021/acsami.4c04302

Li, F., Wang, P., Weir, M. D., Fouad, A. F., and Xu, H. H. (2014). Evaluation of antibacterial and remineralizing nanocomposite and adhesive in rat tooth cavity model. *Acta Biomater* 10, 2804–2813. doi: 10.1016/j.actbio.2014.02.033

Liang, K., Wang, S., Tao, S., Xiao, S., Zhou, H., Wang, P., et al. (2019). Dental remineralization via poly(amido amine) and restorative materials containing calcium phosphate nanoparticles. *Int. J. Oral. Sci.* 11, 15. doi: 10.1038/s41368-019-0048-z

Liu, Y., Huang, Y., Kim, D., Ren, Z., Oh, M. J., Cormode, D. P., et al. (2021). Ferumoxytol nanoparticles target biofilms causing tooth decay in the human mouth. *Nano Lett.* 21, 9442–9449. doi: 10.1021/acs.nanolett.1c02702

Liu, Y., Kohno, T., Tsuboi, R., Kitagawa, H., and Imazato, S. (2020). Acidity-induced release of zinc ion from BioUnion(TM) filler and its inhibitory effects against Streptococcus mutans. *Dent. Mater J.* 39, 547–553. doi: 10.4012/dmj.2019-061

Liu, Y., Naha, P. C., Hwang, G., Kim, D., Huang, Y., Simon-Soro, A., et al. (2018b). Topical ferumoxytol nanoparticles disrupt biofilms and prevent tooth decay *in vivo* via intrinsic catalytic activity. *Nat. Commun.* 9, 2920. doi: 10.1038/s41467-018-05342-x

Liu, H. Y., Prentice, E. L., and Webber, M. A. (2024). Mechanisms of antimicrobial resistance in biofilms. *NPJ Antimicrob. Resist.* 2, 27. doi: 10.1038/s44259-024-00046-3

Liu, Y., Zhang, L., Niu, L. N., Yu, T., Xu, H. H. K., Weir, M. D., et al. (2018a). Antibacterial and remineralizing orthodontic adhesive containing quaternary ammonium resin monomer and amorphous calcium phosphate nanoparticles. *J. Dent.* 72, 53–63. doi: 10.1016/j.jdent.2018.03.004

Lykourinou, V., Chen, Y., Wang, X. S., Meng, L., Hoang, T., Ming, L. J., et al. (2011). Immobilization of MP-11 into a mesoporous metal-organic framework, MP-11@mesoMOF: a new platform for enzymatic catalysis. *J. Am. Chem. Soc.* 133, 10382–10385. doi: 10.1021/ja2038003

Ma, L., Zheng, J. J., Zhou, N., Zhang, R., Fang, L., Yang, Y., et al. (2024). A natural biogenic nanozyme for scavenging superoxide radicals. *Nat. Commun.* 15, 233. doi: 10.1038/s41467-023-44463-w

Madhyastha, P. S., Naik, D. G., Natarajan, S., and Vinodhini, R. S. (2025). Influence of time interval, temperature, and storage condition on fluoride release and recharge from silorane-based restorative materials. *Dent. J. (Basel)* 13 (5), 197. doi: 10.3390/dj13050197

Meghwanshi, G. K., Kaur, N., Verma, S., Dabi, N. K., Vashishtha, A., Charan, P. D., et al. (2020). Enzymes for pharmaceutical and therapeutic applications. *Biotechnol. Appl. Biochem.* 67, 586–601. doi: 10.1002/bab.1919

Menezes-Silva, R., Velasco, S. R. M., BRESCIANi, E., Bastos, R. D. S., and Navarro, M. F. L. (2021). A prospective and randomized clinical trial evaluating the effectiveness of ART restorations with high-viscosity glass-ionomer cement versus conventional restorations with resin composite in Class II cavities of permanent teeth: two-year follow-up. *J. Appl. Oral. Sci.* 29, e20200609. doi: 10.1590/1678-7757-2020-0609

Meng, W., Huang, L., Guo, J., Xin, Q., Liu, J., and Hu, Y. (2024). Innovative nanomedicine delivery: targeting tumor microenvironment to defeat drug resistance. *Pharmaceutics* 16(12), 1549. doi: 10.3390/pharmaceutics16121549

Ming, J., Zhu, T., Yang, W., Shi, Y., Huang, D., Li, J., et al. (2020). Pd@Pt-GOx/HA as a novel enzymatic cascade nanoreactor for high-efficiency starving-enhanced chemodynamic cancer therapy. *ACS Appl. Mater Interfaces* 12, 51249–51262. doi: 10.1021/acsami.0c15211

Mokeem, L. S., Martini Garcia, I., Balhaddad, A. A., Lan, Y., Seifu, D., Weir, M. D., et al. (2024). Multifunctional dental adhesives formulated with silane-coated magnetic fe(3)O(4)@m-siO(2) core-shell particles to counteract adhesive interfacial breakdown. *ACS Appl. Mater Interfaces* 16, 2120–2139. doi: 10.1021/acsami.3c15157

Monjarás-Ávila, A. J., Hardan, L., Cuevas-Suárez, C. E., Alonso, N. V. Z., Fernández-Barrera, M., Moussa, C., et al. (2025). Systematic review and meta-analysis of remineralizing agents: outcomes on white spot lesions. *Bioengineering (Basel)* 12 (1), 93. doi: 10.3390/bioengineering12010093

Montoya, C., Roldan, L., Yu, M., Valliani, S., Ta, C., Yang, M., et al. (2023). Smart dental materials for antimicrobial applications. *Bioact Mater* 24, 1–19. doi: 10.1016/j.bioactmat.2022.12.002

Morawska-Wilk, A., Kensy, J., Kiryk, S., Kotela, A., Kiryk, J., Michalak, M., et al. (2025). Evaluation of factors influencing fluoride release from dental nanocomposite materials: A systematic review. *Nanomaterials (Basel)* 15 (9), 651. doi: 10.3390/nano15090651

Mu, Y., Wang, Y., Huang, L., Weng, Z., Zhong, T., Yu, S., et al. (2025). Yellow light and ultrasound Dual-responsive strontium-doped zinc oxide composites for dental caries prevention and remineralization. *Bioact Mater* 47, 403–416. doi: 10.1016/j.bioactmat.2025.01.029

Naha, P. C., Liu, Y., Hwang, G., Huang, Y., Gubara, S., Jonnakuti, V., et al. (2019). Dextran-coated iron oxide nanoparticles as biomimetic catalysts for localized and pH-activated biofilm disruption. *ACS Nano* 13, 4960–4971. doi: 10.1021/acsnano.8b08702

Nazemisalman, B., Niaz, S., Darvish, S., Notash, A., Ramazani, A., and Luchian, I. (2024). The antibacterial properties of a reinforced zinc oxide eugenol combined with cloisite 5A nanoclay: an *in-vitro* study. *J. Funct. Biomater* 15 (7), 198. doi: 10.3390/jfb15070198

Patil, P., Gupta, A., Kishlay, K., Rathaur, S., Vaidya, N., Sharma, M., et al. (2025). Comparative Evaluation of the Antimicrobial Efficacy of Endodontic Sealers Against Staphylococcus aureus and Streptococcus mutans: An *In Vitro* Study. *Cureus* 17, e80435. doi: 10.7759/cureus.80435

Pereira, C. A., Costa, A. C., Carreira, C. M., Junqueira, J. C., and Jorge, A. O. (2013). Photodynamic inactivation of Streptococcus mutans and Streptococcus sanguinis biofilms *in vitro*. *Lasers Med. Sci.* 28, 859–864. doi: 10.1007/s10103-012-1175-3

Piszko, P. J., Piszko, A., Kiryk, S., Kiryk, J., Kensy, J., Michalak, M., et al. (2025). Fluoride release from two commercially available dental fluoride gels-*in* vitro study. *Gels* 11(2), 135. doi: 10.3390/gels11020135

Puttipanampai, O., Panpisut, P., and Sitthisettapong, T. (2025). Assessment of fluoride-releasing materials in remineralization of adjacent demineralized enamel. *Appl. Sci.* 15 (4), 2077. doi: 10.3390/app15042077

Qi, J., Si, C., Liu, H., Li, H., Kong, C., Wang, Y., et al. (2025). Advances of metal-based nanomaterials in the prevention and treatment of oral infections. *Adv. Healthc Mater* 14, e2500416. doi: 10.1002/adhm.202500416

Rodríguez-Gómez, F. D., Monferrer, D., Penon, O., and Rivera-Gil, P. (2025). Regulatory pathways and guidelines for nanotechnology-enabled health products: a comparative review of EU and US frameworks. *Front. Med. (Lausanne)* 12, 1544393. doi: 10.3389/fmed.2025.1544393

Rostami, A., Molabashi, V., Ganji, S., Moosavi, S. P., Koushki, A., Fathi-Karkan, S., et al. (2025). Chlorhexidine loaded nanomaterials for dental plaque control: enhanced antibacterial activity and biocompatibility. *BioMed. Microdevices* 27, 28. doi: 10.1007/s10544-025-00755-0

Sahli, C., Moya, S. E., Lomas, J. S., Gravier-Pelletier, C., Briandet, R., and Hémadi, M. (2022). Recent advances in nanotechnology for eradicating bacterial biofilm. *Theranostics* 12, 2383–2405. doi: 10.7150/thno.67296

Sajithkumar, A., Shenoy, M., Vinod, K. R., and Nadakkavukkaran, D. (2025). Nanotechnology applications in oral pathology: A scoping review. *J. Oral. Maxillofac. Pathol.* 29, 127–136. doi: 10.4103/jomfp.jomfp_187_24

Sales-Junior, R. A., de Bessa, M. S., Oliveira, F. J. D., Barbosa, B. F. S., Santos, K. S., Owen, M., et al. (2025). Multifaceted characterization of antibacterial resin composites: A scoping review on efficacy, properties, and *in vivo* performance. *Jpn Dent. Sci. Rev.* 61, 112–137. doi: 10.1016/j.jdsr.2025.05.003

Sangha, J. S., Barrett, P., Curtis, T. P., Métris, A., Jakubovics, N. S., and Ofiteru, I. D. (2024). Effects of glucose and lactate on Streptococcus mutans abundance in a novel multispecies oral biofilm model. *Microbiol. Spectr.* 12, e0371323. doi: 10.1128/spectrum.03713-23

Schwendicke, F., Walsh, T., Lamont, T., Al-Yaseen, W., Bjørndal, L., Clarkson, J. E., et al. (2021). Interventions for treating cavitated or dentine carious lesions. *Cochrane Database Syst. Rev.* 7, Cd013039. doi: 10.1002/14651858.CD013039.pub2

Senol, G., Kirakli, C., and Halilçolar, H. (2007). *In vitro* antibacterial activities of oral care products against ventilator-associated pneumonia pathogens. *Am. J. Infect. Control* 35, 531–535. doi: 10.1016/j.ajic.2006.10.016

Sereda, G., Ahammadullah, A., Wijewantha, N., and Solano, Y. A. (2023). Acid-triggered release of eugenol and fluoride by desensitizing macro- and nanoparticles. *J. Funct. Biomater* 14 (1), 42. doi: 10.3390/jfb14010042

Sileika, T. S., Barrett, D. G., Zhang, R., Lau, K. H., and Messersmith, P. B. (2013). Colorless multifunctional coatings inspired by polyphenols found in tea, chocolate, and wine. *Angew Chem. Int. Ed Engl.* 52, 10766–10770. doi: 10.1002/anie.201304922

Sivakumar, I., Arunachalam, K. S., Sajjan, S., Ramaraju, A. V., Rao, B., and Kamaraj, B. (2014). Incorporation of antimicrobial macromolecules in acrylic denture base resins: a research composition and update. *J. Prosthodont* 23, 284–290. doi: 10.1111/jopr.12105

Sowmya, R., Karthick Raja Namasivayam, S., and Krithika Shree, S. (2024). A critical review on nano-selenium based materials: synthesis, biomedicine applications and biocompatibility assessment. *J. Inorganic Organometallic Polymers Materials* 34, 3037–3055. doi: 10.1007/s10904-023-02959-4

Springsteen, G., and Wang, B. (2002). A detailed examination of boronic acid–diol complexation. *Tetrahedron* 58, 5291–5300. doi: 10.1016/S0040-4020(02)00489-1

Tapponi, S., Yusuf, A., Alsaafin, F., and Hussain, Z. (2025). Breaking barriers with pH-responsive nanocarriers: a new frontier in precision oncology. *Int. J. Pharm.* 682, 125931. doi: 10.1016/j.ijpharm.2025.125931

Venkataiah, V. S., Krithikadatta, J., Teja, K. V., Mehta, D., and Doble, M. (2025). Ion release dynamics of bioactive resin cement under variable pH conditions. *Front. Oral. Health* 6, 1564838. doi: 10.3389/froh.2025.1564838

Vilela, A., Ferreira, L., Biscaia, P., da Silva, K., Beltrame, F., Camargo, G., et al. (2023). Preparation, characterization and stability study of eugenol-loaded eudragit RS100 nanocapsules for dental sensitivity reduction. *Braz. Arch. Biol. Technol.* 66. doi: 10.1590/1678-4324-ssbfar-2023230300

Wang, T., Dong, D., Chen, T., Zhu, J., Wang, S., Wen, W., et al. (2022). Acidity-responsive cascade nanoreactor based on metal-nanozyme and glucose oxidase combination for starving and photothermal-enhanced chemodynamic antibacterial therapy. *Chem. Eng. J.* 446, 137172. doi: 10.1016/j.cej.2022.137172

Wang, J., Li, L., Hu, X., Zhou, L., and Hu, J. (2024). pH-responsive on-demand release of eugenol from metal-organic frameworks for synergistic bacterial killing. *Dalton Trans.* 53, 2826–2832. doi: 10.1039/D3DT04216B

Wang, Y., Liu, C., Ren, Y., Song, J., Fan, K., Gao, L., et al. (2024). Nanomaterial-based strategies for attenuating T-cell-mediated immunodepression in stroke patients: advancing research perspectives. *Int. J. Nanomedicine* 19, 5793–5812. doi: 10.2147/IJN.S456632

Wang, K., Wang, S., Yin, J., Yang, Q., Yu, Y., and Chen, L. (2023). Long-term application of silver nanoparticles in dental restoration materials: potential toxic injury to the CNS. *J. Mater Sci. Mater Med.* 34, 52. doi: 10.1007/s10856-023-06753-z

Wendler, M., Stenger, A., Ripper, J., Priewich, E., Belli, R., and Lohbauer, U. (2021). Mechanical degradation of contemporary CAD/CAM resin composite materials after water ageing. *Dent. Mater* 37, 1156–1167. doi: 10.1016/j.dental.2021.04.002

Wu, J., Weir, M. D., Melo, M. A., and Xu, H. H. (2015). Development of novel self-healing and antibacterial dental composite containing calcium phosphate nanoparticles. *J. Dent.* 43, 317–326. doi: 10.1016/j.jdent.2015.01.009

Wu, J., Xie, X., Zhou, H., Tay, F. R., Weir, M. D., Melo, M. A. S., et al. (2019). Development of a new class of self-healing and therapeutic dental resins. *Polymer Degradation Stability* 163, 87–99. doi: 10.1016/j.polymdegradstab.2019.02.024

Xia, Y., Yang, L., Xu, S., Xia, Y., Peng, L., Wu, Y., et al. (2025). Trapping effect of surface deficient cocrystal synergizes with bimetallic nanoparticles against bacterial infection in wounds. *J. Colloid Interface Sci.* 695, 137805. doi: 10.1016/j.jcis.2025.137805

Xiu, Z. M., Ma, J., and Alvarez, P. J. (2011). Differential effect of common ligands and molecular oxygen on antimicrobial activity of silver nanoparticles versus silver ions. *Environ. Sci. Technol.* 45, 9003–9008. doi: 10.1021/es201918f

Xu, Y., You, Y., Yi, L., Wu, X., Zhao, Y., Yu, J., et al. (2023). Dental plaque-inspired versatile nanosystem for caries prevention and tooth restoration. *Bioact Mater* 20, 418–433. doi: 10.1016/j.bioactmat.2022.06.010

Xue, J., Wang, J., Feng, D., Huang, H., and Wang, M. (2020). Application of antimicrobial polymers in the development of dental resin composite. *Molecules* 25 (20), 4738. doi: 10.3390/molecules25204738

Yamauchi, M., Nigauri, A., Yamamoto, K., Nakazato, G., Kawano, J., and Kimura, K. (1989). Antibacterial actions of denture base resin on oral bacteria. *Nihon Hotetsu Shika Gakkai Zasshi* 33, 571–576. doi: 10.2186/jjps.33.571

Yang, H., Niu, S., Guo, M., and Xue, Y. (2024). Molecular mechanisms of silver nanoparticle-induced neurotoxic injury and new perspectives for its neurotoxicity studies: A critical review. *Environ. pollut.* 362, 124934. doi: 10.1016/j.envpol.2024.124934

Yi, J., Weir, M. D., Melo, M. A. S., Li, T., Lynch, C. D., Oates, T. W., et al. (2019). Novel rechargeable nano-CaF(2) orthodontic cement with high levels of long-term fluoride release. *J. Dent.* 90, 103214. doi: 10.1016/j.jdent.2019.103214

Yuan, H., Bai, H., Liu, L., Lv, F., and Wang, S. (2015). A glucose-powered antimicrobial system using organic-inorganic assembled network materials. *Chem. Commun. (Camb)* 51, 722–724. doi: 10.1039/C4CC07533A

Zhang, N., Chen, C., Melo, M. A., Bai, Y. X., Cheng, L., and Xu, H. H. (2015). A novel protein-repellent dental composite containing 2-methacryloyloxyethyl phosphorylcholine. *Int. J. Oral. Sci.* 7, 103–109. doi: 10.1038/ijos.2014.77

Zhang, Y., Jiang, Z. T., Wang, Y., Wang, H. Y., Hong, S., Li, W., et al. (2024). A supramolecular nanoformulation with adaptive photothermal/photodynamic transformation for preventing dental caries. *ACS Nano* 18, 27340–27357. doi: 10.1021/acsnano.4c06051

Zhang, Q., Ma, Q., Wang, Y., Wu, H., and Zou, J. (2021). Molecular mechanisms of inhibiting glucosyltransferases for biofilm formation in Streptococcus mutans. *Int. J. Oral. Sci.* 13, 30. doi: 10.1038/s41368-021-00137-1

Zhang, Y., Tsitkov, S., and Hess, H. (2018). Complex dynamics in a two-enzyme reaction network with substrate competition. *Nat. Catalysis* 1, 276–281. doi: 10.1038/s41929-018-0053-1

Zhang, J., Yang, Y., Chen, Y., Chen, X., Li, A., Wang, J., et al. (2024). A review of new generation of dental restorative resin composites with antibacterial, remineralizing and self-healing capabilities. *Discov. Nano* 19, 189. doi: 10.1186/s11671-024-04151-0

Zhao, A., Sun, J., and Liu, Y. (2023). Understanding bacterial biofilms: From definition to treatment strategies. *Front. Cell Infect. Microbiol.* 13, 1137947. doi: 10.3389/fcimb.2023.1137947

Zhou, W., Peng, X., Zhou, X., Bonavente, A., Weir, M. D., Melo, M. A. S., et al. (2020). Novel nanocomposite inhibiting caries at the enamel restoration margins in an *in vitro* saliva-derived biofilm secondary caries model. *Int. J. Mol. Sci.* 21(17), 6369. doi: 10.3390/ijms21176369

Zhu, X., Guo, J., Yang, Y., and Liu, J. (2023). Macrophage polarization induced by bacteria-responsive antibiotic-loaded nanozymes for multidrug resistance-bacterial infections management. *Small* 19, e2204928. doi: 10.1002/smll.202204928

Zhu, J., He, L., Xu, X., Wu, H., Li, J., Yan, B., et al. (2025). Bioheterojunctions prevent tooth caries via cascade antibacterial strategy. *J. Dent. Res.* 104, 1095–1104. doi: 10.1177/00220345251329334

frontiers | Frontiers in Cellular and Infection Microbiology

TYPE Original Research
PUBLISHED 14 October 2025
DOI 10.3389/fcimb.2025.1633342

OPEN ACCESS

EDITED BY
Keke Zhang,
Wenzhou Medical University, China

REVIEWED BY
Zhenting Xiang,
Temple University, United States
Megan L. Falsetta,
University of Rochester, United States

*CORRESPONDENCE
Yan-song Ma
mayansong0911@126.com
Yu-xing Bai
byuxing@ccmu.edu.cn

RECEIVED 22 May 2025
ACCEPTED 29 September 2025
PUBLISHED 14 October 2025

CITATION
Gao H-y, Yang H, Wang H-m, Li H-m, Ma Y-s and Bai Y-x (2025) Arginine inhibits cross-kingdom interactions and synergistic cariogenicity between *Streptococcus mutans* and *Candida albicans*. *Front. Cell. Infect. Microbiol.* 15:1633342. doi: 10.3389/fcimb.2025.1633342

Arginine inhibits cross-kingdom interactions and synergistic cariogenicity between *Streptococcus mutans* and *Candida albicans*

Hong-yu Gao, Hao Yang, Hong-mei Wang, Hao-ming Li, Yan-song Ma* and Yu-xing Bai*

Department of Orthodontics, Beijing Stomatological Hospital, Capital Medical University, Beijing, China

Introduction: *Streptococcus mutans* and *Candida albicans* are common pathogenic organisms from the oral microbial community, and are associated with the pathogenesis of caries. We investigated the repressive effects of arginine on the cross-kingdom interactions and synergistic cariogenicity between *S. mutans* and *C. albicans*.

Methods: The effect of arginine on the growth of *S. mutans* and *C. albicans* in the planktonic state was reflected by analyzing growth curves and pH measurements. Biofilm biomass was measured using growth curves, crystal violet staining, and colony-forming unit measurements; fluorescence *in situ* hybridization indicated the physical relationship between *S. mutans* and *C. albicans* in biofilms. The cariogenic properties of dual-species biofilms were analyzed through extracellular polysaccharide and lactic acid production assessments.

Results: Arginine inhibited the planktonic growth and biofilm formation of *S. mutans* and *C. albicans*, with reduced biofilm formation, biomass, and physical adhesion between strains. Moreover, arginine suppressed the production of extracellular polysaccharides and lactic acid. In addition, short-term arginine treatment effectively inhibited the growth of *S. mutans* and *C. albicans*.

Conclusion: L-Arginine inhibited both mono- and dual-species growth of *S. mutans* and *C. albicans*. Thus, L-arginine may serve as a novel approach to inhibit the cross-kingdom interactions and synergistic cariogenicity of *S. mutans* and *C. albicans*.

KEYWORDS

***Streptococcus mutans*, *Candida albicans*, arginine, cariogenicity, cross-kingdom interaction**

1 Introduction

The most prevalent major oral disease is deciduous tooth caries, which is estimated to affect 43% of the world's population, followed by dental caries of permanent dentition, with an average global prevalence of 29%, according to the World Health Organization (Cherian et al., 2023). Untreated dental caries affects masticatory function, speech, smile characteristics, and psychology, as well as quality of life. Plaque attached to the tooth surface is the main biological factor leading to dental caries. Numerous cariogenic bacteria, including *Streptococcus mutans*, *Actinomyces gerencseriae*, *Propionibacterium acidifaciens*, and *Scardovia wiggsiae*, have been identified in recent studies, revealing multiple observed synergistic interactions (Jenkinson, 2011; Pang et al., 2021).

In recent years, fungi, particularly *Candida albicans*, have garnered attention for their cariogenic potential. Recent studies have proposed that *C. albicans* is also involved in the formation of caries and that *S. mutans* and *C. albicans* have a synergistic cariogenic effect. *S. mutans* and *C. albicans* co-exist in high enrichment and have been co-detected in a variety of oral disease models, such as early childhood caries (Xiao et al., 2018; Lu et al., 2023), root caries (Du et al., 2021), white spot lesions (Klaus et al., 2016; Beerens et al., 2017; Yang et al., 2023), and denture stomatitis (Baena-Monroy et al., 2005; Clemente et al., 2023). Research has demonstrated that cross-kingdom interactions between cariogenic bacteria and fungi enhance the formation of cariogenic biofilms (Koo et al., 2018; Wan et al., 2021). The synergistic pathogenicity of *S. mutans* and *C. albicans* is manifested in physical adhesion, metabolic promotion, acid production, and cross-feeding (Du et al., 2022; Li et al., 2023). *S. mutans* and *C. albicans* utilize sucrose to synthesize exopolysaccharides and produce massive cross-kingdom biofilms. Moreover, their symbiotic effects promote carbohydrate metabolism and upregulate the expression of virulence genes, increasing the biomass of, enhancing the active metabolism in, decreasing the pH of, and increasing the cariogenicity of the dual-species biofilm of *S. mutans* and *C. albicans* (He et al., 2017; Xiao et al., 2023).

Approaches to inhibit cross-kingdom interactions between *S. mutans* and *C. albicans* may be important in preventing dental caries. In most clinical treatments for infections caused by microorganisms, antibiotics or antifungal drugs are used; however, resistance and dysbiosis caused by broad-spectrum antimicrobial drugs limit their use in the treatment of biofilm-associated infections. The development of biofilm-targeted therapeutic strategies to disrupt the growth of polymicrobial biofilms is urgently needed to combat oral diseases and maintain oral health; many approaches, such as natural compounds, chemical compounds, nanomaterials, and photodynamic therapy, have been investigated in this regard (Li et al., 2023; Philip et al., 2018).

One category of natural products that has become a focus of interest is probiotics and prebiotics. Prebiotics are defined as substrates that are selectively utilized by host microorganisms, conferring a health benefit (Gibson et al., 2017). Arginine is a semi-essential amino acid that plays a role in protein synthesis, substance metabolism, immune regulation, anti-inflammatory and antioxidant activities, and various signaling pathways (Wei et al., 2023). Arginine, considered an oral prebiotic, is mainly derived from diet and host saliva and catabolized and metabolized by bacteria via the arginine deiminase system, producing ammonia as a major product. The protonation of ammonia to ammonium increases the pH, which creates a less cariogenic environment (Kuriki et al., 2021).

Arginine is widely reported to inhibit the growth of *S. mutans*, indicating its inhibitory role in the development of caries by affecting the microbiome of the oral microenvironment (Huang et al., 2017). At present, studies on the effect of arginine on *C. albicans* are limited and inconclusive. To the best of our knowledge, no study has investigated whether arginine inhibits the synergistic cariogenic effects of *C. albicans* and *S. mutans*.

In this study, we aimed to investigate whether arginine exerts an inhibitory effect on the growth of *S. mutans* and *C. albicans*, with the expectation of finding new preventive and therapeutic options for inhibiting their synergistic cariogenicity. We proposed the following null hypotheses: 1. Arginine does not inhibit the growth of *S. mutans* and *C. albicans* in single cultures; 2. Arginine does not inhibit the co-culture growth of *S. mutans* and *C. albicans*; and 3. Arginine does not inhibit the synergistic cariogenic effects of *S. mutans* and *C. albicans*.

2 Materials and methods

2.1 Strains and growth conditions

Standard wild-type *S. mutans* UA159 and *C. albicans* SC5314, inoculated from frozen glycerol stocks, were used in all experiments. *Streptococcus mutans* strains were cultivated in brain heart infusion (BHI) broth, and *C. albicans* strains were cultivated in yeast peptone dextrose (YPD) broth at 37°C under aerobic conditions with 5% CO_2 overnight (without shaking). Cells were grown to the mid-exponential phase and harvested by centrifugation (5000 rpm, 5 min, 4°C). *S. mutans* and *C. albicans* were inoculated into BHI broth supplemented with a 1% (w/v) sucrose (BHI-S), with or without 100 mM L-arginine at the concentration for which the optical density of the suspensions at 600 nm (OD_{600nm}) reached 0.005 for the subsequent experiments. BHI-S medium was autoclaved and the required amount of L-arginine (0.1742 g per 10 mL) was added aseptically to achieve a final concentration of 100 mM. The solution was then vortexed until fully dissolved, after which it was sterilized by passing it through a 0.22 μm membrane filter. The experiments were performed in triplicate.

2.2 Effects of arginine on planktonic cultures of *S. mutans* and *C. albicans*

2.2.1 Growth curves

Planktonic growth of *S. mutans* and *C. albicans* co-cultures and monocultures, with or without arginine, was monitored at 4, 6, 8,

10, 12, 14, 16, 20, 22, and 24 h based on the optical density of the culture supernatant. By measuring the optical density at 600 nm (OD_{600nm}) using a diluphotometer (Implen, Munich, Germany), microbial growth analysis was performed. The microbial culture was shaken well and added to the cuvette in a volume of 2 mL, whereas a cuvette containing 2 mL of BHI-S was used as a blank control. For microbial cultures at later stages of growth, we measured absorbance by adding a volume of 200 µL culture to 1800 µL phosphate-buffered saline (PBS) and diluting it 10-fold. The control consisted of an equal volume of BHI-S broth as the measured sample, and the total volume was brought to 2 ml with PBS. Growth curves were then plotted to assess the effect of arginine on growth.

2.2.2 pH test

Changes in the pH of the supernatant during incubation can reflect the degree of acid production by both microorganisms and the effect of arginine. A pH meter (Orion 868, Thermo Fisher Scientific, Waltham, MA, USA) was used to measure the pH of the supernatants obtained from *S. mutans*, *C. albicans*, and dual-species cultures in the planktonic state after incubation for 4, 6, 8, 12, 20, and 24 h.

2.3 Effect of arginine on biofilm growth and cariogenicity of *S. mutans* and *C. albicans*

Biofilm growth was monitored based on the analyses of the absorbance of the cultures, crystal violet (CV) staining, colony-forming units (CFUs), and lactic acid production. Equal volumes of the suspensions of each strain were inoculated into the wells of 24-well microtiter plates (1 mL each) and 96-well microtiter plates (100 µL each). The plates were incubated at 37°C in the presence of 5% CO_2.

2.3.1 Growth curve

Biofilm growth curves were measured using 96-well plates. Growth curves were constructed by measuring OD_{600nm} using a multimode microplate reader (SpectraMax iD3, Molecular Devices, San Jose, CA, USA). The kinetic data were acquired by programming the microplate reader to automatically record the optical density at one-hour intervals. These values were then plotted as a line graph.

2.3.2 Crystal violet staining

Biofilm biomass, formed in the presence or absence of arginine, was evaluated by CV staining after 4, 8, or 24 h of incubation. The biofilms were washed twice with PBS and stained with 0.1% (w/v) CV for 15 min. Thereafter, plates were washed twice with PBS to remove the unbound stain and dissolved in 600 µL of 100% ethanol for 30 min. The biofilm concentration was determined by measuring the optical density of the samples at 570 nm (OD_{570nm}) (Liu et al., 2022).

2.3.3 CFU measurement

After incubation for 4, 8, and 24 h, the biofilms of *S. mutans* and *C. albicans* in single- and dual-species cultures were analyzed to determine the CFU/mL of each strain. At each time point, biofilms were washed twice with PBS, were disrupted by sonication and then harvested, serially diluted, and plated on YPD agar supplemented with kanamycin and streptomycin (to culture *C. albicans* while inhibiting the growth of *S. mutans*) and BHI agar supplemented with amphotericin B (to culture *S. mutans* while inhibiting the growth of *C. albicans*). Plates were incubated at 37°C with 5% CO_2 for 24 h, after which CFUs were counted.

2.3.4 Lactic acid production assay

Mature biofilms were cultured in buffered peptone water supplemented with 0.2% (w/v) sucrose at 37°C with 5% CO_2 for 3 h after rinsing with PBS. The concentrations of lactic acid produced by the biofilms were measured using an L-Lactic Acid Assay Kit (Nanjing Jiancheng, Nanjing, China) according to the manufacturer's instructions (Lu et al., 2022).

2.3.5 Exopolysaccharide production assay

Congo red (CR) staining was performed to evaluate the production of exopolysaccharides (EPS). After 24 h of incubation in 96-well plates, the biofilms were washed using PBS, and each well was stained with a mixture of 100 µL BHI-S and 50 µL Congo red (0.5 mM). After staining, the supernatants from each well were transferred to microtiter plates; the absorbance of the supernatants was measured at 490 nm in triplicate. Optical density values were used to measure EPS production as per the following formula: OD of EPS production = OD of blank control group supernatant CR– OD of experiment group supernatant (Kulshrestha et al., 2016).

2.3.6 Fluorescence *in situ* hybridization

S. mutans and *C. albicans* were inoculated into confocal Petri dishes containing BHI-S with or without 100 mM arginine at an initial concentration of OD_{600nm} = 0.005, and incubated for 4 h. Thereafter, samples were fixed with 4% paraformaldehyde, eluted twice using PBS solution, and dried at room temperature.

The solutions were prepared as required for the experiment. The hybridization solution comprised 20 mM trimethylolamine hydrochloride, 0.9 M NaCl, 0.01% sodium dodecyl sulfate, and 20% deionized formamide; the pH was 7.5 and the solution was stored at 4°C. The elution solution comprised 215 mM NaCl, 20 mM tris(hydroxymethyl)aminomethane, and 5 mM ethylene diaminetetraacetic acid; the pH was 7.5 and the solution was stored at room temperature. In addition, we prepared 20x SSC solution (3 M NaCl, 0.3 M sodium citrate), which was stored at room temperature.

The *S. mutans* fluorescent probe (ATTO488-5′-ACTCCAG ACTTTCCTGAC-3′, Ex 502 nm/Em 524 nm) and *C. albicans* fluorescent probe (TexasRed X-5′- GCCAAGGCTTATA CTCGCT-3′, Ex 596 nm/Em 615 nm) were diluted to 100 pmol/μL with enzyme-free sterile water and added to the prepared 100 μL hybridization solution so that the final concentration of each probe was 1 pmol/μL. After vortexing and oscillating for mixing, the hybridization solution containing fluorescent probes was evenly covered with the plaque and hybridized at 46°C for 3 h. The hybridized biofilm was placed in the elution solution and eluted at 48°C for 15 min. The biofilm was eluted at 37°C for 10 min using 0.1x SSC solution, and the process was repeated twice. After drying away from light, the plaques were sealed with an anti-fade sealer and stored in a dark box for subsequent imaging analysis.

Imaging analysis was performed using a Zeiss LSM 780 laser confocal scanning microscope, with a laser emission wavelength of 488 nm/561 nm, laser power of 2.0%, and an xy-axis image size of 1024 × 1024 pixels. The whole layer of the biofilm was captured along the Z-axis of the biofilm during the imaging process, with Z-axis layers swept at an interval of 1 μm. Three images were taken from each group of samples. The Imaris 10.2 (Bitplane, Switzerland) software was used to construct the 3D structure of the biofilm and perform post-image processing. The heights of the biofilm xz and yz planes were measured to compare the thickness of the biofilms in the experimental and control groups, and to compare the differences in interspecies distances between *S. mutans* and *C. albicans*, in order to assess the effect of arginine on the interspecies adhesion of *S. mutans* and *C. albicans*.

2.4 Short-term treatment of arginine on biofilm growth and cariogenicity of *S. mutans* and *C. albicans*

After 4 h of incubation without arginine, the medium was changed to BHI-S medium containing 100 mM arginine, followed by incubation for 10 min. After the treatment, the medium was again changed to the original one, and the incubation was continued. This was performed to evaluate the short-term effect of arginine after 24 h.

As described in sections 2.2 and 2.3, the change in the absorbance of the solutions was measured to evaluate the planktonic growth; we also performed CV staining and measurement of the CFU counts for all the biofilms.

2.5 Statistical analyses

Biofilm CV staining, biomass, thickness of the biofilm, interspecies distances, EPS production, and lactic acid production were analyzed using IBM SPSS 27.0 (IBM, Armonk, NY, USA). The Shapiro–Wilk test was used to determine whether the data were normally distributed. T-tests and one-way analysis of variance (ANOVA) were used for data conforming to the normal distribution, whereas Mann–Whitney U tests and Kruskal–Wallis tests were used otherwise. Statistical significance was set at values of $p < 0.05$.

3 Results

3.1 Arginine inhibited the planktonic growth of both *S. mutans* and *C. albicans*

Our results showed that *C. albicans* promoted the growth of *S. mutans* when co-cultured in the planktonic state, with a decrease in the pH of the supernatant. Absorbance value measurements of the bacterial broths after 24 h incubation showed that the addition of 100 mM arginine significantly inhibited the growth of both *S. mutans* and *C. albicans*, as well as the symbiotic growth of the dual-species culture in the planktonic state (Figures 1A–C).

The results of pH testing of the planktonic culture solution showed that *S. mutans* had a stronger acid-producing ability than did *C. albicans*, which may lower the pH below the demineralization threshold, and could lead to the emergence of enamel demineralization, corroborating the pathogenicity of *S. mutans* and the synergistic effect of *S. mutans* and *C. albicans* in caries. In the supernatants of *S. mutans* and *C. albicans* monocultures and their co-cultures (all in the planktonic state), the addition of arginine minimized the pH decrease and maintained the pH at a level above the demineralization threshold (Figures 1D–F).

This suggests that arginine may reduce the effect on enamel demineralization by reducing the acid-producing properties of *S. mutans* and *C. albicans*, and by maintaining a non-cariogenic alkaline environment.

3.2 Arginine inhibited the formation of both *S. mutans* and *C. albicans* biofilms

Our results demonstrated a symbiotic promotion of growth for *S. mutans* and *C. albicans* when co-cultured in the biofilm state. The presence of *C. albicans* enabled the growth of *S. mutans*, and the co-culture biofilms exhibited thicker and larger biomass. The biofilm growth curves of *S. mutans*, *C. albicans*, and dual-species cultures showed decreased biofilm formation rates in the presence of arginine in the growth medium, with growth curves ultimately showing a reduction in the biomass, a delay in the onset of the rapid growth phase, and a slowing of the growth rate. The inhibitory effect of arginine on the growth of *S. mutans* monoculture biofilms was the most pronounced, with essentially no growth (Figure 2A).

The CV staining and CFU counts of single-species and double-species biofilms were performed at three selected time points, namely the early 4 h incubation, the middle 8 h incubation, and the late stage 24 h incubation stages of growth. Moreover, CV staining showed that the addition of 100 mM arginine inhibited biofilm formation (Figures 2B–D).

The CFU counts of *S. mutans*, *C. albicans*, and dual-species biofilms observed after incubation for 4, 8, and 24 h were used to determine the effects of arginine on biofilm biomass. Our results

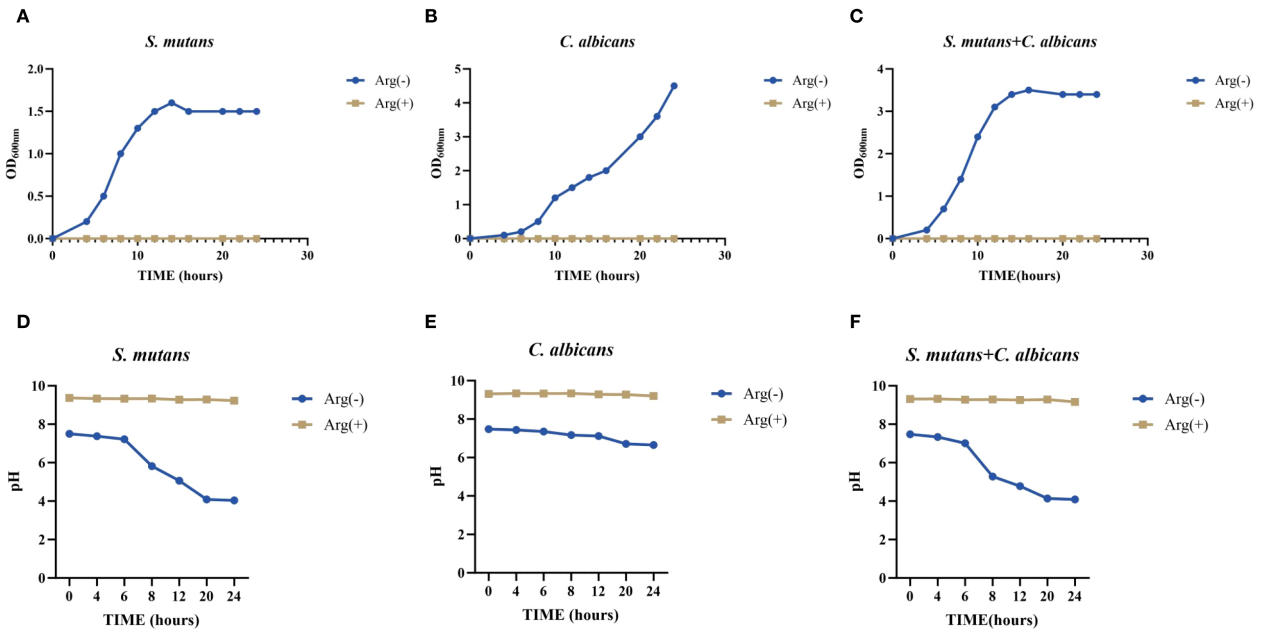

FIGURE 1
Planktonic growth curve and pH of *Streptococcus mutans* and *Candida albicans* in non-treated control group (0 mM arginine) and treated group (100 mM arginine). Planktonic growth curves of *S. mutans* **(A)**, *C. albicans* **(B)**, and dual-species **(C)** after incubation for 4, 6, 8, 10, 12, 14, 16, 20, 22, and 24 h Planktonic pH of *S. mutans* **(D)**, *C. albicans* **(E)**, and dual-species **(F)** after incubation for 4, 6, 8, 12, 20, and 24 h.

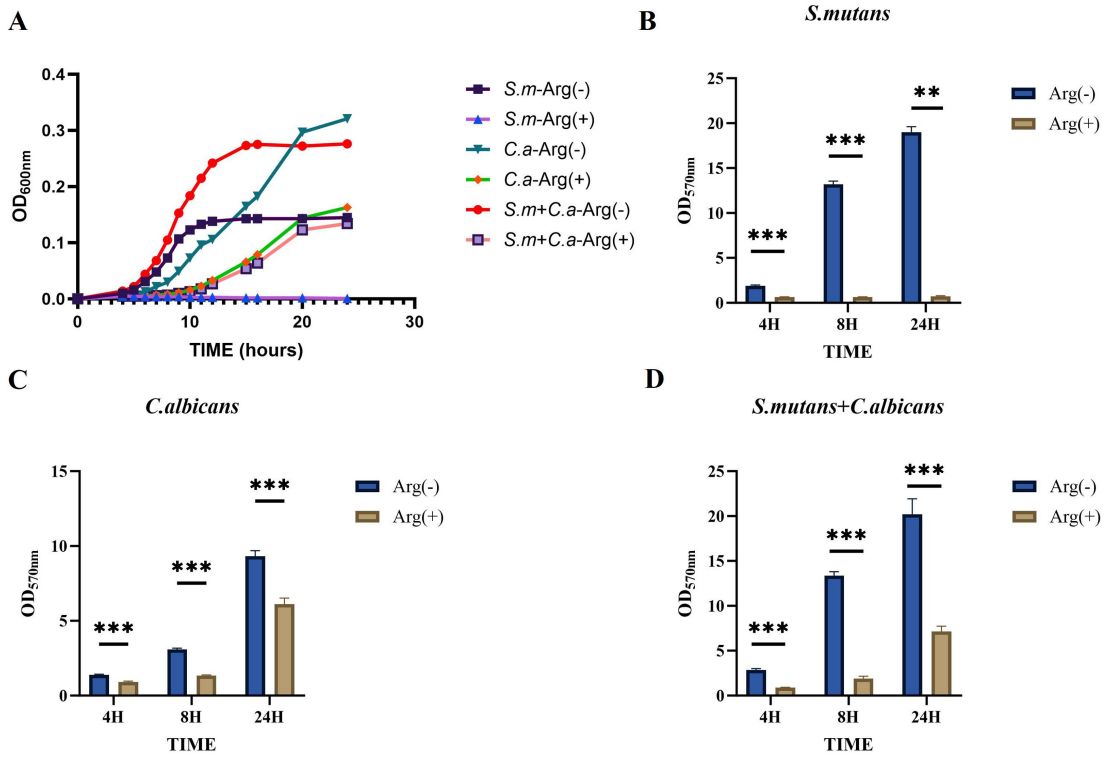

FIGURE 2
Biofilm growth of *Streptococcus mutans* and *Candida albicans* in non-treated control group (0 mM arginine) and treated group (100 mM arginine). Biofilm growth curves of *S. mutans*, *C. albicans*, and dual-species **(A)**. Biofilm mass determined by crystal violet staining of *S. mutans* **(B)**, *C. albicans* **(C)**, and dual-species **(D)**. Values are expressed as the mean and SD. Student's *t*-test and Mann–Whitney U tests were used to compare biomass between the control and experimental groups (*$p < 0.05$, **$p < 0.01$, and ***$p < 0.001$).

10.3389/fcimb.2025.1633342

showed that co-culture of *S. mutans* and *C. albicans* resulted in more colonies of *S. mutans* and *C. albicans* compared with the respective number of colonies in monoculture biofilms at the three assayed time points. Arginine reduced the counts of *S. mutans* and *C. albicans* in the biofilms. The counts of both *S. mutans* and *C. albicans* in the single-species biofilm were significantly lower than those of the two organisms in the dual-species co-culture biofilm (Figure 3). CFU counts of *S. mutans* and *C. albicans* were consistent with the previous results of biofilm CV staining, both of which demonstrated that the addition of arginine reduced the biofilm biomass of microorganisms, resulting in a reduction in biofilm production. Our results indicate that arginine may inhibit the formation of cariogenic biofilm by decreasing the biomass of biofilm, thereby achieving a caries-inhibiting effect.

FISH staining was performed on single- and dual-species biofilms of *S. mutans* and *C. albicans* after 4 h of incubation. Biofilms were observed using a confocal fluorescence microscope. Both monoculture (Figure 4) and dual-culture (Figure 5) biofilms of *S. mutans* and *C. albicans* showed a decrease in biomass after the addition of 100 mM arginine, and this result was in line with the trend of the results of biofilm CFU counting. Moreover, biofilm thicknesses were significantly decreased after the addition of 100 mM arginine. The reduction of both biomass and biofilm thickness indicated that arginine could inhibit biofilm formation (Figure 6). Simultaneously, the interspecies distance of *S. mutans* and *C. albicans* in the co-cultured biofilm increased after the addition of 100 mM arginine (Figure 7).

The biomass of *S. mutans* and *C. albicans* in the biofilm was reduced, the physical contact between the strains was sparse, and the biofilm became loosely packed. The synergistic cariogenic effect between *S. mutans* and *C. albicans* included their physical adhesion, and their close association contributed to the biomass accumulation of the co-cultured biofilm and stabilization of the biofilm structure, which may also be one of the ways that arginine inhibited the co-cultivated biofilm of *S. mutans* and *C. albicans*.

The metabolism of *S. mutans* for acid production from dietary sugars and the production of extracellular polysaccharides (EPSs) for biofilm generation are crucial indicators of its cariogenicity. The production of lactic acid and EPSs by co-cultured biofilm was increased compared with that observed in the *S. mutans* single-species biofilm, thus increasing in the cariogenicity of the co-cultured biofilm, in line with the synergistic cariogenic effects of *S. mutans* and *C. albicans* as reported in previous studies. *S. mutans* and dual-species biofilms exhibited higher lactic acid production than *C. albicans* biofilms. L-Arginine (100 mM) inhibited biofilm lactate production, substantially reducing levels compared with those observed without arginine (Figure 8A). The addition of arginine decreased the level of EPSs produced, leading to the suppression of biofilm formation. This finding was consistent with the biofilm CV staining results, suggesting that arginine had an inhibitory effect on the cariogenicity of the co-cultured biofilms (Figure 8B).

In summary, the addition of arginine to the culture medium inhibited the formation of *S. mutans* and *C. albicans* single- and

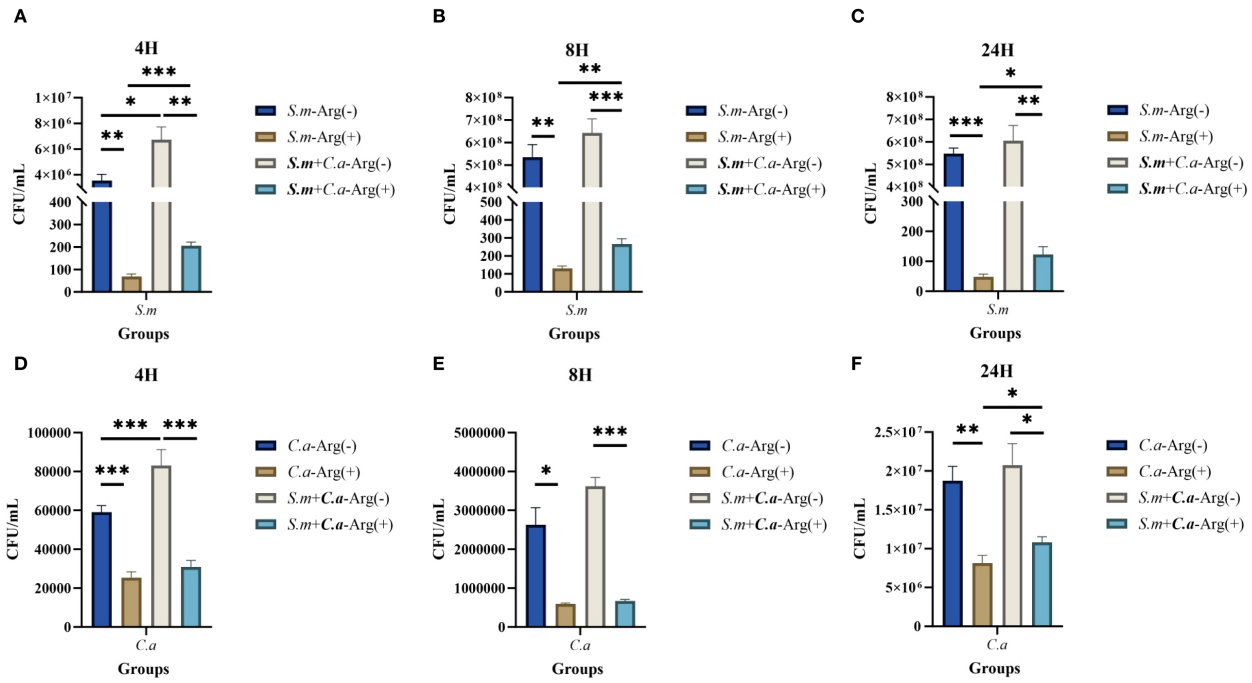

FIGURE 3
Colony forming units (CFUs) of single- and dual-species biofilms. Mean and SD of CFU/mL of *Streptococcus mutans* after incubation for 4 **(A)**, 8 **(B)**, and 24 **(C)** h and *Candida albicans* after incubation for 4 **(D)**, 8 **(E)**, and 24 **(F)** h in single- and dual-species biofilm viable cells obtained for the control group (0 mM arginine) and treated group (100 mM arginine). One-way ANOVA and Kruskal–Wallis tests were used to compare the control and experimental groups (*$p < 0.05$, **$p < 0.01$, and ***$p < 0.001$).

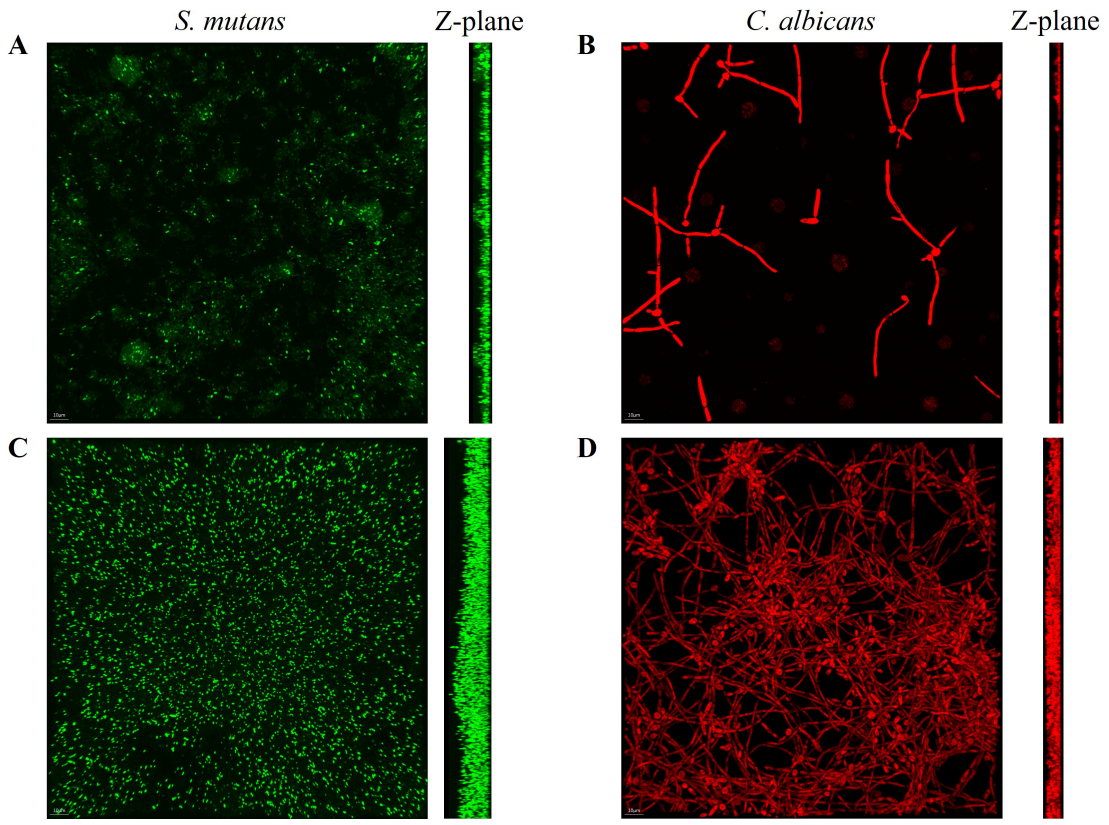

FIGURE 4
Fluorescence *in situ* hybridization staining images of biofilms of *Streptococcus mutans* biofilms in the experimental group **(A)** and control group **(C)**, and *Candida albicans* biofilms in the experimental group **(B)** and control group **(D)** after 4 h of incubation, with the Z-plane denoting biofilm thickness.

dual-species biofilms, resulting in the suppression of biofilm formation and a decrease in biofilm biomass, as well as the production of extracellular polysaccharides and lactic acid within the biofilms.

3.3 Short-term arginine treatment inhibited the growth of both *S. mutans* and *C. albicans*

We treated *S. mutans* and *C. albicans* with 100 mM arginine for 10 min after 4 h of incubation. Short-term treatment with arginine similarly inhibited the planktonic and biofilm growth of both single- and dual-species cultures but was not as effective as the long-term treatment of adding arginine to the culture medium. These results suggest that arginine inhibits the planktonic growth of *S. mutans*, *C. albicans*, and the dual-species culture (Figure 9A). Biofilm CV staining and analysis of the CFU counts (Figures 9B–D) demonstrated that short-term treatment of biofilms with arginine also reduced biofilm formation, resulting in a decrease in biofilm biomass. However, some of these results demonstrated no statistically significant differences.

4 Discussion

In the present study, we demonstrated the potential of arginine as a prebiotic agent that may serve as a novel caries control measure by exerting inhibitory effects on cavity-causing microorganisms. Our results showed that the use of arginine as a prebiotic inhibited both mono- and dual-species growth of *S. mutans* and *C. albicans* and reduced the production of EPSs and lactic acid in biofilms. Thus, our null hypothesis that arginine does not affect the growth and synergistic cariogenic effects of *S. mutans* and *C. albicans* is rejected.

S. mutans and *C. albicans* have been shown to co-exist in several models of oral diseases, especially caries, and are important in disease development. Although fluoride is a known standard of care for the prevention of caries, its effects on oral biofilms are limited (Dang et al., 2016). The use of broad-spectrum antimicrobials, such as chlorhexidine, may alter the composition of the oral flora by non-selectively destroying bacteria and allowing antimicrobial-resistant bacteria to flourish. Given the synergistic cariogenic effects between *S. mutans* and *C. albicans*, approaches targeting microorganisms or cross-kingdom interactions may be effective in treating or preventing caries.

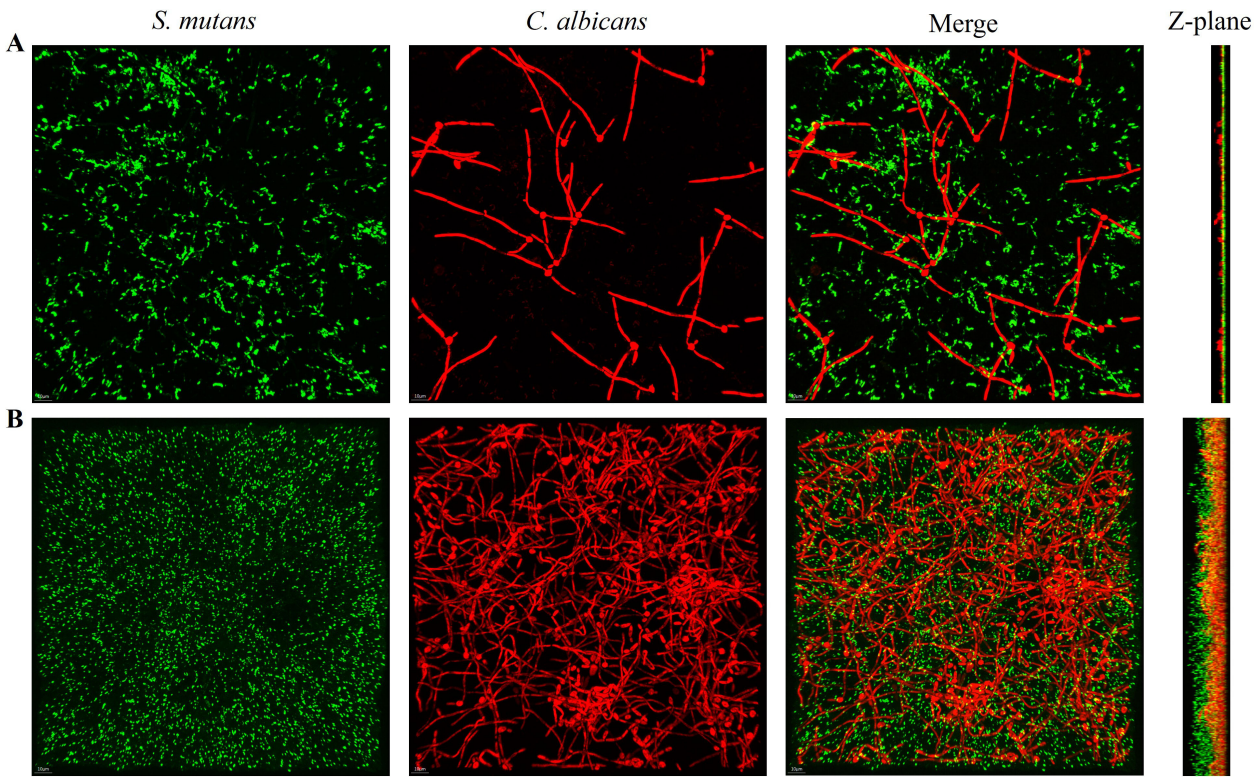

FIGURE 5
Fluorescence *in situ* hybridization staining images of *Streptococcus mutans* and *Candida albicans* co-cultured biofilms with the addition of 100 mM arginine **(A)** and in the control group **(B)** after 4 h of incubation, with the Z-plane indicating biofilm thickness.

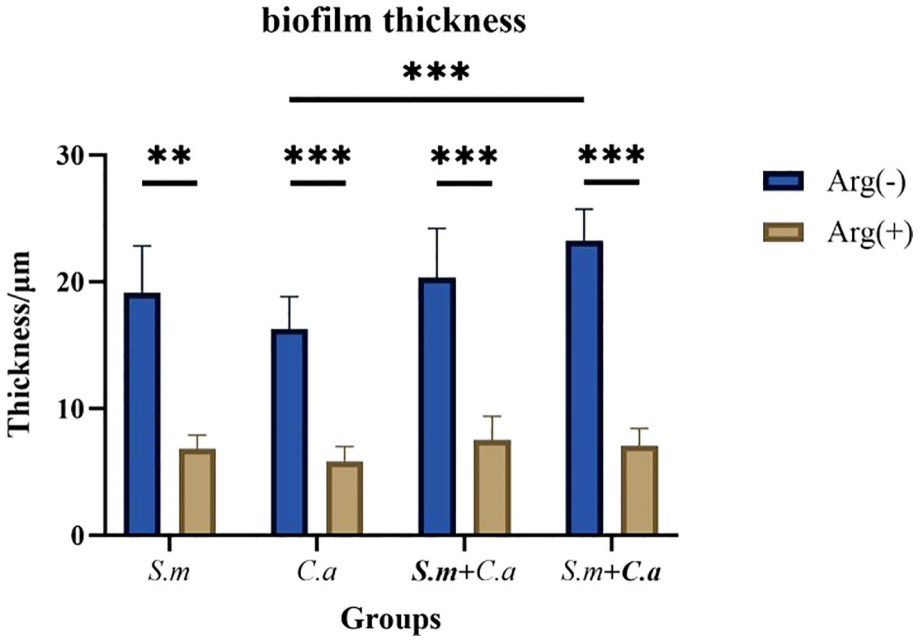

FIGURE 6
Thickness measurements of *Streptococcus mutans* and *Candida albicans* monoculture and co-culture biofilms after 4 h of incubation with 100 mM and 0 mM arginine (*$p < 0.05$, **$p < 0.01$, and ***$p < 0.001$).

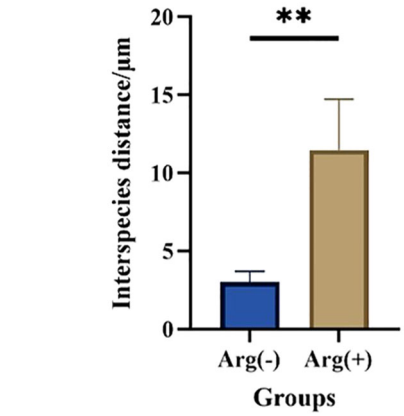

FIGURE 7
Interspecies distance measurements of *Streptococcus mutans* and *Candida albicans* in co-cultured biofilms after 4 h of incubation with 100 mM and 0 mM arginine (**$p < 0.01$).

Therapeutic approaches targeting *S. mutans* and *C. albicans* biofilms include natural compounds, antimicrobial peptides, nanomaterials, antimicrobial photodynamic therapy, and combination therapy, all of which have demonstrated good inhibitory effects as antimicrobial therapies (Khan et al., 2021; Li et al., 2023). Arginine has shown promise in preventing and treating dental caries in several studies. Arginine is metabolized by five main pathways: (1) to creatine and homoarginine by arginine glycine amidinotransferase; (2) biosynthesized to guanidine butyramine and carbon dioxide by decarboxylation of arginine decarboxylase; (3) produced to citrulline and nitric oxide by nitric oxide synthase; (4) decomposed to ornithine and urea by arginases; and (5) metabolized to ammonia and citrulline by arginine deiminase (Wei et al., 2023). Arginine can be metabolized by microorganisms with arginine deiminase systems, such as *Streptococcus gordonii*, to produce ammonia, which increases the environmental pH and reduces the occurrence of enamel demineralization (Jing et al., 2022). In contrast, *S. mutans* does not have an arginine deiminase system and cannot metabolize arginine. Most of these studies focused on the effects of arginine against *S. mutans* showed that arginine negatively impacts *S. mutans* biofilm formation ability, pathogenicity, metabolism, and tolerance to environmental stressors (Huang et al., 2017). Several studies have examined the effects of the addition of arginine to fluoridated toothpaste and found that a fluoridated toothpaste containing 1.5% arginine exhibited more prominent anti-caries effects (Yin et al., 2013; Li et al., 2015). Arginine-containing toothpaste favorably modifies the bacterial composition to a healthier community (Nascimento et al., 2014). In addition, arginine has been added to products such as mouth rinses (Wang et al., 2012; Yu et al., 2017), varnishes (Shapira et al., 1994), and confections (Acevedo et al., 2008) to study its caries-controlling effects. Furthermore, 8% arginine has been reported to be effective in treating dentin hypersensitivity (Hirsiger et al., 2019).

C. albicans can encode arginases that metabolize arginine (Schaefer et al., 2020). However, relatively few studies have focused on the effects of arginine on the growth of *C. albicans* and have indicated different effects than those on *S. mutans*. Ghosh et al. demonstrated that arginine supplementation stimulates hyphal growth in *C. albicans* (transition from yeast to hyphal form is a critical virulence factor in *C. albicans*) (Ghosh et al., 2009). Another study reported that the addition of 0.2% arginine promoted cross-kingdom interactions between *C. albicans* and *Actinomyces viscosus* in root caries (Xiong et al., 2022). In contrast, Koopman et al. demonstrated that arginine supplementation enhanced the resilience of the oral

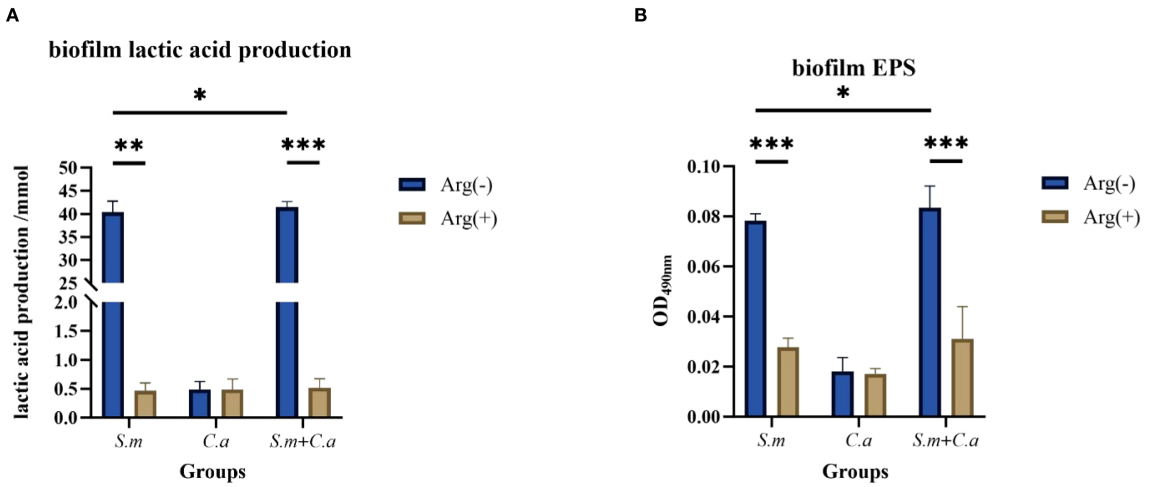

FIGURE 8
Lactic acid **(A)** and extracellular polysaccharide **(B)** production in single- and dual-species biofilms in the control group (0 mM arginine) and experimental group (100 mM arginine). Values are expressed as the mean and SD. Student's *t*-test and Mann–Whitney U tests were used to compare biomass between the control and experimental groups (*$p < 0.05$, **$p < 0.01$, and ***$p < 0.001$).

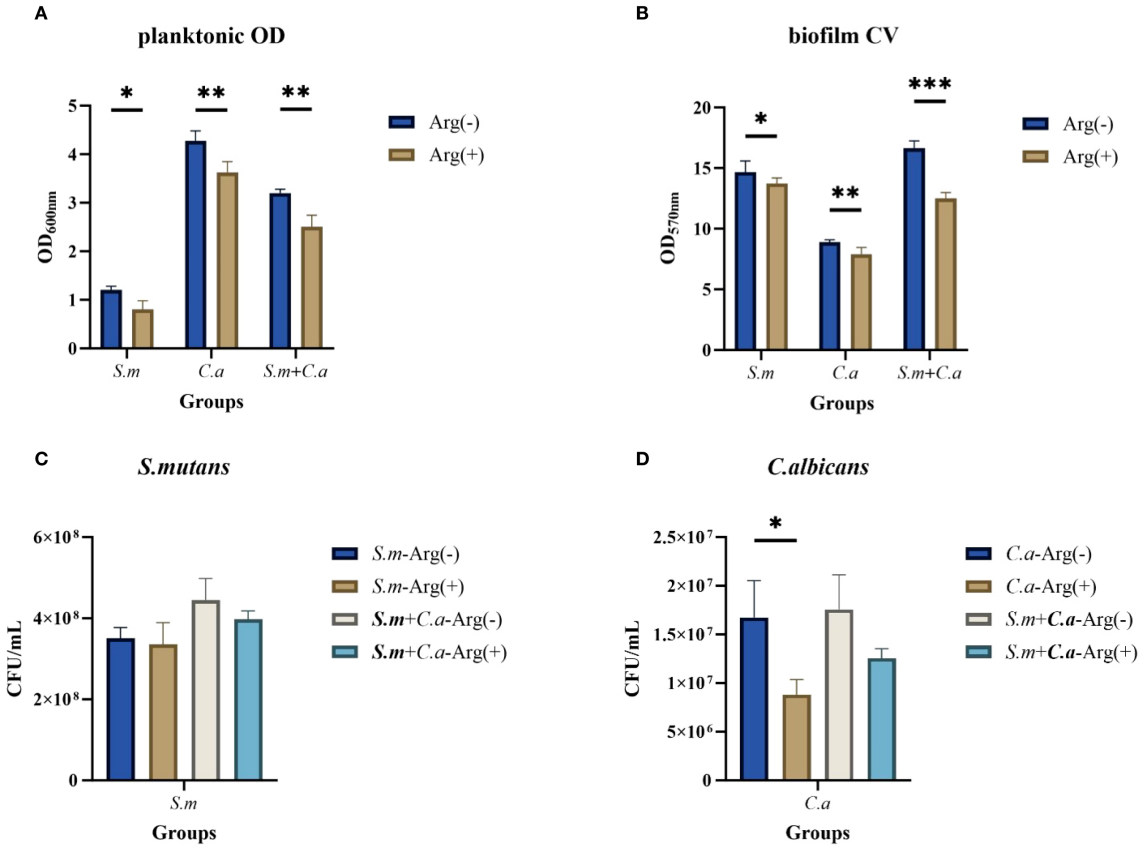

FIGURE 9
Short-term effect of arginine on planktonic and biofilm growth of *Streptococcus mutans* and *Candida albicans*. Planktonic solution absorbance in non-treated control group (0 mM arginine) and treated group (100 mM arginine, treated for 10 min after 4 h incubation) **(A)**. Biofilm mass determined by crystal violet staining **(B)** and CFU/mL of *S. mutans* **(C)** and *C. albicans* **(D)** in single- and dual-species biofilm viable cells obtained for the control group (0 mM arginine) and experimental group (100 mM arginine, treated for 10 min after 4-h incubation). Values are expressed as the mean and SD. Student's *t*-test and Mann–Whitney U tests were used to compare biomass between the control and experimental groups (*$p < 0.05$, **$p < 0.01$, and ***$p < 0.001$).

microenvironment against acidification and suppressed *C. albicans* outgrowth (Koopman et al., 2015). However, to the best of our knowledge, no prior studies have examined the effects of arginine on the combined growth of *S. mutans* and *C. albicans*.

Our study focused on whether arginine has an inhibitory effect on *S. mutans* and *C. albicans*, with the goal of guiding the clinical application of arginine and exploring novel methods for inhibiting the development of caries. Previous studies reported that toothpastes supplemented with 1.5% arginine were used for the prevention of dental caries. Similarly, we used 100 mM arginine and investigated its effects on the growth of *S. mutans*, *C. albicans*, and their dual-species co-cultures. In the present study, a high concentration of arginine (100 mM) inhibited the growth of both single- and dual-species cultures in the planktonic and biofilm states. Biofilm CV staining, CFU quantification, and FISH showed that arginine inhibited biofilm formation by reducing both biomass and physical adhesion. These results lead to the rejection of our null hypotheses, indicating that the effect of arginine not only inhibits the growth of *S. mutans* and *C. albicans* in both single- and dual-species cultures but also suppresses the synergistic cariogenic effects of these organisms. The effect of arginine on *S. mutans* was consistent with that reported in previous studies. Our results also demonstrated that arginine inhibited the growth of *C. albicans*, consistent with prior findings. However, discrepancies with certain previous findings suggest that the effect of arginine on *C. albicans* growth is concentration-dependent; higher concentrations (such as the 100 mM arginine used in this study) appear to exert stronger inhibitory effect.

Our results showed that *S. mutans* and *C. albicans* co-culture enhanced the growth and cariogenic properties of *S. mutans*. Previous studies have demonstrated that the presence of *C. albicans* increases *S. mutans* metabolism, including the upregulation of genes involved in glycolytic carbohydrate metabolism (*eno*) and galactose metabolism (*lacC* and *lacG*), as well as genes related to acid production (*ldh*) and acid stress tolerance (*fabM* and *atpD*). Additionally, the downregulation of genes associated with ammonia production (*arcA* and *ureC*) allows the pH to drop below the demineralization threshold (Du et al., 2021; Xiao et al., 2023). *S. mutans* is a major producer of extracellular polysaccharides in dental plaque biofilms, converting dietary sucrose to extracellular glucans primarily through glucosyltransferases (Gtfs) (Krzyściak et al., 2014). Gtfb secreted

by *S. mutans* binds tightly to the mannan layer of *C. albicans*, resulting in the production of a large amount of extracellular α-glucan on the fungal surface, contributing to the bacterial-fungal association and biofilm formation (Hwang et al., 2017; Bowen et al., 2018; Falsetta et al., 2014).

Additionally, arginine has been shown to increase the pH of the oral microenvironment, as its metabolism leads to the production of ammonia, and downregulates genes associated with the production of extracellular polysaccharides (*gtfB*) in *S. mutans*, thereby affecting its cariogenic properties (Chakraborty and Burne, 2017). Our results indicate that the production of extracellular polysaccharides and lactic acid within the dual-species biofilm decreased after the addition of arginine, while also maintaining a higher pH, which reduces the initiation and progression of demineralization and caries. These findings suggest that arginine has an inhibitory effect on the co-cultured biofilm and reduces the pathogenicity of *S. mutans* and *C. albicans*, representing a novel approach to preventing caries.

Our results showed that the co-culture of *S. mutans* and *C. albicans* enhanced the growth of both organisms and the cariogenic properties of the co-cultured biofilms. The inhibition of growth of both *S. mutans* and *C. albicans*, along with the reduction of biomass, physical adhesion, EPS production, and lactic acid production in the co-cultured biofilms after the addition of arginine, may explain how arginine reduces the cariogenicity of *S. mutans* and *C. albicans*, presenting a new strategy for caries prevention.

Arginine exerts different inhibitory effects on *C. albicans* and *S. mutans*, presumably due to their different modes of action toward fungi and bacteria. In *S. mutans*, arginine significantly impacts physiological homeostasis and gene regulation. Arginine inhibits growth, suppresses virulence and compromises stress tolerance (Chakraborty and Burne, 2017). Recent evidence shows that arginine can weaken the *S. mutans* cell wall, ultimately causing lysis (Liu et al., 2022).

In contrast, the effect of arginine against *C. albicans* is believed to resemble the action of cationic surfactants, primarily targeting the plasma-membrane lipids (Fait et al., 2023). As arginine has a more profound and multifaceted impact on the physiology and transcriptome of *S. mutans*, its inhibitory effect is more pronounced. Consequently, when *S. mutans* and *C. albicans* are co-cultured, the pronounced suppression of the former disrupts their cross-kingdom synergy and markedly restricts the overall growth of the dual-species community.

We also investigated whether the short-term application of arginine affected the growth of *S. mutans* and *C. albicans*; the inhibitory effects of arginine against the growth of these bacteria were similar. Short-term treatments reduced the biomass of *S. mutans* and *C. albicans* in the planktonic state. Similarly, in the biofilm state, a reduction in biofilm biomass was noted, although the CFU counts of *S. mutans* and *C. albicans* showed no statistically significant differences. It is encouraging to note that short-term treatment with arginine also inhibited the formation of *S. mutans* and *C. albicans* biofilms. This suggests adding arginine to toothpaste, mouthwash, and other oral cleansing products, in conjunction with regular oral hygiene, could be effective in inhibiting the growth of caries-causing bacteria and preventing the development of caries. Further research is needed to determine the duration and effectiveness of the short-term application of L-arginine.

Arginine may help prevent dental caries due to its effect on the growth of both *S. mutans* and *C. albicans*. This inhibition results in a decrease in biofilm biomass, which, in turn, reduces cariogenic biofilm production. Moreover, arginine affects the physical adhesion of these microbes, thereby affecting the formation of a symbiotic biofilm. Arginine may also suppress the expression of virulence factors in *S. mutans*, leading to reduced production of EPSs and lactic acid, as well as maintaining a higher pH. Collectively, these changes contribute to a decrease in the onset and progression of demineralization and caries. Moreover, the cross-kingdom cariogenic effect of *S. mutans* and *C. albicans* can enhance the cariogenicity of *S. mutans*. Arginine could reduce the production of extracellular polysaccharides and lactic acid, which become more abundant during co-culture, as reflected in the reduced cariogenicity of *S. mutans*. This suggests that the inhibitory effect of arginine may stem from its action on the cross-kingdom interactions between *S. mutans* and *C. albicans*. However, further studies are required to determine whether the mechanisms underlying the inhibitory effects of arginine are associated with its action on the growth of a single microorganism or its effect on the cross-kingdom interactions between both microorganisms. Moreover, future studies should investigate the mechanisms by which the inhibitory effect of arginine are mediated through the regulation of genes in these two pathogens.

5 Conclusion

L-Arginine inhibited the growth and biofilm formation of *S. mutans* and *C. albicans*, both monocultured and co-cultured. Moreover, L-arginine suppressed the bacterial growth-associated reduction in pH, as well as the production of EPSs and lactic acid. Our findings suggest that L-arginine can serve as a potential candidate to inhibit the synergistic cariogenicity of *S. mutans* and *C. albicans*.

Data availability statement

The raw data supporting the conclusions of this article will be made available by the authors, without undue reservation.

Author contributions

H-YG: Data curation, Formal Analysis, Investigation, Methodology, Validation, Visualization, Writing – original draft, Writing – review & editing. HY: Formal Analysis, Investigation, Writing – review & editing. H-MW: Formal Analysis, Writing – review & editing. H-ML: Writing – review & editing, Formal Analysis. Y-SM: Conceptualization, Funding acquisition, Supervision, Writing – review & editing, Investigation, Project

administration. Y-XB: Conceptualization, Funding acquisition, Supervision, Writing – review & editing.

Funding

The author(s) declare financial support was received for the research and/or publication of this article. This work has been funded by Beijing Hospitals Authority Youth Programme (QML20231504); Beijing Hospitals Authority Clinical medicine Development of special funding support (ZLRK202330) and International Orthodontic Foundation Young Grant (2023IOFY14).

Conflict of interest

The authors declare that the research was conducted in the absence of any commercial or financial relationships that could be construed as a potential conflict of interest.

Generative AI statement

The author(s) declare that no Generative AI was used in the creation of this manuscript.

Any alternative text (alt text) provided alongside figures in this article has been generated by Frontiers with the support of artificial intelligence and reasonable efforts have been made to ensure accuracy, including review by the authors wherever possible. If you identify any issues, please contact us.

Publisher's note

References

Acevedo, A. M., Montero, M., Rojas-Sanchez, F., Machado, C., Rivera, L. E., Wolff, M., et al. (2008). Clinical evaluation of the ability of caviStat in a mint confection to inhibit the development of dental caries in children. *J. Clin. Dent.* 19, 1–85.

Baena-Monroy, T., Moreno-Maldonado, V., Franco-Martínez, F., Aldape-Barrios, B., Quindós, G., and Sánchez-Vargas, L. O. (2005). Candida albicans, staphylococcus aureus and streptococcus mutans colonization in patients wearing dental prosthesis. *Med. Oral Patol. Oral Cir. Bucal.* 10 (Suppl1), E27–E39.

Beerens, M. W., ten Cate, J. M., and van der Veen, M. H. (2017). Microbial profile of dental plaque associated to white spot lesions in orthodontic patients immediately after the bracket removal. *Arch. Oral. Biol.* 78, 88–93. doi: 10.1016/j.archoralbio.2017.02.011

Bowen, W. H., Burne, R. A., Wu, H., and Koo, H. (2018). Oral biofilms: pathogens, matrix and polymicrobial interactions in microenvironments. *Trends Microbiol.* 26, 229–425. doi: 10.1016/j.tim.2017.09.008

Chakraborty, B., and Burne, R. A. (2017). Effects of arginine on streptococcus mutans growth, virulence gene expression, and stress tolerance. *Appl. Environ. Microbiol.* 83, e00496–e00175. doi: 10.1128/AEM.00496-17

Cherian, J. M., Kurian, N., Varghese, K. G., and Thomas, H. A. (2023). World health organization's global oral health status report: paediatric dentistry in the spotlight. *J. Paediatrics Child Health* 59 , 925–265. doi: 10.1111/jpc.16427

Clemente, L. M., Ribeiro, A. B., Fortes, C. V., Ribeiro, A. B., Oliveira, V. de Cássia, Macedo, A. P., et al. (2023). Risk factors and immunological biomarkers in denture stomatitis: an observational cross-sectional study. *Arch. Oral. Biol.* 155, 105799. doi: 10.1016/j.archoralbio.2023.105799

Dang, M.-H., Jung, J.-E., Lee, D.-W., Song, K.-Y., and Jeon, J.-G. (2016). Recovery of acid production in streptococcus mutans biofilms after short-term fluoride treatment. *Caries Res.* 50, 363–715. doi: 10.1159/000446408

Du, Q., Ren, B., He, J., Peng, X., Guo, Q., Zheng, L., et al. (2021). Candida albicans promotes tooth decay by inducing oral microbial dysbiosis. *ISME J.* 15 , 894–908. doi: 10.1038/s41396-020-00823-8

Du, Q., Ren, B., Xuedong, Z., Zhang, L., and Xu, X. (2022). Cross-kingdom interaction between candida albicans and oral bacteria. *Front. Microbiol.* 13. doi: 10.3389/fmicb.2022.911623

Fait, M. E., Grillo, P. D., Garrote, G. L., Prieto, E. D., Vázquez, R. F., Saparrat, M. C. N., et al. (2023). 'Biocidal and antibiofilm activities of arginine-based surfactants against Candida isolates'. *Amino Acids* 55, 1083–1102. doi: 10.1007/s00726-023-03296-z

Falsetta, M. L., Klein, M. I., Colonne, P. M., Scott-Anne, K., Gregoire, S., Pai, C.-H., et al. (2014). Symbiotic relationship between streptococcus mutans and candida albicans synergizes virulence of plaque biofilms *in vivo*. *Infection Immun.* 82 , 1968–1981. doi: 10.1128/IAI.00087-14

Ghosh, S., Navarathna, D. H.M.L. P., Roberts, D. D., Cooper, J. T., Atkin, A. L., Petro, T. M., et al. (2009). Arginine-induced germ tube formation in candida albicans is essential for escape from murine macrophage line RAW 264.7. *Infection Immun.* 77, 1596–16055. doi: 10.1128/IAI.01452-08

Gibson, G. R., Hutkins, R., Sanders, M. E., Prescott, S. L., Reimer, R. A., Salminen, S. J., et al. (2017). Expert consensus document: the international scientific association for probiotics and prebiotics (ISAPP) consensus statement on the definition and scope of prebiotics. *Nat. Rev. Gastroenterol Hepatol.* 14 , 491–502. doi: 10.1038/nrgastro.2017.75

He, J., Kim, D., Zhou, X., Ahn, S.-J., Burne, R. A., Richards, V. P., et al. (2017). RNA-seq reveals enhanced sugar metabolism in streptococcus mutans co-cultured with candida albicans within mixed-species biofilms. *Front. Microbiol.* 8. doi: 10.3389/fmicb.2017.01036

Hirsiger, C., Schmidlin, P. R., Michaelis, M., Hirsch, C., Attin, T., Heumann, C., et al. (2019). Efficacy of 8% Arginine on dentin hypersensitivity: A multicenter clinical trial in 273 patients over 24 weeks. *J. Dentistry* 83, 1–6. doi: 10.1016/j.jdent.2019.01.002

Huang, X., Zhang, K., Deng, M., Exterkate, R. A.M., Liu, C., Zhou, X., et al. (2017). Effect of arginine on the growth and biofilm formation of oral bacteria. *Arch. Oral. Biol.* 82, 256–262. doi: 10.1016/j.archoralbio.2017.06.026

Hwang, G., Liu, Y., Kim, D., Li, Y., Krysan, D. J., and Koo, H. (2017). Candida albicans mannans mediate streptococcus mutans exoenzyme gtfB binding to modulate cross-kingdom biofilm development *in vivo*. *PloS Pathog.* 13, e10064075. doi: 10.1371/journal.ppat.1006407

Jenkinson, H. F. (2011). Beyond the oral microbiome. *Environ. Microbiol.* 13 , 3077–3087. doi: 10.1111/j.1462-2920.2011.02573.x

Jing, M., Zheng, T., Gong, T., Yan, J., Chen, J., Lin, Y., et al. (2022). AhrC negatively regulates *streptococcus mutans* arginine biosynthesis. *Microbiol. Spectr.* 10, e0072122. doi: 10.1128/spectrum.00721-22

Khan, F., Bamunuarachchi, N. I., Pham, D. T. N., Tabassum, N., Khan, M. S. A., and Kim, Y.-M. (2021). Mixed biofilms of pathogenic candida-bacteria: regulation mechanisms and treatment strategies. *Crit. Rev. Microbiol.* 47, 699–7275. doi: 10.1080/1040841X.2021.1921696

Klaus, K., Eichenauer, J., Sprenger, R., and Ruf, S. (2016). Oral microbiota carriage in patients with multibracket appliance in relation to the quality of oral hygiene. *Head Face Med.* 12, 28. doi: 10.1186/s13005-016-0125-x

Koo, H., Andes, D. R., and Damian, J.K. (2018). Candida–streptococcal interactions in biofilm-associated oral diseases. *PloS Pathog.* 14, e10073425. doi: 10.1371/journal.ppat.1007342

Koopman, J. E., Röling, W. F.M., Buijs, M. J., Sissons, C. H., ten Cate, J. M., Bart, J., et al. (2015). Stability and resilience of oral microcosms toward acidification and candida outgrowth by arginine supplementation. *Microbial Ecol.* 69, 422–335. doi: 10.1007/s00248-014-0535-x

Krzyściak, W., Jurczak, A., Kościelniak, D., Bystrowska, B., and Skalniak, A. (2014). The virulence of streptococcus mutans and the ability to form biofilms. *Eur. J. Clin. Microbiol. Infect. Dis.* 33 , 499–515. doi: 10.1007/s10096-013-1993-7

Kulshrestha, S., Khan, S., Ehtisham Khan, M., Misba, L., and Khan, A. U. (2016). Calcium fluoride nanoparticles induced suppression of streptococcus mutans biofilm: an *in vitro* and *in vivo* approach. *Appl. Microbiol. Biotechnol.* 100, 1901–1145. doi: 10.1007/s00253-015-7154-4

Kuriki, N., Asahi, Y., Sotozono, M., Machi, H., Noiri, Y., Hayashi, M., et al. (2021). Next-generation sequencing for determining the effect of arginine on human dental biofilms using an. *In Situ Model. Pharmacy: J. Pharm. Educ. Pract.* 9, 185. doi: 10.3390/pharmacy9010018

Li, X., Zhong, Y., Jiang, X., Hu, D., Mateo, L. R., Morrison, B. M. Jr., et al. (2015). Randomized clinical trial of the efficacy of dentifrices containing 1.5% Arginine, an insoluble calcium compound and 1450 ppm fluoride over two years. *J. Clin. Dent.* 26, 7–125.

Li, Y., Huang, S., Du, J., Wu, M., and Huang, X. (2023). Current and prospective therapeutic strategies: tackling candida albicans and streptococcus mutans cross-kingdom biofilm. *Front. Cell. Infection Microbiol.* 13. doi: 10.3389/fcimb.2023.1106231

Liu, Y., Liu, S., Zhi, Q., Zhuang, P., Zhang, R., Zhang, Z., et al. (2022). Arginine-induced metabolomic perturbation in streptococcus mutans. *J. Oral. Microbiol.* 14, 20151665. doi: 10.1080/20002297.2021.2015166

Lu, Y., Lei, L., Deng, Y., Zhang, H., Xia, M., Wei, Xi, et al. (2022). RNase III coding genes modulate the cross-kingdom biofilm of streptococcus mutans and candida albicans. *Front. Microbiol.* 13. doi: 10.3389/fmicb.2022.957879

Lu, Y., Lin, Y., Li, M., and He, J. (2023). Roles of streptococcus mutans-candida albicans interaction in early childhood caries: A literature review. *Front. Cell. Infection Microbiol.* 13. doi: 10.3389/fcimb.2023.1151532

Nascimento, M. M., Browngardt, C., Xiaohui, X., Klepac-Ceraj, V., Paster, B. J., and Burne, R. A. (2014). The effect of arginine on oral biofilm communities. *Mol. Oral. Microbiol.* 29 , 45–54. doi: 10.1111/omi.12044

Pang, L., Wang, Y., Ye, Y., Zhou, Y., Zhi, Q., and Huancai, L. (2021). Metagenomic analysis of dental plaque on pit and fissure sites with and without caries among adolescents. *Front. Cell. Infection Microbiol.* 11. doi: 10.3389/fcimb.2021.740981

Philip, N., Suneja, B., and Walsh, L. J. (2018). Ecological approaches to dental caries prevention: paradigm shift or shibboleth? *Caries Res.* 52 , 153–165. doi: 10.1159/000484985

Schaefer, K., Wagener, J., Ames, R. M., Christou, S., MacCallum, D. M., Bates, S., et al. (2020). Three related enzymes in *candida albicans* achieve arginine- and agmatine-dependent metabolism that is essential for growth and fungal virulence. *mBio.* 11, e01845–e01820. doi: 10.1128/mBio.01845-20

Shapira, J., Sgan-Cohen, H. D., Stabholz, A., Sela, M. N., Schurr, D., and Goultschin, J. (1994). Clinical and microbiological effects of chlorhexidine and arginine sustained-release varnishes in the mentally retarded. *Special Care Dentistry: Off. Publ. Am. Assoc. Hosp. Dentists Acad. Dentistry Handicapped Am. Soc. Geriatric Dentistry* 14 , 158–163. doi: 10.1111/j.1754-4505.1994.tb01124.x

Wan, S. X., Tian, J., Liu, Y., Dhall, A., Koo, H., and Hwang, G. (2021). Cross-kingdom cell-to-cell interactions in cariogenic biofilm initiation. *J. Dental Res.* 100 , 74–81. doi: 10.1177/0022034520950286

Wang, X. L., Cheng, C. Y., Peng, D., Wang, B., and Gan, Y. H. (2012). Dental plaque pH recovery effect of arginine bicarbonate rinse *in vivo*. *Chin. J. Dental Res.* 15, 115–205.

Wei, Yu, Wang, Z., Liu, Y., Liao, B., Zong, Y., Shi, Y., et al. (2023). Extracellular vesicles of candida albicans regulate its own growth through the L-arginine/nitric oxide pathway. *Appl. Microbiol. Biotechnol.* 107 , 355–367. doi: 10.1007/s00253-022-12300-7

Xiao, J., Huang, X., Alkhers, N., Alzamil, H., Alzoubi, S., Wu, T. T., et al. (2018). Candida albicans and early childhood caries: A systematic review and meta-analysis. *Caries Res.* 52 , 102–112. doi: 10.1159/000481833

Xiao, J., Zeng, Y., Rustchenko, E., Huang, X., Wu, T. T., and Megan, L.F. (2023). Dual transcriptome of streptococcus mutans and candida albicans interplay in biofilms. *J. Oral. Microbiol.* 15, 21440475. doi: 10.1080/20002297.2022.2144047

Xiong, K., Zhu, H., Li, Y., Ji, M., Yan, Y., Chen, X., et al. (2022). The arginine biosynthesis pathway of candida albicans regulates its cross-kingdom interaction with actinomyces viscosus to promote root caries. *Microbiol. Spectr.* 10 , e0078222. doi: 10.1128/spectrum.00782-22

Yang, H., Ma, Y., Xie, X., Wang, H., Li, X., Fang, D., et al. (2023). Candida albicans enriched in orthodontic derived white spot lesions and shaped focal supragingival bacteriome. *Front. Microbiol.* 14. doi: 10.3389/fmicb.2023.1084850

Yin, W., Hu, D. Y., Fan, X., Feng, Y., Zhang, Y. P., Cummins, D., et al. (2013). A clinical investigation using quantitative light-induced fluorescence (QLF) of the anticaries efficacy of a dentifrice containing 1.5% Arginine and 1450 ppm fluoride as sodium monofluorophosphate. *J. Clin. Dentistry* 24, A15–A22. doi: 10.1016/j.jdent.2010.04.004

Yu, Y., Wang, X., Ge, C., Wang, B., Cheng, C., and Gan, Y.-H. (2017). Effects of rinsing with arginine bicarbonate and urea solutions on initial enamel lesions in situ. *Oral. Dis.* 23 , 353–359. doi: 10.1111/odi.12618

frontiers | Frontiers in Cellular and Infection Microbiology

TYPE Original Research
PUBLISHED 20 October 2025
DOI 10.3389/fcimb.2025.1670139

OPEN ACCESS

EDITED BY
Keke Zhang,
Wenzhou Medical University, China

REVIEWED BY
Lin Zeng,
University of Florida, United States
Noura Ahmed,
Salt Lake Community College, United States

*CORRESPONDENCE
Junghyun Kim
dvmhyun@jbnu.ac.kr
Dongyeop Kim
biofilmkim@jbnu.ac.kr

†These authors have contributed equally to this work and share first authorship

RECEIVED 21 July 2025
ACCEPTED 06 October 2025
PUBLISHED 20 October 2025

CITATION
Han S, Rajitha K, Park S, Lim J, Jung H-Y, Kim J and Kim D (2025) Unveiling the impact of allulose on oral microbiota and biofilm formation via a cariogenic potential assessment platform. *Front. Cell. Infect. Microbiol.* 15:1670139. doi: 10.3389/fcimb.2025.1670139

Unveiling the impact of allulose on oral microbiota and biofilm formation via a cariogenic potential assessment platform

Seunghun Han[1†], Kuthirakkal Rajitha[1†], Sungbin Park[1†], Jaeeui Lim[1], Hee-Young Jung[1], Junghyun Kim[2,3*] and Dongyeop Kim[1,3*]

[1]Department of Preventive Dentistry, School of Dentistry, Jeonbuk National University, Jeonju, Republic of Korea, [2]Department of Oral Pathology, School of Dentistry, Jeonbuk National University, Jeonju, Republic of Korea, [3]Institute of Oral Bioscience, Jeonbuk National University, Jeonju, Republic of Korea

Introduction: The increased consumption of refined carbohydrates, particularly sucrose, has contributed to metabolic disorders and oral diseases such as dental caries by promoting dysbiotic biofilm formation and reducing microbial diversity. Allulose, a rare sugar with physicochemical properties similar to sucrose, has been suggested to offer metabolic health benefits; however, its impact on oral biofilm ecology remains unclear.

Methods: We evaluated the cariogenic potential of allulose using a multi-tiered in vitro platform consisting of single-species planktonic and biofilm models, a dual-species biofilm model involving *Streptococcus mutans* (pathogen) and *Streptococcus oralis* (commensal), and a saliva-derived microcosm biofilm model. Key virulence indicators, including bacterial growth, acid production, biofilm biomass, exopolysaccharide (EPS) synthesis, and microbial community composition, were quantitatively assessed.

Results: Compared to sucrose, glucose, and fructose, allulose supported reduced bacterial growth and acid production, showing a profile similar to non-fermentable sugar alcohols such as xylitol and erythritol. Biofilms developed under allulose conditions lacked the dense EPS-enmeshed microcolonies and dome-shaped architecture characteristic of sucrose-induced S. mutans-dominant biofilms. In the saliva-derived microcosm model, allulose-treated biofilms maintained higher microbial diversity and preserved health-compatible genera such as *Neisseria*, *Haemophilus*, *Veillonella*, and *Granulicatella*.

Discussion: These findings demonstrate that allulose supports lower bacterial virulence activity and minimal biofilm formation compared to common dietary sugars while preserving microbial diversity. This highlights its potential as a non-cariogenic sugar alternative with microbiome-conscious benefits and provides ecological insight into how allulose may modulate oral biofilm structure and function.

KEYWORDS

oral biofilm, extracellular polymeric substances, dental caries, Streptococcus mutans, microcosm

Introduction

The evolution of human diets has been accompanied by an increased refined carbohydrate consumption, which has increased metabolic disorders, such as obesity and diabetes, as well as oral health issues, such as dental caries. The habitual intake of refined sugars, particularly sucrose, promotes oral biofilm formation by reducing microbial diversity and fostering pathogenic microorganisms (Bowen et al., 2018). *Streptococcus mutans* is widely recognized as a primary etiological agent owing to its strong biofilm-forming ability and acidogenic properties (Palmer et al., 2010; Hajishengallis et al., 2017).

Among the fermentable dietary sugars, sucrose plays a crucial role in caries development (Forssten et al., 2010; Sheiham and James, 2015; Benahmed et al., 2021), significantly contributing to dental biofilm accumulation and pathogenicity (Leme et al., 2006; Bowen et al., 2018). It serves as a key substrate for the synthesis of exopolysaccharides (EPS), specifically glucans, catalyzed by glucosyltransferases (Gtfs) secreted by *S. mutans*. These EPS glucans facilitate bacterial adhesion to tooth surfaces, promote biofilm accumulation, and enhance the structural stability of biofilms (Bowen and Koo, 2011; Klein et al., 2015; Kim et al., 2020, 2022). Additionally, water-insoluble glucans trap nutrients and sugars within biofilms, creating an environment conducive to bacterial proliferation.

During sucrose metabolism, *S. mutans* produces acidic metabolites, which reduce the biofilm pH and accelerate enamel demineralization and dental caries progression (Bowen et al., 2018). The metabolic activity of *S. mutans* within dental plaques is central to dental caries development (Parisotto et al., 2010; Durso et al., 2014; Zhang et al., 2022). Although other microorganisms within the biofilm can also be considered cariogenic, *S. mutans* possesses several potential characteristics such as rapid dietary carbohydrate transport and fermentation, acidic byproduct production, extracellular and intracellular polysaccharide synthesis, and stress-responsive carbohydrate metabolism (Banas, 2004; Beighton, 2005; Kanasi et al., 2010).

Considering the critical role of dietary sugars in EPS synthesis and biofilm development, efforts to mitigate dental caries have primarily focused on reducing sugar consumption and enhancing oral hygiene practices (Philip et al., 2018). However, sugar reduction alone is not always feasible owing to dietary habits and lifestyle choices. Consequently, developing non-cariogenic sugar substitutes has attracted attention as an alternative approach. Non-nutritive sweeteners, including synthetic and naturally occurring compounds such as sugar alcohols (polyols), have been widely studied as they interfere with bacterial metabolism and inhibit biofilm formation (Milgrom et al., 2012; Rice et al., 2020; Staszczyk et al., 2020). Despite their potential, the effectiveness of these sugar alternatives varies, causing gastrointestinal side effects and offering limited long-term benefits (Mäkinen, 2016).

D-Allulose, a naturally occurring monosaccharide classified as a rare sugar, is found in small amounts in maple syrup, dried figs or raisins, and brown sugar. It is a fructose epimer via enzymatic treatment with epimerases, with 70% sweetness of sucrose and minimal caloric content (Hu et al., 2021). Clinical studies have suggested that allulose consumption positively influences metabolic health, including improved plasma glucose control, insulin regulation, and weight management, showing benefits in healthy populations and individuals with type 2 diabetes (Hasturk, 2018; Document, 2019; Daniel et al., 2022; Lee et al., 2022). In addition, it has been generally recognized as safe (GRAS) by the United States Food and Drug Administration (FDA), allowing its use as a food ingredient (FDA, 2023).

Clinical and controlled feeding studies have shown that allulose is not efficiently metabolized in mammalian systems (Iida et al., 2010; Iwasaki et al., 2018), but its effects on oral microbial ecology—including biofilm interactions—remain poorly explored. Despite the promising attributes of allulose, few studies have explored its effects on oral biofilm formation and microbial diversity. In this study, the effects of dietary carbohydrates on oral microbial cariogenicity were assessed across various ecological models using a multi-tiered platform (Figure 1), including single-species planktonic and biofilm, dual-species models involving *S. mutans* and *S. oralis*, and saliva-derived microcosm biofilm experiments with increasing complexity. Each model was used to assess key virulence parameters, including bacterial growth, glycolytic pH drop, biofilm biomass, EPS synthesis, and microbial community composition. The cariogenic potential of allulose has been systematically compared to that of conventional fermentable sugars, such as sucrose, glucose, and fructose (Benahmed et al., 2021), as well as with that of non-fermentable sugar alcohols, such as xylitol and erythritol (Razak et al., 2017; Jeong et al., 2024). Using clinically relevant oral biofilm models, including a hydroxyapatite disc model that mimics the enamel surface and a saliva-based model simulating the oral microbiome, this study provides novel insights into the ecological impact of allulose and highlights its potential as a preventive strategy against dental caries.

Materials and methods

Bacterial strains and culture conditions

S. mutans UA159 (an established cariogenic dental pathogen and well-characterized EPS producer) was used to generate single- and multi-species biofilms. For inoculum preparation, *S. mutans* was cultured to the mid-exponential phase [optical density at 600 nm (OD_{600}) approximately 1.0] in ultrafiltered (10-kDa molecular-mass cutoff membrane; Millipore, MA, USA) tryptone–yeast extract broth [UFTYE; 2.5% tryptone and 1.5% yeast extract (BD Biosciences, San Jose, CA, USA)] with 1% (w/v) glucose at 37°C under 5% CO_2 as previously described (Kim et al., 2017).

Sweetener supplementation

The effects of different sweeteners on *S. mutans* biofilm formation and microbial dynamics were evaluated using a panel of common dietary sugars, such as sucrose, glucose, and fructose

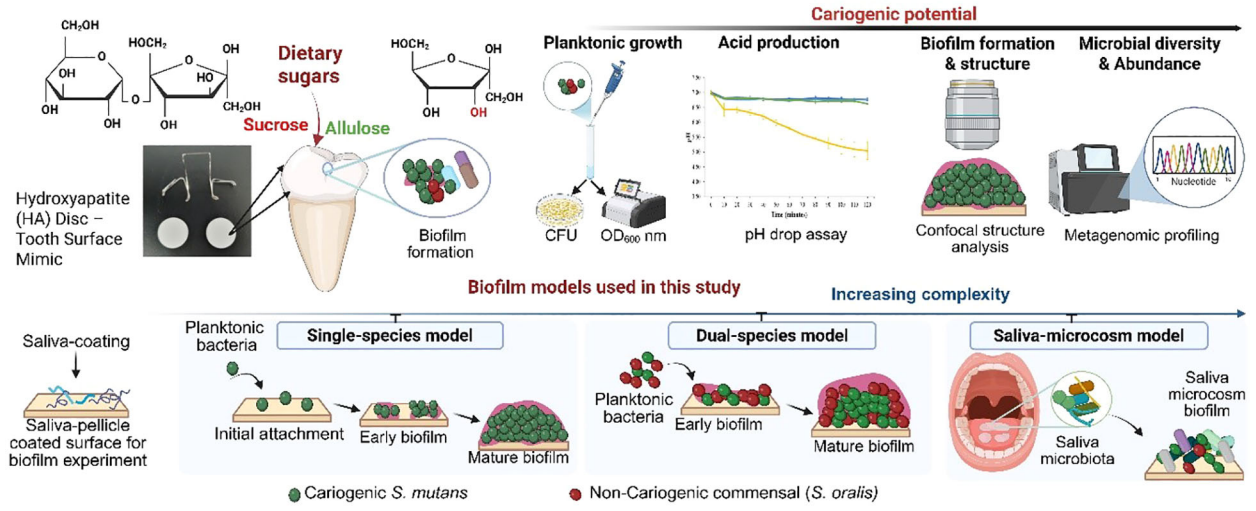

FIGURE 1
Schematic representation of the overall experimental approach to assess the cariogenic potential of dietary sugars using biofilm models of increasing complexity. The study evaluates the impact of sucrose and allulose on *Streptococcus mutans* biofilm formation and oral microbial communities. The biofilm models progress in complexity: single-species (*S. mutans*), dual-species (*S. mutans* and *Streptococcus oralis*), and a saliva-derived microcosm model that simulates the natural oral environment. This comprehensive approach provides mechanistic insights into the role of dietary sugars in biofilm development and microbial dysbiosis. Figure created using BioRender.

(Sigma-Aldrich, Saint Louis, MO, USA), and sugar substitutes, such as allulose (Samyang Co., Seongnam, Korea), xylitol (Sigma-Aldrich), and erythritol (Samyang Co.). Each sweetener was freshly prepared at 1% (w/v) final concentration in sterile UFTYE medium based on previous studies demonstrating its physiological relevance in stimulating dietary sugar exposure in the oral cavity (Benahmed et al., 2021). The UFTYE medium (without additional sugars) was used for the baseline comparison, and basal culture medium was used for both planktonic and biofilm models. To replicate normal dietary sugar exposure and oral clearance patterns, the medium was replaced twice daily (at 19 h and 28 h).

Planktonic growth assay

To assess the cariogenic potential of each sweetener, planktonic growth kinetics and acid production by *S. mutans* were evaluated in UFTYE medium supplemented with 1% glucose, fructose, allulose, xylitol, or erythritol. UFTYE medium without additional sugars served as a blank control. Growth was monitored by measuring the OD_{600} at 30 min intervals for 24 h.

Glycolytic pH drop assay in planktonic cells

Glycolytic acid production by *S. mutans* was assessed using a pH drop assay as previously described (Jeon et al., 2011; Jung et al., 2022). Briefly, planktonic cultures were harvested, washed once, and resuspended in salt solution (50 mM KCl + 1 mM $MgCl_2$). The suspension pH was adjusted to 7.0 using 0.2 M KOH. Each sweetener was added at 1% (w/v) final concentration and the pH was recorded at 10 min intervals over 120 min using a calibrated glass pH electrode (Orion 3-Star, Thermo Scientific, Waltham, MA, USA).

Gene expression analysis by quantitative real-time polymerase chain reaction

RNA was extracted and purified using protocols optimized for *in vitro* biofilm formation (He et al., 2017). Total RNA was isolated and treated with on-column DNase using a RNeasy Micro kit (Qiagen, Valencia, CA, USA). The RNAs were further treated with a second DNase I (Turbo DNase, Applied Biosystems/Ambion) and purified using the Qiagen RNeasy MinElute Cleanup Kit (Qiagen). Complementary DNA (cDNA) was synthesized from 0.5 µg purified RNA using the iScript cDNA synthesis kit (Bio-Rad Laboratories, Hercules, CA, USA) (Cai et al., 2018). Quantitative real-time polymerase chain reaction (qRT-PCR) was performed using the Applied Biosystems StepOne Real-Time PCR system with gene-specific primers targeting *gtfB*, *gtfC*, *gtfD*, *ftf*, *dexA*, *pdhA*, *adhE*, *ldh*, *atpD*, and *16S rRNA* as previously described (Jeon et al., 2009; He et al., 2017; Cai et al., 2018). Gene expression was analyzed using the comparative ΔΔCt method, normalizing each target gene to 16S rRNA as the internal reference.

Single-species biofilm model

To replicate the smooth surfaces of the pellicle-coated tooth, biofilms were formed on saliva-coated hydroxyapatite (sHA) disc (surface area: 2.7 ± 0.2 cm^2) vertically suspended in 24-well plates using a specifically designed wire specimen holder (Xiao et al., 2012; Kim et al., 2018). Filter-sterilized human whole saliva was collected

from healthy donors as previously described (Koo et al., 2000). Hydroxyapatite (HA) discs were immersed in cell-free saliva for 1 h to stimulate salivary pellicle formation. The discs were then vertically suspended in a 24-well plate using custom-made holders; inoculated with *S. mutans* (10^5 colony-forming unit (CFU)/mL; mid-exponential growth phase) in 2.8 mL UFTYE medium supplemented with 1% (w/v) sucrose, glucose, fructose, allulose, xylitol, or erythritol; and incubated at 37°C under 5% CO_2. The inoculum size reflected the typical *S. mutans* levels in the saliva of caries-active individuals (Ren et al., 2022). The sweetener-containing media were changed at 19 h and 28 h to stimulate eating (meal-like) episodes under continuous sugar exposure. Biofilms were harvested and analyzed at 19, 23, and 43 h post-incubation. Sucrose served as the control (cariogenic reference) for head-to-head comparison.

Acidogenicity of pre-formed biofilms

To assess the glycolytic activity, a pH drop assay was performed on pre-formed biofilms cultivated on sHA discs. *S. mutans* biofilms were grown for 43 h in UFTYE medium supplemented with 1% (w/v) sucrose. At 43 h, the discs were transferred to fresh solutions containing 1% (w/v) sweetener, and pH was recorded at 10-min intervals over 120 min to monitor acid production. The initial rate of acid production, which is considered the best indicator of the acid production capacity of the biofilm, was determined from the pH values.

Dual-species biofilm model

A dual-species biofilm model was developed using the cariogenic pathogen *S. mutans* UA159 and oral commensal *S. oralis* KCTC 13038 [originated from ATCC 35037; obtained from Korean Collection for Type Cultures (KCTC), Jeongeup, Korea]. Bacterial suspensions were prepared and mixed to obtain final inoculum concentrations of 10^5 and 10^7 CFU/mL for *S. mutans* and *S. oralis*, respectively. Consistent with the ecological plaque hypothesis, this mixed inoculum was cultured in UFTYE medium containing 0.1% (w/v) sucrose (cariogenic reference) for 19 h to establish an initial colonization community. The discs were then transferred to UFTYE containing 1% sucrose to stimulate a cariogenic challenge at 19 h. The culture medium was changed at 28 h, and the biofilms were harvested at 43 h to determine the viable bacterial count, expressed as CFU per biofilm, using blood agar plating.

Saliva-derived microcosm biofilm model

To simulate a clinically relevant oral microenvironment, a saliva-derived microcosm biofilm model was established using sHA discs (Liu et al., 2023) with slight modifications. The saliva-originated microbial consortium was centrifuged at 3,000× *g* for 10 min to remove the host cells, and the salivary microbiome (saliva collected from healthy individuals, as qualified *S. mutans* absence) was inoculated for initial binding (1 h). Next, approximately 10^5 CFU/mL *S. mutans* was inoculated into UFTYE medium containing 1% (w/v) sucrose or allulose, or UFTYE medium without additional sugars (blank).

Biofilm imaging using confocal microscopy

The biofilms formed under each condition were examined using confocal microscopy. The bacterial cells were stained with 2.5 μM SYTO 9 green-fluorescent nucleic acid stain (485/498 nm; Molecular Probes Inc., Eugene, OR, USA), while EPS was labeled with 1 μM Alexa Fluor 647–dextran conjugate (647/668 nm; Molecular Probes Inc.) The 3D biofilm architecture was acquired using a C2+ confocal microscope (Nikon, Tokyo, Japan) with 20× (0.75 numerical aperture (NA)). NIS-Elements software version 5.21 (Nikon) was used to create 3D renderings to visualize the biofilm architecture (Jung et al., 2022).

Metagenome profiling of saliva-derived microcosm biofilms

Microcosm biofilm samples were collected from the sHA discs and eluted in phosphate-buffered saline (PBS). Genomic DNA was extracted using the FastDNA® Spin Kit for Soil (MP Biomedicals, USA) and quantified using a BioTek Epoch™ spectrophotometer. DNA quality was verified using 1% agarose gel electrophoresis. The V3–V4 region of the bacterial *16S rRNA* gene was amplified using the universal primers 341F and 805R with overhang Illumina adapter sequences following the Nextera™ consensus design. Polymerase chain reaction (PCR) amplification was conducted in two steps: the first round of target amplification and the second round of indexing. The first PCR included 25 cycles using Takara Ex Taq polymerase, and the second PCR consisted of eight indexing cycles. Libraries were purified using AMPure XP beads (Beckman Coulter) and quantified using the Quant-iT PicoGreen dsDNA Assay Kit. Library quality was assessed using an Agilent 2100 Bioanalyzer, and sequencing was performed using the Illumina MiSeq platform with the MiSeq Reagent Kit v2 (500 cycles). Chimeric sequences were detected and removed using the UCHIME method and embedded in the EzBioCloud database (Yoon et al., 2017). Downstream analysis included alpha- and beta-diversity metrics (e.g., Shannon index and Bray–Curtis distance) and relative abundance profiling across taxonomic ranks. The *16S rRNA* gene sequences are available in the NCBI Sequence Read Archive (BioProject accession number: PRJNA1269248).

Statistical analysis

All data are presented as mean ± standard deviation (SD). For comparisons involving multiple groups against a single control, a

one-way analysis of variance (ANOVA) followed by Dunnett's multiple comparison test was applied. Interspecies CFU comparisons were analyzed using non-parametric Kruskal–Wallis tests with Dunn's *post-hoc* correction. For gene expression analysis, ΔCt values were evaluated using one-way ANOVA followed by Holm–Šídák's multiple comparisons test. Statistical significance was set at $p<0.05$. Analyses were performed using GraphPad Prism version 10.4.0 (GraphPad Software, San Diego, CA, USA).

Results and discussion

Planktonic growth and acid production of *S. mutans* in response to various sweeteners

To evaluate allulose with fermentable sugars and non-fermentable polyols in a controlled setting, the initial phase of the cariogenic evaluation platform concentrated on a single-species model using the key cariogenic pathogen *S. mutans* (Hajishengallis et al., 2017; Kim et al., 2020). To assess how different sweeteners affect the planktonic growth kinetics (OD_{600}) and the acid production (pH drop assay), *S. mutans* was cultured in a UFTYE defined medium supplemented with 1% (w/v) sweetener. Basal medium UFTYE (blank) is a complex medium that contains low-molecular-weight nutrients (<10 kDa). The minimal growth observed in the UFTYE medium without additional sugars likely reflects the utilization of these residual nutrients. The growth curves showed that glucose and fructose supported robust bacterial growth with an extended exponential phase, reaching the stationary phase (OD_{600}: approximately 1.0, Figure 2A). These observations align with previous findings that fermentable carbohydrates serve as a preferred and rapidly metabolizable energy source that fuels bacterial proliferation (Jurakova et al., 2023). Moreover, these sugars induced a steep pH drop, with the final pH value dropping to 4.20 ± 0.04 within 30 min, indicating high acid production from glycolytic fermentation (Figure 2B).

Conversely, although allulose had a structural resemblance to fructose, it did not promote exponential growth and exhibited only marginal acidification (Figures 2A, B). The growth in the presence of allulose supplementation remained constant at OD_{600} approximately 0.3, and the pH remained above 5.0 (critical pH for enamel demineralization) over 120 min with a reduction in acid production by 99% compared to that in the presence of sucrose,

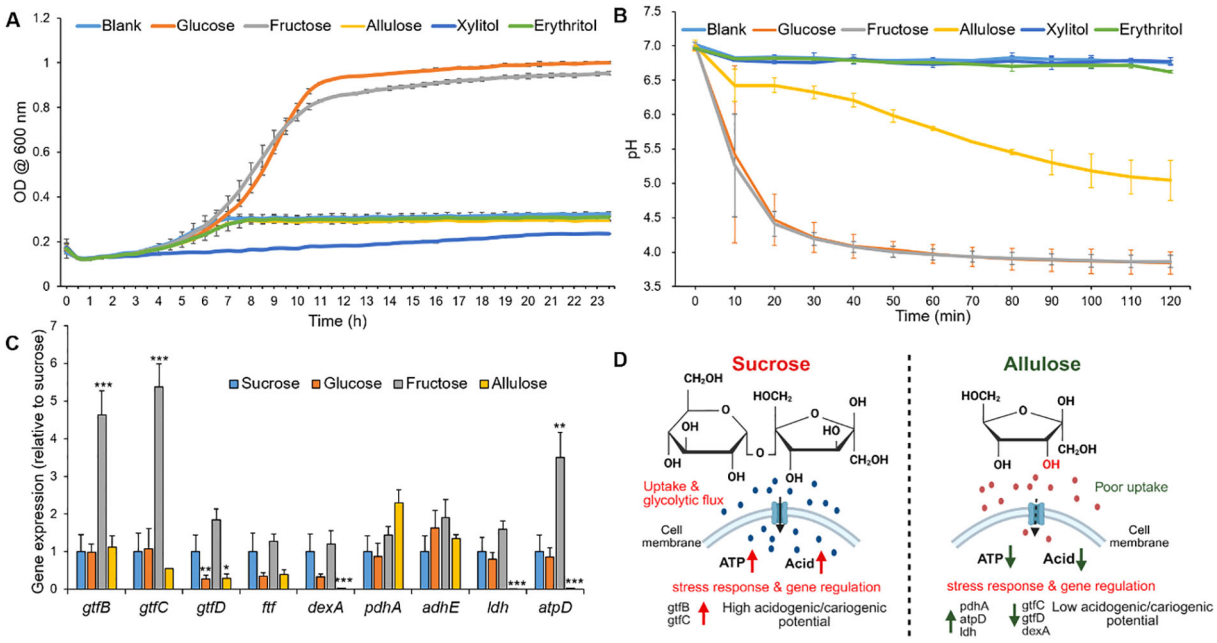

FIGURE 2
Bacterial growth curve, glycolytic pH drop, and relative gene expression of *Streptococcus mutans* in response to different sweeteners. **(A)** Growth curve of *S. mutans* measured as optical density at 600 nm (OD_{600}) over time in a UFTYE medium supplemented with 1% (w/v) glucose, fructose, allulose, xylitol, or erythritol. The UFTYE medium without any sugar supplementation was used as a blank control. **(B)** pH drop assay of *S. mutans* in the presence of different sweeteners. Different sweeteners were added to 50 mM KCl + 1 mM $MgCl_2$ solution (pH=7) to obtain a concentration of 1% (w/v), and pH changes were assessed over 120 min. The data are presented as mean ± standard deviation (n=3). **(C)** Relative gene expression of *S. mutans* planktonic cells in response to different sweeteners at 19 h. Bar graph shows the relative expression levels of key genes associated with biofilm formation (*gtfB*, *gtfC*, *gtfD*, *ftf*), extracellular matrix (*dexA*), energy metabolism (*pdhA*, *adhE*, *atpD*), and acid production (*ldh*) in *S. mutans* cultured in UFTYE medium supplemented with 1% (w/v) sucrose, glucose, fructose, or allulose. Xylitol and erythritol were excluded from gene expression analysis due to minimal growth, which precluded reliable RNA extraction. Data represent mean ± standard deviation from biological replicates (n=6). Only statistically significant differences compared to the sucrose group are indicated with asterisks: *$p<0.05$; **$p<0.01$; ***$p<0.001$. All other comparisons were not significant (ns). **(D)** Conceptual working model summarizing observed phenotypes under sucrose versus allulose, including bacterial growth, glycolytic pH drop, EPS production, and gene expression profiles. The schematic is illustrative and created using BioRender.

indicating the absence of key metabolic pathways for effectively metabolizing allulose. This growth profile highlights that, under the conditions tested, allulose supported minimal bacterial growth and acid production compared to conventional sugars. Xylitol and erythritol also failed to support exponential growth and acid production, establishing their roles as non-fermentable sugar alcohols (Figures 2A, B) (Mäkinen, 2010; Jeong et al., 2024).

Dynamics of cariogenicity-associated genes in response to allulose and other fermentable sugars

To elucidate the molecular basis underlying the observed differences in planktonic growth and acid production, we examined the expression of key virulence genes in 19 h-old *S. mutans* cells cultured in the presence of different dietary sweeteners (Figure 2C). Planktonic gene expression is important because it may indicate the ability of free cells to colonize a pre-formed biofilm or a new surface (Durso et al., 2014). The cariogenicity of *S. mutans* is closely linked to its ability to synthesize extracellular glucans and produce acids via carbohydrate fermentation.

Glucosyltransferase (Gtf catalyzes EPS synthesis and forms a protective scaffold that supports biofilm integrity under external stress (Wang et al., 2018). Specifically, *gtfB* and *gtfC* are associated with insoluble and soluble glucan production, whereas *gtfD* contributes to soluble glucan production (Zhao et al., 2014). In our study, *gtfB* and *gtfC* expression were significantly upregulated in the presence of fructose than in the presence of sucrose ($p<0.0001$), consistent with prior findings on fructose-mediated EPS-related gene induction (Shemesh et al., 2006). In contrast, *gtfD* was significantly downregulated in the presence of allulose ($p<0.05$), which may limit the primer availability for initial EPS synthesis, thereby impairing biofilm formation.

Notably, *gtfB* expression remained unaffected by allulose exposure. Since environmental stress often triggers *gtfB* upregulation to promote adhesion and glucan synthesis (Zhang et al., 2022), its stable expression in the presence of allulose may represent a compensatory mechanism for surface attachment in nutrient-limited or metabolically inactive states. It is important to note that transcriptional levels may not always correspond to enzymatic activity because post-transcriptional regulation can modulate the final protein function (Zhang et al., 2021).

Unlike *gtf* genes, *ftf* expression, which is involved in fructan synthesis, remained unchanged in the presence of all sweeteners, suggesting a limited role of fructan-mediated EPS under these experimental conditions. Interestingly, the significant downregulation of *dexA*, which encodes the dextranase responsible for glucan degradation during biofilm remodeling, suggests that, under allulose conditions, EPS synthesis and biofilm maturation pathways were less active compared to fermentable sugars (Igarashi et al., 2002).

pdhA, which encodes a component of the pyruvate dehydrogenase complex, was upregulated in the presence of allulose. This enzyme links glycolysis to the tricarboxylic acid (TCA) cycle by converting pyruvate into acetyl-CoA, suggesting a shift toward alternative energy metabolism in response to inefficient allulose fermentation. This metabolic reprogramming was consistent with previous findings under carbohydrate-limited conditions (Lemos and Burne, 2008), indicating that under allulose conditions, *S. mutans* exhibited a low-metabolic, low-virulence-like state.

In terms of acidogenicity, the expression of *ldh*, which encodes lactate dehydrogenase, a key enzyme in lactic acid production, was significantly lower in the presence of allulose than in the presence of sucrose ($p<0.001$), correlating with the reduced acid production. Similarly, *atpD*, encoding the β-subunit of the F_1F_0–ATPase complex responsible for proton extrusion under acidic conditions, was highly expressed in the presence of fructose ($p<0.01$), reflecting increased acid stress. Conversely, its significant downregulation in the presence of allulose ($p<0.001$) supports the notion that allulose imposes minimal acidogenic stress, further reinforcing its low cariogenic potential.

Taken together, the gene expression profiling and phenotypic data on growth and acid production support a less-cariogenic profile for allulose under the tested conditions (Figure 2D). Its inability to activate key virulence pathways, including those involved in EPS synthesis (*gtfD*), acid production (*ldh*), and acid tolerance (*atpD*), aligns it with the properties of non-cariogenic sugar alcohols, such as xylitol and erythritol (Mäkinen, 2011; Milgrom et al., 2012; Runnel et al., 2013; De Cock, 2018).

Modulation of *S. mutans* biofilm formation and EPS synthesis by sweeteners

To assess the effects of dietary sugars on biofilm development and EPS production, which are key indicators of cariogenic potential, we employed a sHA disc model to simulate a pellicle-formed tooth surface (Figure 3A). *S. mutans* was incubated for 43 h in the presence of 1% (w/v) various sweeteners, and the mature biofilm biomass was quantified in terms of CFU and dry weight (Figures 3B, C). The three-dimensional (3D) architecture of the biofilm, consisting of both bacterial cells and EPS, was visualized using confocal microscopy (Figure 3D).

Quantitative data (Figures 3A, B) showed that sucrose yielded significantly higher CFU counts and dry biofilm weights ($p<0.001$) than all the other sugars. This further validates its established role as a high-carbohydrate sugar that enhances bacterial cell attachment and EPS production (Banas and Vickerman, 2003; Duarte et al., 2008; Razak et al., 2017). The dense, well-defined, dome-shaped microcolonies embedded in the EPS matrix under sucrose supplementation (Figures 3D, E) were consistent with those reported in previous reports on the sucrose-driven upregulation of Gtf exoenzymes, which are crucial for water-insoluble glucan synthesis and robust biofilm development. In contrast, supplementation with other fermentable sugars, such as glucose and fructose, resulted in comparatively less biomass with a dispersed cell–EPS arrangement (Figure 3D). These results indicate that, although these monosaccharides are fermentable,

10.3389/fcimb.2025.1670139

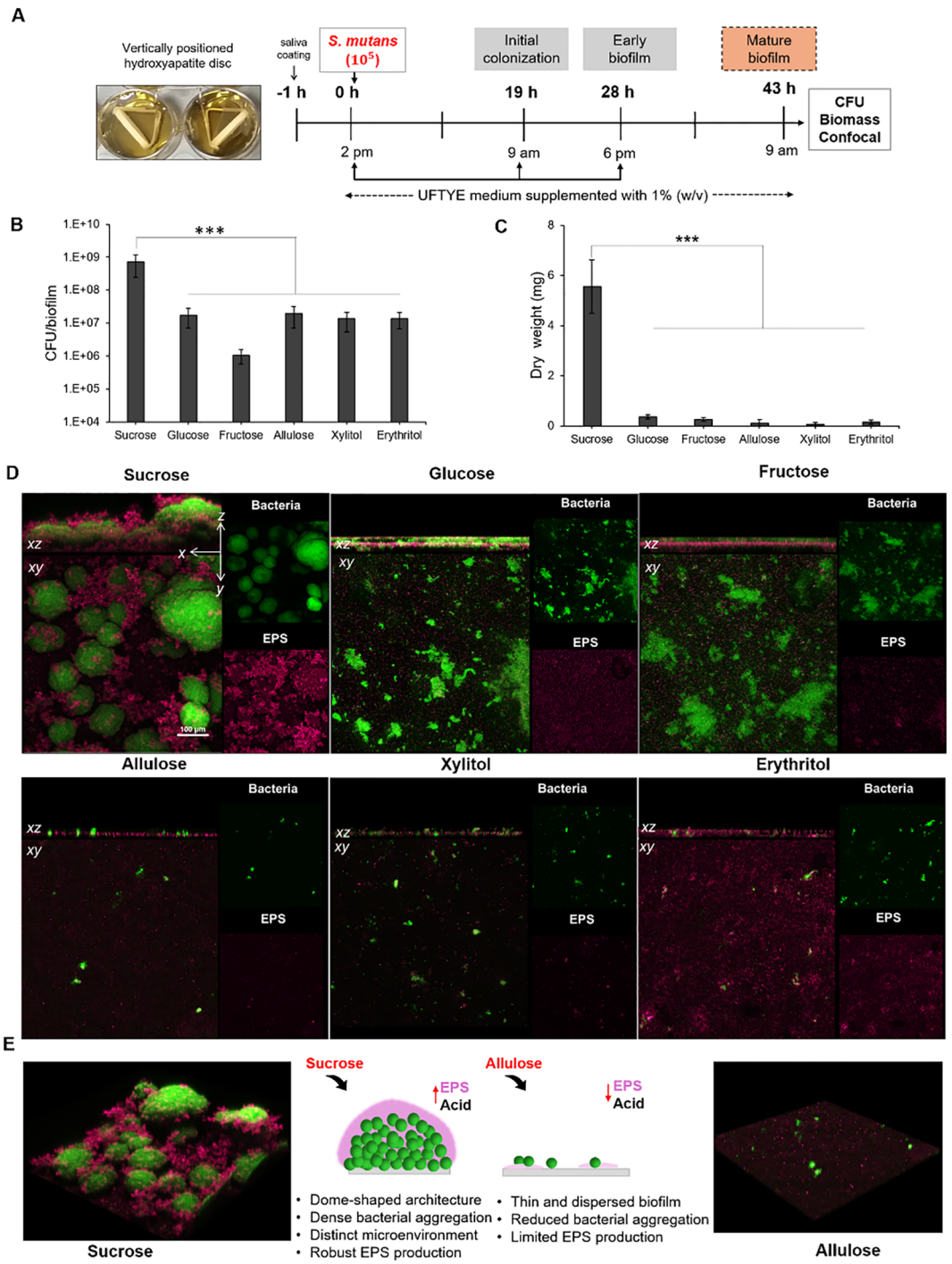

FIGURE 3
Experimental workflow and microbiological analysis of *Streptococcus mutans* biofilm architecture at 43 h. **(A)** Experimental design for *S. mutans* biofilm formation on the saliva-coated hydroxyapatite (sHA) discs. Biofilms were cultured in UFTYE media supplemented with 1% (w/v) sweetener at 37°C and 5% CO_2. The culture medium was changed twice daily (at 19 h and 28 h). Biofilm quantification in terms of **(B)** colony-forming units (CFU)/biofilm and **(C)** dry weight. **(D)** Confocal images showing the structural and spatial organization of 43-h-old *S. mutans* biofilm grown in the presence of various sweeteners. **(E)** Representative 3D confocal microscopy images showing biofilm formation in the presence of sucrose (left) and allulose (right). Green represents bacterial cells, while magenta indicates the extracellular polysaccharide (EPS) matrix. The data are presented as mean ± standard deviation (n=5). One-way analysis of variance (ANOVA) followed by Dunnett's multiple comparisons test was used to compare each treatment group with the sucrose control. ***p<0.0001.

they cannot replace the dual role of sucrose as a fuel for acid production and a key substrate for water-insoluble EPS biosynthesis.

Biofilms developed in the presence of allulose showed significantly reduced CFU counts and dry weights, similar to those developed in the presence of xylitol and erythritol (Figures 3A, B). Confocal imaging further showed that biofilms formed under allulose conditions lacked the dense, matrix-rich structures typical of sucrose-induced *S. mutans* biofilms (Figures 3D, E). The initial inhibition of biofilm formation in the presence of allulose can be attributed to reduced planktonic growth compared to that in the presence of fermentable sugars, correlating with the gene expression data showing a more complicated adaptive response. The upregulation of genes associated with metabolic stress and compensatory energy pathways (*pdhA* and *adhE*, respectively; Figure 2C) indicates that *S. mutans* may activate adaptive strategies under nutrient-limited conditions rather than simply undergoing growth arrest. These results suggest that biofilms under allulose conditions were characterized by reduced biomass, less EPS, and altered metabolic programming compared to fermentable sugars.

Taken together, the results of the single-species *S. mutans* biofilm provide consistent evidence that, under the conditions tested, allulose exhibits fewer cariogenic phenotypes compared to fermentable sugars and shows functional similarities to previously reported sugar alcohols (Miyasawa-Hori et al., 2006; Park et al., 2014). Our study further showed that biofilm architecture and EPS accumulation are the main indicators of cariogenic potential, and the sHA biofilm model is pertinent for evaluating dietary sugar under near-physiological conditions.

Acidogenic potential of sweeteners in mature *S. mutans* biofilm

Assessing how pre-formed oral biofilms respond to altered sugar exposure is necessary to comprehend how dietary sugar variations affect the cariogenic behavior of established biofilms. This was evaluated by a glycolytic pH drop assay using a 43 h-old *S. mutans* biofilm grown on tooth mimetics (Figure 4). To mimic the dietary changes, biofilms grown in the presence of 1% sucrose were exposed to various fermentable and non-fermentable sweeteners, and the pH drop was monitored for 120 min. The results show that sucrose supports the highest H^+ ion release (1.95 μM/min) and reaches a pH of 4.5 within 20 min of exposure, which further establishes its role as a fuel for both bacterial metabolisms, followed by acid production and EPS-associated proton accumulation (Duarte et al., 2008; Razak et al., 2017; Jurakova et al., 2023). The acidogenic profile of fructose was similar to that of sucrose than that of glucose, which is consistent with earlier findings on the expression of fructose-induced virulence factors in *S. mutans* (Shemesh et al., 2006).

Conversely, allulose-, xylitol-, or erythritol-supplemented biofilms maintained near-neutral pH throughout the assay period, with 98%, 99%, and 99% reduction in acid production, respectively, within 30 min compared to the sucrose-supplemented biofilm

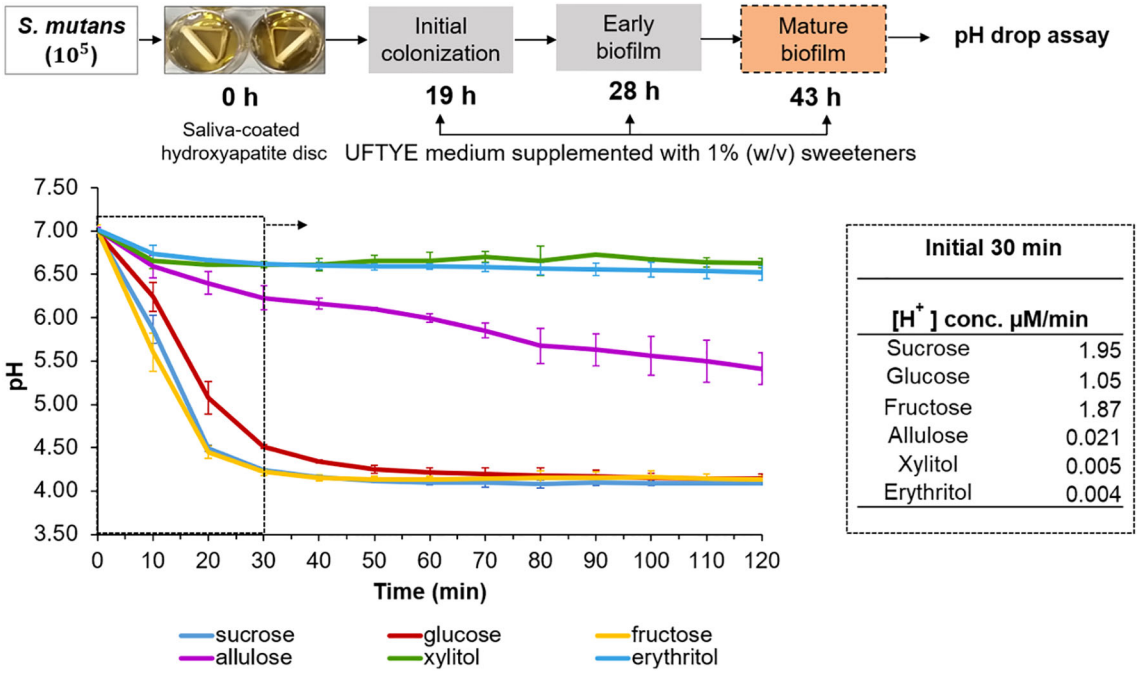

FIGURE 4
pH drop assay with pre-formed *Streptococcus mutans* biofilm in the presence of different sweeteners. The top panel illustrates the experimental design where *S. mutans* biofilms were grown on saliva-coated hydroxyapatite (sHA) discs in UFTYE medium supplemented with 1% (w/v) sucrose. The pH drop assay was performed at 43 h in the presence of different sweeteners. The bottom panel presents the pH drop over time, showing acid production from bacterial metabolism. Data are presented as the mean of two biologically different experiments.

(Figure 4). This result confirms that they serve as poorly fermentable substrates for *S. mutans* metabolism.

Although the oral cavity generally maintains a near-neutral pH, localized acidification from dietary sugars can promote enamel demineralization, favor acid-tolerant microbiota proliferation, and disrupt biofilm homeostasis (Marsh, 1994; Welin-Neilands and Svensater, 2007; Ikäläinen et al., 2024). Poor oral hygiene may exacerbate these effects by allowing the aciduric biofilms to mature and persist (Sälzer et al., 2020). In this context, alternative sweeteners, such as allulose, may help suppress acid accumulation, even in 3D-structured biofilms.

Modulation of interspecies balance in a dual-species biofilm model by sweeteners

Microbial interactions play crucial roles in the modulation of health and disease. Cooperative and competitive interactions among oral pathogens and commensals, as well as their composition, are modulated by ecological factors, such as nutrients and pH (Marsh, 2003). In the second phase of our cariogenic assessment platform, we evaluated the impact of dietary sugar (as it is the major nutrient source) on the dual-species biofilm model using *S. mutans* as the oral pathogen and *S. oralis* as the commensal bacterium (Figure 5A). The results show that supplementation with 1% (w/v) sucrose, glucose, or fructose selectively enriched *S. mutans* over *S. oralis* (p<0.001, Figure 5B). *S. mutans* enrichment in the presence of fermentable sugars such as sucrose, glucose, and fructose is driven by its robust metabolic and ecological adaptations. *S. mutans* can produce acid and survive in low-acid conditions because of its highly efficient fermentable sugar uptake system and virulence-associated gene expression. Particularly, sucrose can serve as both a substrate and precursor for EPS matrix synthesis for dense, acidic, and robust biofilm formation (Koo et al., 2010). Previous reports have shown that *S. mutans* can compete with commensal species, such as *S. oralis*, and dominate biofilms through bacteriocin production and a quorum-sensing mechanism (Li et al., 2002; Kreth et al., 2005). Conversely, *S. oralis* is an early colonizer associated with healthy oral biofilms, sensitive to acidic conditions, and lacks EPS production capacity, which makes it vulnerable to sugar-rich and acidic environments. This clearly shows the ecological imbalance that can shift the biofilm into a dysbiotic state with enhanced cariogenic potential.

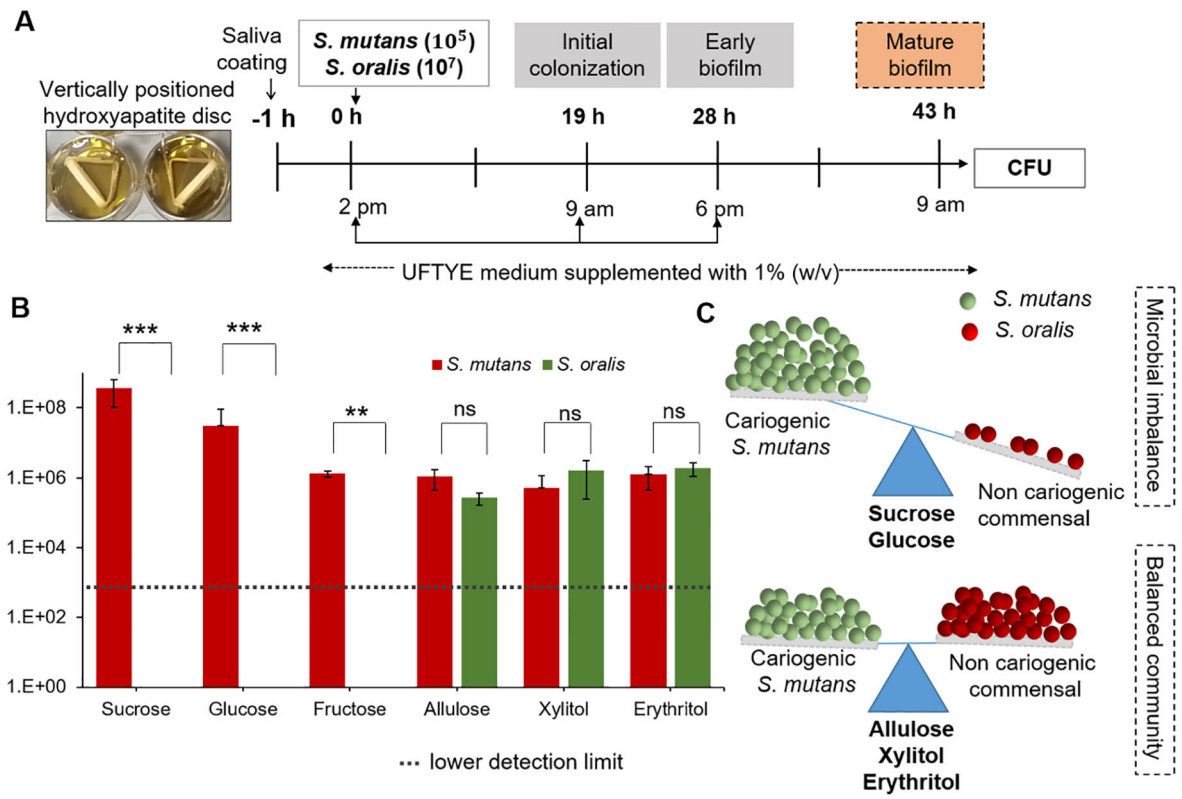

FIGURE 5
Impact of different sweeteners on *Streptococcus mutans* and *Streptococcus oralis* interspecies biofilm formation. **(A)** Experimental design for interspecies biofilm formation of *S. mutans and S. oralis* saliva-coated hydroxyapatite (sHA) discs. The biofilms were cultured in UFTYE medium supplemented with 1% (w/v) sweetener at 37°C and 5% CO_2. **(B)** Quantification of *S. mutans* and *S. oralis* colony-forming units (CFU) in 43 h-old biofilms grown in the presence of different sweeteners. **(C)** Schematic representation of microbial balance shift induced by different sweeteners, illustrating the impact of sugar supplementation on the dominance of *S. mutans* (cariogenic) and *S. oralis* (commensal species). Data are presented as mean ± standard deviation (n=8). Pairwise comparisons between *S. mutans* and *S. oralis* in the presence of each sweetener were performed using Dunn's multiple comparisons test following Kruskal–Wallis analysis. ***p<0.0001; **p<0.001; ns, not significant.

In contrast, allulose, xylitol, and erythritol maintained a balanced microbial composition, with no significant overgrowth of *S. mutans* toward *S. oralis* (Figure 5B). Previous studies have shown that the balance of *S. oralis* abundance in oral biofilms can be beneficial for dental health because these commensals secrete hydrogen peroxide, which can interfere with *S. mutans* growth and colonization (Kim et al., 2022). These findings align with the ecological plaque hypothesis, indicating the importance of non- or less-fermentable sugars such as allulose in reducing acid production and suppressing the overgrowth of acid-tolerant species over that of sensitive commensal bacteria in oral biofilms (Marsh, 1994, 2003). Therefore, oral microbial homeostasis and cariogenic biofilm formation control depend on the preservation of the balance between *S. mutans* and *S. oralis* (Figure 5C).

Ecological modulation in saliva-derived multi-species microcosm biofilm model by allulose

Next, we used HA discs coated with pooled whole saliva to stimulate a clinically relevant polymicrobial environment and support early colonization by native microbes. The ecological response to allulose was evaluated under caries-promoting conditions by supplementation with 1% (w/v) sucrose, followed by adding *S. mutans*, and compared with that of the no-added-carbohydrate saliva control. Changes in biofilm structure and community profile were examined in early (19 h) and mature (43 h) biofilms (Figure 6A).

Confocal imaging revealed significant architectural differences between the biofilms grown under sucrose and allulose supplementation. Early biofilm maturation, in terms of significant bacterial adhesion and EPS deposition, was observed in sucrose-supplemented biofilms at 19 h (Figure 6B). In contrast, the saliva-only control (without sugar addition) showed moderate bacterial attachment with little or no EPS, whereas the allulose-supplemented biofilms showed sparse bacterial colonization with minimal EPS deposition. Minimal baseline growth or biofilm may have resulted from trace amounts of sugars in the UFTYE medium; however, all groups were cultured under the same basal medium to ensure comparability. Upon extended incubation for 43 h, sucrose induced the development of dense dome-shaped microcolonies with a robust EPS matrix. The allulose-supplemented biofilm maintained a reduced biofilm structure with minimal bacteria and EPS, suggesting that biofilms under allulose conditions remained thinner and less structured over time compared to sucrose-treated biofilms; as expected, biofilms developed in the saliva-only group remained less organized and thinner.

Following confocal imaging, diversity analysis showed that the bacterial community structure was distinct among the groups (Figure 7). Alpha-diversity, in terms of the Shannon index, which is a measure of both richness and evenness (Kitikidou et al., 2024), was significantly lower in the sucrose-supplemented biofilm than in the no-sugar-added control and allulose-supplemented biofilms in early and mature stages, respectively (Figures 7A, B; p=2.8E−2). Interestingly, allulose maintained the highest Shannon diversity index compared to the other two sweeteners at both 19 and 43 h. This suggests the ecological neutrality of allulose under the tested conditions by maintaining or promoting microbial diversity. Beta-diversity analysis (principal coordinate analysis based on the Bray–Curtis distance) revealed distinct clustering of microbial communities by treatment and time point. At both early (19 h) and mature (43 h) stages, sucrose-treated biofilms showed strong separation from both the allulose-supplemented and no-sugar-added control biofilms, indicating a marked shift in microbial community composition toward a dysbiotic state. In contrast, allulose-treated communities clustered closer to the no-sugar-added control communities, suggesting the maintenance of a more health-compatible microbial community (Figure 7C). Sucrose significantly reduced community diversity by selectively promoting the growth of acidogenic and aciduric *Streptococcus* and *Lactobacillus* species. In contrast, the relative abundance was maintained or increased under allulose supplementation compared to that without any supplementation (Figure 7A).

Biofilm development is a multistep process that begins with the attachment of early colonizers via specific or non-specific interactions with pellicle-coated surfaces (Marsh and Bradshaw, 1995; Dang and Lovell, 2000; Rickard et al., 2003). Favorable conditions promote microcolony formation by primary colonizers, subsequently facilitating secondary (late) colonizers to adhere primarily through co-aggregation (Rickard et al., 2003). Genera such as *Streptococcus*, *Actinomyces*, *Haemophilus*, *Veillonella*, and *Neisseria* are well-established early colonizers (Ritz, 1967; Foster and Kolenbrander, 2004; Dige et al., 2009; Huang et al., 2011). In this study, the presence of all these genera (except *Actinomyces)* in the allulose-treated and blank (saliva-origin microbiome) groups supported the establishment of a health-associated early biofilm community. *Veillonella* species convert the lactic acid produced by fermentative bacteria, such as *Streptococcus* sp., into weak acids, which may reduce the enamel demineralization rate (Geddes, 1972; Mikx and Van der Hoeven, 1975). The enrichment and maintenance of *Veillonella* sp. in the allulose-treated group than in the no-sugar-added group confirmed a more balanced community with metabolic cooperation (Figure 7A).

Additionally, the presence of *Neisseria*, *Haemophilus*, *Granulicatella*, *Fusobacterium*, and *Veillonella* further supports the establishment of a healthy nitrate-reducing biofilm with a beneficial role in maintaining oral homeostasis (Hyde et al., 2014). Notably, *Fusobacterium* plays a key bridging role in plaque development, promoting co-aggregation and supporting anaerobic colonizers (Bradshaw et al., 1998; Kolenbrander et al., 1999; Rickard et al., 2003). Hence, its presence in the allulose-supplemented group suggests a diverse microbial community structure, where microbial connectivity and balance were preserved (Figures 7A–C).

Altogether, our microbial community analysis data align with the "ecological plaque hypothesis," which explains that environmental shifts owing to acid production from dietary sugar fermentation can select acid-tolerating species such as *Streptococcus* and *Lactobacillus*, developing dysbiotic, caries-associated biofilms. By dealing with these detrimental and virulent factors, the allulose-treated microcosms retained microbial interactions, community

10.3389/fcimb.2025.1670139

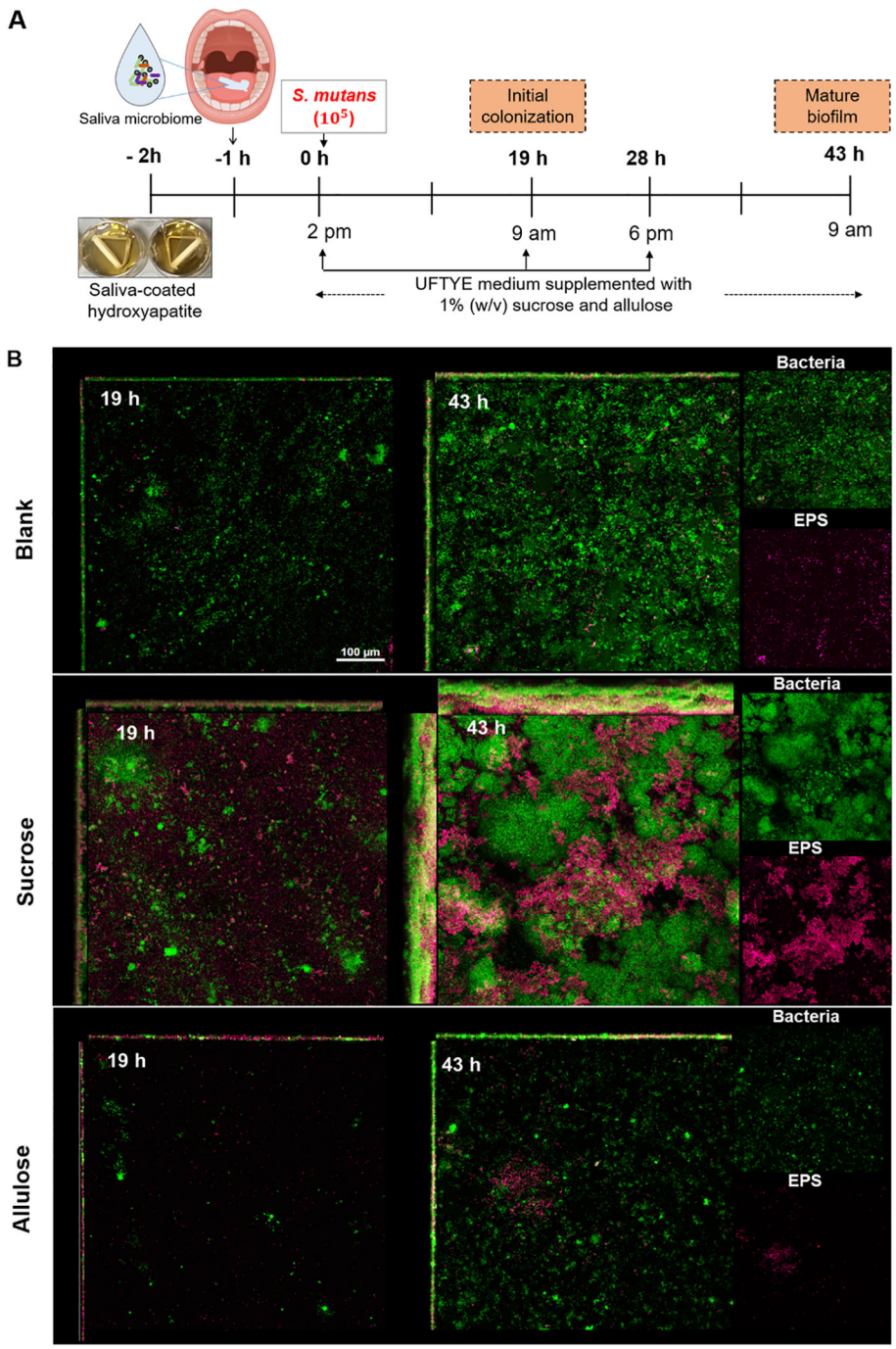

FIGURE 6
Biofilm development and extracellular polysaccharide (EPS) production in a saliva-derived microcosm model in the presence of 1% (w/v) sucrose or allulose. **(A)** Schematic representation of an ex vivo microcosm biofilm model using saliva-coated hydroxyapatite (sHA) discs. The discs were first incubated with the saliva from healthy donors for 1 h to allow initial microbial colonization, followed by incubation in UFTYE media supplemented with 1% (w/v) sucrose or allulose and inoculated with *S. mutans*. UFTYE media without any sweetener supplementation served as the blank control. **(B)** Confocal laser scanning microscopy images of biofilms grown at 19 and 43 h. Green and magenta represent bacterial cells and the extracellular polysaccharides (EPS), respectively.

diversity, and spatial organization, which are key characteristics of health-compatible biofilms.

In this study, we used a multi-tiered platform to investigate the ecological and functional effects of allulose on oral biofilm development. Using a biologically relevant model that included single-species planktonic, biofilm, dual-species biofilm, and saliva-derived microcosms, we systematically showed that allulose does not support the key virulence traits typically promoted by commonly used fermentable sugars such as sucrose, fructose, and glucose. Allulose consistently resulted in lower growth,

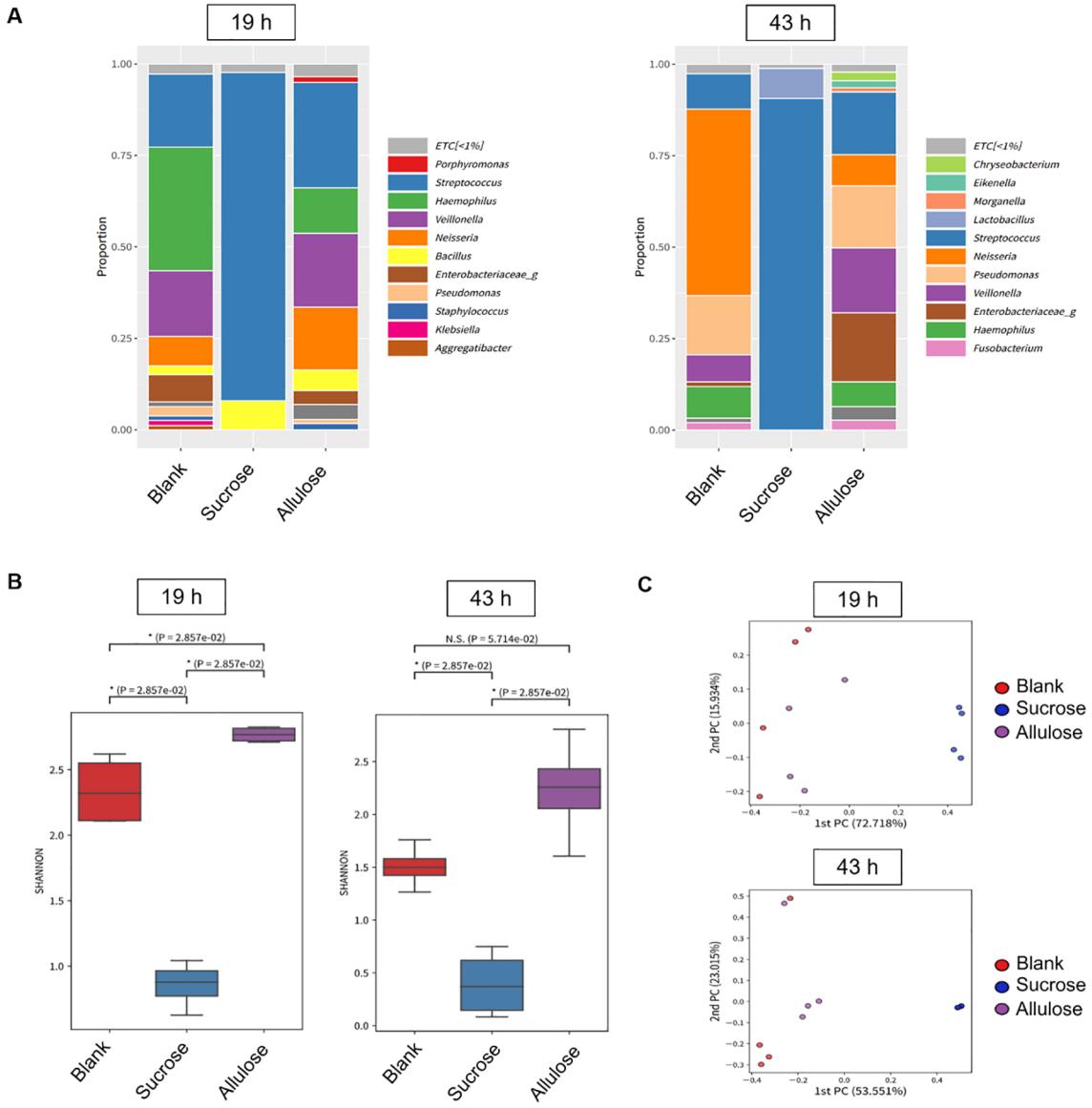

FIGURE 7
Microbial diversity and community structure in biofilm grown in the presence of 1% (w/v) sucrose or allulose. **(A)** Relative abundance of bacterial genera in 19 (left) and 43 h (right) biofilms grown on saliva-coated hydroxyapatite (sHA) discs with 1% (w/v) sucrose, allulose, or no sugar (blank). **(B)** Alpha-diversity (Shannon index) of microbial communities among treatment groups at 19 and 43 h. **(C)** Principal coordinate analysis (PCoA) of beta-diversity (Bray–Curtis distance) across treatment groups.

acidogenicity, and EPS matrix formation compared to fermentable sugars, while preserving the ecological equilibrium of commensal bacteria (*S. oralis*). Additionally, it preserved many health-compatible taxa such as *Neisseria*, *Haemophilus*, *Granulicatella*, and *Veillonella* and maintained high alpha-diversity, indicating microbial equilibrium and ecological resilience. The follow-up experiment will apply shotgun metagenomics to identify species-level community shifts and functional gene analyses to link taxonomic shifts to cariogenic traits.

The overall findings of our study indicate that allulose is a microbiome-friendly sugar substitute that may limit cariogenic shifts under *in vitro* conditions. While promising, the translational potential of allulose as an alternative to established cariostatic agents, such as xylitol and erythritol, warrants further investigation.

We acknowledge the limitations of this platform, particularly the inability of the continuous sugar exposure model to accurately mimic the dynamic nature of dietary intake. Future research should aim to improve the ecological relevance of cariogenic evaluations by incorporating a feast–famine strategy. In addition, future research should evaluate the composition of plaques, the dynamics of salivary pH, and the incidence of caries over time to validate these *in vitro* results using *in vivo* models, including clinical trials. Ecological engineering of oral microbiota may also be clarified by further studies on the interactions of allulose with fluoride, oral prebiotics, or probiotics. Overall, this study establishes a strong

foundation for developing next-generation microbiome-conscious sugar alternatives that support oral and systemic health.

Data availability statement

The datasets presented in this study can be found in online repositories. The names of the repository/repositories and accession number(s) can be found below: https://www.ncbi.nlm.nih.gov/genbank/, PRJNA1269248.

Ethics statement

The studies involving humans were approved by Institutional Review Board of Jeonbuk National University (IRB ref. JBNU 2021-12-008-003). The studies were conducted in accordance with the local legislation and institutional requirements. The participants provided their written informed consent to participate in this study.

Author contributions

SH: Formal analysis, Investigation, Methodology, Visualization, Writing – original draft. KR: Formal analysis, Validation, Visualization, Writing – original draft. SP: Formal analysis, Investigation, Methodology, Validation, Visualization, Writing – review & editing. JL: Investigation, Methodology, Writing – review & editing. HJ: Investigation, Methodology, Validation, Writing – review & editing. JK: Conceptualization, Methodology, Resources, Writing – review & editing. DK: Conceptualization, Funding acquisition, Methodology, Project administration, Supervision, Visualization, Writing – review & editing, Writing – original draft.

Funding

The author(s) declare financial support was received for the research and/or publication of this article. This work was supported in part by the National Research Foundation (NRF) [grant number RS-2021-NR061314 to DK] and the Bio & Medical Technology Development Program of NRF [grant number RS-2022-NR067350 to DK], funded by the Korean government (MIST).

Acknowledgments

High-purity allulose and erythritol were provided by Samyang Co. (Seongnam, Korea).

Conflict of interest

The authors declare that the research was conducted in the absence of any commercial or financial relationships that could be construed as a potential conflict of interest.

The author(s) declared that they were an editorial board member of Frontiers, at the time of submission. This had no impact on the peer review process and the final decision.

Generative AI statement

The authors declare that Generative AI was used in the creation of this manuscript. The author(s) used ChatGPT in order to improve the language and readability of the manuscript.

Any alternative text (alt text) provided alongside figures in this article has been generated by Frontiers with the support of artificial intelligence and reasonable efforts have been made to ensure accuracy, including review by the authors wherever possible. If you identify any issues, please contact us.

Publisher's note

References

Banas, J. A. (2004). Virulence properties of Streptococcus mutans. *Front. Biosci.* 9, 1267–1277. doi: 10.2741/1305

Banas, J., and Vickerman, M. (2003). Glucan-binding proteins of the oral streptococci. *Crit. Rev. Oral. Biol. Med.* 14, 89–99. doi: 10.1177/154411130301400203

Beighton, D. (2005). The complex oral microflora of high-risk individuals and groups and its role in the caries process. *Community Dent. Oral. Epidemiol.* 33, 248–255. doi: 10.1111/j.1600-0528.2005.00232.x

Benahmed, A. G., Gasmi, A., Dadar, M., Arshad, M., and Bjørklund, G. (2021). The role of sugar-rich diet and salivary proteins in dental plaque formation and oral health. *J. Oral. Biosci.* 63, 134–141. doi: 10.1016/j.job.2021.01.007

Bowen, W. H., Burne, R. A., Wu, H., and Koo, H. (2018). Oral biofilms: pathogens, matrix, and polymicrobial interactions in microenvironments. *Trends Microbiol.* 26, 229–242. doi: 10.1016/j.tim.2017.09.008

Bowen, W., and Koo, H. (2011). Biology of *Streptococcus mutans*-derived glucosyltransferases: role in extracellular matrix formation of cariogenic biofilms. *Caries Res.* 45, 69–86. doi: 10.1159/000324598

Bradshaw, D. J., Marsh, P. D., Watson, G. K., and Allison, C. (1998). Role of *Fusobacterium nucleatum* and coaggregation in anaerobe survival in planktonic and biofilm oral microbial communities during aeration. *Infect. Immun.* 66, 4729–4732. doi: 10.1128/IAI.66.10.4729-4732.1998

Cai, J.-N., Jung, J.-E., Lee, M.-H., Choi, H.-M., and Jeon, J. G. (2018). Sucrose challenges to *Streptococcus mutans* biofilms and the curve fitting for the biofilm changes. *FEMS Microbiol. Ecol.* 94, fiy091. doi: 10.1093/femsec/fiy091

Dang, H., and Lovell, C. R. (2000). Bacterial primary colonization and early succession on surfaces in marine waters as determined by amplified rRNA gene restriction analysis and sequence analysis of 16S rRNA genes. *Appl. Environ. Microbiol.* 66, 467–475. doi: 10.1128/AEM.66.2.467-475.2000

Daniel, H., Hauner, H., Hornef, M., and Clavel, T. (2022). Allulose in human diet: the knowns and the unknowns. *Br. J. Nutr.* 128, 172–178. doi: 10.1017/S0007114521003172

De Cock, P. (2018). Erythritol functional roles in oral-systemic health. *Adv. Dent. Res.* 29, 104–109. doi: 10.1177/0022034517736499

Dige, I., Nyengaard, J. R., Kilian, M., and Nyvad, B. (2009). Application of stereological principles for quantification of bacteria in intact dental biofilms. *Oral. Microbiol. Immunol.* 24, 69–75. doi: 10.1111/j.1399-302X.2008.00482.x

Document, G. (2019). *The Declaration of Allulose and Calories from Allulose on Nutrition and Supplement Facts Labels: Guidance for Industry* (MD, USA: Center for Food Safety and Applied Nutrition College Park).

Duarte, S., Klein, M., Aires, C., Cury, J., Bowen, W., and Koo, H. (2008). Influences of starch and sucrose on *Streptococcus mutans* biofilms. *Oral. Microbiol. Immunol.* 23, 206–212. doi: 10.1111/j.1399-302X.2007.00412.x

Durso, S. C., Vieira, L., Cruz, J., Azevedo, C., Rodrigues, P., and Simionato, M. R. L. (2014). Sucrose substitutes affect the cariogenic potential of *Streptococcus mutans* biofilms. *Caries Res.* 48, 214–222. doi: 10.1159/000354410

Forssten, S. D., Björklund, M., and Ouwehand, A. C. (2010). *Streptococcus mutans*, caries and simulation models. *Nutrients* 2, 290–298. doi: 10.3390/nu2030290

Foster, J. S., and Kolenbrander, P. E. (2004). Development of a multispecies oral bacterial community in a saliva-conditioned flow cell. *Appl. Environ. Microbiol.* 70, 4340–4348. doi: 10.1128/AEM.70.7.4340-4348.2004

Geddes, D. A. (1972). The production of l (+) and d (–) lactic acid and volatile acids by human dental plaque and the effect of plaque buffering and acidic strength on pH. *Arch. Oral. Biol.* 17, 537–545. doi: 10.1016/0003-9969(72)90069-6

Hajishengallis, E., Parsaei, Y., Klein, M. I., and Koo, H. (2017). Advances in the microbial etiology and pathogenesis of early childhood caries. *Mol. Oral. Microbiol.* 32, 24–34. doi: 10.1111/omi.12152

Hasturk, H. (2018). *A clinical study on the effect of allulose, a low-calorie sugar, on* in vivo *dental plaque pH* (Boston, MA, USA: Forsyth Institute).

He, J., Kim, D., Zhou, X., Ahn, S.-J., Burne, R. A., Richards, V. P., et al. (2017). RNA-Seq reveals enhanced sugar metabolism in *Streptococcus mutans* co-cultured with Candida albicans within mixed-species biofilms. *Front. Microbiol.* 8, 1036. doi: 10.3389/fmicb.2017.01036

Hu, M., Li, M., Jiang, B., and Zhang, T. (2021). Bioproduction of D-allulose: Properties, applications, purification, and future perspectives. *Compr. Rev. Food Sci. Food Saf.* 20, 6012–6026. doi: 10.1111/1541-4337.12859

Huang, R., Li, M., and Gregory, R. L. (2011). Bacterial interactions in dental biofilm. *Virulence* 2, 435–444. doi: 10.4161/viru.2.5.16140

Hyde, E. R., Andrade, F., Vaksman, Z., Parthasarathy, K., Jiang, H., Parthasarathy, D. K., et al. (2014). Metagenomic analysis of nitrate-reducing bacteria in the oral cavity: implications for nitric oxide homeostasis. *PloS One* 9, e88645. doi: 10.1371/journal.pone.0088645

Igarashi, T., Morisaki, H., Yamamoto, A., and Goto, N. (2002). An essential amino acid residue for catalytic activity of the dextranase of *Streptococcus mutans*. *Oral. Microbiol. Immunol.* 17, 193–196. doi: 10.1034/j.1399-302X.2002.170310.x

Iida, T., Hayashi, N., Yamada, T., Yoshikawa, Y., Miyazato, S., Kishimoto, Y., et al. (2010). Failure of d-psicose absorbed in the small intestine to metabolize into energy and its low large intestinal fermentability in humans. *Metabolism* 59, 206–214. doi: 10.1016/j.metabol.2009.07.018

Ikäläinen, H., Guzman, C., Saari, M., Söderling, E., and Loimaranta, V. (2024). Real-time acid production and extracellular matrix formation in mature biofilms of three *Streptococcus mutans* strains with special reference to xylitol. *Biofilm* 8, 100219. doi: 10.1016/j.bioflm.2024.100219

Iwasaki, Y., Sendo, M., Dezaki, K., Hira, T., Sato, T., Nakata, M., et al. (2018). GLP-1 release and vagal afferent activation mediate the beneficial metabolic and chronotherapeutic effects of D-allulose. *Nat. Commun.* 9, 113. doi: 10.1038/s41467-017-02488-y

Jeon, J. G., Klein, M. I., Xiao, J., Gregoire, S., Rosalen, P. L., and Koo, H. (2009). Influences of naturally occurring agents in combination with fluoride on gene expression and structural organization of *Streptococcus mutans* in biofilms. *BMC Microbiol.* 9, 1–10. doi: 10.1186/1471-2180-9-228

Jeon, J. G., Pandit, S., Xiao, J., Gregoire, S., Falsetta, M. L., Klein, M. I., et al. (2011). Influences of trans-trans farnesol, a membrane-targeting sesquiterpenoid, on *Streptococcus mutans* physiology and survival within mixed-species oral biofilms. *Int. J. Oral. Sci.* 3, 98–106. doi: 10.4248/IJOS11038

Jeong, G.-J., Khan, F., Tabassum, N., and Kim, Y.-M. (2024). Alteration of oral microbial biofilms by sweeteners. *Biofilm* 7, 100171. doi: 10.1016/j.bioflm.2023.100171

Jung, H.-Y., Cai, J.-N., Yoo, S. C., Kim, S.-H., Jeon, J.-G., and Kim, D. (2022). Collagen peptide in a combinatorial treatment with *Lactobacillus rhamnosus* inhibits the cariogenic properties of *Streptococcus mutans*: An *in vitro* study. *Int. J. Mol. Sci.* 23, 1860. doi: 10.3390/ijms23031860

Jurakova, V., Farková, V., Kucera, J., Dadakova, K., Zapletalova, M., Paskova, K., et al. (2023). Gene expression and metabolic activity of *Streptococcus mutans* during exposure to dietary carbohydrates glucose, sucrose, lactose, and xylitol. *Mol. Oral. Microbiol.* 38, 424–441. doi: 10.1111/omi.12428

Kanasi, E., Johansson, I., Lu, S. C., Kressin, N. R., Nunn, M. E., Kent, R. Jr., et al. (2010). Microbial risk markers for childhood caries in pediatricians' offices. *J. Dent. Res.* 89, 378–383. doi: 10.1177/0022034509360010

Kim, D., Barraza, J. P., Arthur, R. A., Hara, A., Lewis, K., Liu, Y., et al. (2020). Spatial mapping of polymicrobial communities reveals a precise biogeography associated with human dental caries. *Proc. Natl. Acad. Sci. U.S.A.* 117, 12375–12386. doi: 10.1073/pnas.1919099117

Kim, D., Ito, T., Hara, A., Li, Y., Kreth, J., and Koo, H. (2022). Antagonistic interactions by a high H_2O_2-producing commensal streptococcus modulate caries development by Streptococcus mutans. *Mol. Oral. Microbiol.* 37, 244–255. doi: 10.1111/omi.12394

Kim, D., Liu, Y., Benhamou, R. I., Sanchez, H., Simón-Soro, Á., Li, Y., et al. (2018). Bacterial-derived exopolysaccharides enhance antifungal drug tolerance in a cross-kingdom oral biofilm. *ISME J.* 12, 1427–1442. doi: 10.1038/s41396-018-0113-1

Kim, D., Sengupta, A., Niepa, T. H., Lee, B.-H., Weljie, A., Freitas-Blanco, V. S., et al. (2017). *Candida albicans* stimulates *Streptococcus mutans* microcolony development via cross-kingdom biofilm-derived metabolites. *Sci. Rep.* 7, 41332. doi: 10.1038/srep41332

Kitikidou, K., Milios, E., Stampoulidis, A., Pipinis, E., and Radoglou, K. (2024). Using biodiversity indices effectively: considerations for forest management. *Ecologies* 5, 42–51. doi: 10.3390/ecologies5010003

Klein, M. I., Hwang, G., Santos, P. H., Campanella, O. H., and Koo, H. (2015). *Streptococcus mutans*-derived extracellular matrix in cariogenic oral biofilms. *Front. Cell. Infect. Microbiol.* 5, 10. doi: 10.3389/fcimb.2015.00010

Kolenbrander, P. E., Andersen, R. N., Clemans, D. L., Whittaker, C. J., and Klier, C. M. (1999). Potential role of functionally similar coaggregation mediators in bacterial succession. *Dental plaque revisited: Oral. biofilms Health Dis.* 171-186.

Koo, H., Vacca Smith, A. M., Bowen, W. H., Rosalen, P. L., Cury, J. A., and Park, Y. K. (2000). Effects of Apis mellifera propolis on the activities of streptococcal glucosyltransferases in solution and adsorbed onto saliva–coated hydroxyapatite. *Caries Res.* 34, 418–426. doi: 10.1159/000016617

Koo, H., Xiao, J., Klein, M., and Jeon, J. (2010). Exopolysaccharides produced by *Streptococcus mutans* glucosyltransferases modulate the establishment of microcolonies within multispecies biofilms. *J. Bacteriol.* 192, 3024–3032. doi: 10.1128/JB.01649-09

Kreth, J., Merritt, J., Shi, W., and Qi, F. (2005). Competition and coexistence between *Streptococcus mutans* and *Streptococcus sanguinis* in the dental biofilm. *J. Bacteriol.* 187, 7193–7203. doi: 10.1128/JB.187.21.7193-7203.2005

Lee, H.-Y., Lee, G.-H., Hoang, T.-H., Park, S.-A., Lee, J., Lim, J., et al. (2022). D-allulose ameliorates hyperglycemia through IRE1α sulfonation-RIDD-sirt1 decay axis in the skeletal muscle. *Antioxid. Redox Signal.* 37, 229–245. doi: 10.1089/ars.2021.0207

Leme, A. P., Koo, H., Bellato, C., Bedi, G., and Cury, J. (2006). The role of sucrose in cariogenic dental biofilm formation—new insight. *J. Dent. Res.* 85, 878–887. doi: 10.1177/154405910608501002

Lemos, J. A., and Burne, R. A. (2008). A model of efficiency: stress tolerance by *Streptococcus mutans*. *Microbiology* 154, 3247–3255. doi: 10.1099/mic.0.2008/023770-0

Li, Y.-H., Tang, N., Aspiras, M. B., Lau, P. C., Lee, J. H., Ellen, R. P., et al. (2002). A quorum-sensing signaling system essential for genetic competence in *Streptococcus mutans* is involved in biofilm formation. *J. Bacteriol.* 184, 2699–2708. doi: 10.1128/JB.184.10.2699-2708.2002

Liu, Y., Daniel, S. G., Kim, H.-E., Koo, H., Korostoff, J., Teles, F., et al. (2023). Addition of cariogenic pathogens to complex oral microflora drives significant changes in biofilm compositions and functionalities. *Microbiome* 11, 123. doi: 10.1186/s40168-023-01561-7

Mäkinen, K. K. (2010). Sugar alcohols, caries incidence, and remineralization of caries lesions: a literature review. *Int. J. Dent.* 2010, 981072. doi: 10.1155/2010/981072

Mäkinen, K. K. (2011). Sugar alcohol sweeteners as alternatives to sugar with special consideration of xylitol. *Med. Princ. Pract.* 20, 303–320. doi: 10.1159/000324534

Mäkinen, K. K. (2016). Gastrointestinal disturbances associated with the consumption of sugar alcohols with special consideration of xylitol: scientific review and instructions for dentists and other health-care professionals. *Int. J. Dent.* 2016, 5967907. doi: 10.1155/2016/5967907

Marsh, P. D. (1994). Microbial ecology of dental plaque and its significance in health and disease. *Adv. Dent. Res.* 8, 263–271. doi: 10.1177/08959374940080022001

Marsh, P. D. (2003). Are dental diseases examples of ecological catastrophes? *Microbiology* 149, 279–294. doi: 10.1099/mic.0.26082-0

Marsh, P. D., and Bradshaw, D. J. (1995). Dental plaque as a biofilm. *J. Ind. Microbiol.* 15, 169–175. doi: 10.1007/BF01569822

Mikx, F., and van der Hoeven, J. (1975). Symbiosis of *Streptococcus mutans* and *Veillonella alcalescens* in mixed continuous cultures. *Arch. Oral. Biol.* 20, 407–410. doi: 10.1016/0003-9969(75)90224-1

Milgrom, P., Söderling, E., Nelson, S., Chi, D., and Nakai, Y. (2012). Clinical evidence for polyol efficacy. *Adv. Dent. Res.* 24, 112–116. doi: 10.1177/0022034512449467

Miyasawa-Hori, H., Aizawa, S., and Takahashi, N. (2006). Difference in the xylitol sensitivity of acid production among *Streptococcus mutans* strains and the biochemical mechanism. *Oral. Microbiol. Immunol.* 21, 201–205. doi: 10.1111/j.1399-302X.2006.00273.x

Palmer, C., Kent, R.Jr., Loo, C., Hughes, C., Stutius, E., Pradhan, N., et al. (2010). Diet and caries-associated bacteria in severe early childhood caries. *J. Dent. Res.* 89, 1224–1229. doi: 10.1177/0022034510376543

Parisotto, T. M., Steiner-Oliveira, C., Silva, C. M. S. E., Rodrigues, L. K. A., and Nobre-dos-Santos, M. (2010). Early childhood caries and mutans streptococci: a systematic review. *Oral. Health Prev. Dent.* 8(1), 59-70.

Park, Y.-N., Jeong, S.-S., Zeng, J., Kim, S.-H., Hong, S.-J., Ohk, S.-H., et al. (2014). Anti-cariogenic effects of erythritol on growth and adhesion of *Streptococcus mutans*. *Food Sci. Biotechnol.* 23, 1587–1591. doi: 10.1007/s10068-014-0215-0

Philip, N., Suneja, B., and Walsh, L. J. (2018). Ecological approaches to dental caries prevention: paradigm shift or shibboleth? *Caries Res.* 52, 153–165. doi: 10.1159/000484985

Razak, F. A., Baharuddin, B. A., Akbar, E. F. M., Norizan, A. H., Ibrahim, N. F., and Musa, M. Y. (2017). Alternative sweeteners influence the biomass of oral biofilm. *Arch. Oral. Biol.* 80, 180–184. doi: 10.1016/j.archoralbio.2017.04.014

Ren, Z., Jeckel, H., Simon-Soro, A., Xiang, Z., Liu, Y., Cavalcanti, I. M., et al. (2022). Interkingdom assemblages in human saliva display group-level surface mobility and disease-promoting emergent functions. *Proc. Natl. Acad. Sci. U.S.A.* 119, e2209699119. doi: 10.1073/pnas.2209699119

Rice, T., Zannini, E., K. Arendt, E., and Coffey, A. (2020). A review of polyols–biotechnological production, food applications, regulation, labeling and health effects. *Crit. Rev. Food Sci. Nutr.* 60, 2034–2051. doi: 10.1080/10408398.2019.1625859

Rickard, A. H., Gilbert, P., High, N. J., Kolenbrander, P. E., and Handley, P. S. (2003). Bacterial coaggregation: an integral process in the development of multi-species biofilms. *Trends Microbiol.* 11, 94–100. doi: 10.1016/S0966-842X(02)00034-3

Ritz, H. (1967). Microbial population shifts in developing human dental plaque. *Arch. Oral. Biol.* 12, 1561–1568. doi: 10.1016/0003-9969(67)90190-2

Runnel, R., Mäkinen, K. K., Honkala, S., Olak, J., Mäkinen, P. L., Nõmmela, R., et al. (2013). Effect of three-year consumption of erythritol, xylitol and sorbitol candies on various plaque and salivary caries-related variables. *J. Dent.* 41, 1236–1244. doi: 10.1016/j.jdent.2013.09.007

Sälzer, S., Graetz, C., Dörfer, C. E., Slot, D. E., and van der Weijden, F. A. (2020). Contemporary practices for mechanical oral hygiene to prevent periodontal disease. *Periodontol. 2000* 84, 35–44. doi: 10.1111/prd.12332

Sheiham, A., and James, W. (2015). Diet and dental caries: the pivotal role of free sugars reemphasized. *J. Dent. Res.* 94, 1341–1347. doi: 10.1177/0022034515590377

Shemesh, M., Tam, A., Feldman, M., and Steinberg, D. (2006). Differential expression profiles of Streptococcus mutans ftf, gtf and vicR genes in the presence of dietary carbohydrates at early and late exponential growth phases. *Carbohydr. Res.* 341, 2090–2097. doi: 10.1016/j.carres.2006.05.010

Staszczyk, M., Jurczak, A., Magacz, M., Kościelniak, D., Gregorczyk-Maga, I., Jamka-Kasprzyk, M., et al. (2020). Effect of polyols and selected dental materials on the ability to create a cariogenic biofilm–on children caries-associated *Streptococcus mutans* isolates. *Int. J. Environ. Res. Public Health* 17, 3720. doi: 10.3390/ijerph17103720

US Food and Drug Administration (FDA) (2023). *Generally Recognized as Safe (GRAS) Notice (GRN) No. 1029: D-psicose. Silver Spring, MD: U.S. Food and Drug Administration*.

Wang, Y., Wang, X., Jiang, W., Wang, K., Luo, J., Li, W., et al. (2018). Antimicrobial peptide GH12 suppresses cariogenic virulence factors of *Streptococcus mutans*. *J. Oral. Microbiol.* 10, 1442089. doi: 10.1080/20002297.2018.1442089

Welin-Neilands, J., and Svensater, G. (2007). Acid tolerance of biofilm cells of *Streptococcus mutans*. *Appl. Environ. Microbiol.* 73, 5633–5638. doi: 10.1128/AEM.01049-07

Xiao, J., Klein, M. I., Falsetta, M. L., Lu, B., Delahunty, C. M., Yates, J. R. III, et al. (2012). The exopolysaccharide matrix modulates the interaction between 3D architecture and virulence of a mixed-species oral biofilm. *PloS Pathog.* 8, e1002623. doi: 10.1371/journal.ppat.1002623

Yoon, S.-H., Ha, S.-M., Kwon, S., Lim, J., Kim, Y., Seo, H., et al. (2017). Introducing EzBioCloud: a taxonomically united database of 16S rRNA gene sequences and whole-genome assemblies. *Int. J. Syst. Evol. Microbiol.* 67, 1613–1617. doi: 10.1099/ijsem.0.001755

Zhang, Q., Ma, Q., Wang, Y., Wu, H., and Zou, J. (2021). Molecular mechanisms of inhibiting glucosyltransferases for biofilm formation in *Streptococcus mutans*. *Int. J. Oral. Sci.* 13, 30. doi: 10.1038/s41368-021-00137-1

Zhang, L., Shen, Y., Qiu, L., Yu, F., Hu, X., Wang, M., et al. (2022). The suppression effect of SCH-79797 on *Streptococcus mutans* biofilm formation. *J. Oral. Microbiol.* 14, 2061113. doi: 10.1080/20002297.2022.2061113

Zhao, W., Li, W., Lin, J., Chen, Z., and Yu, D. (2014). Effect of sucrose concentration on sucrose-dependent adhesion and glucosyltransferase expression of *S. mutans* in children with severe early-childhood caries (S-ECC). *Nutrients* 6, 3572–3586. doi: 10.3390/nu6093572

Frontiers in
Cellular and Infection Microbiology

Investigates how microorganisms interact with their hosts

Explores bacteria, fungi, parasites, viruses, endosymbionts, prions and all microbial pathogens as well as the microbiota and its effect on health and disease in various hosts.

Discover the latest Research Topics

See more →

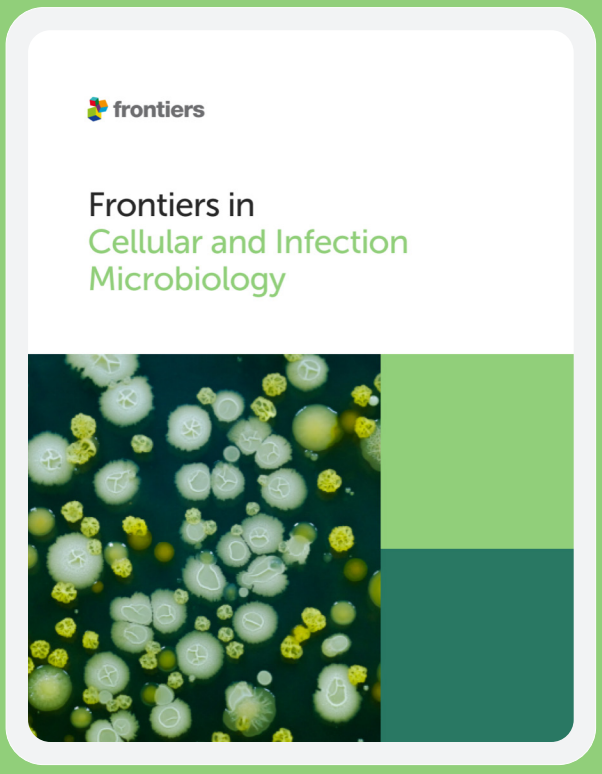

Frontiers

Avenue du Tribunal-Fédéral 34
1005 Lausanne, Switzerland
frontiersin.org

Contact us

+41 (0)21 510 17 00
frontiersin.org/about/contact